Final Report for the Design of a VTOL Firefighter Aircraft

Group 14

Floris Benschop	F.B.	5562457
Xander Bonenkamp	X.B.	5491770
Jorrit Greep	J.G.	5284236
Sjoerd Heijnen	S.H.	5286565
Emma Janssen	E.J.	5090660
Marinka Jongeneel	M.J.	5544300
Ivo L'Ortije	I.L.	5482704
Merel Luijpen	M.L.	5328608
Ruben van der Plas	R.P.	5549922
Marco Smits	M.S.	5474558

Delft University of Technology

TU Delft

Final Report for the Design of a VTOL Firefighter Aircraft

Group 14

by

Floris Benschop	F.B.	5562457
Xander Bonenkamp	X.B.	5491770
Jorrit Greep	J.G.	5284236
Sjoerd Heijnen	S.H.	5286565
Emma Janssen	E.J.	5090660
Marinka Jongeneel	M.J.	5544300
Ivo L'Ortije	I.L.	5482704
Merel Luijpen	M.L.	5328608
Ruben van der Plas	R.P.	5549922
Marco Smits	M.S.	5474558

Project duration:	April 22, 2024 – June 28, 2024
Tutor:	Dr. Calvin Rans
Coaches:	Dr. Vincent Meijer, Adhyanth Giri Ajay
Group TA:	Crina Mihalache
Institution:	Delft University of Technology
Course :	AE3200 Design Synthesis Exercise
Cover Image:	Adapted from Sandra J. Milburn, 2019

TU Delft

Executive Overview

Contributors: Jorrit
Authors: Jorrit

As wildfires are becoming more frequent and severe every year, posing significant threats to both natural environments and human societies and infrastructure, new and innovative ways of firefighting are needed. To tackle this problem, this project aims to design a Vertical Take-Off and Landing (VTOL) aircraft that combines the versatility of firefighting helicopters with the capacity and speed of conventional firefighting aircraft. For this reason, the Compound High-performance Emergency Extinguishing, Transport, and Aid Helicopter (CHEETAH) was created.

Firefighting Needs

The mission of our project is to develop an aircraft that can make the greatest possible impact on an aerial firefighting fleet. This means CHEETAH will need to bridge the gap between heavy tanker aircraft that can only refill at an airbase and low-capacity scooper aircraft that can refill anywhere. This leads to the project objective statement:

"To design a multirole VTOL aerial firefighter, that has a higher capacity, has more range and reaches a higher speed than a helicopter while being more versatile than a fixed-wing aircraft."

To achieve this goal, we have established a set of stakeholder requirements that guide our design process. These requirements ensure that the aircraft will effectively bridge the gap between the current capabilities of firefighting helicopters and fixed-wing aircraft. Below is a table summarising the key requirements:

Table 1: *Leading user requirements.*

Identifier	Requirement
FTF-UR-01	The aircraft shall suppress wildfires effectively using water and/or retardant.
FTF-UR-02	The aircraft shall have Vertical Take-off and Landing (VTOL) capability.
FTF-UR-03	The aircraft shall have the ability to refill water tanks in a hover.
FTF-UR-04	The aircraft shall have a water/retardant tank capacity of at least 10 000 L.
FTF-UR-05	The aircraft shall have a maximum cruise speed of at least 400 km/h.

A market analysis also supports CHEETAH's case. Current firefighting aircraft are either not purpose-built or are ageing designs. On top of this, due to the increasing frequency and severity of wildfires, the aerial firefighting market is projected to expand significantly, reaching between $7.3 billion and $16.2 billion in the next decade. CHEETAH can make up a significant portion of this as its VTOL capabilities ensure temporary airbases can be set up for remote wildfires and its high speed and capacity aligns with the frequency and severity of the wildfires.

In the current aerospace market, sustainable aircraft are highly sought after. However, emissions from the aircraft are negligible compared to those from wildfires, with the entire aviation industry emitting only half of what wildfires emit on a yearly basis, meaning CHEETAH's impact would not be significant on the environment. Therefore the decision was made to design for performance rather than sustainability. Naturally, where possible, sustainable choices are integrated throughout the design process to achieve the best possible balance between performance and environmental impact.

Final Design

The final design of CHEETAH can be seen in Figure 1 below.

Figure 1: *Final design of CHEETAH.*

CHEETAH will have a main rotor with eight blades, four forward-facing propellers and four engines powering them. A box wing will be fitted to the fuselage, with a fuel tank inside the wing box. An H-tail was chosen to ensure the stability and control of the aircraft. A rear ramp door is the primary access point to the cargo hold.

A removable water tank holding 10 000 L of water can be fitted inside the cargo hold. The tank can be put in and taken out of the hold using a winch fitted at the base of the tail. The cabin can also be fitted for a crew cabin and cargo missions. The modularity of the design adds to CHEETAH's already good versatility.

Propulsion System

The main rotor will have a radius of 11.5 m, provide a torque of 16.4 kNm and requires 16.4 MW to run. This was determined using momentum theory and blade element theory. The radius was set from a structural need, as the deflection of the rotor had to be minimised. A larger radius would have been beneficial for efficiency. The high power requirement follows from the effects of flapping on the main rotor. This is a phenomenon that occurs due to the variation in the amount of lift created on different sides of the rotor due to the forward velocity of the aircraft. If produced this rotor will be one of the biggest in the world, however, due to the large Maximum Take-off Weight (MTOW), this is justified.

The forward-facing propellers were sized with the constraint that the tip velocity of the blades should not exceed 95% of the speed of sound at sea level. With the initial sizing two Hartzell HC-B5M (A-2) props were selected. With more accurate drag estimations the number of propellers was doubled to four, as the speed requirement of 400 km/h would otherwise not be met. This required an extra 4.8 MW to run. The propellers will be driven by the main engines through a driveshaft running through the wings. Due to the high power requirements, CHEETAH will have 4 General Electric T408 engines generating a total of 22.4 MW.

Box wing Design

The aerodynamic design of CHEETAH is complicated by the interference of the rotor and propellers on the box wing design. The wing will need to generate 350 kN of lift and will do so with a wing area of 94 m^2 and an aspect ratio of 8. Airfoil analysis was performed using XFLR5 to select a low-drag airfoil for the wing. From the analysis in XFLR5, the LS(1)-0417 came out best. After preliminary sizings were established for the wing, the effects of these interferences and the effects of the box wing design were quantified.

After drag estimations with ANSYS Fluent proved inaccurate, a statistical analysis was performed. Using statistical equations from Roskam's Aircraft Design the drag of the aircraft was estimated at 32.2 kN in cruise conditions.

For more accurate analysis of the aerodynamics of the wing and aircraft, high-fidelity Computational Fluid Dynamics (CFD) and wind tunnel tests can be performed.

Stability and Control

A centre of gravity analysis was performed using mass estimations and locations for all subsystems. This gave a range of 4.65 m to 4.8 m as measured from the nose. This analysis formed the groundwork for further stability calculations. From the mass estimations, an MTOW of 35 500 kg was found.

To ensure static stability in hover, the rotor was placed close to the centre of gravity. For forward flight scissor plots were created that gave the stability margins of the aircraft. An analysis was also performed for yaw stability, as at low speeds the empennage would not be sufficient to control the aircraft. Therefore the forward-facing propellers will be used to generate a differential thrust until a forward velocity of 270 km/h is reached.

Dynamic stability was analysed for the eigenmotions of both planes and helicopters. From these calculations, it turned out that in forward flight all eigenmotions are stable. In hover two out of the four eigenmotions are unstable, both in the longitudinal direction. In further design phases, this will need to be taken into account and mitigated.

The landing gear was sized using historical data, giving a tyre diameter of 86 cm. The placement was done such that CHEETAH is stable while taxiing and landing.

Structural Characteristics

The structural analysis of the rotor was performed for the case that 10.000 L of water will be dropped at once. For the rotor deflection, a structural idealisation using boom areas was used. This gave a maximum deflection due to the dropping of the blades of 0.72 m and adding this to the flapping effect of the rotor the maximum deflection will be 2.2 m. The mass of the blades was estimated at 257 kg. It will likely decrease after a more detailed analysis as several effects that would counter this deflection like coning were not yet taken into account.

An analysis of the structure of the box wing proved the structural rigidity of the design. A comparison was made between a box wing and a straight wing to evaluate the design, the results of which are shown in the table below.

Table 2: *Structural and aerodynamic efficiency of both wings.*

	Box wing	**Straight wing**
L/D	21.9	41.8
Weight per side [kg]	235	3919

From this table follows that a conventional straight wing would be unfeasible due to the mass the wings would have. Though the straight wing is twice as efficient from an aerodynamic standpoint, the box wing is more than 10 times as light.

The material selection was based on both the structural characteristics and the operating environment of the aircraft. For the fuselage aluminium alloy 2024 (Al2024) is chosen for its corrosion resistance, low density, and high service temperature. For the water tank aluminium alloy 6061 (Al6061) is selected for its lightweight and corrosion-resistant properties, proven effective in previous aerospace applications. For the rotor and propeller Blades bi-axial composites are used for their strength and durability.

System Characteristics

The design of the water tank has to fit the modular design philosophy of CHEETAH. This means it needs to be removable and therefore fit through the rear cargo door. On top of this, the tank had to be shaped around the spars of the lower wing going through the fuselage. An important design consideration for the water tank was the effect of sloshing on the stability of the aircraft. To prevent sloshing when the aircraft is moving baffles will be placed in the water tank. The Helitank HP10000 firefighting hover pump was selected as a snorkel for CHEETAH, giving it the ability to fill the tanks in one minute completely on electric power. Additional tanks for retardant are placed on top of the water tank.

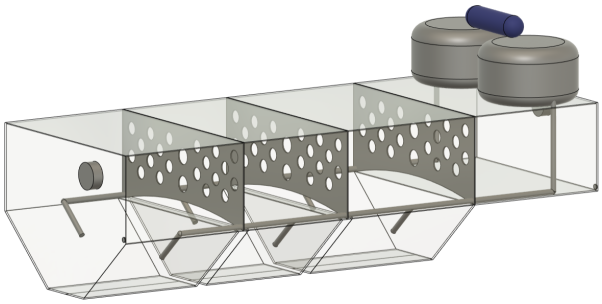

Figure 2: *Interior of the water tank, with retardant pipes and anti-sloshing baffles.*

The fuel tanks have a capacity of just under 10 000 L. They will be placed in the wings and under the floor in front of the water tank. The fuel tanks also contain baffles to reduce the effects of sloshing.

Performance

The range of CHEETAH is calculated with a payload-range diagram. From this a range at MTOW of 1390 km and a ferry range of 1840 km is calculated. The ferry range can be further increased to 3975 km by including an auxiliary fuel tank in the cargo bay.

The transition from hover flight at take-off to forward flight at cruise level is analysed using a simulation. The conclusion from this model is that most available power should be directed towards the aircraft's climb performance instead of forward velocity. This model is still very preliminary and there are a lot of aspects and phenomena that should be incorporated before the model's confidence level will be acceptable, but it gives a good indication of what the transition phase will look like.

A *V-n* diagram was set up to determine the operational limits of the aircraft. This diagram shows compliance with the CS-25 regulations, as the aircraft is able to sustain loads between -1 g and 3.25 g.

Further Design

To continue the design; a financial breakdown, risk analysis and verification and validation were performed. A cost breakdown is done for production and development, which combined with the market analysis will mean 392 units are sold at a $42.5 million.

Technical risks are identified and mitigated, which is shown in a risk map. Mitigations in case of system failures are also set up to improve the safety of the crew. These mitigations will need to be taken into account in further stages of development to ensure smooth continuation of the project.

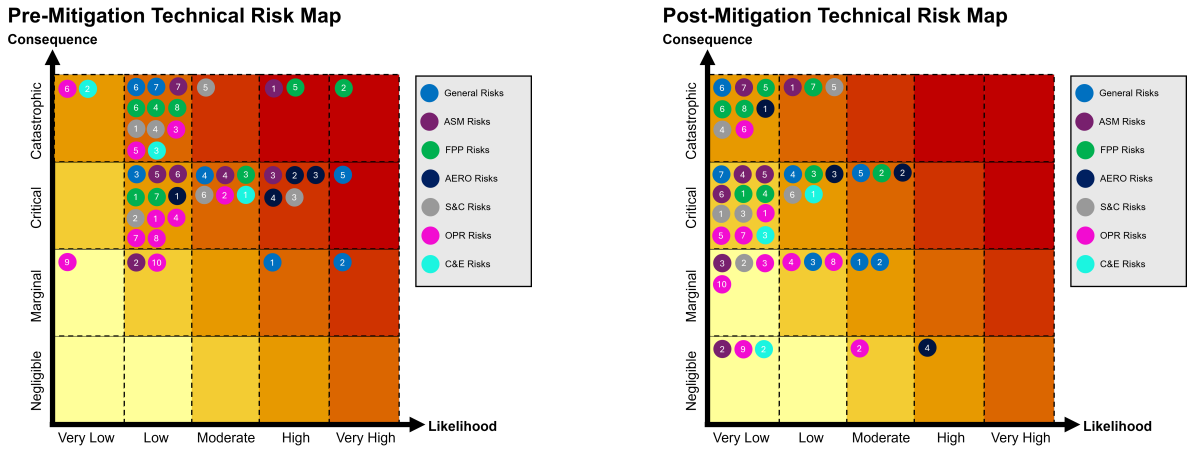

(a) *Technical risk map pre-mitigation.*

(b) *Technical risk map post-mitigation.*

Figure 3: *Technical Risk Maps*

The models created and used in the design process of CHEETAH are largely verified during the creation of the model and validated using sanity checks. More extensive verification and validation will not be possible due to the time constraints of the project, but will need to be performed if the project continues.

Using a compliance matrix the feasibility of the design is tested. Requirements that are not met are largely not met because little or no development has been done on that aspect. This shows the importance of a prolonged detailed design phase to continue the project. The viability of the design can also be tested further using simulations of firefighting missions and case studies. From analysing the feasibility of the design from a requirement and financial perspective, the conclusion was made that the project is viable in the current aerial firefighting environment. The only doubts stem from an ethical perspective, as a large number of CHEETAHs will likely be sold to military organisations in order to be financially stable. However, since the aircraft will not be used in direct combat situations, the positive impact CHEETAH could potentially have on firefighting operations was deemed more significant than the negative impact of selling CHEETAH to military organisations.

Since the project is deemed feasible to continue a manufacturing, assembly and integration plan is set up alongside other post-DSE activities. The project will first continue into a detailed design phase, after which another feasibility check will be performed. Should it pass, a prototype will be developed and tested, with which certifications can be obtained. Once certifications are obtained production of the aircraft will be started up and the first deliveries will start. To support parties that procure CHEETAH, pilot training and maintenance programmes will be set up.

Contents

Nomenclature

Abbr.	Description
AoA	Angle of Attack
AC	Alternating Current
ADF	Automatic Distance Finder
ADIRS	Air Data Inertial Reference System
APU	Auxiliary Power Unit
ASM	Aerospace Structures and Materials
ATC	Air Traffic Control
BSc	Bachelor of Science
BEM	Blade Element Method
C&O	Control & Operations
CAD	Computer Assisted Design
CFD	Computational Fluid Dynamics
CG	Centre of Gravity
CHEETAH	Compound High-performance Emergency Extinguishing, Transport, and Aid Helicopter
CSAR	Combat Search and Rescue
COD	Carrier Onboard Delivery
DC	Direct Current
DL	Disc Loading
DSE	Design Synthesis Excercise
FBD	Free Body Diagram
FBS	Functional Breakdown Structure
FFD	Functional Flow Diagram
FHA	Functional Hazard Analysis
FMEA	Failure Mode Effect Analysis
FPP	Flight Performance and Propulsion
GPU	Ground Power Unit
HLD	High Lift Device
HS	High Strength
HVAC	Heating, Ventilation, and Air Conditioning
ICAO	International Civil Aviation Organization
IFR	Instrument Flight Rules
LiDAR	Light Detection And Ranging
MAI	Manufacturing, Assembly, Integration
MLG	Main Landing Gear
MTOW	Maximum Take-Off Weight
NA	Not Adressed
NATO	North Atlantic Treaty Organization
NDT	Non Destructive Testing
NLG	Nose Landing Gear
OBIGGS	On-Board Inert Gas Generating System
OEW	Operational Empty Weight
RAMS	Reliability, Availability, Maintainability and Safety
RANS	Reynolds Averaged Navier Stokes
RDTE	Research, Development, Testing and Evaluation
ROI	Return on Investment
RPM	Rotations per minute
SC	Special Conditions
SE	System Engineering
SM	Stability Margin
SWOT	Strengths, Weaknesses, Opportunities and Threats
V&V	Verification & Validation
VFR	Visual Flight Rules
VTOL	Vertical Take-Off and Landing

Symbol	Description	Unit
α	Angle of attack	°
β	Flapping angle	°
γ	Lock number	-
δ	Rotor blade tip deflection	m
δ_α	Aileron deflection	°
δ_t	Transverse wing deflection	m
δ_a	Axial wing deflection	m
δ_i	Span efficiency factor	-
$\frac{d\epsilon}{d\alpha}$	Downwash gradient	-
η	Efficiency	-
η	Dynamic viscosity	Ns/m^2
θ	Pitch angle	°
θ	Blade twist	°
λ	Taper ratio	-
$\Lambda_{1/4}$	Quarter chord sweep	°
Λ	Wing dihedral angle	°
ν	Dynamic viscosity	m^2/s
ρ	Density	kg/m^3
σ	Solidity	-
ϕ	Induced angle	°
ψ	Azimuth angle	°
Ω	Rotor rotational speed	rad/s or RPM

Symbol	Description	Unit
AR	Aspect ratio	-
A	Disc area	m^2
a	Lift gradient	/rad
b	Span	m
b	Wing box width	m
b	Distance landing gear to CG	m
$BSFC$	Brake-specific fuel consumption	$lb/(h \cdot hp)$
c	Chord length	m
$\bar{c}$	Mean chord	m
c_p	Specific fuel consumption	g / (sW)
C_D	Drag coefficient	-
C_{D_0}	Zero-lift drag coefficient	-
C_{D_i}	Induced drag	-
C_m	moment coefficient	-
C_L	Lift coefficient	-
C_l	Lift coefficient (wing)	-

Symbol	Description	Unit
C_t	Thrust coefficient	-
D	Drag	N
DL	Disc loading	N/m^2
d	diameter	m
d	distance	m
e	Aerodynamic efficiency	-
E	Elastic modulus	GPa
F	Load per tire	Pa
F	Factor	-
g	Gravitational constant	m/s^2
h	Height	m
I	Area Moment of Inertia	m^4
L	Lift	N
L	Length	m
l	Length	m
M	Reaction moment	Nm
N	Number	-
n	Number of points of the airfoil	-
n	Number of rotor blades	-
P	Power available	W
P	Load on one rotor blade	N
P	Roll rate	° / s
q_∞	Dynamic Pressure	$kg/(m \cdot s^2)$
R	Radius	m
R	Range	km
R	Reaction force	N
RC	Rate of climb	m/s
r	Local radius	m
Re	Reynolds number	-
S	Surface area	m^2
T	Torque	Nm
T	Thrust	N
t	thickness	m
V	Velocity	m/s
v_i	Induced velocity	m/s
v	Wing deflection	m
W	Weight	N
w	Distributed load	N/m
x	X-location	m
y	Y-location/Spanwise location	m
z	Z-location	m

1 | Introduction

Contributors: Ruben
Authors: Ruben

Wildfires all over the globe become increasingly frequent and intense each year, resulting in short- and long-term consequences for both human well-being and planetary health. Wildfires emit carbon dioxide levels comparable to the annual emissions of the European Union, significantly contributing to the worldwide climate crisis. This accentuates the need for the global community to address the rise in wildfires as a major threat. Each year, wildfire smoke is estimated to cause 340,000 early deaths due to breathing and heart problems. Additionally, the 2019-2020 Australian wildfires killed or displaced an estimated three billion animals.[2] At this critical stage, aerial firefighting is crucial for preventing the spread of wildfires and saving lives. Aerial firefighting acts as a last resort when fires become uncontrollable, and the decisions made by pilots are vital. [3]

Figure 1.1: *Koala wildfire survivor.* [1]

Aerial firefighting against forest fires is performed by helicopters and airplanes, occasionally purpose-built for firefighting tasks but often adapted for other uses. The benefits of helicopters are that they offer high refuelling and operational flexibility. On the other side, airplanes are attractive for their greater range and payload capacity. In short, there is a gap between the performance characteristics of firefighting helicopters and firefighting airplanes. To fill this gap, a Vertical Take-Off and Landing (VTOL) aircraft is designed, named CHEETAH (Compound High-performance Emergency Extinguishing, Transport, and Aid Helicopter), which combines the versatility of firefighting helicopters with the capacity, range, and speed of conventional firefighting aircraft. Due to its modular water tank, CHEETAH is a versatile compound helicopter that can also be used for missions as a medivac. Its capability to fly at 400 km/h and carry approximately 10,000 litres of water makes CHEETAH uniquely suited for combating forest fires.

Before the final design of the CHEETAH can be described, the reader needs to have an understanding of the firefighting missions and the requirements for the overall design. This fundamental mission analysis is given in Chapter 2 whereafter the mission is analysed from a market analysis perspective in Chapter 3. In this market analysis, the stakeholders involved in the design are analysed and market risks are outlined. Because the final design needs to fulfil certain sustainability goals, Chapter 4 describes an extensive sustainability strategy including all its contributors when it comes to sustainability and the environment.

After establishing the mission, market, and sustainability contexts, the pre-design analysis is done and the internal and external layout of the final design of the CHEETAH is outlined in Chapter 5. Next to a detailed layout description, the modularity and multirole functionality of CHEETAH are described. Once the final design is set, the main rotor and forward propulsion system are described in Chapter 6. This propulsive analysis is followed by an analysis of the aerodynamics of the aircraft. In this chapter, Chapter 7, the overall aerodynamics is covered and a detailed analysis of the box wing is done.

[1] Striking Photograph of Koala Wildfire Survivor Helps Raise Funds for Australia Emergency Efforts, https://www.rewild.org/press/striking-photograph-of-koala-wildfire-survivor-helps-raise-funds-for-australia-emergency-efforts [retrieved 19th June 2024]

[2] Wildfires: A Crisis Raging out of Control, https://wwf.panda.org/discover/our_focus/forests_practice/forest_publications_news_and_reports/fires_forests/ [retrieved 19th June 2024]

[3] The Crucial Role Of Aerial Firefighting, https://firebuyer.com/the-crucial-role-of-aerial-firefighting/ [retrieved 19th June 2024]

Figure 1.2: *Final design of CHEETAH.*

Vertical takeoff and landing capabilities offer significant advantages but also pose stability challenges. These are addressed in Chapter 8, which outlines the overall controllability and stability of CHEETAH. This chapter is followed by a comprehensive analysis of the structural and material characteristics, which is described in Chapter 9. In addition to conducting a structural analysis, a material trade-off is performed, and a manufacturing plan is developed. Following the analysis of the aircraft in terms of propulsion, controllability, stability, and structures, Chapter 10 details the system characteristics of the aircraft. Thereafter, the aircraft performance and emissions are described in Chapter 11.

As a continuation of the market analysis, the return on investments is defined in Chapter 12. The technical risks and the Reliability, Availability, Maintainability and Safety (RAMS) characteristics are outlined in Chapter 13. Finally, the verification and validation procedures are described in Chapter 14 and the further development of the CHEETAH is outlined in Chapter 15.

2 | The Firefighting Mission

This chapter describes the design mission and how this mission is achieved. A need, mission and project objective statement are established that will drive the design. The requirements that came from these statements are given, as well as the mission profile. Furthermore, the logistic diagram, the Functional Flow Diagram (FFD) and the Functional Breakdown Structure (FBS) are iterated after the baseline report [1].

2.1. Project Description

Contributors: Emma
Authors: Emma

In the past decades, wildfires have become a more and more escalating threat, as their intensity and frequency is growing dramatically. These wildfires endanger both nature and human society. The increasing severity of these fires asks for new advanced solutions and innovative technologies in firefighting. Therefore, the following need statement is formulated:

"New firefighting aircraft are needed to effectively neutralise the threat wildfires pose to nature and society as they become increasingly intense and widespread."

From this, the team's mission statement is established:

"To aid in controlling wildfires, an aircraft will be designed to make the biggest possible impact on any firefighting fleet."

This then leads to the project objective statement, which describes the goal of the project:

"To design a multirole VTOL aerial firefighter, that has a higher capacity, has more range and reaches a higher speed than a helicopter while being more versatile than a fixed-wing aircraft."

2.2. Requirements

Contributors: Emma
Authors: Emma

In order to achieve the project objective and the mission statement, requirements that support this goal were set up. First, the user requirements were specified. These are requirements directly given by the client or will be relevant for possible future users. Based on these user requirements, the system requirements will be established. The user requirements are given in Table 2.1.

Table 2.1: *List of user requirements.*

Identifier	Requirement
FTF-UR-01	The aircraft shall suppress wildfires effectively using water and/or retardant.
FTF-UR-02	The aircraft shall have Vertical Take-off and Landing (VTOL) capability.
FTF-UR-03	The aircraft shall have the ability to refill water tanks in a hover.
FTF-UR-04	The aircraft shall have a water/retardant tank capacity of at least 10,000 L.
FTF-UR-05	The aircraft shall have a maximum cruise speed of at least 400 km/h.
FTF-UR-06	Make the aircraft reliability and operational availability equal to or better than that of comparable aircraft.
FTF-UR-07	The aircraft shall provide a systems and avionics architecture that will enable autonomous operations in cruise.
FTF-UR-08	The aircraft shall be capable of Visual Flight Rules (VFR) flight with an autopilot.
FTF-UR-09	The aircraft shall be capable of Instrument Flight Rules (IFR) flight with an autopilot.
FTF-UR-10	The aircraft shall be capable of flight in known icing conditions.
FTF-UR-11	The aircraft shall meet applicable certification rules in CS Part 25/29 depending on applicability.

The user requirements are then translated into stakeholder requirements, which are broken down into technical system requirements, linked to different stakeholders, and identified by the third group of three letters in the requirement identifier. These requirements are shown in Table 2.3. Table 2.2 lists to what stakeholders the identifiers in Table 2.1 and Table 2.3 are referring.

Table 2.2: *Requirement identifier explanation*

Identifier	Meaning	Identifier	Meaning
FTF	Fight the Fire	**INV**	Investors
SYS	System	**LOC**	Locals
UR	User	**OWN**	Aircraft owner
AIR	Airbases	**PIL**	Pilot
ATC	Air traffic control	**REG**	Regulatory agencies
FDS	Fire departments	**GFC**	Ground firefighter crew
SUP	Fuel/retardant suppliers		

Table 2.3: *List of system requirements.*

Identifier	Requirement
FTF-SYS-FDS-01.1	The aircraft shall be able to drop retardant at least twice per refill.
FTF-SYS-FDS-01.2	The aircraft shall withstand the effects of sloshing liquids in the tank.
FTF-SYS-FDS-01.3	The aircraft shall remain longitudinally statically stable during the release phase of the water and retardant.
FTF-SYS-FDS-02.1	The aircraft shall have a water/retardant tank capacity of at least 10 000 L.
FTF-SYS-FDS-03.1	The aircraft shall have a ferry range of at least 3000 km.
FTF-SYS-FDS-03.2	The aircraft shall have a minimum endurance of 3 hours.
FTF-SYS-FDS-03.3	The aircraft shall have a full retardant tank range of at least 500 km in cruise.
FTF-SYS-FDS-04.1	The aircraft shall have a cruise speed of at least 400 km/h.
FTF-SYS-FDS-05.1	The aircraft shall have VTOL capability.
FTF-SYS-FDS-05.2	The aircraft shall be able to refill the water tanks while hovering.
FTF-SYS-FDS-05.3	The aircraft shall be able to drop all its water/retardant load at once (spot-dropping).
FTF-SYS-FDS-05.4	The aircraft shall be able to drop its water/retardant load over a longer distance (line-dropping).
FTF-SYS-FDS-05.5	The aircraft shall be able to be (re)filled with water and retardant by ground tanking equipment.
FTF-SYS-FDS-05.6	The aircraft shall be equipped with a system to monitor the fire visually.
FTF-SYS-FDS-05.7	The aircraft shall be equipped with a system to monitor the infrared radiation emitted by the fire.
FTF-SYS-FDS-05.8	The aircraft shall be able to evacuate people.
FTF-SYS-FDS-05.9	The aircraft shall be able to drop objects in forward flight.
FTF-SYS-FDS-05.10	The aircraft shall be able to drop objects in hover.
FTF-SYS-FDS-05.11	The aircraft shall be able to drop personnel in forward flight.
FTF-SYS-FDS-05.12	The aircraft shall be able to drop personnel in hover.
FTF-SYS-FDS-05.13	The aircraft shall be able to adjust the water/retardant dispersion settings.
FTF-SYS-FDS-05.14	The aircraft shall be capable of stable hovering at different altitudes.
FTF-SYS-FDS-05.15	The aircraft shall sustain no structural damage when accelerating between -1 and +3.25 g at MTOW.
FTF-SYS-FDS-05.16	The aircraft shall have a service ceiling of 5000 m above sea level.

Continued on next page

Table 2.3 – continued from previous page

Identifier	Requirement
FTF-SYS-FDS-05.17	The aircraft shall be capable of a minimum rate of climb (ROC) of 5.5 m/s at MTOW in hover mode at sea level.
FTF-SYS-FDS-06.1	The aircraft shall have a maintenance downtime of less than 10 hours per operational hour.
FTF-SYS-FDS-06.2	The aircraft shall be able to take off within 30 minutes from an emergency call.
FTF-SYS-FDS-06.3	The aircraft shall make use of proven technology.
FTF-SYS-FDS-06.4	The aircraft shall be able to be serviced by an Approved Maintenance Organisation (AMO).
FTF-SYS-FDS-06.5	The aircraft shall be compatible with a widely used refuelling system.
FTF-SYS-FDS-06.6	The aircraft shall have a turnaround time of 20 minutes.
FTF-SYS-FDS-07.1	The aircraft shall be able to operate in known icing conditions.
FTF-SYS-FDS-07.2	The aircraft shall be resistant to corrosion caused by (salty) water.
FTF-SYS-FDS-07.3	The aircraft shall be able to operate as required, despite heat generated by the fire whilst flying in the air above the fire.
FTF-SYS-FDS-08.1	The aircraft shall contain a night vision system for the pilots.
FTF-SYS-FDS-09.1	The aircraft shall contain a system that enhances the pilot's perception in smoke.
FTF-SYS-PIL-01.1	The aircraft shall be capable of autopiloted flight in compliance with VFR.
FTF-SYS-PIL-01.2	The aircraft shall be capable of autopiloted flight in compliance with IFR.
FTF-SYS-PIL-01.3	The aircraft shall be equipped with an auto-land feature.
FTF-SYS-PIL-02.1	The aircraft shall not require higher physical control effort from the pilot compared to the Sikorsky S-70 Firehawk.
FTF-SYS-PIL-03.1	The aircraft shall be statically longitudinally stable.
FTF-SYS-PIL-03.2	The avionics software used shall be user-friendly and similar to use as existing aircraft.
FTF-SYS-PIL-04.1	The aircraft shall be equipped with safety features to ensure the safety of the crew when flying over a fire.
FTF-SYS-PIL-04.2	The aircraft shall be equipped with safety features to ensure the safety of the crew in case of an aircraft malfunction (e.g. crash or emergency landing).
FTF-SYS-PIL-04.3	The aircraft shall be able to sustain one-engine-inoperative flight.
FTF-SYS-PIL-04.4	The aircraft shall have crash-resistant fuel systems.
FTF-SYS-PIL-05.1	The aircraft shall be ergonomic such that a 95th% percentile male can fly missions of endurance specified in FTF-SYS-FDS-03.2 without inducing physical discomfort.
FTF-SYS-INV-01.1	The preliminary design of the aircraft shall be performed by a team of 10 students working full-time.
FTF-SYS-INV-02.1	The aircraft design shall be modular.
FTF-SYS-INV-02.2	The aircraft shall be capable of search and rescue missions.
FTF-SYS-INV-02.3	The aircraft shall be capable of cargo missions.
FTF-SYS-INV-02.4	The aircraft shall be capable of landing on a surface as soft and as wet and boggy grass.
FTF-SYS-OWN-01.1	The aircraft shall comply with environmental regulations for the coming 20 years, from 2024 onwards.
FTF-SYS-OWN-02.1	The aircraft shall have a unit cost of less than 63 million euros.
FTF-SYS-GFC-01.1	The aircraft shall be equipped with radio communication equipment capable of reaching ground crews.
FTF-SYS-ATC-01.1	The aircraft shall be equipped with radio communication equipment capable of reaching air traffic control.
FTF-SYS-ATC-01.2	The aircraft shall be equipped with satellite communication equipment.

Continued on next page

Table 2.3 – continued from previous page

Identifier	Requirement
FTF-SYS-ATC-02.1	The aircraft shall not make use of low observable (LO) Technology materials.
FTF-SYS-ATC-02.2	The aircraft shall be equipped with a transponder.
FTF-SYS-LOC-01.1	The aircraft shall be able to create fire lines.
FTF-SYS-REG-01.1	The aircraft shall be compliant with icing conditions requirements as stated in CS25.1419.
FTF-SYS-REG-01.2	The aircraft shall be compliant with one engine inoperative climb rate requirements as stated in CS29.67.
FTF-SYS-REG-01.3	The aircraft shall be compliant with engine power ratings as stated in CS-E 40.
FTF-SYS-REG-01.4	The aircraft shall be compliant with engine fire requirements as stated in CS-E 130.
FTF-SYS-REG-01.5	The aircraft shall be compliant with critical engine part integrity requirements as stated in CS-E 515.
FTF-SYS-REG-01.6	The aircraft shall be compliant with ingestion of foreign matter requirements as stated in CS-E 540.
FTF-SYS-REG-01.7	The aircraft shall be compliant with cockpit visibility requirements as stated in CS29.773.
FTF-SYS-REG-01.8	The aircraft shall be compliant with fire protection requirements of critical parts as stated in CS29.855.
FTF-SYS-REG-01.9	The aircraft shall be compliant with emergency evacuation requirements as stated in CS25.803.
FTF-SYS-REG-01.10	The aircraft shall be compliant with the installation of systems requirements as stated in CS25.901.
FTF-SYS-REG-01.11	The aircraft shall be compliant with engine placement requirements as stated in CS29.903.
FTF-SYS-REG-01.12	The aircraft shall be compliant with gust and turbulence requirements as stated in CS25.341.
FTF-SYS-REG-01.13	The aircraft shall be compliant with deformation characteristics as stated in CS25.305.
FTF-SYS-REG-01.14	The aircraft shall be compliant with landing gear requirements as stated in CS29.731.
~~**FTF-SYS-REG-02.1**~~	~~The aircraft shall have SC certification for water deflectors during water collecting operations.~~ → Discarded, only applies to scoopers, which the design is not.
FTF-SYS-REG-02.2	The aircraft shall have SC certification for fireproof systems.
~~**FTF-SYS-REG-02.3**~~	~~The aircraft shall have SC certification to utilise a water scooping device.~~ → Discarded, only applies to scoopers, which the design is not.
FTF-SYS-REG-02.4	The aircraft shall have SC certification to utilise a refilling device while hovering.
FTF-SYS-REG-02.5	The aircraft shall have SC certification to carry a drop tank.
FTF-SYS-REG-02.6	The aircraft shall have SC certification to withstand water-load conditions.
~~**FTF-SYS-REG-02.7**~~	~~The aircraft shall have SC certification to land on water.~~ → Discarded, only applies to scoopers, which the design is not.
FTF-SYS-REG-02.8	The aircraft shall have SC certification according to VTOL.2235 regarding the proof of structure.
FTF-SYS-REG-02.9	The aircraft shall have SC certification in accordance with VTOL.2230, VTOL.2235 and VTOL.2240 for each critical loading condition.
FTF-SYS-REG-02.10	The aircraft shall have SC certification in accordance with VTOL.2500 b) and VTOL.2510 for the development of the Flight Guidance Systems (FGS).
FTF-SYS-AIR-02.1	The aircraft shall be compliant with engine power ratings as stated in CS-E 40.

Continued on next page

Table 2.3 – continued from previous page

Identifier	Requirement
FTF-SYS-SUP-01.1	The aircraft shall operate within a temperature range specified by the construction materials supplier.
FTF-SYS-SUP-01.2	The aircraft shall be able to operate with a widely available type of fuel for the chosen engine configuration.
FTF-SYS-SUP-01.3	The aircraft shall be able to host off-the-shelf avionic systems.

2.3. Mission profile

Contributors: Emma
Authors: Emma

A flight profile diagram that relates to the main firefighting mission was constructed for the midterm report [2]. A low-level and high-level profile diagram were made. They are given in Figure 2.1 and Figure 2.2. The low-level diagram is an example of what the mission could look like.

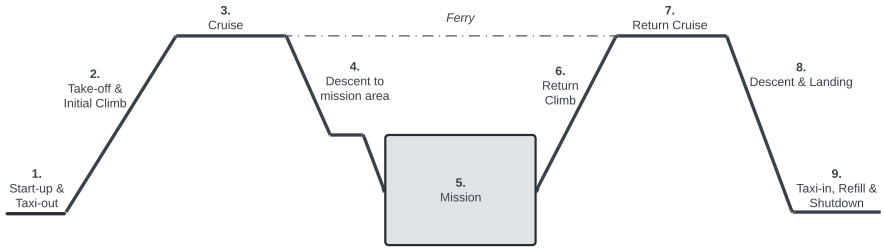

Figure 2.1: *High-level flight profile diagram.*

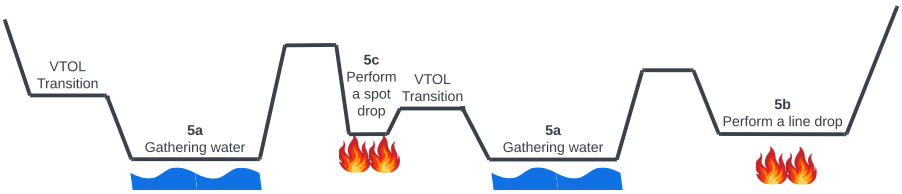

Figure 2.2: *Example low-level flight profile diagram for the mission phase.*

2.4. Logistics Concept Description Iteration

Contributors: Floris
Authors: Floris

In the logistics section of the midterm report [2], the potential modularity was not addressed. As CHEETAH has a modular retardant tank, this modularity now has to be addressed.

The tank can be moved within the fuselage by CHEETAH itself. However CHEETAH can not lift the tank up and down outside the fuselage, so to safely load and unload the water tank, and other modules, one should only (un)load the water tank on the main base, where a cargo loader is available to put the tank on the ground, or in storage. This will then be a part of ground handling, as can be seen on Figure 2.3, which is an updated version of Figure 7.9 (a) from the midterm report [2].

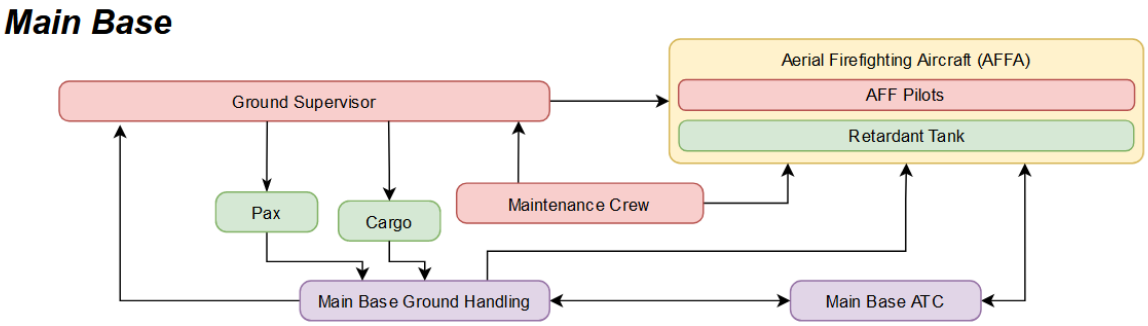

Figure 2.3: *Interactions for the main base phase.*

2.5. Functional Flow Diagram Iteration

Contributors: Ruben, Xander
Authors: Ruben, Xander

To reach the project objective as stated in Section 2.1, a Functional Flow Diagram (FFD) is constructed (see Appendix A). In the baseline report [1], the FFD showed how and when the different phases from the design to the decommissioning of the aircraft occur throughout its entire lifespan. First of all, the Lifecycle FFD was given in which the lifecycle is outlined in a structured overview. Secondly, the Operational FFD outlines the operation segment. While the overall structure of these diagrams remains consistent with the current design stage, there have been some minor iterations and changes following further project development. These iterations are described in this section.

First of all, in the Operational FFD, the function *F-5.2* has been removed. After a coordinated subsystem trade-off, described in the midterm report [2], the team decided to reload the water tanks exclusively by hovering. Consequently, the scooping water reloading option was eliminated from the diagram. This results in a single-option water reloading process, where the first function is the transition to a vertical flight configuration, followed by the function of refilling the tank by hovering using a snorkel and concluding with the transition back to a horizontal flight configuration.

Secondly, the options for take-off and landing were re-evaluated. In the conceptual design phase, both conventional and vertical take-off and landing were considered and included in the Operational FFD. For this design phase, the team decided to retain both options, recognising the benefits of having the flexibility to land conventionally and vertically. This decision was made because the team believes that maintaining both options will enhance take-off and landing efficiency, ultimately leading to improved overall performance of the aircraft.

Another change made to the Operational FFD concerns the payload function. In the baseline report, a distinction was made between dropping and picking up payloads. However, since these functions are nearly identical, the team decided to replace this OR statement with the options of aerial payload dropping or ground payload handling. Aerial payload dropping involves the function of dropping the payload in flight and picking it up while hovering. Ground payload handling starts with a transition from horizontal to vertical flight configuration, followed by a vertical landing. The aircraft will then pick up or deliver the payload, take off vertically, and transition back to horizontal flight configuration. Furthermore, to define the dropping of payload in a better way, the types of payload were determined, ranging from pesticides or seeds being dropped from the air to personnel or evacuees being picked up or dropped off on the ground.

Finally, some small changes were made to the Lifecycle FFD. First of all, the function *L-2* is renamed to Production Preparation and function *L-3* to Production Execution. After a revision of the whole diagram, the team thought to make a clearer distinction between these functions by renaming them in this way. Furthermore, these functions are worked out with the knowledge of the production plan from the midterm report [2].

2.6. Functional Breakdown Structure Iteration

Contributors: Ruben, Xander
Authors: Ruben, Xander

The main functions identified in the FFD are now broken down into smaller functions but are still aggregates of a large amount of even smaller functions. The chosen 'size' is the desired level of detail to easily identify what the system needs to be able to perform, while not going too far into detail. The Functional Breakdown Structure (FBS) can be found in Appendix A.

The changes made are as follows:

- With the removal of scooping as a to-be-performed function, all sub-functions of this function disappear as well.
- With the concept defined, the transition between hover and conventional flight is now shaped. Though originally the tilting of a system was assumed to be used, this is not the case for this specific concept and as a result, the performed actions are the slowing/speeding up of the main rotor and switching between providing counteracting torque and forward thrust by the forward pointed propellers.
- With the payload defined, the need for landing before dropping off/picking up the payload was identified. This changed the FBS slightly. Manoeuvring for example is now part of the landing, taking out some functions for the payload system. The payload pickup/dropping system has been chosen as a simple ramp door at the back of the fuselage, and this has been changed in the FBS as well.

3 | Market Analysis

Performing a market analysis for CHEETAH is of importance in the aircraft design process. This helps to inform the design team and guides decisions by providing a comprehensive overview of the current and future market. By identifying key stakeholders, performing a current and future market analysis, exploring alternative uses and assessing the market gaps, the design team can ensure that CHEETAH meets the needs of the aerial firefighting market. Market risks will also be identified, this allows for mitigation to be performed.

3.1. Stakeholders

Contributors: Emma, Floris, Merel
Authors: Merel

In a design process, stakeholders are the individuals and organisations involved in the development of the product, making them important to the design team. For the design of the multirole VTOL aerial firefighting aircraft, a list of stakeholders has been established. An overview of all stakeholders and their identifiers is listed in Table 3.1. In the baseline report [1], all the stakeholders are elaborated on. One additional stakeholder was identified; alternative users. This stakeholder was identified after the concept selection, as the modular nature of CHEETAH enables use outside of aerial firefighting situations.

Alternative users **[ALT]**

- Alternative users are those who can buy and use the aircraft for non-firefighting operations. These can include, but are not limited to, search and rescue missions, seed bombing, offshore operations and possibly even military purposes.

Table 3.1: *List of stakeholders and stakeholder identifiers.*

Identifier	Stakeholder	Identifier	Stakeholder
AIR	Airbases	**LOC**	Locals
ALT	Alternative users	**MAI**	Maintenance instance
ATC	Air traffic control	**MAN**	Manufacturer
CRW	Air crew	**OWN**	Aircraft owner
FDS	Fire departments	**PIL**	Pilot
GFC	Ground firefighter crew	**REG**	Regulatory agencies
GOV	Government	**SUP**	Fuel/retardant suppliers
INV	Investors		

In Figure 3.1, the role of each stakeholder is displayed. The alternative users fall in the "keep informed" category. This entails that they would have to be thoroughly informed; however, their influence on the actual design is minimal. This is due to the large amount of potential alternative uses of the aircraft, which makes it impractical to account for all possible alternative users during the design process. CHEETAH is designed primarily as an aerial firefighting aircraft with modular traits. Therefore the firefighting functionality will be more important than the modular aspect during the design phase.

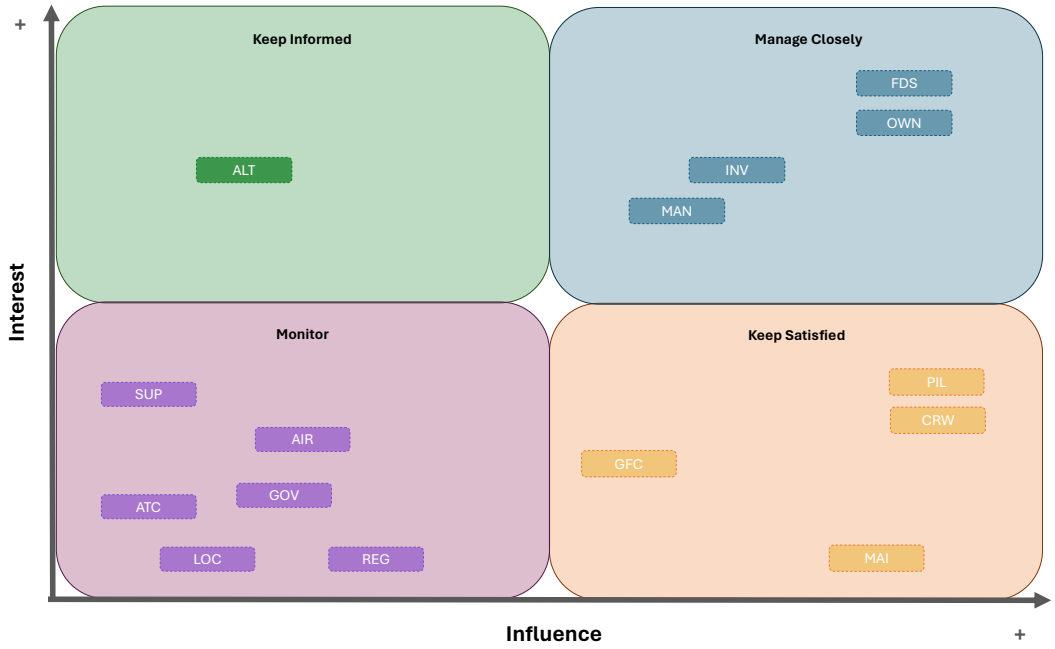

Figure 3.1: *Stakeholder map, showing the group into which each stakeholder is categorised.*

Displaying all the stakeholders in a stakeholder map and dividing them into four groups, each with different needs, ensures that the design team knows which stakeholders require more attention and therefore need to be managed closely and which ones just need to be informed, satisfied, or monitored. Even within the four groups, there are differences between stakeholders. If they are placed more to the right in Figure 3.1, they exert more influence on the design. This map enables the team to keep all stakeholders invested in the project while avoiding mismanagement of time on less important parties or missing out on possible opportunities.

3.2. Current and Future Market

Contributors: Merel
Authors: Merel

A thorough market analysis is important as it can influence design decisions. For this reason, understanding the market that the Aerial firefighting CHEETAH will be released into and operate in during its lifetime as well as the current market state, is crucial. This knowledge enables the team to identify current and future competitors, as well as opportunities. Additionally, it helps the team identify the market gap that the design of CHEETAH will fill.

3.2.1. Current Market Analysis

The aerial firefighting market is ever-changing, heavily influenced by climate change, which is causing an increased wildfire risk. Forest fires now burn nearly twice as much tree coverage compared to 20 years ago [3], consequently driving up demand for aerial firefighting vehicles. Certain regions have always been more prone to the occurrence of wildfires due to climate conditions and the available amount of flammable materials. However, forest fires also occur outside of these locations. As can be seen in Figure 3.2, wildfires are a global phenomenon, not limited to a specific continent. This causes aerial firefighting vehicles to deal with a wide range of challenging scenarios, including changing terrain, scarce water resources, remote wildfire locations and corrosion risks by salty water, among others.

This causes aerial firefighting vehicles to deal with a wide range of challenging scenarios, including changing terrain, scarce water resources, remote wildfire locations, and corrosion risks due to salty water, among others.

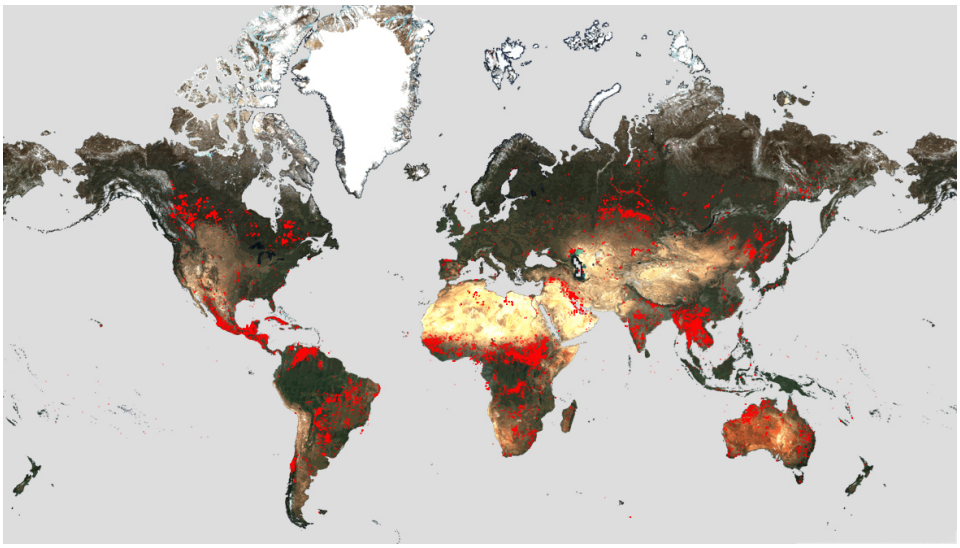

Figure 3.2: *Global wildfire map: May 2016 to June 2023, using data from the World Fire Atlas [4]. Each dot represents a wildfire occurrence, note that the dots do not indicate the intensity of the wildfire.*

The wildfire season varies by region, allowing aerial firefighting vehicles to be leased for the duration of a region's wildfire season. Once this season ends, they are transported to another location. These seasons can even vary within a country. For instance, North and South Australia have opposite fire seasons.

Aerial Firefighters

The current aerial firefighting market is mainly dominated by retrofitted aircraft. These aircraft are not specifically designed for use in firefighting situations. Most of them originate from the military sector, as they are designed for higher g-loads than commercial airliners. This is useful during firefighting situations as they require high manoeuvrability. The exception to this is the Canadair CL-415, which is the only purpose-built firefighting aircraft of the last 40 years.

Aerial firefighters can be divided into two categories; fixed-wing and rotorcraft aircraft. In fixed-wing aircraft, a distinction can be made between 'scooper' and 'tanker' aircraft. Scoopers can scoop up water during the mission whereas tankers have to return to base to be filled with retardant. Rotorcraft are usually able to collect water during their mission by using a bucket or a snorkel device.

Compound Helicopters

Currently, no compound helicopters are being used in the aerial firefighting sector. They are in service in other sectors, primarily military, due to their high performance in both manoeuvrability and speed.

3.2.2. Future Market Predictions

Because of the influence of climate change on wildfires, researching future as well as current wildfire risks is important when designing an aircraft that should not only be an excellent aerial firefighter in the current climate but also in the future. As highlighted in the baseline report [1], wildfires are predicted to increase in both frequency and intensity. However, that is not the only future challenge; the area prone to wildfires will also grow. This means that there will be a future need for aerial firefighting in many different environments. These new environments all come with their own challenges that should be kept in mind during the design phase, such as the availability of water, airbase locations, and terrain. The length of the wildfire season is already increasing in some areas. An example of this is Canada, where the increased length of the Quebec wildfire season prevents the Quebec Fire Department from leasing their CL-415 to the Los Angeles County Fire Department for the duration of the California fire season [5]. This demonstrates that there will be an increased need for aerial firefighting aircraft in the future.

Aerial Firefighters

There are two main types of potential competitors in the future market. The first type is retrofitted military aircraft. As older military aircraft retire, it is a possibility that VTOL aircraft such as the V-22 Osprey will be

retrofitted for aerial firefighting use. However, no such plans have been announced at the moment. The second type of competitor is new purpose-built firefighting aircraft. In the near future, only two of these aircraft designs have been announced; the DHC-515, of which 22 have already been pre-ordered by European customers [1] and the Hynaero Fregate F-100 [6]. Both of these aircraft are purpose-built firefighting fixed-wing aircraft with scooping capabilities, this can be seen in Figure 3.3. They have similar capacities to CHEETAH, with the DHC-515 being able to scoop up 7000 L and the F-100 able to scoop up to 10 000 L. However, their lack of VTOL and hovering capabilities makes them very different from CHEETAH. As explained in the baseline report, the production of other new aerial firefighting aircraft within the coming few years is highly unlikely due to regulations [1].

(a) *The DHC-515.*[1] **(b)** *The Hynaero Fregate F-100.*[2]

Figure 3.3: *The two purpose-built firefighting scoopers that have been announced to enter the market in the near future.*

3.2.3. Alternative Uses

The modular nature of CHEETAH allows for the aircraft to be useful outside of firefighting situations. The modular tank can be easily removed, providing space for cargo or passengers in the back of the aircraft. With its VTOL capabilities, high speed from the forward propellers and excellent manoeuvrability, the aircraft can be used for various missions. For example, it can be used for search and rescue, medical emergencies, transport of people or cargo to remote areas and seed bombing. Additionally, it could be of great use for transporting personnel to windmill construction sites or oil rigs due to its VTOL capabilities and excellent resistance to salty water.

3.2.4. Market Gaps

Research of both the current market and future market expectations for the identification of market gaps. The aerial firefighting market is dynamic and growing. It is expected that the firefighting market will grow from $4.95 billion in 2022 [7] to between $7.3 [7] and $16.2 [8] billion in the next decade. The market gap identified in the baseline report, which is to bridge the gap between the capacity of the bigger tankers and the VTOL and scooping capabilities of a rotorcraft, remains relevant [1]. Additionally, the purpose-built design enables the team to prioritise pilot safety and implement specific firefighting features to help navigate the turbulence, heavy smoke and heat of wildfires at speeds uncommon for rotorcraft. The aircraft is also unique in its VTOL hovering capabilities, allowing it to take off and land in remote areas and draw water from smaller sources using its snorkel device. These hovering capabilities also enable CHEETAH to perform accurate drop loads on fires while its high speed allows it to lay lines of retardant to prevent the fires from spreading. The aircraft can be filled with water both on base and in-flight and mix it with its own foam concentrate to create up to 100 000 L of retardant foam. These features ensure that CHEETAH is the aerial firefighting VTOL that can fulfil the roles of both a rotorcraft and a fixed-wing aircraft, providing the greatest possible impact to any firefighting organisation at any location worldwide. The modular nature of the water tank enables CHEETAH to also be used in search and rescue situations, medical evacuations and other types of transport in the toughest of terrains. This broadens the market opportunities even more, as alternative users also become possible investors and buyers of CHEETAH.

[1] De Havilland, https://dehavilland.com/en/news/posts/de-havilland-aircraft-of-canada-limited-launches-dhc-515-firefighter
[2] Skies magazine, https://skiesmag.com/press-releases/altitude-aerospace-and-hynaero-sign-cooperation-agreement/

3.3. Market Risks

Contributors: Merel
Authors: Merel

After having observed the market behaviour and the market gap that the team aims to fill with the CHEETAH, several market risks can be identified. These risks represent possible occurrences that can negatively influence the success of CHEETAH on the market. Being aware of and informed about these risks allows for mitigation or monitoring, thereby limiting the chances of the design failing market-wise. The first step in such a risk analysis is a Strengths, Weaknesses, Opportunities and Threats (SWOT) analysis. This analysis shows the strengths and weaknesses within the team, as well as the opportunities and threats posed by external factors. The SWOT analysis can be found in the baseline report [1]. Based on this SWOT analysis a list of risks was composed. An iterated, more extensive overview of these market risks can be found in Table 3.2.

Table 3.2: *Iterated market risks overview.*

ID	Description	Drivers
MAR1	Unreliable market analysis	No reliable information available about similar aircraft, time constraint
MAR2	Sub-optimal design choices	Limited resources available during the design process
MAR3	Lack of funding from governmental organisations	Geopolitical events requiring more funds
MAR4	Lack of funding from private investors	Lack of trust in a small startup
MAR5	Disappointing sales	Competition, flawed market analysis
MAR6	Regulatory challenges	No regulations yet for the new design
MAR7	Safety concerns	Concerns arising because of new design
MAR8	Bad publicity	Internal issues being made public, outside opinions
MAR9	No investments in new technology	Global economy crash causing a recession
MAR10	Competitors filling the market gap	Other companies fill in the existing market gap first
MAR11	Use of outdated technologies	Advancements in aviation technology used in the design render the product obsolete
MAR12	Supply chain disruption	Dependence of the design on specific components or materials
MAR13	Strict environmental regulations	Stricter environmental laws at certain locations affecting operations and design of the CH
MAR14	Inflation on operational costs	Higher maintenance and operational costs than expected leading to financial strain and a decrease in sales
MAR15	Shortage of certified personnel	Difficulties with finding qualified people to work on maintenance, design and operations
MAR16	Changing needs in the firefighting sector by region	The variability in firefighting needs and requirements across different regions was not researched enough
MAR17	Limited market reach	Difficulty in gaining a presence in the international markets as a startup
MAR18	Difficulties with existing systems	Integrating with existing firefighting infrastructure and protocols turns out to be difficult
MAR19	Difficulties with intellectual property	Disputes concerning used technologies and designs
MAR20	Customer fear of change	Reluctance from existing instances to work with new technologies and methods

4 | Sustainability Strategy

The sustainability strategy for the CHEETAH project is an integral part of the design and development process, addressing the urgent need to mitigate the environmental impact of firefighting operations. As wildfires become increasingly intense and widespread, it is crucial that firefighting technologies not only combat these disasters effectively but also do so in an environmentally responsible manner. This chapter details the comprehensive approach taken to ensure that CHEETAH operates with a minimal ecological footprint. By integrating advanced materials, sustainable fuels, and eco-friendly manufacturing processes, the CHEETAH project aims to set a new standard in sustainable aviation. This strategy ensures that while enhancing firefighting capabilities, the project also aligns with broader environmental goals and regulations, promoting a balanced approach to technological innovation and environmental responsibility.

4.1. Wildfire Impact

Contributors: Sjoerd
Authors: Sjoerd

There are two main players in the case concerning the CHEETAH mission design. First, there are the wildfires and thereafter there is the CHEETAH design fighting the wildfires. This section will cover the negative as well as any positive impacts regarding wildfires.

Wildfires play a crucial role in maintaining healthy ecosystems by facilitating nutrient cycling, reducing disease and pest prevalence, and promoting new growth. Earlier research discusses how wildfires release nutrients that have been locked into the top layers of the earth. These newly released nutrients will enhance plant regrowth and biodiversity, stimulating new species to develop [9][10]. Similarly, research has proved that wildfires can and are used to decrease pest populations in forests and prevent the spread of diseases [11]. Wildfires have always been around for the past millennia and lots of ecosystems have adapted to the dynamic cycle of destruction and regrowth [12]. Moreover, controlled wildfires have been used to prevent any unforeseen wildfires or to mitigate the impact of these wildfires [11].

Next to a positive impact, wildfires can also have severe negative impacts on both the environment and human communities. Wildfires destroy vast areas of vegetation every year and in turn, cause soil erosion as loss of plant life as plants serve to anchor the soil [13]. Additionally, wildfires form a direct threat to wildlife and their habitats which poses long-term impacts on biodiversity [14]. Wildfires significantly impact the local air quality as smoke particles from wildfires can lead to human health risks [15]. Furthermore, large amounts of carbon dioxide are released during wildfires which contribute to global climate change [16]. Water quality suffers from wildfires as well, as wildfires can contaminate drinking water supplies and aquatic ecosystems [17]. Finally, wildfires closer to populated areas can have immense impacts on human life, property and consequently the economics accompanying the surrounding societies [18][19].

4.2. Aircraft Impact

Contributors: Sjoerd
Authors: Sjoerd

To account for all the negative effects of wildfires, a firefighting aircraft design has been proposed that should aid in controlling wildfires by making the biggest possible impact on any firefighting fleet. The impact is defined as the effectiveness of fighting wildfires. Aircraft, however, also come with their environmental impact and these should also be analysed to properly sketch the situation. The positive impact of a firefighting aircraft, like the CHEETAH, is mitigating all the negative impacts of wildfires. For this mitigation, it is important to identify what negative wildfire consequences are most effective and impactful to design. Unfortunately, aircraft have a negative footprint on the environment as well. These are mostly due to noise pollution, carbon emissions and the depletion of raw materials [20].

4.3. Discussion and Environmental Statistics

Contributors: Sjoerd
Authors: Sjoerd

From the positive and negative impacts of wildfires, it can be concluded that wildfires have always been part of the world's environment and many ecosystems have adapted themselves in such a way that they can re-grow and expand their biodiversity after a destructive fire. The problems, however, arise in two main aspects, the first being soil erosion as the earth is vulnerable to such erosion in the short-term aftermath of a wildfire by the absence of soil anchoring by vegetation. The most important risk of wildfires is the interaction between human life and settlement in combination with wildfires, as wildfires pose great risks to human health, property and economics.

On the other side, the positive and negative effects of (firefighting) aircraft have been discussed. To make an impact on the environment that is as sustainable as possible, CHEETAH will have to be designed in such a way that it reduces the negative effects of wildfires as much as possible while mitigating its own negative impact as far as possible.

The dilemma that arises with this is that often a trade-off will be required between the positive and negative environmental impact of CHEETAH. To shed light on this matter, emission statistics of both wildfires and firefighting aircraft have been informed for the baseline and midterm report and a further emissions analysis has been done in Section 11.4 within Chapter 11 [1][2]. The conclusion is that the emissions of a firefighting aircraft fleet are dwarfed by wildfire emissions as mentioned Section 11.4. However, it should be noted that, as mentioned in Section 4.1, the ecosystem has adapted to a cycle of burning down and regrowing. In contrast, aircraft predominantly use nonrenewable fossil fuels so this argument would not be fully valid if the frequency of forest fires wouldn't significantly increase suddenly. However, The issue is that this frequency increase is occurring and therefore firefighting departments might have to intervene to maintain the balance [21]. Moreover, an argument supporting firefighting performance is the health and safety of citizens, as directly rescuing people from the hazards of wildfires would always be paramount over a relatively marginal amount of carbon emissions.

In conclusion of the research, CHEETAH is designed to fight wildfires with the main goal of ensuring health and safety for citizens. In the case of wildfires, every second counts regarding this health and safety and therefore the CHEETAH design should mostly be designed for performance which can save, not only lots of damage to people's property but also lives. That does not mean, however, that sustainability can be fully neglected. The CHEETAH design still contributes to the world's carbon footprint and therefore a strategy is required to **minimise the environmental impact as long as this does not compromise the performance of the aircraft**. In Section 4.4 the policies and strategy will be discussed which will realise this vision.

4.4. Policies and Strategy

Contributors: Sjoerd
Authors: Sjoerd

The sustainability policies and strategies were first discussed in the baseline report and have not been iterated upon for this report [1]. In this section, the policies will be briefly repeated and elaboration will be given on how the policies have been incorporated up until now and how they will be implemented in the future. An overview of all the sustainability policies is listed in Table 4.1.

Aerospace Structural and Manufacturing (ASM) Sustainability: The ASM department significantly impacts the CHEETAH design's sustainability. SUSP-ASM-01 has been implemented by bearing in mind the CO_2 emissions of all considered materials. These emissions include those due to raw material delving, material processing and treatment. The manufacturing sustainability is considered by limiting the outsourcing of part manufacturing. By producing the parts in-house, the control on implementing the stated policy will be maximised. Furthermore, SUSP-ASM-02 and SUSP-ASM-03 have been considered during the material selection process by implementing materials that are resistant to fatigue in the first place. Consequently, when the parts have been damaged by fatigue or impact, materials have been selected such that they are repairable instead of having to be replaced. By SUSP-ASM-04, structures have been designed to be relatively easy to disassemble and materials have been considered, which are recyclable. Finally, by SUSP-ASM-05, the structure has been designed and will be further designed in the future with the philosophy of maximising the strength-

Table 4.1: *Sustainability policy table.*

ID	Policy
SUSP-ASM-01	Minimise manufacturing and material emissions
SUSP-ASM-02	Maximise material durability
SUSP-ASM-03	Design for easy structure maintenance
SUSP-ASM-04	Design for easy structure disassembly
SUSP-ASM-05	Minimise material redundancy
SUSP-FPP-01	Minimise fuel consumption
SUSP-FPP-02	Maximise flight performance
SUSP-FPP-03	Design for sustainable fuel types
SUSP-FPP-04	Maximise propulsive system durability
SUSP-FPP-05	Design for easy propulsive system maintenance
SUSP-CO-01	Design for efficient fire fighting
SUSP-CO-02	Design for seed-bombing
SUSP-AERO-01	Maximise aerodynamic efficiency
SUSP-SE-01	Integrating sustainability of departments

over-weight ratio such that redundancy of material is minimised.

Flight Performance and Propulsive (FPP) Sustainability: The major contributor when it comes to operational sustainability is the FPP department. During the engine selection process, SUSP-FPP-01, SUSP-FPP-03 and SUSP-FPP-04 have been considered as the trade-off included criteria of most efficient specific fuel consumption. Durability and maintainability of the engines have been taken into account, however, the engine type of all options was the same and relatively similar durability and maintainability within this type of engine was assumed. Also, more exact specifications for each of the engine options were not found. Moreover, SUSP-FPP-03 has not been considered yet. The performance requirements included a required power which can only be accomplished by a limited amount of engines, as 6 or more engines would be complicated to install. The engine options did not allow for an option which was designed specifically for sustainable fuel. However, in collaboration with the engine manufacturers, perhaps some design modifications can be implemented that would allow for sustainable fuel.

Control & Operational (C&O) Sustainability: To maximise the sustainability impact, CHEETAH should also be designed to effectively fight fires. This minimises the required mission time and thus fuel consumption. SUSP-CO-01 includes designing for pilot controllability and manoeuvrability, as well as designing the dropping system such that CHEETAH will most efficiently perform its missions. This policy has also been accounted for by allowing for hover capability which allows for a wider variety of disposable water sources and the application of foam retardant mix tanks. Furthermore, the seed-bombing modularity (SUSP-CO-02) would improve sustainability as CHEETAH would be able to efficiently plant new forests in areas that have been affected by wildfires. However, such a new tank will still need to be designed.

Aerodynamic Sustainability: Optimising the aerodynamics efficiency (SUSP-AERO-01) entails reducing the amount of drag of the aircraft while ensuring its performance. The policy was implemented by optimising the overall lift-over-drag ratio of CHEETAH. More specifically this was done by minimising the drag of the fuselage and maximising the lift-over-drag ratio of the box wing design.

System Engineering (SE) Sustainability: All departments are integrated by the department of System Engineering which is responsible for the sustainability of the aircraft. The related policy, SUSP-SE-01, has been implemented by communicating design decisions within the group and making sure that sustainable choices would not mutually.

5 | Final Design

The goal of this entire project is to design a VTOL aerial firefighting aircraft. The result of this project is CHEETAH, Compound High-performance Emergency Extinguishing, Transport, and Aid Helicopter. In this chapter, the main systems and design parameters of CHEETAH are presented. Finally, the multirole aspects of CHEETAH are discussed and a sensitivity analysis is performed to explore how the design may change if certain parameters are slightly altered.

5.1. Final Design Sizing and Properties

Authors: Emma, Marco

In this section, all sizing parameters of CHEETAH are presented. In Table 5.1, all dimensions and values describing the layout of CHEETAH are listed. How all these values are exactly determined is explained in the next chapters of this report.

Table 5.1: *Sizing and dimensions of the final design.*

Parameter	Value	Unit
Fuselage		
Outer length (nose to tail)	22.3	m
Outer height	2.6	m
Outer width	2.5	m
Cabin outer height	2.0	m
Cabin inner height	1.9	m
Cabin floor length	5.6	m
Cabin roof length	8.7	m
Tail boom length	8.9	m
Rear door length	3.0	m
Rear door width	2.3	m
Belly height	0.6	m
Cockpit length	1.3	m
Wheelbase	6.9	m
Main rotor		
Disc radius	11.5	m
Blade chord	0.7	m
Number of blades	8	-
Twist (root to tip)	-8	deg
Blade airfoil	NACA 0012	-
Forward propellers		
Propeller	HC-B5MA-2	
Disc radius	1.2	m
Number of blades	5	m
Propulsion		
Engine	GE T408	
Number of engines	4	-

Parameter	Value	Unit
Top wing		
Airfoil	LS(1)-0417	-
Area	46.9	m^2
Span	19.4	m
Aspect ratio	8	-
Root chord	3.46	m
Tip chord	1.38	m
Taper ratio	0.4	-
Root angle of attack	3	deg
Tip angle of attack	3	deg
Anhedral angle	8	deg
Bottom wing		
Airfoil	LS(1)-0417	-
Area	46.9	m^2
Span	19.4	m
Aspect ratio	8	-
Root chord	3.46	m
Tip chord	1.38	m
Taper ratio	0.4	-
Root angle of attack	3	deg
Tip angle of attack	3	deg
Dihedral angle	5	deg

Parameter	Value	Unit
Vertical tail		
Airfoil	NACA 0015	-
Area	10	m^2
Span	3.16	m
Aspect ratio	1	-
Root chord	1.58	m
Tip chord	1.58	m
Horizontal tail		
Airfoil	NACA 0015	-
Area	6.19	m^2
Span	6.69	m
Aspect ratio	7.23	-
Root chord	1.67	m
Tip chord	1.67	m

Parameter	Value	Unit
Undercarriage		
Track	6.93	m
Wheelbase	2.7	m
No. of wheels (nose;main)	2;4	-
Main wheel diameter	0.86	m
Main wheel width	0.29	m
Nose wheel diameter	0.86	m
Nose wheel width	0.29	m
Water tank		
Volume	10 000	L
Length	5	m
Width	2	m
Door width	0.6	m
Height	1.4	m
Drop area	2.1	m^2

5.2. External Layout

Contributors: Marco
Authors: Marco

For the final design, some key design decisions have been made. In this section, the most important points of the external layout are briefly outlined, and references are given to the sections where the subsystems are treated more in detail. A full three-view drawing of CHEETAH can be found in Appendix B.

- **Propulsion:**
  - Rotor: this component remains eight-bladed and is similar in size to the previous iteration, as found in [2], but it is placed somewhat higher with respect to the fuselage (Section 6.1);
  - Propellers: their number has increased to four. Instead of being powered by separate engines, they are connected via driveshafts to the main engines (Section 6.2);
  - Engines: there is now one more engine, bringing the total to four (Section 6.3);
- **Aerodynamics:**
  - Wing: the choice was made to have a box wing, i.e. two wings mounted above one another at the root, and meet at the tip. The wing has a higher span than in the previous iteration. Fuel tanks are mounted inside the wing box of each wing (Chapter 7);
  - Tail: the H-tail concept from previously was retained, but for stability reasons, the size of the horizontal and vertical stabilisers increased, and the tail was placed further aft (Section 8.2 & Section 8.3);
  - Control surfaces: CHEETAH has control surfaces in all three axes like a conventional fixed-wing aircraft: ailerons, elevators, and rudders (Section 8.5).
- **Fuselage:**
  - Access: the rear ramp door remains the principal access point to the cabin, and it is supplemented by escape hatches in case of emergency. The cockpit is still accessible via doors on either side. While the final sizing of these doors has not been completed, CHEETAH will comply with emergency evacuation requirements from CS25.803;

  - Landing gear: this still has a tricycle configuration, although the nose gear has two separate struts to limit the volume needed when retracted.

5.3. Internal Layout

Contributors: Marco
Authors: Marco

A large factor in determining the outer dimensions of CHEETAH, and consequently critical properties like drag, is understanding its interior dimensions. For this purpose, an initial sizing has been drafted for each system. First, in Subsection 5.3.1, a quick overview of the internal systems is given, to supplement the three-view drawing in Appendix B. Then, in Subsection 5.3.2, the connections between these systems are explained, both in terms of hardware and software. Again in Appendix B, block diagrams are shown to graphically illustrate the system components and their connections.

5.3.1. System Layout

In the following list, the most important internal systems of CHEETAH are shortly explained, with references to the sections where the respective systems are treated more in detail.

- **Water/Retardant System:**
  - Water tank: this is still removable like in the last iteration. It is partially placed below the floor level (Subsection 10.1.1);
  - Retardant tank: an extra tank is attached to the water tank to mix retardant with the water (Subsection 10.1.2);
  - Snorkel and pump: the pump choice has not changed since the last iteration. The snorkel will be 4.5 m long (Subsection 10.1.4).
- **Fuel Tanks:** these are now placed in the wing box of each wing and are supplemented by a tank between the nose landing gear bay and the water tank dropping mechanism (Section 10.2);
- **Hydraulic System:** CHEETAH will have a full hydraulic system to power the control surfaces, the landing gear, and the water/retardant dropping doors (Section 10.3);
- **Electrical System:** this system has not been explored in depth, as it will not contribute a large amount to the feasibility of the end product, but it will at least consist of the following components: alternators to obtain electrical power from the engines, an auxiliary power unit to back up the engines, transformer rectifier units to convert Alternating Current (A/C) to Direct Current (D/C), inverters to convert D/C to A/C, batteries to store energy, transformers to adapt the power to the specific systems, and circuit breakers to protect the entire system. Additionally, a Ground Power Unit (GPU) can be connected when parked, so that the engines do not need to be running all the time. More information about which system uses which power can be found in [2];
- **Avionics:**
  - Avionics architecture: to reduce pilot training, a user-friendly off-the-shelf system will be chosen. It consists of flight computers, fly-by-wire sensors, a flight data recorder and cockpit voice recorder, instruments and displays, and a vision enhancement system;
  - Flight computers: the computers can be split into different components that each fulfil a different function. Examples are the Flight Control Computer, which sends signals to the control surfaces based on commanded inputs from the (auto)pilot, the Display Management Computer, which gathers all the information that will be presented to the pilot, and the Flight Management Computer, which tracks the route CHEETAH should fly. The entire avionics system is reported in the Software & Data Handling Block Diagram in Appendix B;
  - Autopilot: like the rest of the avionics system, the autopilot will also be based on an off-the-shelf solution. As stated in requirements **FTF-SYS-PIL-01.1** to **01.3**, the autopilot will be able to function in visual flight rules (VFR) and instrument flight rules (IFR) conditions, and it will be able to perform autonomous landings;

  - Vision enhancement system: this system is included to increase pilots' visibility in smoke or darkness. It consists of a variety of sensors, such as Light Detection And Ranging (LiDAR) scanners, infrared sensors, radar, and a heads-up display for the pilot.

- **Communication and Navigation Systems:**
  - Flight data sensors: these are the standard sensors mounted on most conventional aircraft, like the pitot-static system, weather radar, and an Air Data Inertial Reference System (ADIRS);
  - Fire monitoring system: this system aids the fire department using the aircraft to more easily obtain data from the fire. It will collect data through at least cameras, infrared sensors, and Light Detection And Ranging scanners (LiDAR). As this system has not been looked into too deeply, more sensors may be added;
  - Communication system: included in this system are a transponder, antennae to communicate with Air Traffic Control (ATC) and ground crews via radio, and an antenna to communicate with satellites.

- **Cockpit & Cabin, Multirole Items:**
  - Cockpit: the cockpit is sized such that a 95th percentile male can comfortably sit in the pilot's seat [22]. The cockpit visibility is such that it complies with the requirements specified in CS29.773;
  - Environmental Control System: this system includes equipment to make CHEETAH's occupants more comfortable. The components are the oxygen system, to supply oxygen to the occupants when flying at a high altitude, the fire suppression system, to extinguish fires that occur on the aircraft itself, the Heating, Ventilating and Air Conditioning (HVAC) system, to provide a pleasant temperature inside the cabin, and the anti-ice system, to ensure safe operations in icing conditions;
  - Winch: this component was kept, it is placed above the ramp door in the tail. The winch can be used to hoist cargo and people, this can be useful in for example rescue operations;
  - Internal mounting for seats, cargo, and stretchers: these have not been sized yet, but CHEETAH will contain mountings for relevant industry-standard systems;
  - Cabin size: the main driver for cabin dimensions was the requirement for 10,000 L of water, but the cabin ended up a bit larger: 5.6 m in length, 2.4 m in width, and 1.9 m in height. This means that the cabin is spacious enough to accommodate people standing upright, but that it can also fit two standardised 463L pallets, with a footprint of 275 cm by 224 cm [23], or three LD-3 standardised containers, which have a footprint of 157 cm by 201 cm [24].

5.3.2. Block Diagrams

The components mentioned in the previous subsection do not comprise everything included onboard CHEETAH. More components, and the systems to which they belong, are reported on the Hardware Block Diagram. Their interconnections are shown with arrows, where each colour represents a different type of flow.

Being a modern aircraft, and one with an unconventional propulsion/lifting system at that, CHEETAH has an extensive amount of software installed. In the Software & Data Handling Block Diagram, the different computers are shown, including the different data that is shared between them. What was displayed as 'Flight Computers' on the Hardware Block Diagram, is now split into multiple different components, in order to better visualise the different functions of the software.

The last constructed block diagram is the one showing the electronics. All systems that need to be powered with electricity are grouped into systems needing AC and DC. This diagram is a revised form of the one presented in the midterm report [2]. All block diagrams are found in Appendix B.

5.4. Modularity and Multirole Functionality

Contributors: Emma
Authors: Emma

One of the important design drivers of CHEETAH is the modularity of the design and the multirole functionality that comes with it. The design is initially made to fight wildfires. In firefighting mode, a water tank with a capacity of 10 000 L is installed in the fuselage. This takes up almost all usable fuselage space, but allows for multiple drops and in-flight refilling to provide even more extinguishing drops.

If the mission does not require direct firefighting, the water tank can be removed and a floor can be placed inside the fuselage. This allows for some more mission options. Firstly, CHEETAH allows for crews or goods to be transported and dropped at desired locations. Due to the hover capabilities, the helicopter does not have to land in order to get troops to the ground. Therefore, CHEETAH allows for more flexibility in where the troops can be dropped. These troops can for example be firefighting crew that are needed at the wildfire. Goods that are dropped can also be firefighting related, but another option is dropping medical goods or food to disaster areas, where ground accessibility is limited. Goods can be dropped both in hover and horizontal flight.

Furthermore, CHEETAH can be used for search and rescue missions when the water tank is not installed. Due to its large range, manoeuvrability and hover capability it can search a lot of area and also the places that are inaccessible from the ground. Equipment is installed that allows CHEETAH to search and rescue in bad weather or at night as well. Furthermore, once the people who need to be rescued are located, they can be rescued very close to their location since no runway is required due to CHEETAHs VTOL capabilities. This leads to another role of CHEETAH, which is medical evacuation. When no water tank is installed, there is enough space for medical equipment, which allows the helicopter to be used as a medical helper.

CHEETAH can also be deployed for the army. Because of the same reasons given as before, like manoeuvrability, hover and VTOL capabilities, CHEETAH is highly suitable for this. In the military, often dropping or evacuation missions are executed.

Lastly, another mission of CHEETAH is seed bombing. The soil where a wildfire took place is very fertile once the fire is extinguished. Therefore, CHEETAH can be used to drop seed balls on this area. The seed balls contain many seeds, to foster new growth of trees.

6 | Propulsion System Design

CHEETAH utilises multiple propellers and a rotor to provide both lift and thrust. These are to be analysed in detail, specifically for various speeds of the aircraft. First, the main rotor shall be analysed, in an attempt to size the rotor and determine the amount of power needed to drive the rotor. Then, the main propellers are sized and their required power is to be analysed as well. With the required power known, an engine selection can be done.

6.1. Main Rotor Design

Contributors: Ruben, Xander
Authors: Xander

Previously, the main rotor was sized using momentum methods. This method however has its limitations, especially when the flight direction of the rotor is not aligned with its rotational axis. For this, a more sophisticated method is to be applied, the Blade Element Method (BEM).

6.1.1. Helicopter principles

In order to grasp some of the principles that will be applied in BEM, it is important to discuss some of the "ailments" typical for helicopters in forward flight. When a helicopter has forward speed, the velocity over the blades varies with the azimuth angle of the blade ψ as seen in Figure 6.1b.[1] This can be compared to the situation in hover as seen in Figure 6.1a. This means that with forward speed, the advancing blade (azimuth angle of 90°) does not only have a velocity component due to the rotation of the rotor but also due to the forward speed. On the retreating blade however (azimuth angle of 270°), the forward speed of the rotor actually causes a reverse flow over the blade, meaning that the inner span has a completely reversed flow over the blade, signified by a white contour in the figure. The outer portion of the blade does not have as high velocity as the advancing blade either, seriously offsetting the centre of pressure of the rotor.

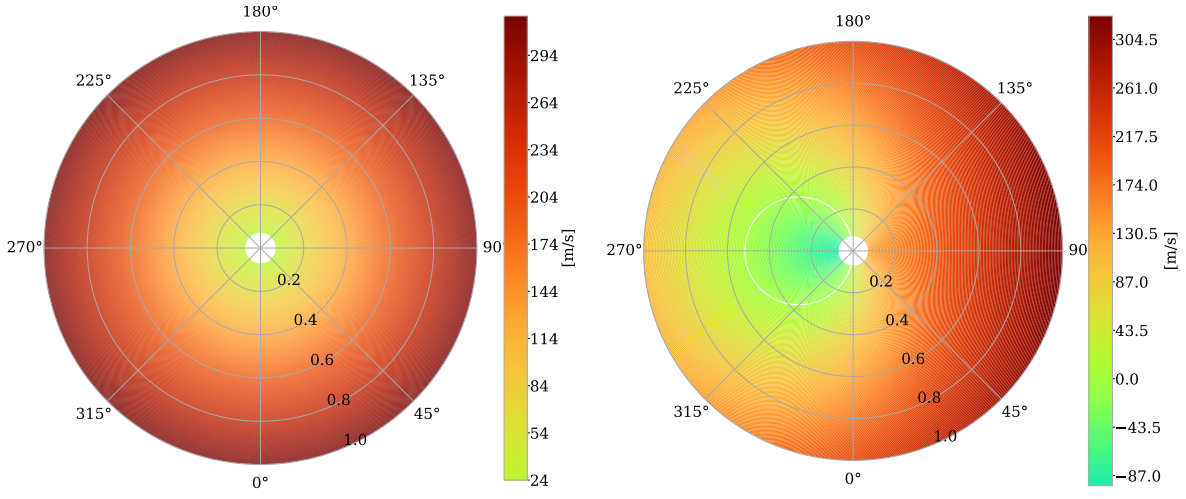

(a) *Hover* (0 km/h. **(b)** *Cruise* 400 km/h.

Figure 6.1: *Velocity distribution over the rotor.*

To produce lift, rotors 'suck' air down, producing a so-called induced velocity. For an ideal twist in hover, this induced velocity is constant over the entire rotor [25]. With a forward cruising velocity, the induced velocity changes over the azimuth angle as depicted in Figure 6.7a. This relationship, as described by Prouty [25], is presented in Equation 6.1. Here, v_i denotes the induced velocity specified in Equation 6.2, r represents the

[1] The azimuth angle is 0 when the blade points in the direction of the tail and seen from above, counter clock-wise is positive.

local radius, R is the total radius of the main rotor blade, and ψ is the azimuth angle.

$$v_{i,local} = v_i \left(1 + \left(\frac{r}{R}\right) cos(\psi)\right) \tag{6.1}$$

The induced velocity used in Equation 6.1 is defined by Equation 6.2, where D represents the drag force, L is the lift force, and ρ denotes the density and RC the rate of climb.

$$v_i = \frac{RC}{2} + \sqrt{\left(\frac{RC}{2}\right)^2 + \frac{DL}{2\rho}} \tag{6.2}$$

Here, r is the local radius, whereas R is the total radius. DL is the discloading in N/m^2 and ρ is the local density in kg/m^3.[2] This varying induced velocity, combined with a varying tangential velocity, results in a different induced angle ϕ across the rotor. This tilts the aerodynamic force of the wing backwards, increasing the required power while decreasing the amount of lift provided, as seen in Figure 6.2. With the twist as a pilot input, constant over the azimuth angles, this varying induced angle ϕ results in a varying angle of attack (AoA) α over the rotor as seen in Figure 6.5. The resulting lift per span is given as well. Combining this with the tangential velocities being higher on the advancing blade side, explains a wildly offset centre of pressure, in this case situated at a distance from the centre of the rotor 25 % greater than the radius of the rotor, making the aircraft not flyable.

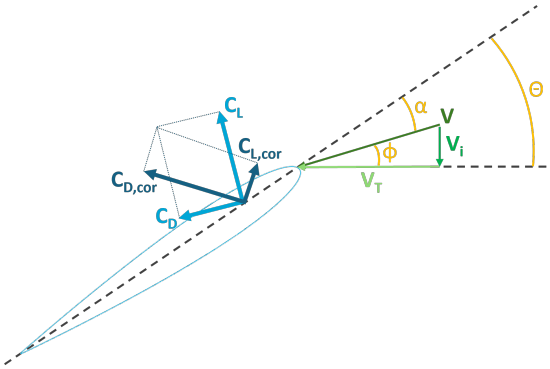

Figure 6.2: *Overview of the angles per blade section and resulting tilting of the aerodynamic force.*

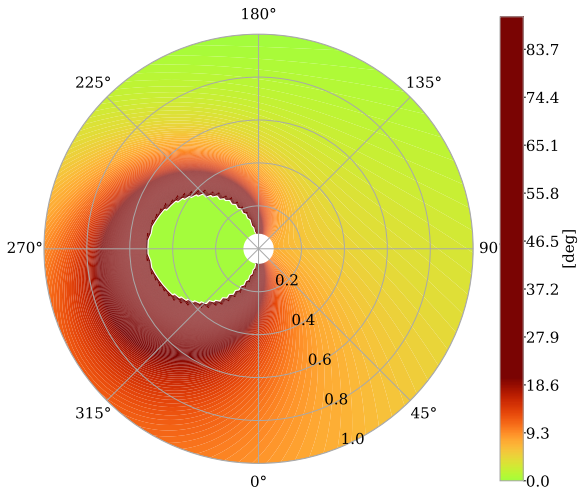

Figure 6.3: *Induced angle° at* 1 g *with a cruise speed of* 400 km/h *without flapping.*

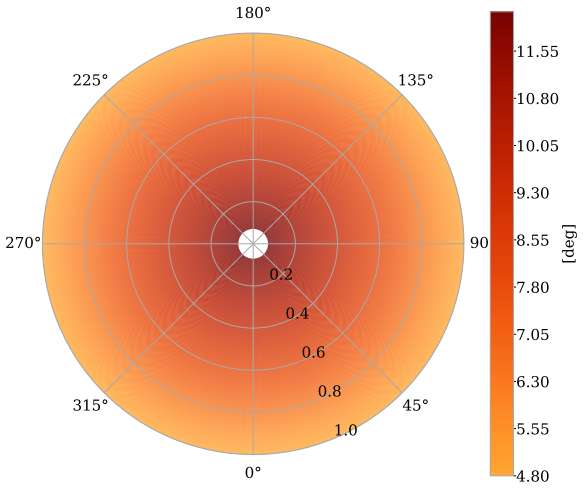

Figure 6.4: *Pitch° at* 1 g *with a cruise speed of* 400 km/h *without flapping.*

[2] The equation for the induced velocity is not valid for forward flight and a different equation is to be used. This mistake however leads to an overestimation of the required power, meaning that the effect of this error is not detrimental to the feasibility of the design.

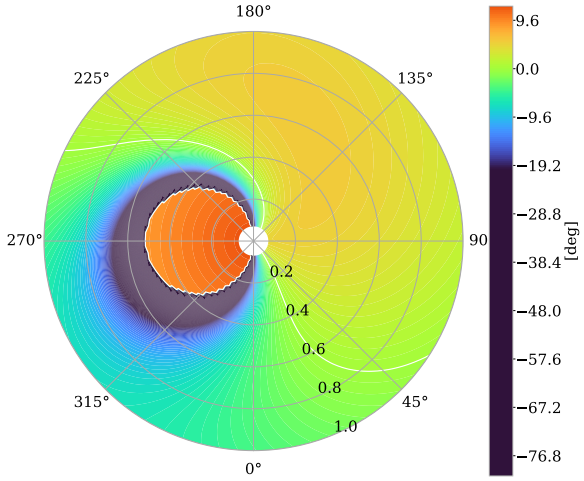

Figure 6.5: *Angle of attack* ° *at* 1 g *with a cruise speed of* 400 km/h *without flapping.*

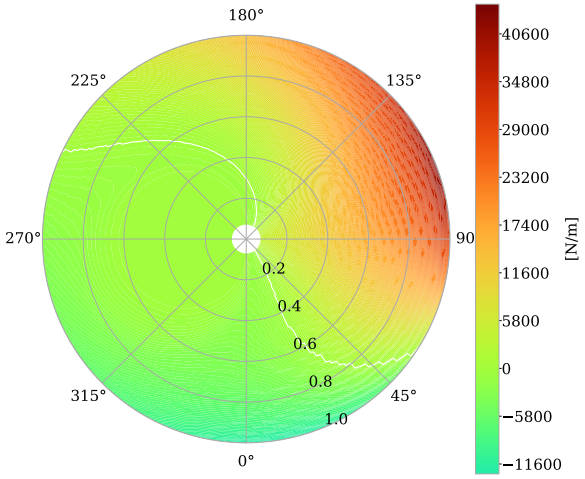

Figure 6.6: *Lift per unit span* N/m *at* 1 g *with a cruise speed of* 400 km/h *without flapping.*

The variation of the velocity combined with the even more complex variation of the AoA over the rotor, results in a very asymmetric lift distribution over the rotor. To fix this, the blade shall be able to move up and down freely, known as flapping. The hinge found on many rotors allowing for this movement is called the flapping hinge. When flapping up, a velocity is induced coming from above the blade, reducing the angle of attack on that side. As a result, the blades shall flap up around the advancing side and vice versa. The weight of the blade, inertia of the blade and centrifugal force acting on the blade hold the blade in equilibrium at a small angle. An effort was made to analyse this flapping motion, but proved to be too difficult. As the restoring centrifugal force and inertia depend on the flapping angle β and its second time-derivative $\dot{\beta}$ respectively, β is dependent on itself and due to time limits, the lack of convergence of β over the iterations could not be fixed. Instead, due to the cyclical nature of the flapping which can be estimated by a 3-term Taylor series [25], the flapping is taken to be

$$\beta = C_1 + C_2 \sin(\psi + C_3) \tag{6.3}$$

where C_1, C_2 and C_3 are the coning, cyclical coning and offset, respectively. This assumption decreases the accuracy of the model, which takes a lot of confidence from determined values, but is the best available. The C_1, C_2 and C_3 parameters are varied to minimise the distance of the centre of pressure from the geometric centre of the rotor. For the simplicity of manufacturing, a linear twist is assumed. It can be seen in Figure 6.7b that for the outer portion of the blade, this can be fairly close and since the outer portion of the blade is the most important anyway due to its higher speeds, performance losses should be minimal.

Plotting the lift distribution with flapping as depicted in Figure 6.8 and comparing it to Figure 6.5 and Figure 6.6, makes it abundantly clear how important flapping is. The centre of pressure is now located in the centre of the rotor. Important to note is how the tip of the advancing blade is producing negative lift, balancing the asymmetric effects caused by the forward speed of the rotor. This is of course not beneficial for performance and will increase the drag and torque of the rotor and thus required power.

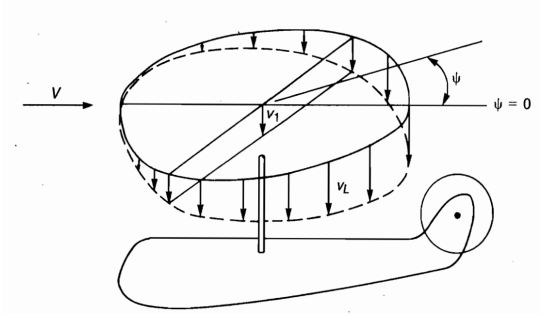

(a) *Velocity distribution over the main rotor in hover.*

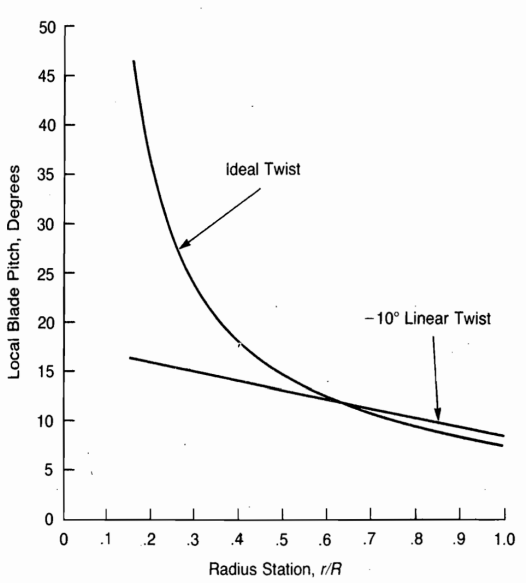

(b) *Velocity distribution over the main rotor in cruise.*

Figure 6.7: *Velocity distribution over the rotor at different speeds [25].*

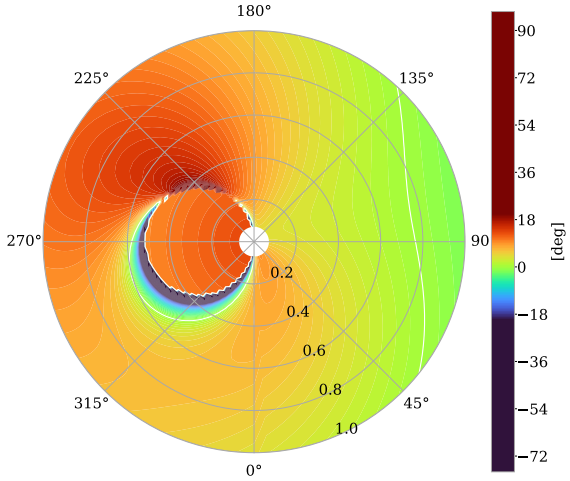

(a) *Angle of attack* °.

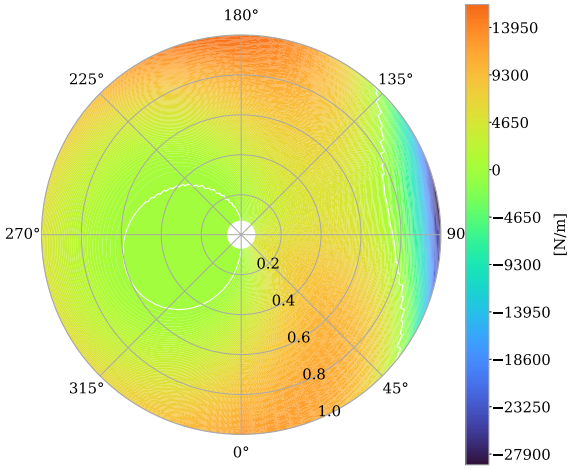

(b) *Lift per unit span* N/m.

Figure 6.8: *AoA and lift distributions over the rotor at* 1 g *with a cruise speed of* 400 km/h *with flapping.*

Due to the complex distribution of the lift, however, the $C1$, $C2$ and $C3$ parameters are not easily determined and prove to be fairly different for various situations. In addition to that, the position of the centre of pressure is highly sensitive to these parameters. Further complicating the matter is the fact that the induced velocity is dependent on the disc-loading (DL), which influences the induced angle ϕ. This means that the collective pitch of the rotor is to be altered to match the load used to compute the induced velocity. For this different pitch θ however, the flapping parameters have to be altered again, as the centre of the lift position is fairly sensitive to the collective pitch. Introducing different flapping parameters fixes this, but again changes the load produced by the rotor, altering the induced velocity. This loop, coupled with high variations and sensitivity of various inputs, requires a few iterations and automation was not accomplished elegantly. Brute-forcing automation by simply trying many values was deemed too slow. For every situation, finding the correct solution by altering various inputs is done by hand, being somewhat costly in terms of time. Automation is possible, but proved to be even less time-efficient. As a direct result, rotor performance is sadly not determined over a range of speeds for example but only for specific, singular cases.

6.1.2. Numerical model using Blade Element Method

The inputs and outputs of the model are tabulated in Table 6.1 Notice how the lift is both an input and output,

Table 6.1: *Inputs and outputs of the rotor model.*

Inputs	Outputs
Blade length	Lift
Blade chord	Torque
Blade twist	Drag
Collective pitch	Power
Rotor rotational speed	
Cruise speed	
Climb speed	
Lift	
C1	
C2	
C3	

which explains part of the need for iterations as discussed in Subsection 6.1.1. Also, note that the rotational speed is often governed by the limiting of the maximum Mach number to 0.95 (which occurs at the tip of the advancing bade).

The blade is divided into a hundred elements, and the blades are analysed for 100 different azimuth angles as well. For every of the ten thousand parts, the induced velocity, tangential velocity and thus induced angle are computed as discussed in Subsection 6.1.1. With the chosen collective pitch and twist, the angle of attack is determined, governing the lift and drag coefficients. These coefficients are determined using a publicly available airfoil analyser, Javafoil, and corrected for both the induced effects as seen in Figure 6.2 and Mach effects using the Prandtl-Glauert correction.[3] When the lift (pointing in the direction of the rotational axis of the rotor) and drag (perpendicular to the lift and length of the blade) are computed over the entire rotor, the total lift, torque, power and drag generated by the rotor are easily computed.

6.1.3. Results

The two main answers to be received are the optimal design and the required power. Those are obviously related as the optimal design should require a minimal amount of power. The NACA0012 airfoil was chosen before as it is a frequently used airfoil and typically produces no moment around its quarter-chord, which is beneficial for rotor blades that are not torsionally stiff. This leaves the radius, twist and chord distribution to be designed for.

For the original design, used as a starting point, flapping angles C_2 proved to go up to 8° and a coning C_1 of 3 degrees was guessed. When dropping 10000 L of water at once, the blade deflected a little under a meter as described in Chapter 9. The length of the blades was reduced to 11.5 m to limit the total deflection to 2 meters, preventing the rotor from hitting the tail. This estimate is fairly conservative as normally, not all water is dropped at once. The chord was not altered, as at the speeds the blades encounter, the Reynolds-numbers influence was limited and therefore not taken into account. For hover, adding or subtracting a twist from the blade had little to no effect on the required power. Therefore, it is kept at an arbitrary $-8°$.

Now, the model can be used to analyse any case with varying loads, forward speeds and climb speeds. Due to the higher human workload per case, a maximum can not simply be found by letting the model evaluate any case and thus, certain design points are to be selected. As will be discussed in Chapter 7, it was clear from previous research that the rotor is barely used in cruise. Therefore, the design point is chosen to be vertical flight, at a load of 1.5 g as seen in Chapter 11, with a vertical speed of 5.5 m/s. The required power is easily determined to be 16.4 MW, with a torque of 652 kNm to be delivered. Altering the load or vertical speed and running the simulation again, quickly shows that this is indeed the most power-intensive phase.

[3] When a more refined method was used to compute the lift coefficients, the Prandtl-Glauert correction was forgotten for the drag coefficients. In the future, comparing the numbers between 2 versions of code when making big changes is recommended.

Coming back to the required power in cruise; the effective L/D can be computed and compared to the L/D of the aircraft. This is done in where L is the lift force, V_c is the velocity in cruise and $P_{cr,req}$ is the required power in cruise.

$$\left(\frac{L}{D}\right)_{\text{eff}} = \frac{LV_{\text{c}}}{P_{\text{cr,req}}} \tag{6.4}$$

Note that this power entails both the power required to drive the rotor and to drive the propellers harder to compensate for the increased drag. At 400 km/h, this effective L/D proves to be 7.5, slightly more than half of the L/D of 14.3 the aircraft without a rotor generates. However, the power required by the rotor does not diminish to zero but stays fairly constant for small loads on the rotor. In addition, adding load on the wing increases the drag created by the wing, not to mention that the wing would have to increase in size too. Some load on the rotor therefore seems desired and obviously, an optimum exists. For a load (the factor of the weight carried by the rotor) of $0, 0.05, 0.08, 0.2, 0.5$ and 1 times the weight, the required power was computed and interpolated using cubic interpolation. Then, the amount of power required to counteract the drag of the wing was computed, simply using the L/D of 21.9 for the wing for every amount of lift generated, and changing the weight of the wing corresponding to the lift it has to generate.

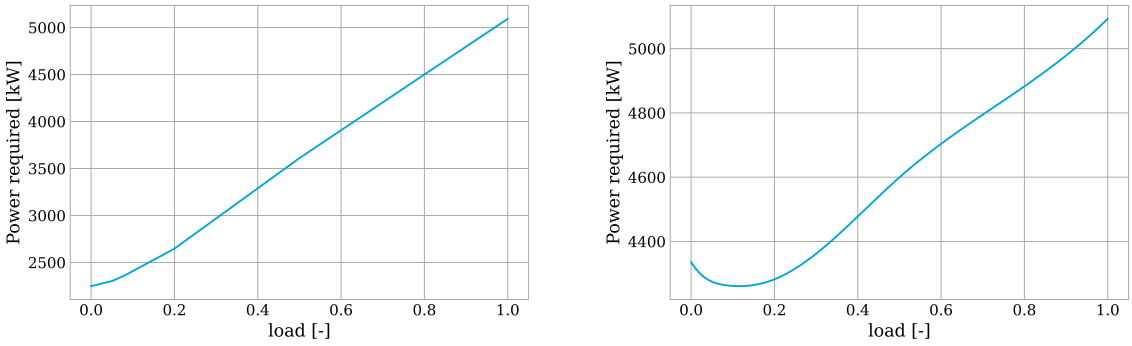

(a) *Power required by rotor.*

(b) *Total power required by aircraft.*

Figure 6.9: *Required power against load provided by the rotor.*

An optimum can be found at 0.11, which is reasonably close to numbers found from literature, prescribed in Chapter 7. This value was however found quite late into the design phase, so the original 0.08 was kept. It can be seen in Figure 6.9 however, that this value barely increases the total required power.

Now, it would be interesting to explore the required power to provide sufficient lift with just the rotor at every speed. Again, due to time constraints, this analysis will not be utilised elsewhere but exploring the effects is still insightful. Computing the power at velocities ranging from 0 km/h to 400 km/h with steps of 50 km/h.

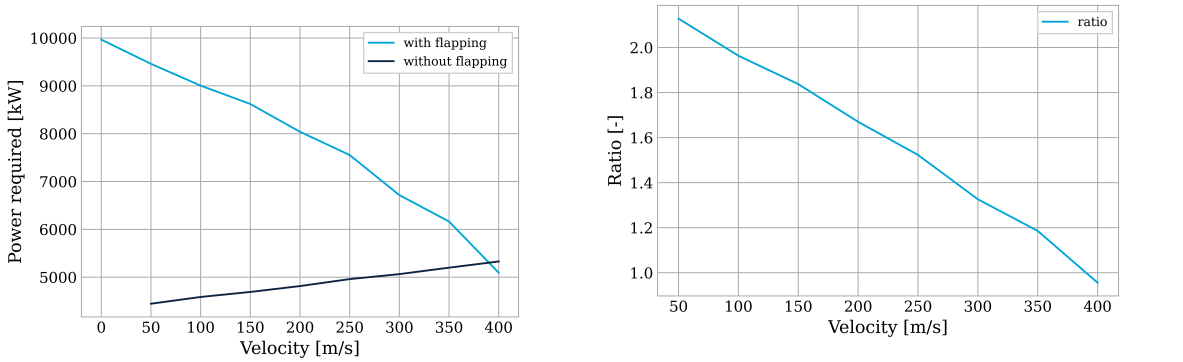

(a) *Required power with and without flapping.*

(b) *Ratio of required power including flapping, over required power without flapping.*

Figure 6.10: *Required power as a function of velocity.*

The most important conclusion from Figure 6.10a is that flapping has a huge effect on the required power, again emphasizing the need for a more accurate model to simulate flapping. When looking at the required

power as a function of the velocity to produce 1 g of thrust, it is apparent that the results are linearly dependent on the speed. The ratio between them seems fairly linear too, which would be beneficial for investigating the performance when converting from hover to forward flight. When flapping is applied, the power required decreases which is an interesting result. The results here could be utilised in doing a better performance analysis, especially since now the performance could be evaluated at any forward speed.

At last, the performance of the rotor at a load of 0.08 g can be analysed. Looking at the lift distribution as displayed in Figure 6.11a, it can be seen that the rotor produces a lot of negative lift. Here, positive power is however still required to turn the rotor and counteract the drag produced by the rotor, as seen in Figure 6.11b, making the rotor inefficient. However, as seen earlier, this is still an optimal point, as a wing is generally more efficient than a rotor.

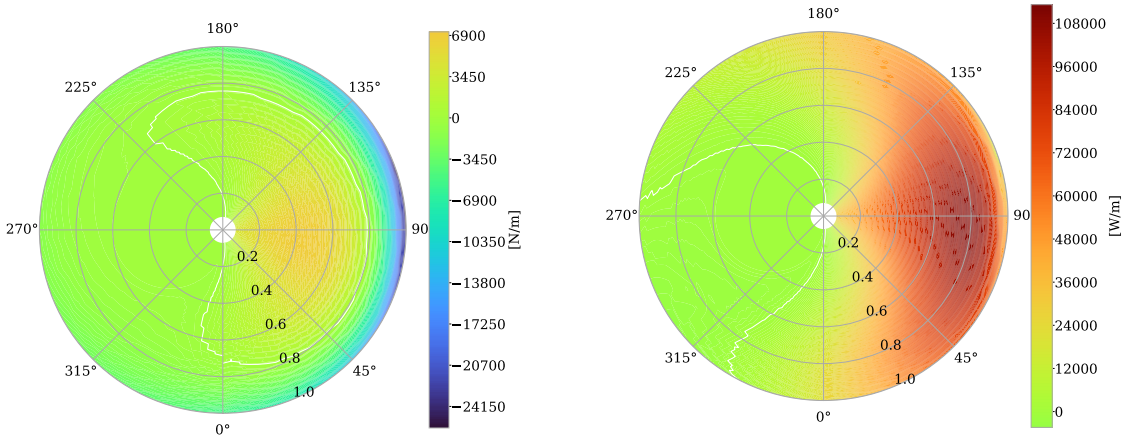

(a) *Lift per unit span* N/m. **(b)** *Power per unit span* W/m.

Figure 6.11: *Lift and power distributions over the rotor at* 0.08 g *with a cruise speed of* 400 km/h.

When a forward speed is applied, the required power is comprised of two parts: The power needed to overcome the extra drag caused by the rotor, only occurring during horizontal flight and the power needed to drive the rotor, a direct result of the torque generated by the rotor. For the power budget, this is not important and the sum is simply taken. [4]

Table 6.2: *Power required for maximum power and cruise.*

	Maximum power	**Cruise**
Velocity [m/s]	0	111.1
Climb velocity [m/s]	5.5	0
Load [-]	1.5	0.08
Power [kW]	16410	2358
Power counteracting drag [kW]	0	920
Power counteracting torque [kW]	16410	1438

6.1.4. Discussion

Various assumptions and errors influence the accuracy and thus confidence in the model. First of all, the erroneous underestimated drag coefficients decrease the required power, meaning that the available power may not be enough after all. The erroneous addition of the rotor drag in the power calculations however increases the required power, meaning that the correct required power leaves more margin.

To prevent errors like this, small verification checks are to be repeated when changes are made to the code, and proper version control is to be applied.

[4] Here, an error was made while separating the powers for the cruise and as a result, the power needed to overcome the drag was counted twice. This however reduces the required power, so will only bring benefits to the design. In the future, checking results should be done simultaneously with writing the program.

Small assumptions or low-effort solutions, like a simple Prandtl-Glauert correction or lift- and drag-coefficients being independent of Reynolds number at high Reynolds numbers like encountered at the rotor blades, can be mitigated but would only give small improvements of accuracy.

The biggest assumption that should be mitigated however is the adopted flapping model. The flapping model was ideally only adopted to demonstrate the ability to centre the centre of pressure of the rotor. The Flapping however alters the AoA, greatly influencing all important outputs of the model like required power and generated drag and torque. Figure 6.10b showcased the dramatic effect of flapping to the most important output; the required power. For the same load, the flapping required to centre the lift of the rotor doubled the required power. In addition, the magnitude of the flapping angles influences the maximum downward deflection. To stop the rotor from hitting the tail, the rotor blades were shortened, analogous to decreasing the aspect ratio of a normal wing. A finer flapping analysis would give more confidence in preventing the rotor from hitting the tail, as well as possibly increasing the length of the blade, increasing the overall efficiency of the rotor.

6.2. Forward Propeller Design

Contributors: Ivo, Marco
Authors: Ivo, Marco

The next step in the design phase is to determine the propeller design. To achieve this, several existing propellers were compared. Initially, certain criteria were established to ensure each propeller was a viable option that met the project's requirements. One of the key requirements was having a cruise speed of 400 km/h. Using Equation 6.5 and Equation 6.6, certain limitations on the design of the propeller can be made, as supersonic tip velocities should be avoided. Taking a margin into account, the tip velocity should not exceed 95% of the speed of sound, giving it a maximum velocity of approximately 326 m/s ($0.95 \cdot 343$ m/s). Knowing the rated rotational speed of the propeller in Rotations Per Minute (RPM) and the propeller's diameter (d), the tip speed due to only rotation can be computed:

$$V_{\text{rot}} = \pi d \left(\frac{\text{RPM}}{60} \right) \tag{6.5}$$

Combining the tip speed due to rotation (V_{rot}) and the cruise speed (V_{c}), the total tip speed can be calculated:

$$V_{\text{tip}} = \sqrt{V_{\text{c}}^2 + V_{\text{rot}}^2} \tag{6.6}$$

This is the absolute maximum velocity encountered on the propeller. To limit this, the propeller needs to be capable of providing sufficient power at a low enough diameter and rated RPM. Only propellers that fit these criteria were considered. To know how much power was required for each propeller, Equation 6.7 was used. In here, T_c is the thrust in cruise. Taking the preliminary drag estimation of about 14 000 N (assuming thrust equalling drag) and an estimated propeller efficiency factor of $\eta_{prop} = 0.8$ [26], this led to a total required power of $P_r = 1950$ kW, or 975 kW per propeller. This process led to the selection of the propellers listed in Table 6.3.

$$P_{\text{r}} = \frac{T_{\text{c}} V_{\text{c}}}{\eta_{\text{prop}}} \tag{6.7}$$

It should be noted that only Hartzell propellers were analysed since it was the only manufacturer whose technical and pricing data was readily available.

In addition to the tip speed, another critical factor in this propeller selection process is the diameter: since the vertical space is constrained by the rotor on one side and the lateral ground clearance on the other, there is not much room to place a large propeller. No in-depth aerodynamic interference analysis between the rotor and the propellers has been performed. Still, it can be assumed that a larger distance between the two will be beneficial for performance. Therefore, a smaller diameter was deemed better. Since all the propellers are capable of providing enough thrust, and the weight differences are not significant, the only other factor

Table 6.3: *Propeller models considered for CHEETAH. Technical data from the Hartzell May 2024 Application Guide,[1] pricing data from the Hartzell 2021 Price List.[2]*

Manu-facturer	Series (model)	Used in	No. of blades	Dia-meter [m]	Weight [kg]	Material	Price [$]	Max. power [kW]	Rated RPM
Hartzell	HC-E5 (A-2)	Pilatus PC-21	5	2.39	79.4	Carbon composite	265851	1230	2000
Hartzell	HC-B5M (A-2)	Embraer EMB 314	5	2.39	100.2	Aluminium alloy	84572	1193	2000
Hartzell	HC-E4 (A-2)	Beechcraft AT-6	4	2.46	70.3	Aluminium alloy	56512	1193	2000
Hartzell	HC-B5M (A-5A)	Antonov AN-38	5	2.85	115.2	Aluminium alloy	92000	1230	1700

that will affect the propeller choice is the price. Therefore, the Hartzell HC-B5MA-2 was chosen as the final propeller.

Later on in the design process, however, it appeared that the actual drag value would be around 32 000 N, an increase of more than twice the original value. Utilising Equation 6.7 again, the total required power now became 4200 kW. In Hartzell's database, there were no propellers powerful enough so that only two were required, so the decision was made to use four of the previously chosen propellers, the Hartzell HC-B5MA-2. The total available power from the forward propellers, therefore, becomes just short of 4800 kW.

The original two propellers were to be placed on the tips of the wings, similar to the Airbus RACER. With the two extra propellers, the choice was to mount them either in a pusher-puller configuration or laterally next to them, a bit more inboard on the wing. Since the interference of two propellers placed behind one another was outside of the scope of this project, it was decided to opt for the latter. The new propellers have been placed as far outboard as possible while keeping a margin of 20 cm to the tips of the outboard propellers. They are mounted on pylons between the upper and lower wings.

Adding two more propellers also allows for an increase in safety in case one of the propellers fails, ensuring that it won't be critical at any stage of the flight. However, it still influences the performance of the compound helicopter. During the cruise, the aircraft's maximum speed would be limited to 230 km/h, and it would lose the ability to climb in hover.

6.3. Engine Selection

Contributors: Ivo
Authors: Ivo

Now that the main rotor design and forward propeller design are determined, an engine choice can be made. As mentioned in the midterm report [2], the engines indicated in Table 6.4 are considered.

Table 6.4: *List of engine models considered.*

Manufacturer	Model	Power [hp]	BSFC $\left[\frac{\text{lb}}{\text{h·hp}}\right]$	Application
Rolls-Royce	AE 1107C	6000	0.426	Bell-Boeing V-22 Osprey [27]
Rolls-Royce	AE 1107F	7000	0.426	Bell V-280 Valor [28]
General Electric	T408	7500	≈ 0.4	Sikorsky CH-53K King Stallion [29]
Rolls-Royce Turbomeca	RTM 322	2270	0.42	Eurocopter X^3 [30]
General Electric	T700-GE-701D	1940	0.462	Sikorsky S-70 [31]

The engines will need to supply power to the main rotor, the forward propellers, and various smaller sub-

[1] Hartzell May 2024 Application Guide, https://hartzellprop.com/MANUALS/159-0000-A.pdf, retrieved 5th June 2024.
[2] Hartzell 2021 Price List, https://hartzellprop.com/wp-content/uploads/2021-Price-List.pdf, retrieved 6th June 2024.

systems. To select the appropriate engines and determine the required quantity, the maximum power usage must first be found.

Two potential phases during flight have been identified where power usage may be maximal. The first phase occurs when the aircraft is climbing at 1.5g in hover. In this scenario, the rotor generates roughly 651500 Nm of torque while consuming 16410 kW of power. The torque is counteracted using differential thrust, with two of the propellers producing reverse thrust. To minimise the power needed to counter the torque, the outer propellers are used at full power, each consuming 1193.1 kW, while the inner propellers operate at 896.8 kW. In total, 20589.8 kW of power is required during this phase. The second phase where significant power may be needed is during climbing on a cruise. During this phase, the rotor operates at 2330.1 kW while all the propellers operate at 1118.1 kW each, resulting in a total of 6802.3 kW. Therefore, to ensure sufficient power can be provided at any stage of the flight while minimising the BSFC, four General Electric T408 engines were chosen, delivering a total of 30000 hp, or 22371 kW of power. Considering a transmission efficiency of 95%, this translates to 28500 hp, or 21252.4 kW of power.

Additionally, these engines provide sufficient power for the aircraft to operate at any stage of the flight with one engine out, except for the hover climb phase. In case that happens, the aircraft will simply stop climbing to reduce the power required from the rotor and the propellers. A more detailed explanation of what happens when the aircraft flies with one engine inoperative will be made in Chapter 13.

7 | Aerodynamic Characteristics

In Chapter 6 it was concluded that CHEETAH would require a significant amount of power to comply with the related requirements. The aerodynamics department of CHEETAH has the ability to alleviate some of this required power through an aerodynamically efficient design. The aerodynamics therefore also influence the total efficiency of CHEETAH and this chapter will elaborate upon what this aerodynamic efficiency entails and how it is planned to be optimised.

7.1. Preliminary Aerodynamic Sizing

Contributors: Sjoerd
Authors: Sjoerd

As a start for the aerodynamic design process, a preliminary geometric wing design was computed, which CHEETAH would require. The first interesting aspect of this geometry would be the utilisation of a box wing design selected in the midterm report [2]. In earlier research [32] [33] it was already conducted that bi-wing or box wing designs involve complex interactions of pressure fields, which will be further examined in Section 7.3. For the preliminary sizing of the wing, these complex interactions will not yet be considered as just a first estimation is the goal of this section. As the wing system will most predominantly be carrying the lift during cruise and since the air density at cruise altitude will be limiting for the dynamic pressure, cruise conditions will be considered for computing the preliminary aerodynamic sizing.

The first wing parameter to be computed would be the required surface area S having a direct dependency on the required lift L, a lift coefficient C_L and the dynamic pressure q_∞, by the lift equation, Equation 7.1.

$$L = C_L q_\infty S \tag{7.1}$$

The required lift stems from the most critical weight at which CHEETAH will operate being the MTOW of the iteration at that time which was 348 200 N. It was found in several studies that compound helicopters would perform most efficiently during cruise when the wing carries 94-91% of the total amount of lift while the rotor will still be operative with a lift load factor of 0.06 to 0.09 [34][35][36]. As discussed earlier, cruise conditions will be considered for the dynamic pressure. Furthermore, an estimation had to be made on the C_L to compute a preliminary value for the surface area of CHEETAH. A relatively conservative estimate of 0.75 was taken based on preliminary airfoil analysis which will be elaborated upon in Section 7.2. Furthermore, for simplification, it was decided that the projected surface area would be equally distributed over the upper and lower wings.

Some other wing geometric properties include the taper ratio, the aspect ratio, possible sweep and the dihedral/anhedral angles. Taper and aspect ratio influence aerodynamic efficiency, which is measured by lift over drag, the structural integrity of the wing design and ultimately also the aircraft's manoeuvrability. With this in mind, and predominantly with the use of the BSc Aerospace Engineering aircraft design course [37], preliminary estimations were made. The course [37] was also used to determine a quarter chord sweep angle of 0° as our aircraft will not be flying at a velocity of more than Mach 0.7. Finally, the dihedral and anhedral angles for both the lower and upper wing were determined, once again based on the aircraft design course, but also keeping in mind the required ground clearance for the later implementation of propellers on the wing tips.

All these values should not be considered any more than a rough estimation of the wing geometry, as they just mark a start for a chain of iterations to optimise the design. In Table 7.1, the values for the preliminary wing geometry are listed.

Table 7.1: *Preliminary Wing Geometry.*

Geometric Property	Symbol	Sizing	Unit
Total Projected Wing Surface Area	S	94	m^2
Aspect Ratio	AR	8	-
Taper Ratio	λ	0.4	-
Quarter chord sweep angle	$\Lambda_{1/4}$	0	deg
Lower wing dihedral angle		5	deg
Upper wing anhedral angle		8	deg

7.2. Wing Airfoil Selection

Contributors: Sjoerd
Authors: Sjoerd

The first aerodynamic characteristic to be determined through analysis has been the wing airfoil selection. This selection procedure entails finding a suitable airfoil with regards to the lift coefficient C_L, the drag coefficient C_D, the aerodynamic moment coefficient C_m and whether the airfoil is optimised for the Reynolds Number Re at which the aircraft will be flying [38]. For the scope of the aerodynamic design of CHEETAH, it was decided to select three airfoils optimised for the expected Reynolds number and to analyse these airfoils using XFLR5 software [39]. The Reynolds number was calculated using Equation 7.2.

$$Re = \frac{V \rho \bar{c}}{\nu} \tag{7.2}$$

Where V is the cruise velocity, $\bar{c}$ the mean aerodynamic chord, ρ and μ the air density and dynamic viscosity at cruise altitude respectively. The calculation results in a Reynolds number of $1.75 \cdot 10^7$ based on which three airfoils were selected for the analysis. Since there is an extreme quantity of existing airfoils, a brief query to ChatGPT[1] has pointed towards some airfoils that should be optimised for the CHEETAH flight conditions. Research has confirmed that three airfoils of the airfoils were indeed viable for the design, these have been further explored. The geometries of the airfoils can be seen in Figure 7.1 and their names read: NACA63-215, LS(1)-0417 and SC(2)-0710.

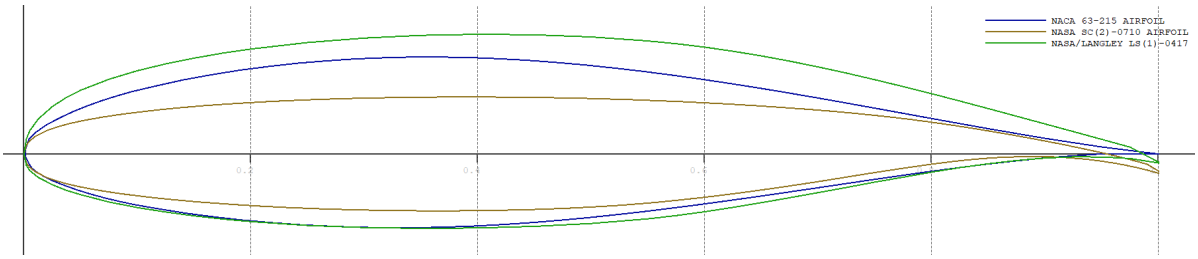

Figure 7.1: *Relative geometry of the selected airfoils. With the thickness of the airfoil on the vertical axis and the chord on the horizontal axis.*

With the use of XFLR5, drag polars and lift curves for all three airfoils were made which can be seen in Figure 7.2 and Figure 7.3. From these two graphs, it is extracted that the SC(2)-0710 and LS(1)-0417 perform better towards the CHEETAH design, as from Figure 7.3 it is found that these two airfoils have a higher lift over drag ratio, which is preferable as drag is favoured to be minimal. Another requirement set for the airfoil was to produce relatively high lift at angles of attack close to 0 deg since the wing is expected to experience an induced angle of attack by the rotor which will reduce the effective angle of attack with respect to the free stream velocity. This phenomenon is further elaborated upon in Section 7.4.

[1] ChatGPT, https://chatgpt.com/

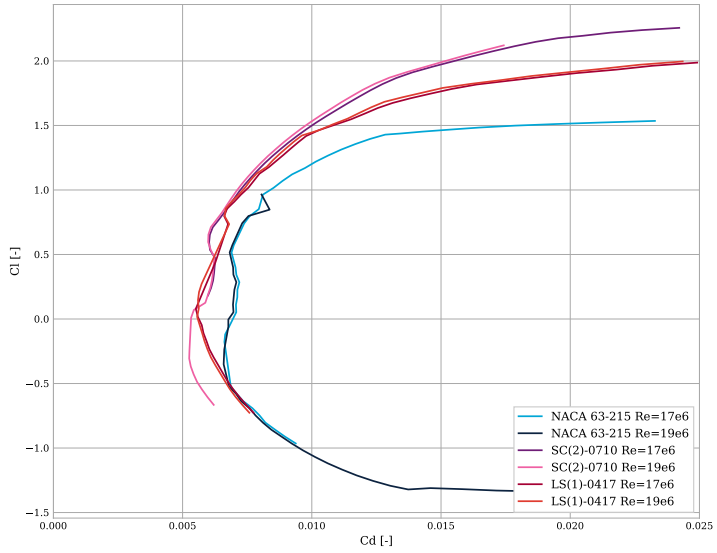

Figure 7.2: *Relation between lift and drag coefficients for selection of airfoils*

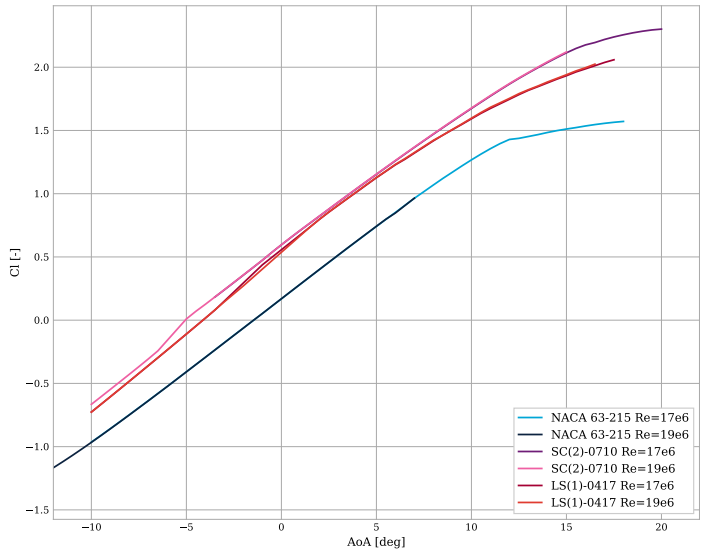

Figure 7.3: *Relation between lift coefficient and AoA for selection of airfoils*

Furthermore, from Chapter 8 it is deduced that the wing will require a negative moment coefficient to ensure stability. Therefore, from Figure 7.4, together with the previous two plots concerning lift and drag, it can be concluded that the NACA63-215 is significantly less suitable and can be discarded. However, making a selection between the SC(2)-0710 and the LS(1)-0417 might need some further analysis.

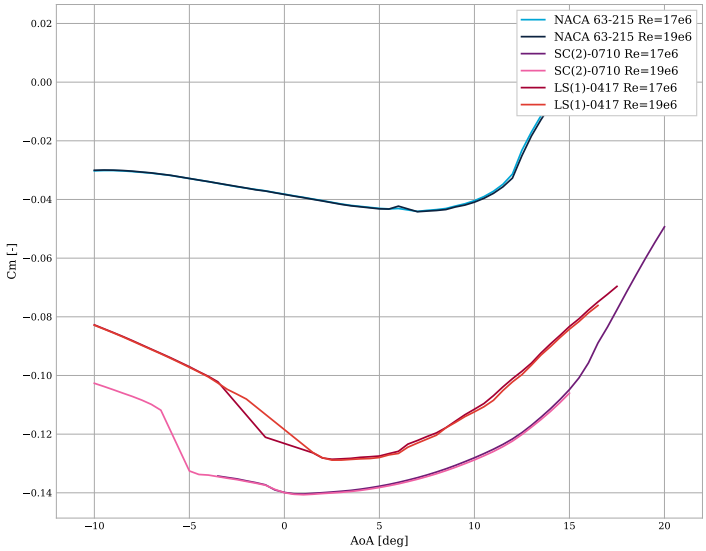

Figure 7.4: *Relation between moment coefficient and AoA for selection of airfoils*

With the NACA63-215 discarded, the focus can be laid towards the other two airfoils for which the pressure coefficient are plotted over the chord of both airfoils at Reynolds number $1.7 \cdot 10^7$ at angles of attack $-1°$, $3°$, and $5°$. These plots can be seen in Figure 7.5.

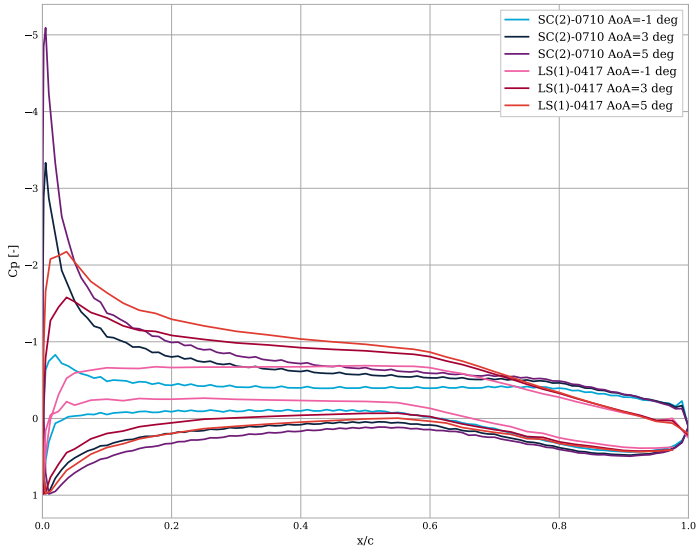

Figure 7.5: *Plot of the pressure coefficient over the chord for the SC(2)-0710 and LS(1)-417 airfoils at Reynolds number 17e+06 at angles of attack $-1°$, $3°$ and $5°$.*

From this graph, it is noted that the SC(2)-0710 has a relatively high-pressure peak at the leading edge of the airfoil, while the LS(1)-0417 seems to have its pressure field more levelled out over the whole chord. The concern is that this higher pressure peak of the SC(2)-0710 will be more prone to interference between the

upper and lower wing of the box wing design. However, since no proper literature regarding this matter was found, no conclusion can be drawn on this contrast between the two airfoils.

Since the other subsystems' calculations do depend on the airfoil selection, a choice was made even though no clear significant aerodynamic differences were found. The LS(1)-0417 has been selected, as the geometry seen in Figure 7.1 would allow for more structural rigidity and space for fuel and control surfaces in respect to the relatively thin SC(2)-0710 airfoil. Therefore, LS(1)-0417 and its properties will be considered for other calculations and design choices.

7.3. Box Wing Characteristics

Contributors: Sjoerd
Authors: Sjoerd

One of the most unique parts of the wing system is the box wing design. This box wing design entails a bi-wing design of two vertically distributed unstaggered wings with dihedral and anhedral angles such that the wing tips, which run into the tip propellers, form a wing geometry.

The incorporation of the wing box for a compound helicopter design was inspired by the Airbus RACER which took its maiden flight in April of 2024 [2]. It is therefore a proven concept, however, it is also very complex and not a lot of studies have been done regarding this specific and unique box wing design. Therefore, selecting the box wing was an aerodynamically challenging choice that comes with several risks and uncertainties as high-fidelity Computational Fluid Dynamics (CFD) software or wind tunnel tests are out of the project's scope.

For the scope of this project, the resources were aimed towards tools that can be used in the limited amount of time available, such that the best attainable understanding and confidence level of a (triangular) box wing design could be reached. These tools include literature research on similar box wing designs and aerodynamic modelling using the XFLR5 software [39].

The box wing design comes with its aerodynamic advantages and disadvantages. The most notable advantage is the reduction of induced drag by obstructing the induction of wing-tip vortices [40]. According to research [33] this reduction of induced drag can go up to 43% for an ideal box wing design. This is an approach which is already widely used in the aerospace field through wing-tip devices which reduce the effect of interference between pressure fields on the top and bottom side of the wing from interfering [41] with one another.

Furthermore, upwash angles could be considered as they can influence the effective angle of attack experienced by a wing. This effect is shown in Figure 7.6 and one can expect that, in the case of another wing right above the one shown, this upper wing would experience a higher effective angle of attack.

Figure 7.6: *Upwash effect of an airfoil.*[3]

Gathering all interfering effects, the efficiency of the lift distribution for a box wing design depends significantly on the height-to-span ratio as found by Prandt. An approximation of this efficiency can be found using Equation 7.3 [33]. Where h/b represents the vertical distance between both wings' surfaces over the total span and e represents the aerodynamic efficiency of a bi-plane. It is noted that a higher height-to-span ratio results in a more efficient lift distribution, which was also expected as this would most likely result in less interference between the pressure fields of both wings. The equation was set up using empirical data and can be used for decision-making regarding box wing geometry.

[2] Airbus2024Racer, https://www.airbus.com/en/innovation/disruptive-concepts/disruptive-design/racer
[3] https://qph.cf2.quoracdn.net/main-qimg-3ff2928d1ac644912a9d692d45bd39f8 [Retrieved 16 June 2024]

$$\frac{1}{e} \approx \frac{1 + 0.45\left(\frac{h}{b}\right)}{1.04 + 2.81\left(\frac{h}{b}\right)} \tag{7.3}$$

As CHEETAH will require the upper and lower wing tips to converge towards each other the height-over-span ratio is not a fully free design parameter. However, it was taken into account by spacing the wingtips 0.4 m apart and connecting them through the engine fairing instead.

Finally, to get some preliminary predictions on the aerodynamic interaction between the upper and lower wing of the box wing design, an XFLR5 simulation was done. The representation of the simplified geometric model can be seen in Figure 7.7 and the lift distribution over these wings is plotted in Figure 7.5. The figure shows the lift-over-span distribution of two different tests. The main test included the box wing as shown in Figure 7.7, while there was also a benchmark test posed which was just a simulation of the lower wing during the same free-stream conditions.

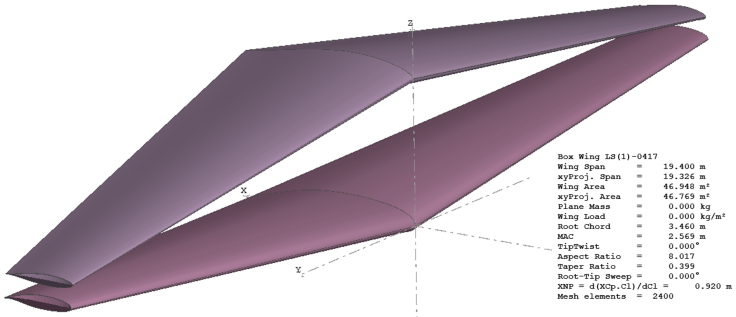

Figure 7.7: *Box wing geometry for aerodynamic analysis using XFLR5.*

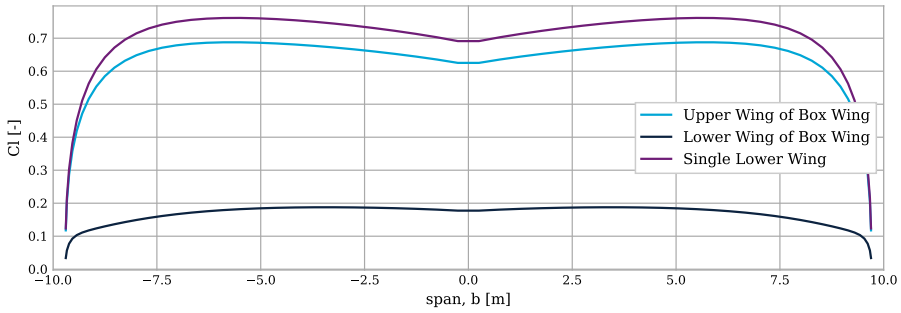

Figure 7.8: *Lift distribution over a box wing and lower wing design with the LS(1)-0417 airfoil and an AoA of 3 degrees.*

Interesting to see in Figure 7.8 is that the lower wing seems to produce a significant amount less lift in the box wing set-up, which is definitely something to look into. However, the validity of this result is debatable since similar box wing studies using high-fidelity CFD software [42] have proven otherwise.

7.4. Aerodynamic Interference

Contributors: Sjoerd
Authors: Sjoerd

The unique aircraft design incorporates a relatively large amount of aerodynamic elements as it combines helicopter and fixed-wing design elements. Moreover, as mentioned in Section 7.3 the design incorporates a box wing design, which also comes with its complications. Summing up all aerodynamic elements, CHEETAH is designed with a main rotor, a fuselage, a box wing, puller propellers and an empennage including horizontal and two vertical stabilisers. In this section, the rotor-wing interference and propellor-wing interferences will be discussed.

Rotor-Wing interference

The most critical element interference was found to be the influence of the main rotor on the wing. This has to do with the main rotor's induced velocity, which significantly influences the incoming velocity vector as seen by the wing leading edge. For example, consider cruise conditions at MTOW where the main rotor provides 8% of the required lift. To calculate the induced velocity by the rotor, Equation 7.4 is used.

$$v_i = \sqrt{\frac{T}{2A\rho}} \tag{7.4}$$

Where v_i is the induced velocity, T is the main rotor thrust or 8% of the total required lift, A is the disk area of the rotor and ρ is the air density at cruise altitude. This results in an induced velocity, normal to the rotor disc, of 17.2 m/s. This induced velocity then decays as it moves further from the rotor and it will do that with a factor as calculated in Equation 7.5 [43]. With T being the thrust generated by the rotor and r being the disk radius of the rotor.

$$V_{\text{i,distance}} = \frac{V_{\text{i,rotor}}}{\left(1 + \frac{h}{2r}\right)} \tag{7.5}$$

Utilising Equation 7.4, Equation 7.5 and the cruise velocity of 400 km/h. The induced velocity angles by the rotor during the cruise are computed by the visualisation of Figure 7.9 and its results are shown in Table 7.2.

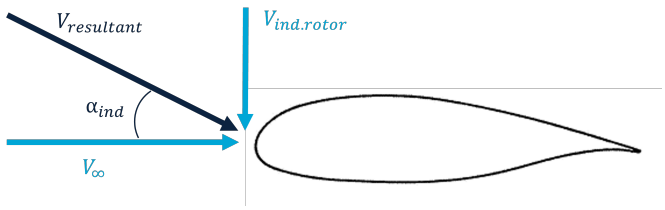

Figure 7.9: *Representation of the induced angle of the rotor on the wing.*

Table 7.2: *Induced angle of attack on the wing by the induced velocity of the rotor during cruise.*

Location	**Induced angle [°] in cruise,** V_∞ = 400 km/h	**Induced angle [°] at** V_∞ = 300 km/h
Upper Wing Root	-2.82	-9.28
Upper Wing Tip	-2.52	-8.31
Lower Wing Root	-1.92	-7.58
Lower Wing Tip	-2.05	-8.10

The induced angles for cruise conditions in Table 7.2 (V_∞ = 400 km/h) seem manageable by for instance designing CHEETAH with a constant AoA. However, in a simple sensitivity analysis at a horizontal velocity of 300 km/h which will be experienced during the transition phase between hover and cruise. It is already noted how much this increases the induced angle, as the induced velocity increases while the free stream velocity decreases. Figure 7.9 visually represents how these velocity alterations will indeed increase the induced AoA. As a side note, the induced velocity vector of the rotor experienced by the wing will be slightly smaller due to the anhedral or dihedral angles. However, by the small angle approximation, this effect is neglected.

Propeller-Wing interference

Besides the main rotor-wing aerodynamic interference, there is also interference between the pusher propellers and the wing since these also produce induce velocities. By Equation 7.4, this induced velocity during cruise conditions will approach 38 m/s which will ensure a local peak in velocity in the wake of the propellers. Consequently, the related wing section will generate more lift by the physics of the lift equation, Equation 7.1, or the increased velocity will cause flow separation over the airfoil, decreasing the local lift.

The induced velocity as mentioned upon now is the normal induced velocity as it is induced normal to the rotor or propeller disks. There is, however, also a tangential induced velocity which is more or less the rotational velocity in the wake of the propeller blades [44]. By literature research, this velocity should not surpass a factor of 0.1 of the normal induced velocity [45], but it does also cause a local induced angle of attack of up to 1.43° in cruise conditions.

Another look should be given to local increases in angles of attack and velocities around the pusher propellers on the wing. With the goal of understanding and optimising the altering aerodynamic conditions on specific sections of the wing.

7.5. Drag Estimation

Contributors: Jorrit
Authors: Jorrit

To further analyse power requirements and verify our engine selection, more accurate drag estimations have to be made. Two methods were proposed to calculate these values: CFD and using statistical methods to estimate the drag of the aircraft. A CFD analysis would likely be the most accurate when executed properly, but would be very time and resource intensive. Using statistical methods would be less accurate, especially with a unique aircraft configuration like CHEETAH.

CFD analysis

To obtain the most accurate values possible without having to do any physical testing, the decision was made to make use of CFD. The solver Ansys Fluent was therefore used to predict CHEETAH's drag. Due to the nature of the created Computer-aided Design (CAD) model, which was not built with CFD in mind, the meshing tool in Ansys did not create a working mesh. Therefore the fuselage, cockpit and tail were analysed in Fluent separately from the boxwing.

The setup used in Fluent was a velocity inlet, pressure outlet system, with far-field outer walls. The fuselage walls had a no-slip condition. The chamber's size was made large enough such that there would be little to no interference from the body on the incoming streamlines, which in this case was taken to be 2 fuselage lengths ahead of the nose of the cockpit. The side and top walls had a distance of 1 fuselage width and 1 fuselage height to the body respectively. The mesh consisted of $1.7 \cdot 10^6$ elements.

The CFD was a Reynolds Averaged Navier Stokes (RANS) simulation with a Spalart–Allmaras turbulence model that ran for 100 iterations. The number of iterations was chosen by analysing the residuals on trial simulations locating after how many iterations convergence occurred. From that, an extra margin of 25% was included in the number of iterations.

After running the simulation, the mesh was inspected again and deemed too inaccurate. The size of the elements meant that the boundary layer would not be represented accurately, which meant that the results of the simulation were not usable. In Figure 7.10 the mesh of the wing is shown. The leading edge of the wing does have a mesh that can be considered accurate enough for the purposes of our simulation. However, the trailing edge has elements that are too large to accurately represent the boundary layer passing over the wing. [46]

Due to these issues with the mesh, a different approach was taken to estimate the drag of the vehicle. The box wing was analysed in XFLR5 and the drag of the fuselage and cockpit were estimated using statistical methods.

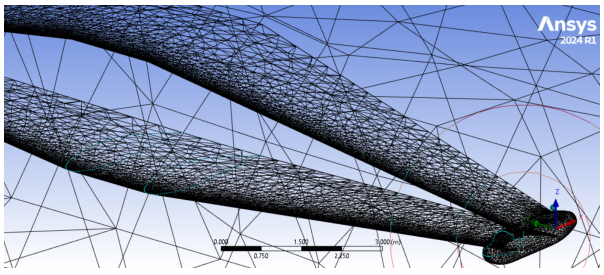

Figure 7.10: *The mesh for the box wing simulation.*

XFLR5

The aerodynamic modelling software XFLR5[39] has already been mentioned in Section 7.3, where it was used to simulate the lift distribution over the wing. In the same matter, the drag was also computed to be 19 kN in cruise conditions. XFLR5 was chosen in the first place since it is a widely validated program that should be able to accurately predict lift and drag values and coefficients for wing designs. However, because the box wing design is still unconventional and because Section 7.3 already posed some doubt on the validity of the lift distribution, uncertainties are still present and more accurate analysis is required if more confidence on the wing drag is required in the future. Furthermore, in Figure 7.7 it can be noted that the wing tips are not connected while it is expected that this connection would reduce the induced velocity by the reduction of wing tip vortices.

Rotor Drag

As described in Chapter 6, the distribution of the drag over the rotor blades and every azimuth angle is known. The drag of the rotor is computed by summing the drag of every element and only considering the related drag components that point in the direction of the flow. The shaft of the rotor, with its cylindrical shape, generates some drag as well but is neglected due to its minimum impact. It is important to remember that, when the drag of the rotor is added to the drag of the aircraft, the power required to overcome this drag is not counted for both the rotor in the model created in Chapter 6.

Statistical Analysis

With the results from the CFD simulation not accurate enough to use, a statistical approach was used to determine the drag of the fuselage. Equations for predicting the fuselage drag were taken from [47]. The drag coefficient for the fuselage can be calculated with:

$$C_{\text{D,fuselage}} = R_{\text{wf}} C_{\text{f,fus}} \left(1 + \frac{60}{\left(\frac{l_f}{d_f}\right)^3} + 0.0025 \left(\frac{l_f}{d_f}\right) \right) \frac{S_{\text{wet,fus}}}{S} \tag{7.6}$$

- R_{wf} is a wing interference factor. From Roskam's aircraft design a value of 1.05 was found. [47]
- $C_{f_{\text{fus}}}$ is the turbulent flat plate skin friction coefficient of the fuselage. For CHEETAH this value is 0.0035.[47]
- l_f is the length of the fuselage.
- d_f is the maximum diameter of the fuselage.
- $S_{\text{wet,fus}}$ is the wetted area of the fuselage.
- S is the wing area.

For this calculation, the fuselage was assumed to be a box with width 2.5 m and height 2.6 m and length 8.6 m. The lift-induced drag was neglected for the fuselage as well, as preliminary calculations for this came out to an insignificant magnitude compared to the zero-lift drag. The drag coefficient for the fuselage was then calculated to be 0.0101.

As the reason for making the drag estimation is for choosing the forward-facing propellers, a calculation was made for the drag at the required 400 km/h at a cruise altitude of 3500 m. The air at cruise altitude has a density of 0.863 kg/m^3.[1] The frontal area of the fuselage of CHEETAH is 6.5 m^2. This could then be added to the drag values obtained from the simulation of the box wing and the obtained drag from the rotor sizing.

$$D = \frac{1}{2} \rho V^2 S C_D \tag{7.7}$$

$$D = D_{\text{fuselage}} + D_{\text{wing}} + D_{\text{rotor}} = 32.2 \text{ kN} \tag{7.8}$$

The total drag CHEETAH will experience during cruise will therefore be 32.2 kN.

[1] ISA Calculator, https://aerotoolbox.com/atmcalc/

7.6. Discussion

Contributors: Sjoerd
Authors: Sjoerd

To conclude the chapter on aerodynamics, it is still an aircraft characteristic with a lot of uncertainties. These uncertainties stem from the wide range of unique aspects that have to do with the CHEETAH design and the interconnection between these aspects, which do not always have published research. The main takeaways and further recommendations will be discussed briefly.

The main risk of the design seems to originate in the rotor-wing interference. In Section 7.4 it was found that, especially in the transition phase, the wing will experience significant induced angles of attack due to the normal induced velocity of the main rotor. This effect has been taken into account by choosing an airfoil that can already generate lift at low angles of attack and the design choice to give the wing a standard angle of attack. To move further, High-lift Devices (HLDs) might be considered. Also, the normal induced velocity has been determined by the use of the moment theory. In practice, the induced velocity is expected to vary over the disk area and the upper wing might protect the lower wing slightly from the induced velocity. A more detailed analysis would be required for more confidence.

Regarding the aerodynamic efficiency, the wing will have to be analysed and designed locally. The interaction of several elements like propellers, fuselage, rotor and the two wing platforms causes local differences in effective angles of attack and velocity. Designing with certain twist angles over the wing is expected to optimise the local sections for their specific conditions.

All of these aerodynamic design iterations should afterwards be analysed using high-fidelity CFDs and wind tunnel tests to increase the confidence of all the aerodynamic properties. The calculations up until now have taken into account relatively high margins. If there is more confidence in the values calculated so far, these margins can be reduced to converge the CHEETAH design towards an optimum.

8 | Stability and Control Characteristics

To have a safe aircraft with comfortable handling qualities it should preferably be statically and dynamically stable in both hover and forward flight. Aerial firefighting is really demanding on the pilots so the aircraft should be easy to handle. The location of the centre of gravity has great influence on this so that is determined first. CHEETAH should be stable in hover, where it will need precise manoeuvring for the water pumping, and in forward flight, where it will encounter turbulent environments above the fires, so the stability is analysed for both cases. After this, the ground stability will be analysed to prevent tip-over. Lastly, the control surfaces will be treated as the aircraft should be manoeuvrable because of the high demands placed on it in the firefighting mission.

8.1. Centre of Gravity

Contributors: Marinka
Authors: Marinka

The Centre of Gravity (CG) can be found using a moment balance where the sum of the product of all the forces and their arms is taken about a reference point at the front and bottom of the fuselage and divided by the total weight. The datum is the front of the fuselage for the x-coordinate and the bottom of the fuselage for the z-coordinates which are the red lines in Figure 8.1. The blue area indicates the water tank and the orange the fuel tank.

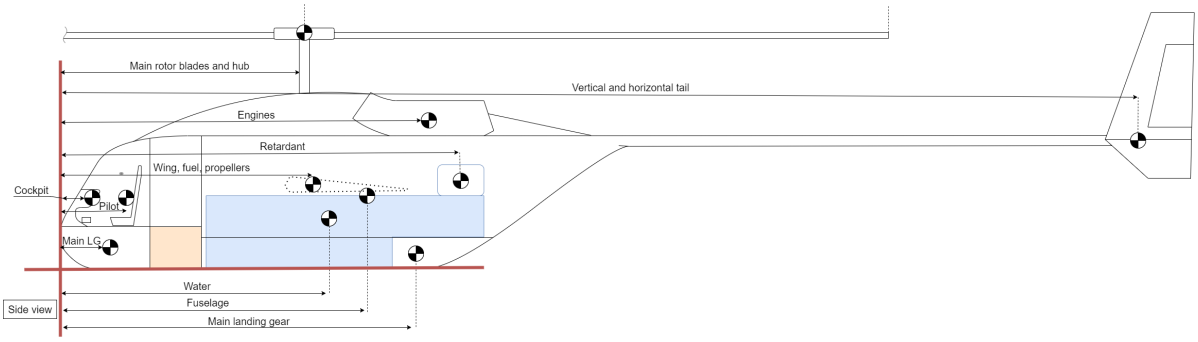

Figure 8.1: *Locations of the datum with red lines and the CG locations*

The weight is dependent on the subsystem dimensions or MTOW so it is an iterative process with calculating the subsystem weight and then recalculating the MTOW until convergence. The estimation was done using statistical equations from Prouty [25]. The procedure can be found in Section 10.4 in more detail. A program was set up to perform this process and find the converged centre of gravity. The values in Table 8.1 are the final values for the weights and locations of several subsystems.

Table 8.1: *Final CG inputs with distances measured from the red datum lines.*

Subsystem	X-location [m]	Y-location [m]	Z-location [m]	Mass [kg]
Main rotor blades	4.8	0	3.3	1200
Main rotor hub	4.8	0	3.3	1500
Wing	4.6	0	1.2	3700
Engines	5.2	0	2.9	2000
Starboard propellers	4.6	8.5	1.2	200
Portside propellers	4.6	-8.5	1.2	200
Nose landing gear	1	0	0.5	210
Main landing gear	6.8	0	0.5	410
Horizontal tail	21.1	0	2.6	80
Vertical tail	21.1	0	2.6	60
Fuselage	5.6	0	1.3	4100
Cockpit	1.1	0	1.3	1900
Pilots	1.25	0	1.3	200
Fuel tank	4.6	0	1.2	800
OEW	**4.65**	**0**	**2.1**	**16300**
Water	4.9	0	0.77	11500
Retardant	7.55	0	1.65	1000
Fuel	4.6	0	1.2	6700
MTOW	**4.8**	**0**	**1.5**	**35500**

An important side note for this table is that the values have been rounded so the values might not properly add up to the total weight. During iterations the rotor was shifted back by 70 cm to ensure that it would be practically above the CG at MTOW with full water tanks.

8.2. Static Stability

Contributors: Marinka
Authors: Marinka

Static stability means that the system will return to an equilibrium situation when disturbed from it. Static instability greatly reduces the handling qualities because that means the pilot constantly has to input corrections.

8.2.1. Hover

From Table 8.1 it can be seen that the CG is 1-15 cm in front of the rotor. This results in a longitudinally statically stable aircraft. When the aircraft pitches up due to a gust the lift gives a restoring moment. In case of a headwind gust on our counterclockwise rotating rotor, the left side will see a reduction in lift and the right side an increase in lift which causes flapback. The rotor thrust tilts backwards a little which reduces the airspeed again and the rotor tilts forward again. The CG is aft of the wing but a gust results in a bigger lift increase of the tail compared to the main wing so a pitch back moment is still present.

In hover, there is also a large torque caused by the rotor. This torque causes a yaw moment which is usually compensated by a tail rotor. In the design, the yaw is counteracted by applying differential thrust on the propellers. One set of propellers provides forward thrust while the other set provides reverse thrust. Like this, the aircraft can also climb without yawing due to rotor torque. In case of one propeller inoperative, there is still enough thrust to counteract the main rotor torque. If a disturbance moves the nose right the left propeller will see an increased incoming airspeed which increases the thrust on that side and in turn is destabilising. However, the tail will move left which will cause a force to the right by the vertical stabiliser to compensate. The arm of this moment is so big that it will be able to compensate for the disturbance.

Lastly, the helicopter is roll-stable in hover because of the damping effect of the wing and vertical fin.

8.2.2. Forward Flight

In forward flight, the helicopter can be made statically stable in the longitudinal direction using the horizontal tail. The minimum size of the tail is found by setting up a scissor plot and inserting the CG range. This was done at multiple speeds and it turns out that lower speeds are more limiting since the lift curve slope of the airfoil of the horizontal stabiliser is higher and it thus produces more lift more quickly at higher speeds. The horizontal stabiliser is sized for 150 km/h. At lower speeds than this, the rotor is the main lift producer and will be used to provide pitch stability using a control system similar to hover.

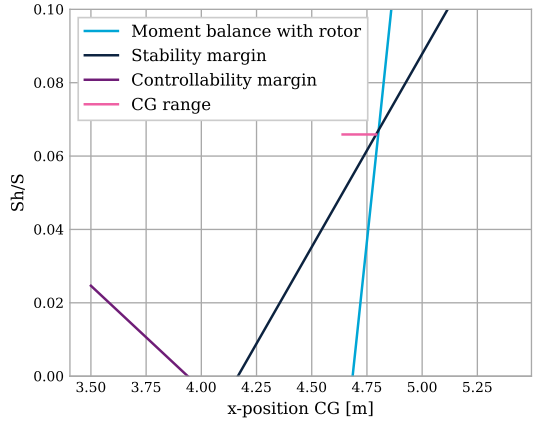

Figure 8.2: *Control and stability at 150 km/h.*

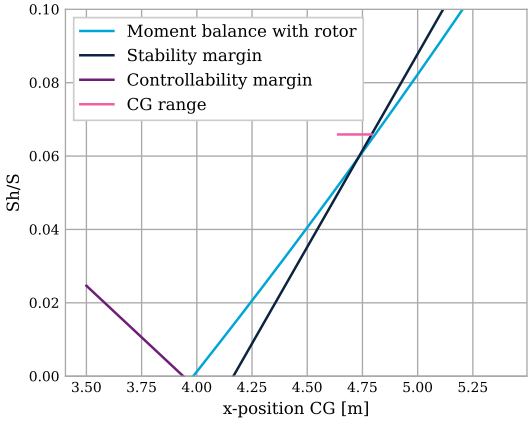

Figure 8.3: *Control and stability at 400 km/h.*

The moment balance with the rotor is derived from setting the moment around the CG to zero and rewriting to solve for the ratio between the horizontal tail and wing area. This yields Equation 8.1.

$$\frac{S_h}{S} = \frac{C_{m_{ac}}\bar{c} + C_l(x_{CG} - x_{ac}) + \frac{T_r}{q_w S}(x_{CG} - x_r)}{C_{l_h}\left(\frac{V_h}{V}\right)^2 (x_{emp} - x_{CG})} \tag{8.1}$$

In this equation S_h is the horizontal tail area, S the wing area, $C_{m_{ac}}$ the wing moment around the aerodynamic centre, $\bar{c}$ the mean aerodynamic chord of the wing, C_l the wing lift coefficient, T_r the rotor thrust, q_w the wing dynamic pressure and C_{l_h} the tail lift coefficient. The stability curve without the rotor is derived from the changes in lift acting at the neutral point due to a change in the angle of attack. The rotor was eliminated here since the effect of a change in the angle of attack on the lift was too complicated to analyse at this stage. The expectation is that the rotor lift would slightly increase. However, due to the small moment arm between the CG and the rotor this will probably not contribute a lot. When rewritten the equation Equation 8.2 becomes.

$$\frac{S_h}{S} = \left(\frac{1}{\frac{C_{l_{\alpha_h}}}{C_{l_\alpha}}\left(1 - \frac{d\epsilon}{d\alpha}\right) l_{h-np}\left(\frac{V_h}{V}\right)^2}\right) x_{CG} - \frac{x_{ac} - SM}{\frac{C_{l_{\alpha_h}}}{C_{l_\alpha}}\left(1 - \frac{d\epsilon}{d\alpha}\right) l_{h-np}\left(\frac{V_h}{V}\right)^2} \tag{8.2}$$

For control, Equation 8.1 was used but instead of the normal lift coefficient a C_{l_h} of $-0.35S_h^{1/3}$ was used which is the maximum for a fixed tail [48]. In this equation C_{l_α} is the lift curve slope, $\frac{d\epsilon}{d\alpha}$ the downwash gradient, l_h the tail arm and the Stability Margin (SM). In Figure 8.2 it is clear that stability is the biggest issue here and controllability will not be much of an issue in forward flight. After an iterative process with the tail area, tail weight and CG location, an optimal area of 6 m^2 is found for the horizontal tail area. This is also able to provide the stability needed during a drop when the CG shifts forward by 15 cm. This sudden shift will cause a pitch forward which will cause an extra angle of attack for the rotor which then tilts back and has a restoring moment. Then the aircraft can also be trimmed for the new CG using the elevator.

The vertical tail was sized to alleviate the differential thrust and provide yaw stability. At maximum speed, the vertical tail can easily counteract the main rotor torque as this is low at that point and the velocity is high

which gives a bigger side force. The torque produced by the rotor is plotted against the counter-torque that the vertical tail will provide at several speeds in Figure 8.4 below. The rotor torque was found from the rotor analysis at various speeds and the side force produced by the vertical tail was found by treating it as a wing and finding the lift.

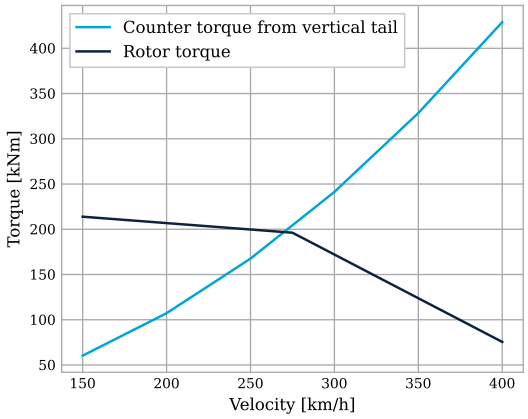

Figure 8.4: *Vertical tail torque versus rotor torque at different velocities.*

Here it is clear that starting at 270 km/h the vertical tail will completely take over and no more differential thrust is needed. Before this point, there is enough power of the engines to provide some differential thrust and still have enough power to reach this speed.

8.3. Dynamic Stability

Contributors: Marinka
Authors: Marinka

Even if an aircraft is statically stable it can still be dynamically unstable so this will also have to be analysed. To do this, the equations of motion are set up, derivatives are taken and rewritten to matrix form.

8.3.1. Hover

To simplify the analysis, the equations of motion matrix for hover and the stability derivatives were taken from Prouty [25]. Here it is assumed that in hover the longitudinal and lateral-directional coupling is weak enough to be ignored. All stability and control derivatives were only taken from the main rotor as this is the main factor influencing the stability in hover. Furthermore, all the values in the following equations are given in imperial units. The mass moment of inertia of the entire aircraft is still unknown so it is assumed they are similar to those of the Sikorsky CH53E Super Stallion.

The characteristic equation which is found by expanding the determinant of the matrix is given by Equation 8.3.

$$\begin{aligned} s^4 - \left[\frac{1}{MTOW}\left(\frac{\partial X}{\partial \dot{x}} + \frac{\partial Z}{\partial \dot{z}}\right) + \frac{1}{I_{yy}}\frac{\partial M}{\partial q}\right] s^3 + \frac{\partial Z}{\partial \dot{z}}\left[\frac{1}{MTOW^2}\frac{\partial X}{\partial \dot{x}} + \frac{1}{MTOW\, I_{yy}}\frac{\partial M}{\partial q}\right] s^2 \\ + \frac{g}{I_{yy}}\frac{\partial M}{\partial \dot{x}} s - \frac{g}{MTOW\, I_{yy}}\frac{\partial M}{\partial \dot{x}}\frac{\partial Z}{\partial \dot{z}} = 0 \end{aligned} \tag{8.3}$$

In this equation, MTOW is the maximum take-off mass. X and Z are the forces in the x- and z-direction, M the moment around the y-axis, I_{yy} the mass moment of inertia around y and q the pitch rate. All the derivatives are used as described in Table 9.1 and 9.2 of [25]. A table with the used inputs for these derivatives is given below in Table 8.2.

Table 8.2: *Values for dynamic stability in hover at sea level.*

Variable	Symbol	Value	Unit
Maximum take-off weight	MTOW	35 500	kg
Density	ρ	1.225	kg/m^3
Blade area	A_b	64.4	m^2
Rotational speed	Ω	18.685	rad/s
Blade radius	R	11.5	m
Thrust coefficient ratio	$\frac{C_t}{\sigma}$	0.029	-
Rotor blade lift slope	a	0.1	1/deg
Twist at 0% span	θ_0	5	deg
Twist at 75% span	$\theta_{.75}$	4.685	deg
Twist at 100% span	θ_1	4.58	deg
Induced velocity	v_i	18.5	m/s
Solidity	σ	0.155	-
Induced efficiency factor	e	0.8	-
Lock number	γ	13.4	
Rotor height	h_M	3.2	m
Pitch moment of inertia [49]	I_{yy}	270 000	kg·m^2
Yaw moment of inertia [49]	I_{zz}	250 000	kg·m^2
Torque coefficient ratio	$\frac{C_Q}{\sigma}$	0.0012	-

Using Python the roots of Equation 8.3 are found to be a complex pair -1.67+2.58j and -1.67-2.58j and the real roots 2.82+0.j and 0.013 +0.j. These values seem large compared to other helicopters but at least they are a good indication of the sign of eigenvalue. This means CHEETAH is dynamically stable in longitudinal direction in one mode and unstable in two modes. An automatic control system will have to be implemented to stabilise the helicopter.

In lateral direction, it is also assumed that the mode is entirely decoupled from the longitudinal direction which results in Equation 8.4. In this equation N is the moment around the z-axis, r the yaw rate and I_{zz} the area moment of inertia around the z-axis.

$$s = \frac{\partial N}{\partial r}\left(\frac{1}{I_{zz}}\right) \tag{8.4}$$

Filling in the derivatives from Prouty results in an eigenvalue of -0.7 which means dynamic stability in hover.

8.3.2. Forward Flight

In forward flight, the stability of a helicopter is not governed by the main rotor anymore as the fuselage, tails and, in our case, the wing also start playing a major role in the stability. The decoupling of longitudinal and lateral-directional modes is not valid anymore as they have a large influence on each other in helicopters. This would mean solving a system of 6 equations to find the eigenvalues for forward flight which is more complicated. Instead of this approximate solutions are used for several stability modes. Also the effects of the main rotor are ignored because in this case the analysis will be done for 400 km/h and there are too many unknowns related to flapping to get an accurate result for those derivatives. All the downwash and interference effects of the main rotor that were accounted for in the stability derivatives are also set to zero.

Table 8.3: *Values for dynamic stability in forward flight at 3500 m.*

Variable	Symbol	Value	Unit
Airspeed	V	400	km/h
Density	ρ	0.863	kg/m^3
Horizontal tail area	S_h	6	m^2
Corrected horizontal lift slope [25]	a_h	0.065	deg
Span efficiency factor [25]	δ_i	0.03	-
Velocity ratio with wing [25]	$\frac{V_h}{V_i}$	2	
Horizontal tail effective aspect ratio [25]	AR_h	7.8	
Zero-lift drag coefficient NACA 0015	$C_{d,0_h}$	0.00634	
Downwash due to winged fuselage [25]	$\frac{d\epsilon_F}{d\alpha_F}$	0.41	
Vertical tail area	S_v	10	m^2
Vertical tail aspect ratio	AR_v	2	
Wing surface	S	94	m^2
Wing drag coefficient	C_{d_w}	0.040	
Roll moment of inertia	I_{xx}	56000	kg·m^2

Starting with the phugoid, it is assumed that there is little change in angle of attack which means the equation in Z-direction drops out. This results in the following characteristic equation.

$$\begin{aligned} &I_{yy}s^3 - \left(\frac{I_{yy}}{MTOW}\frac{\partial X}{\partial \dot{x}} + \frac{\partial M}{\partial q}\right)s^2 \\ &+ \frac{1}{MTOW}\left[\frac{\partial X}{\partial \dot{x}}\frac{\partial M}{\partial q} \quad + \left(\frac{\partial X}{\partial q} - MTOW\left(\bar{V}\bar{\Theta}\right)\right)\frac{\partial M}{\partial \dot{x}}\right]s + g\frac{\partial M}{\partial \dot{x}} = 0 \end{aligned} \tag{8.5}$$

In this equation V is the average velocity and Θ the average pitch. For the first two derivatives in this equation only the horizontal tail has a significant contribution. $\frac{\partial X}{\partial q}$ drops out as it is only influenced by the rotor.

Finding the roots with Python results in -0.62+0.84j -0.62-0.84j and 0.87+0.j. So it is an unstable mode.

The next mode to be analysed is the short period which has Equation 8.6 as characteristic equation. This assumes that there is no speed change during the motion as it is short.

$$\begin{aligned} &s^2 + \left[\frac{-I_{yy}\frac{\partial Z}{\partial \dot{z}} + \frac{\partial M}{\partial q}\left(\frac{\partial Z}{\partial \dot{z}} - MTOW\right) - \left(\frac{\partial Z}{\partial q} + MTOW\,\bar{V}\right)\frac{\partial M}{\partial \dot{z}}}{I_{yy}\left(MTOW - \frac{\partial Z}{\partial \dot{z}}\right)}\right]s \\ &+ \left[\frac{\frac{\partial Z}{\partial \dot{z}}\frac{\partial M}{\partial q} - \left(\frac{\partial Z}{\partial q} + MTOW\,\bar{V}\right)\frac{\partial M}{\partial \dot{z}}}{I_{yy}\left(MTOW - \frac{\partial Z}{\partial \dot{z}}\right)}\right] = 0 \end{aligned} \tag{8.6}$$

$\frac{\partial Z}{\partial \dot{z}}$ and $\frac{\partial M}{\partial \dot{z}}$ fall out because the downwash of the main rotor on the horizontal tail is set to zero. Solving for the roots yields -5.39+2.28j and -5.39-2.28j.

The next mode is the Dutch roll which has Equation 8.7 as characteristic equation. In this case more assumptions need to be made. The aircraft CG has to follow a straight flight path, the cubic is approximated by a quadratic using Bairstow's method which is an algorithm for finding polynomial roots and $\frac{\partial N}{\partial r}$ and $\frac{\partial N}{\partial \dot{y}}$ are the main derivatives affecting this mode.

$$s^2 - \left(\frac{1}{I_{zz}}\right)\frac{\partial N}{\partial r}s + \frac{\bar{V}}{I_{zz}}\left(\frac{\partial N}{\partial \dot{y}}\right) = 0 \tag{8.7}$$

Evaluating this results in values of -3.59 and 2.56 which means this is unstable.

Lastly, the spiral mode has to be evaluated by finding the sign of Equation 8.8. If it is negative this mode will be unstable.

$$E = \frac{g}{I_{xx} I_{zz}} \left[\frac{\partial R}{\partial \dot{y}} \frac{\partial N}{\partial r} - \frac{\partial N}{\partial \dot{y}} \frac{\partial R}{\partial r} \right] \tag{8.8}$$

Solving this equation gives a result of 1.32 so the aircraft is spiral stable.

8.4. Ground Stability

Contributors: Emma
Authors: Emma

Ground stability is mostly dependent on the design of the landing gear. The first step is to determine the size of the wheels. For wheel sizing for helicopters, both the maximum load per wheel and inflation pressure can be scaled up by a factor of 1.5 compared to the wheel sizing for regular fixed-wing aircraft [50]. The loads on the tires are highest during "regular" horizontal takeoff and landing. The tire inflation pressure and maximum load per tire is based on these conditions. CHEETAH does have a fixed wing, but since it will take off and land vertically and therefore will not experience these limiting loads, the factor of 1.5 is also considered for the tire selection of this compound helicopter. For the sizing of the tires, the method of Torenbeek is used [51]. First, the inflation pressure is determined. Requirement **FTF-SYS-INV-02.4** states: *The aircraft shall be capable of landing on a surface as soft and as wet as boggy grass.* Therefore, the inflation pressure for wet, boggy grass is used. As can be seen in Figure 8.5, this is equal to 2.1-3.2 kg/cm^2 for fixed wing aircraft, and thus equal to 3.15-4.8 kg/cm^2 for aircraft with VTOL capabilities.

TYPE OF LANDING SURFACE	Maximum tire pressure kg/cm^2	lb/sq.in.
Large, properly maintained airports (concrete runway)	8.5 - 14	120 - 200
Small tarmac runway, good foundation	5 - 6.3	70 - 90
Small tarmac runway, poor foundation	3.5 - 5	50 - 70
Hard grass, depending on soil	3.2 - 4.2	45 - 60
Wet, boggy grass	2.1 - 3.2	30 - 45
Hard desert sand	2.8 - 4.2	40 - 60
Soft, loose desert sand	1.8 - 2.5	25 - 35

Figure 8.5: *Tire pressure recommendations for different ground surfaces [51], with the pressure used highlighted in yellow.*

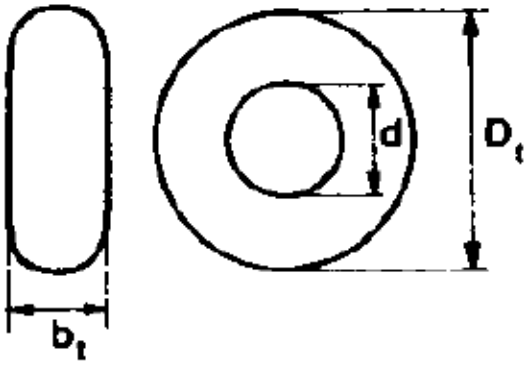

Figure 8.6: *Explanation of the tire code [51].*

Then, the static load per tire is determined. For this, it is assumed that the helicopter will have one nose landing gear strut, with two wheels, and two main landing gear struts, with each two wheels as well. It is assumed that the nose landing gear experiences 1/3 and the main landing gear 2/3 of the weight of the helicopter. With 2 nose wheels and 4 main wheels this means that every wheel experiences the same static load. This assumption is made with the given that for almost all existing helicopters, the same, or almost the same, size nose and main wheels are used, meaning the loads on the wheels are about the same [52]. With the MTOW being 35 500 kg, the load on each wheel is equal to 5925 kg. However, helicopter tires are designed for 1.5 times more weight than fixed wing aircraft. Therefore, the **aircraft**-tire-load that needs to be looked for is 1.5 times lower than the desired **helicopter**-tire-load. This is equal to 3950 kg. To clarify, if the tire under a regular airplane can carry a load of 3950 kg, the tire can carry a load of 1.5 * 3950 kg = 5925 kg under a helicopter.

With the tire pressure and static load determined, the Torenbeek tire sizing plots can be used to find the corresponding tire diameter. The plots can be seen in Figure 8.7 and Figure 8.8. In these plots, the required tire for each combination of static load and inflation pressure is given. The yellow vertical lines show the inflation pressure range and the yellow horizontal line is the load per tire. The only tire that intersects these

values is the **34 x 11.75 - 14** tire, which is highlighted in yellow. Where 34 is the tire diameter D_t, 11.75 is the tire width b_t and 14 is the tire inner diameter d, all given in inches. Clarification of what these dimensions are is given in Figure 8.6. Converting to SI units, the wheels have an outer diameter of 86.4 cm, an inner diameter of 35.6 cm and a width of 29.8 cm.

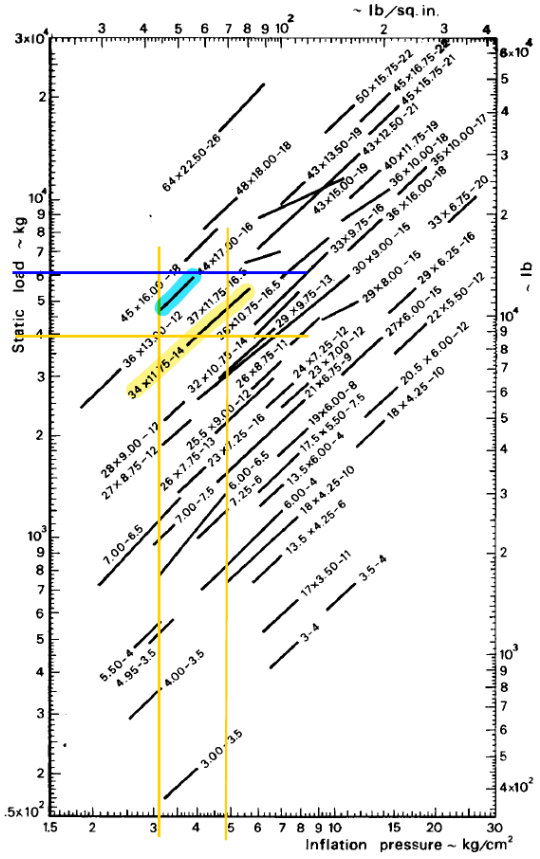

Figure 8.7: *Tire sizing plot: British sizes. [51]*

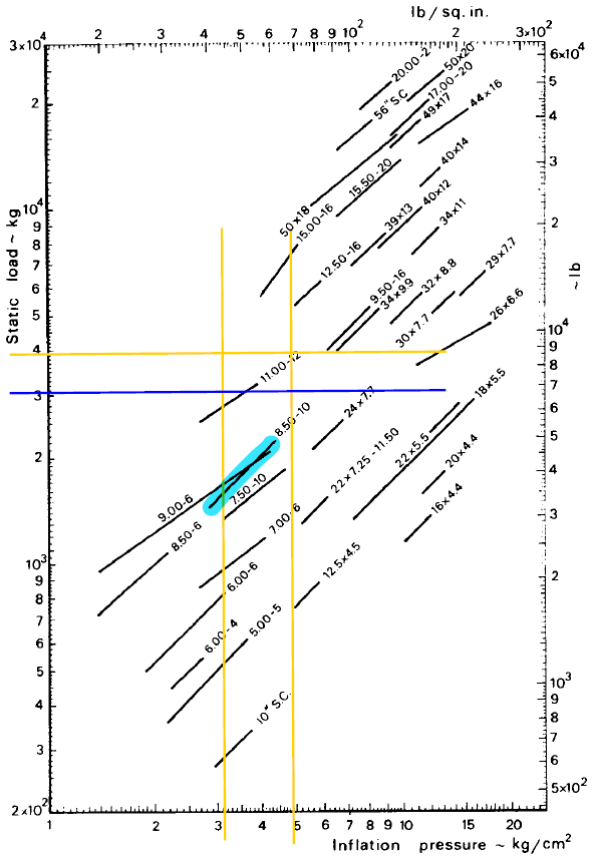

Figure 8.8: *Tire sizing plot: American sizes [51].*

To verify that the Torenbeek method also works for helicopters, two reference helicopters were considered with this method. In Figure 8.7, the blue horizontal line is the load on a single tire of the Mil Mi-26. The Mi-26 has a tire with a diameter of 112 cm and a width of 45 cm [52]. This is equal to 44.1 inch and 17.7 inch respectively. In Figure 8.7, the line corresponding to this tire is highlighted in blue. As can be seen, this almost exactly crosses the blue vertical line, and it also falls within the inflation pressure margins, as this does not change per helicopter. Secondly, in Figure 8.8 the static load per tire of the CH53-E is given with again a blue vertical line. Furthermore, the tire used on the CH53-E is highlighted in blue. Again it can be seen that this tire falls perfectly within the inflation pressure margins. However, the load per tire is less than calculated from the MTOW. This deviation is on the safe side and would allow the wheels to be smaller, rather than having to be larger. Therefore, as for two similar helicopter the method is partially effective, it is for now assumed that the method is sufficient for the sizing of the tires.

Now the size of the of the tires is determined, the placement of the Nose Landing Gear (NLG) and Main Landing Gear (MLG) is considered. To find the placement of the landing gear for the aircraft to be ground stable, the method in the System Engineering & Aerospace Design course is used [48]. With the X and Z location of the centre of gravity as given in Section 8.1 and the X-location of the main landing gear, the X-location of the nose landing gear and the Y-location of the main landing wheels can be determined. The X-location of the main landing gear is limited by the placement of the water tank. Therefore, there is not much margin for this location. By iteration an optimal value for the X and Y positions of the landing gears is found.

To be ground stable, the main landing gear wheels have to be placed quite far away from the Y axis centre

line. They will have to stick out from the fuselage. To minimise the distance they have from the fuselage, the nose wheel should be placed as far forward as possible. This is due to the geometry as given in Figure 8.9. In this figure, the parameters are given by the equations below [48]. For the aircraft to be stable on the ground, $\Psi < 55°$.

$$\Psi = \arctan\left(\frac{z_{LG}}{c}\right) \quad (8.9) \qquad c = b_N \sin(\alpha) \quad (8.10) \qquad \alpha = \arctan\left(\frac{y_{LG}}{d}\right) \quad (8.11)$$

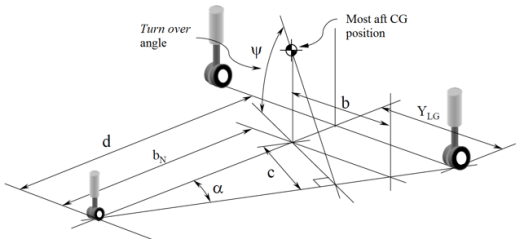

Figure 8.9: *Geometry of the landing gear [48].*

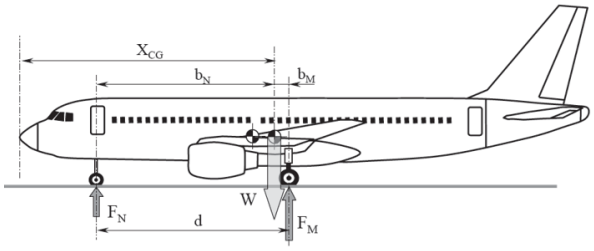

Figure 8.10: *Dimensions of the landing gear[48].*

In Figure 8.10, the necessary dimensions of the landing gear are given. To find the track d, Equation 8.12 from the System Engineering & Aerospace Design course is used [48]. In here, the load fraction is taken as before in the tire sizing and b_M is the X-location of the CG subtracted from the X-location of the main landing gear. These methods result in the following data given in Table 8.4.

$$\frac{F_N}{W} = \frac{b_M}{d} \quad (8.12)$$

Table 8.4: *Landing gear placement dimensions*

Parameter	Symbol	Value [m]
X-position CG	X_{CG}	4.79
Z-position CG (from ground)	Z_{CG}	2.4
Distance CG-MLG	b_M	2.31
Distance NLG-MLG (track)	d	6.93
Distance NLG-CG	b_N	4.62
Y-position MLG	Y_{LG}	2.7
Y-distance of the main landing wheels to the fuselage.		1.45

8.5. Control Surfaces

Contributors: Floris, Marinka
Authors: Floris, Marinka

In forward flight, the control surfaces are used to control the aircraft. At high speed this is more efficient than using the rotor to control the aircraft. The rudder and elevator have not been sized as it was assumed they will not be too big to fit on the tail, but the ailerons have been sized.

Ailerons

In the bachelor Aerospace Engineering at Delft University of Technology, a method for sizing ailerons was presented in the ADSEE-II course [53], and the final equation can be seen in Equation 8.13. This method checks whether the ailerons are sized correctly. As the method includes both a roll rate induced by the ailerons, and a damping coefficient for the wing, it was assumed that for a box wing, the roll rates can be added together.

$$P = -\frac{C_{l_{\delta a}}}{C_{l_P}} \delta_{amax} \frac{2V}{b} \tag{8.13}$$

Where $C_{l_{\delta_a}}$ is the induced roll coefficient, and C_{l_P} is the damping coefficient. $\delta_{a,max}$ is the maximum aileron deflection and V is the airspeed, and b is the wing span. $C_{l_{\delta a}}$ and C_{l_P} can be calculated by using other equations given in that course. It should also be noted that the aileron deflecting downward only deflects 75 %, to minimize the induced yaw, this process is also known as differential ailerons [53]. The large anhedral and dihedral angles are also considered, and the effectiveness of the ailerons is multiplied by the cosine of the respective angles, while the damping is not.

The final aileron dimensions can be found in Table 8.5.

Table 8.5: *Aileron dimensions*

Parameter	Value
Upper Wing	
Aileron start (from wing tip)	2.5 m
Aileron end (from wing tip)	0.3 m
Chord fraction	0.2
Maximum deflection	25°
Lower Wing	
Aileron start (from wing tip)	2.5 m
Aileron end (from wing tip)	0.3 m
Chord fraction	0.2
Maximum deflection	25°

As can be seen, the ailerons are the same in the upper and lower wings, this is done intentionally, as this means that maintenance is easier and fewer parts need to be in storage in order to maintain an aircraft.

8.5.1. Stability sensitivity

Authors: Marinka
Contributors: Marinka

A big portion of the weight of the aircraft is concentrated around the wing which cannot really be shifted because of limits imposed by the end of the fuselage and the door in the front. The main parameter which can easily change and influence the design is the CG of the water. If the water tank is not fully loaded the water could be concentrated towards the back or the front of the tank. Assuming the tank is half-loaded this would mean a CG of the water that is approximately 1.25 m further backwards or forwards. The effect of this shift on the CG of the entire aircraft is plotted below in Figure 8.11.

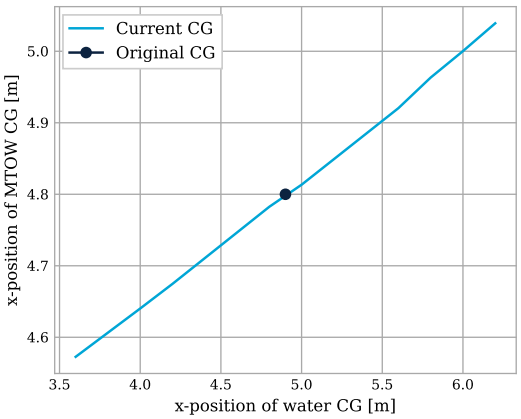

Figure 8.11: *CG location for different water positions*

The MTOW CG shifts approximately 20 cm backwards or forwards due to the shift of the water CG. For hover, a shift backwards of 20 cm would mean static instability due to a CG that is aft of the main rotor. However, 20 cm is still in a range that can be compensated for using the rotor cyclic control[25]. For forward flight, the shift would result in a tail that is 1.3 m^2 bigger which is also an acceptable increase. With this increase in tail area the dynamic stability stays approximately the same with some modes becoming a bit more stable and some a bit more unstable but none of the signs change. In addition to this, the water would realistically be more to the front of the tank if it is only half-filled because the pump and the water doors are in the front. In conclusion, the design is not too sensitive to a change in water CG.

9 | Structural and Material Characteristics

During operation, the firefighting aircraft is subjected to various loads that impose forces and stresses on its structure both in flight and during ground operations. These loads include aerodynamic, gravitational, inertial, ground, dynamic, operation, environmental, and emergency loads. To be able to withstand those loads, it is important to analyse critical aircraft structures and select materials smartly. By understanding the relations between loads, structural integrity, and material properties, the aircraft can be optimised to operate in the challenging conditions a firefighting aircraft is exposed to.

9.1. Structural Characteristics

Contributors: Ruben, Ivo, Xander
Authors: Ruben, Ivo, Xander

From a structural point of view, firefighting aircraft have many characteristics similar to those of general aircraft. This implies that the design and operation of a compound helicopter are known to be feasible and that a comprehensive analysis of all structural systems is not required. For instance, it is known how to size and structurally analyse the compound helicopter's landing gear, which is why this specific analysis is not explicitly conducted in this report. However, what distinguishes CHEETAH is its capability to deploy a payload of 10000 litres of water or retardant. The release of such a substantial load significantly impacts the aircraft's structure, particularly the main rotor blades. With a main rotor radius of 11.5 meters, the water drop exerts considerable influence on the rotor's deflection. Additionally, another interesting structure of CHEETAH is the box wing configuration that delivers lift during the cruise phase. The key points of interest for this box wing are the distributed forces of lift, the structural weight, and the point forces exerted by the engines. In this section, the rotor blades are analysed first, followed by an analysis of the box wing structure.

9.1.1. Rotor Blade Analysis

The operation of dropping 10000 litres of payload has a huge impact on the structure of the compound helicopter. The main goal of the analysis performed in this chapter is to determine the maximum deflection of the rotor blade caused by the drop.

Model & Assumptions

Since the structure of the rotor blade is complex, a simplified model is made to make the structural calculations less complicated. The rotor blade is modelled as a beam with a specific cross-section, where there is a roll support with a rigid connection at the main rotor hub, as visualised in Figure 9.1. The main rotor blade tip, defined as R in this coordinate system, is modelled as a pin connection.

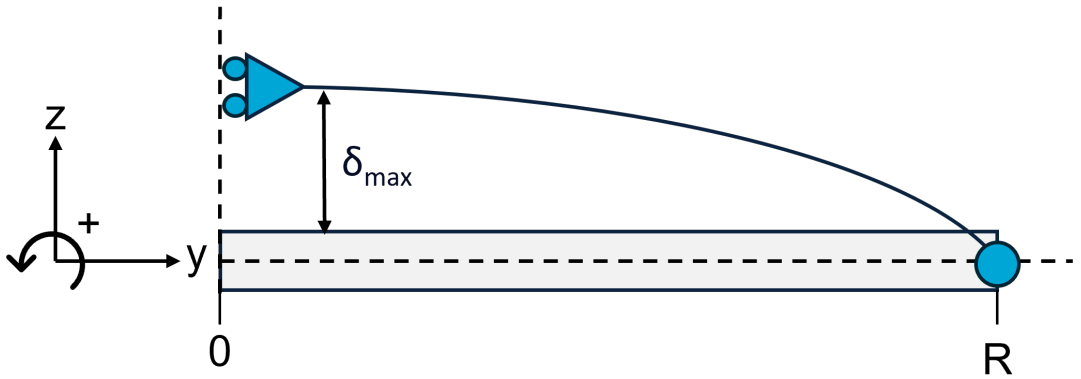

Figure 9.1: *Main rotor blade model.*

To further reduce the complexity of the problem, the following assumptions were made:

- **A01** - The aircraft is in uniform rectilinear motion at the moment of the payload drop, indicating there is force equilibrium in the vertical and horizontal directions before the drop. This means that the deflection of the main rotor blade is only affected by the reduction of weight during the drop.
- **A02** - The payload, so the 10 000 L of water/retardant, is released from the aircraft instantaneously. Therefore, the weight reduction is not modelled as a function of time.
- **A03** - The main rotor blades have a constant cross-section in terms of dimensions and material characteristics over the spanwise location [0, R].
- **A04** - The influence of centrifugal forces, which normally produce axial deformation in the rotor blade due to their rotation, is neglected.

With the basic model and simulation assumptions described, the analysis of the model can now proceed. In this section, three models are created and discussed, each increasing in complexity and fidelity. Figure 9.2, Figure 9.3, Figure 9.4, and Figure 9.5 are used for visualisation of the models and will be further developed upon in this section.

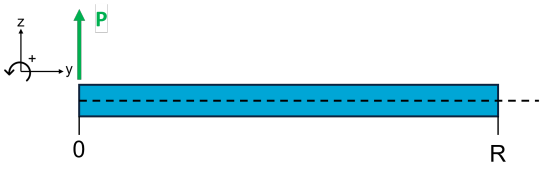

Figure 9.2: *Model with a single point load.*

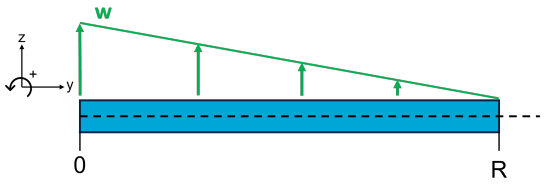

Figure 9.4: *Model with a distributed load.*

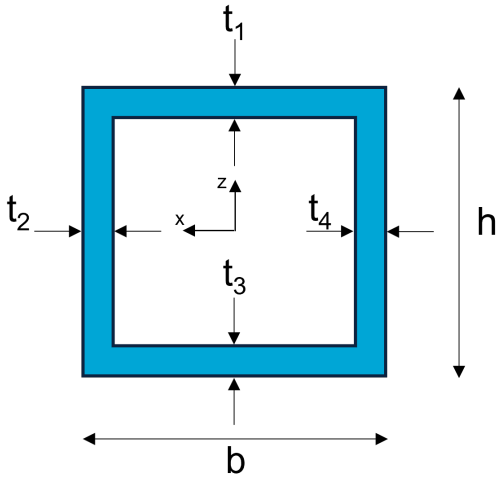

Figure 9.3: *Thin-walled wing box cross-section.*

Figure 9.5: *Boom areas for idealised airfoil cross-section.*

Model 1 - point load & thin-walled cross-section

The first analysis of the deflection of the tip of the main rotor blades is done by applying a simple point load to the hub of the main rotor, see Figure 9.2. This point load is defined by the instantaneous weight decrease due to the payload drop per blade (n=8). Therefore the magnitude of the point force is defined as $P = (10000/8) \cdot g \approx 12258$N. To calculate the deflection of the rotor blade tip, the moment of inertia and thereby the cross-section needs to be defined. A paper about the conceptual sising of multirotor aircraft states that a rotor blade cross-section mainly consists of a wing box and a honeycomb structure, see Figure 9.6 [54]. The main role of the honeycomb structure is to carry the out-of-plane pressure loads and shear loads on the airfoil [55]. Therefore, it can be assumed that the wing box is the primary structural component of the rotor blade responsible for bearing the bending moment.

Figure 9.6: *Cross-section lay-up of the main rotor blade.*

Thus, the cross-section of the main rotor blade is defined as a thin-walled rectangular box, as can be seen in Figure 9.3. For this model, all thicknesses are assumed to be 5% of the chord of the main rotor blades (t_1=t_2=t_3=t_4=0.05 $*$ c). Furthermore, the paper about the conceptual sizing of multirotor aircraft indicates that the base of the wing box should be 15% of the main rotor blade chord [54]. Finally, the height of the wing box is assumed to be 10% of the chord. With these dimensions, the moment of inertia (I_{xx}) can be defined in Equation 9.1. In this equation, c_r is the root chord of the main rotor blade, h_r is the height of the wing box, and t_1, t_2, t_3, and t_4 are the thicknesses defined in Figure 9.3. The moment of inertia is computed by subtracting the inner box ($b_i \times h_i$) from the outer box ($b_o \times h_o$).

$$I_{xx} = \frac{b_o h_o^3}{12} - \frac{b_i h_i^3}{12} = \frac{0.15c_r(0.08c_r)^3}{12} - \frac{(0.15c_r - (t_2 + t_4)) \cdot (0.08c_r - (t_1 + t_3))^3}{12} \tag{9.1}$$

With the moment of inertia of the cross-section of the model defined, the tip deflection due to the instantaneous drop of the payload can be calculated. This is done with Equation 9.2 [56], where P is the point load applied at the rotor hub, L_r the length of the main rotor blade and has a value of 11.5 meters, E_r the Young's modulus of the main rotor blade material and I_{xx} the moment of inertia defined in Equation 9.1. The material of the main rotor blades is assumed to be Epoxy High Strength Carbon Fibre, which has a Young's modulus of 62.7 MPa. The selection of this material will be further described in Section 9.2.

$$\delta_{max} = \frac{PL_r^3}{3E_r I_{xx}} \tag{9.2}$$

By substituting the values in Equation 9.1 and Equation 9.2, a moment of inertia of approximately $1.0 \cdot 10^{-5}$ m^4 and a maximum deflection of roughly 5.14 meters were found. The total mass of the blade was approximated to be 133.65 kg. Although the problem is modelled, the deflection is not representative of what happens in reality.

Model 2 - distributed load & thin-walled cross-section

For the second model, a minor adjustment was made to the first model regarding the loading case. The point load was replaced by a linearly decreasing distributed load w over the whole rotor blade, as can be seen in Figure 9.4. The distributed load is defined in Equation 9.3 and the deflection can be calculated using Equation 9.4 [56], where the rotor length, Young's modulus, cross-section, and thereby I_{xx} remain the same.

$$w = \frac{2P}{L_r} \tag{9.3}$$

$$\delta_{max} = \frac{11wL_r^4}{120E_r I_{xx}} \tag{9.4}$$

Analysing the main rotor blade model for this model results in a maximum deflection of roughly 2.75 meter. The moment of inertia and rotor blade mass remain the same, since the cross-section defined in Figure 9.3 is still used. The maximum deflection is significantly reduced for this load case, yet remains unrealistic. Despite increasing the thicknesses of the upper and lower plates (t_1 and t_3), the deflection remained unrealistic, and the mass of the rotor blade increased rapidly. Given the significant influence of the moment of inertia on the bending moment, and thereby the maximum deflection of the tip, the subsequent focus lies in refining the definition of the cross-section to enhance the rotor's moment of inertia.

Model 3 - distributed load & structural idealisation

Until now, the moment of inertia (I_{xx}) was determined for a thin-walled rectangle representing the wing box. The new method is based on structural idealisation where the skin is represented by boom areas. Using 162 x-

and y-coordinates sourced from Airfoiltools, the boom areas were generated according to the defined points of the airfoil [1]. The distance between the points was then computed and multiplied by the skin thickness (t_{skin}). Based on those boom areas, a new moment of inertia was calculated using Equation 9.5, where n is the number of points of the airfoil, d_i the distance between two points, t_{skin} the skin thickness of the airfoil, c_r the chord of the main rotor, and y_i is the distance from the neutral axis to the boom area. The parameters d_i and y_i need to be scaled by multiplying them with the chord length. This is necessary because these parameters were normalised for a chord length of 1.0, as defined by the airfoil from Airfoiltools. The skin thickness is a variable parameter that can be used to optimise the moment of inertia and thereby the maximum deflection.

$$I_{\text{xx}} = \sum_{i=1}^{n-1} (d_i\, t_{\text{skin}}\, c_{\text{r}})\, (y_{\text{i}} c_{\text{r}})^2 \tag{9.5}$$

Using this new method, the moment of inertia of the main rotor blade increases to approximately $2.75 \cdot 10^{-5}$ m^4 significantly greater than that of the first and second models, indicating that the blade is stiffer with the boom idealisation. Substituting this new value for I_{xx} into Equation 9.4 results in a maximum tip deflection of 0.72 m and a mass of 256.88 kg. The moment of inertia, maximum tip deflection, and mass have already been optimised for the skin thickness. In the design of the main rotor blades, the allowable tip deflection is set to approximately 2 m. Considering about 1.25 m for the flapping of the main rotor blades, the maximum permissible tip deflection is approximately 0.75 m. Therefore, the final maximum deflection for this model is 0.72 m.

Discussion & Recommendation

For the three models, it can be concluded that the moment of inertia is the driving parameter in calculating the maximum deflection of the rotor blade tip. The moment of inertia, and consequently the stiffness of the rotor, increased by 142.5% when the cross-section was idealised using boom areas to represent the skin. This stiffer cross-section reduced the maximum deflection of the tip, δ_{max}, with a factor of approximately 3.82 compared to the deflection obtained in model 2. However, a disadvantage is the significant increase in the mass of the blade. It is, in fact, unrealistic to have a main rotor hub with eight rotor blades, each weighing 256.88 kg.

Table 9.1: *Model parameters comparison.*

Model	$\mathbf{I_{xx}}$	Mass	δ_{max}
Model 1	$1.93 \cdot 10^{-5} m^4$	133.65 kg	5.14 m
Model 2	$1.93 \cdot 10^{-5} m^4$	133.65 kg	2.75 m
Model 3	$2.75 \cdot 10^{-5} m^4$	256.88 kg	0.72 m

The unrealistic value of the weight of the rotor blade may result from the assumptions made. First of all, assumption A02 states that the payload is dropped instantaneously, meaning the rotor is exposed to incredibly high loads. However, in reality, the water is dropped over a longer period, thereby reducing the loads experienced by the rotor and its required stiffness. Secondly, assumption A03 simplifies the problem by making the formulas independent of the spanwise location, as the cross-section is constant in terms of dimensions and material characteristics. However, this may affect the final weight of the rotor blade. A constant cross-section results in a heavier model compared to one where the dimensions decrease along the spanwise location. Additionally, if the load experienced by the rotor blade is less critical, the stiffness can be reduced while still maintaining an acceptable deflection. By doing so, the weight of the rotor blade also goes down, leading to a more realistic value.

Therefore, to make the model of the main rotor blade tip deflection more accurate, the assumptions taken need to have less influence on the final outcome. Furthermore, a model in which the water release is a function of time could be made, thereby reflecting more accurately what would happen during a real firefighting mission, as this would allow the load on the rotor blades to also be modelled as a function of time. Moreover, a recommendation for the construction of the model would be to create a cross-section that varies over the

[1] NACA 0012 AIRFOILS (n0012-il), http://airfoiltools.com/airfoil/details?airfoil=n0012-il [retrieved 11th June 2024]

span. This ensures that the model more accurately represents the real structure and that the resulting values are more reliable. Table 9.2 provides an overview of different helicopters, the number of blades they have, and the mass of a single blade. This table offers an insight into the typical weight range of rotor blades. Since the compound helicopter is most similar to the Silvorsky CH-53E, the mass of its blades can be estimated to be close to 138.43 kg.

Table 9.2: *Mass of the rotor blades of different helicopters [57].*

Helicopter models	Radius [m]	Number of blades [-]	Rotor blade mass [kg]
Aerospatiale A 332 L1	7.79	4	57.96
Bell 206L-3	5.64	2	30.87
Sikorsky CH-53E	12.04	7	138.43

Finally, a vibrational model can be developed in the future to analyse the reaction of the main rotor hub to the decrease in instantaneous load. The main rotor hub and the fuselage can be modelled as two masses connected by a spring. This model will enable calculations to dampen the vibrations resulting from the payload release effectively.

9.1.2. Box Wing Analysis

CHEETAH has a box wing which is an advanced aircraft wing configuration where two horizontal wings are connected at their tips, forming a 'box' structure, see Figure 9.7. This design can improve structural stiffness compared to traditional wing configurations while decreasing aerodynamic efficiency. In this section, the structural efficiency of a box wing over a conventional wing will be discussed and its effect on the efficiency of the entire aircraft.

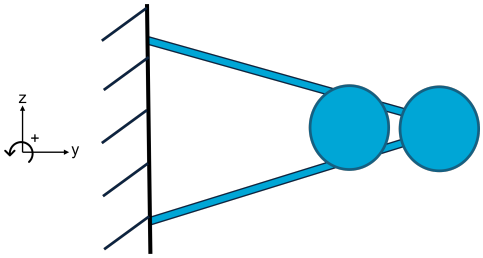

Figure 9.7: *Sketch of the box wing including propellers mounted to the fuselage.*

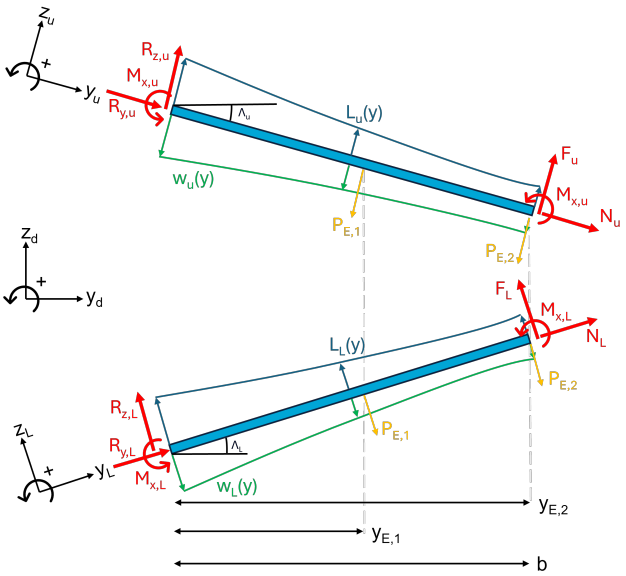

Figure 9.8: *Free body diagram of the box wing in local coordinate system.*

In Figure 9.8, the Free Body Diagram (FBD) can be seen for the upper wing and lower wing. The connection of the upper wing with the lower wing is in the FBD replaced by two internal forces ($R_{x,i}$ & $R_{z,i}$) and an internal bending moment ($M_{x,i}$). The fixed connections at the root of the upper wing and lower wing are replaced by four reaction forces ($R_{x,u}$ & $R_{x,L}$ & $R_{z,i}$ & $R_{z,L}$) and two reaction moments ($M_{x,u}$ & $M_{x,L}$), drawn in a positive direction. It is however important to note that the sum of these moments has to add up to zero as they are internal forces after all. Therefore, the lower internal forces at the tip can be written in terms of the upper forces at the tip:

$$\begin{aligned} &(a) \quad F_{\mathrm{L}} = -F_{\mathrm{U}}\cos(\Lambda_{\mathrm{u}} + \Lambda_{\mathrm{L}}) + N_{\mathrm{U}}\sin(\Lambda_{\mathrm{u}} + \Lambda_{\mathrm{L}}) \\ &(b) \quad N_{\mathrm{L}} = -F_{\mathrm{U}}\sin(\Lambda_{\mathrm{u}} + \Lambda_{\mathrm{L}}) - N_{\mathrm{U}}\cos(\Lambda_{\mathrm{u}} + \Lambda_{\mathrm{L}}) \\ &(c) \quad M_L = -M_U \end{aligned} \tag{9.6}$$

The distributed lift forces represented by $L_u(y)$ for the upper wing and represented by $L_L(y)$ for the lower wing are derived from the C_L-values obtained from XFLR5 in Chapter 7. A list of lift coefficients was derived for the upper wing and lower wing in a box wing configuration along with corresponding chord and span-wise location values. This allows for computing the forces acting on the wing due to the lift. A manoeuvring load and safety factor of 3.25 and 1.5 are applied, respectively.

Besides the distributed lift forces, there is another distributed force known as the distributed weight force $(w_u(y), w_L(y))$. This force was determined by initially estimating the total wing mass of 3700 kg, as detailed in Section 10.4. It was assumed that each wing would have the same mass. Therefore, the total wing mass was divided by four, resulting in a wing mass of 925 kg for each wing. The distributed weight equation was derived based on the assumption that weight is proportional to the cross-sectional area along the span, which means that it is proportional to the volume of the wing as every small element of the wing is cut to be equally long. This assumption led to the derivation of Equation 9.7, where W_{wing} is the weight of each wing, so 925 gN, y is the spanwise location and b/2 is the wing span with a value of 8.44 m.

$$w(y) = \left(\frac{25}{13}W_{\text{wing}}\right)\left(1 - \left(\frac{6}{5}\right)\left(\frac{y}{b}\right) + \left(\frac{9}{25}\right)\left(\left(\frac{y}{b}\right)^2\right)\right)b^{-1} \tag{9.7}$$

In addition to the distributed forces, the upper and lower wings are subjected to point forces from the two propellers attached to the engines. The propellers are located at positions $y_{E,1}$ and $y_{E,2}$, each with a total mass of 100.2 kg. For this structural analysis, it is assumed that the point forces representing the weight of the propellers have a magnitude equal to half the weight of the engine, so each wing supports half of the total weight.

With all forces and moments of the structure established, the moment equations for the lower and upper wings can be formulated. Due to the slenderness of the wing, the internal shear is ignored as its effect is much lower than that of the internal moment. The internal normal force is not small, however, since the structural stiffness of the box wing stems from the fact that a wing can carry normal forces, relieving the bending moment on the other wing and vice versa. Long, slender structures are generally stiffer in the axial direction than transverse direction.

With the moment and second area moment of inertia distribution known and the material selected, the transverse deflection $\delta_t(y)$ can be determined. The second derivative of the transverse deflection is defined as:

$$\frac{d^2\delta_t(y)}{dy^2} = \frac{-M(y)}{E_{\mathrm{w}}I(y)} \tag{9.8}$$

Simply numerically integrating this twice yields the desired result, the upward deflection of the wing. As the only internal normal force is dictated by N_{U} and N_{L}, this internal force is simply constant over the span. With a varying cross-sectional area, the first derivative of the total axial deflection δ_{a} is:

$$\frac{d\delta_a}{dy} = \frac{N}{E_{\mathrm{w}}A(y)} \tag{9.9}$$

This can also be simply integrated to find the total tip deflection. As the ends of the wings are fixed, the difference in their deflections should be zero. First, looking at Figure 9.10, the deflections are first to be transferred into the $z_d - y_d$ reference system, after which the difference in those deflections is to be set to zero by altering the internal forces F_U, N_U and M_U, which dictate F_L, N_L and M_L as per Equation 9.6.

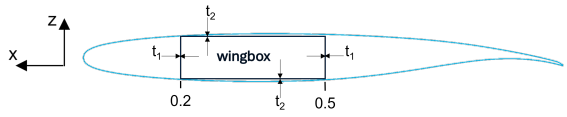

Figure 9.9: *Sketch of the inner wing box of the wings.*

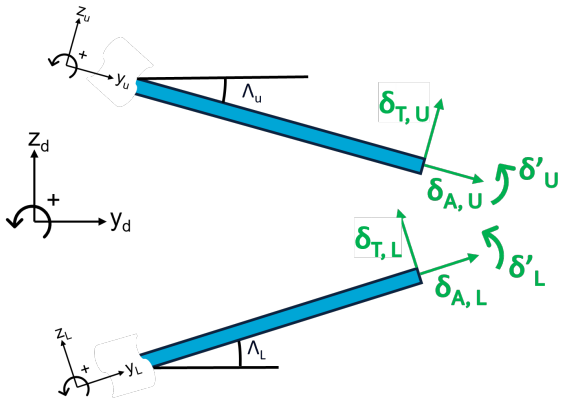

Figure 9.10: *Sketch of the deflections at the tips of the box wing wingtips.*

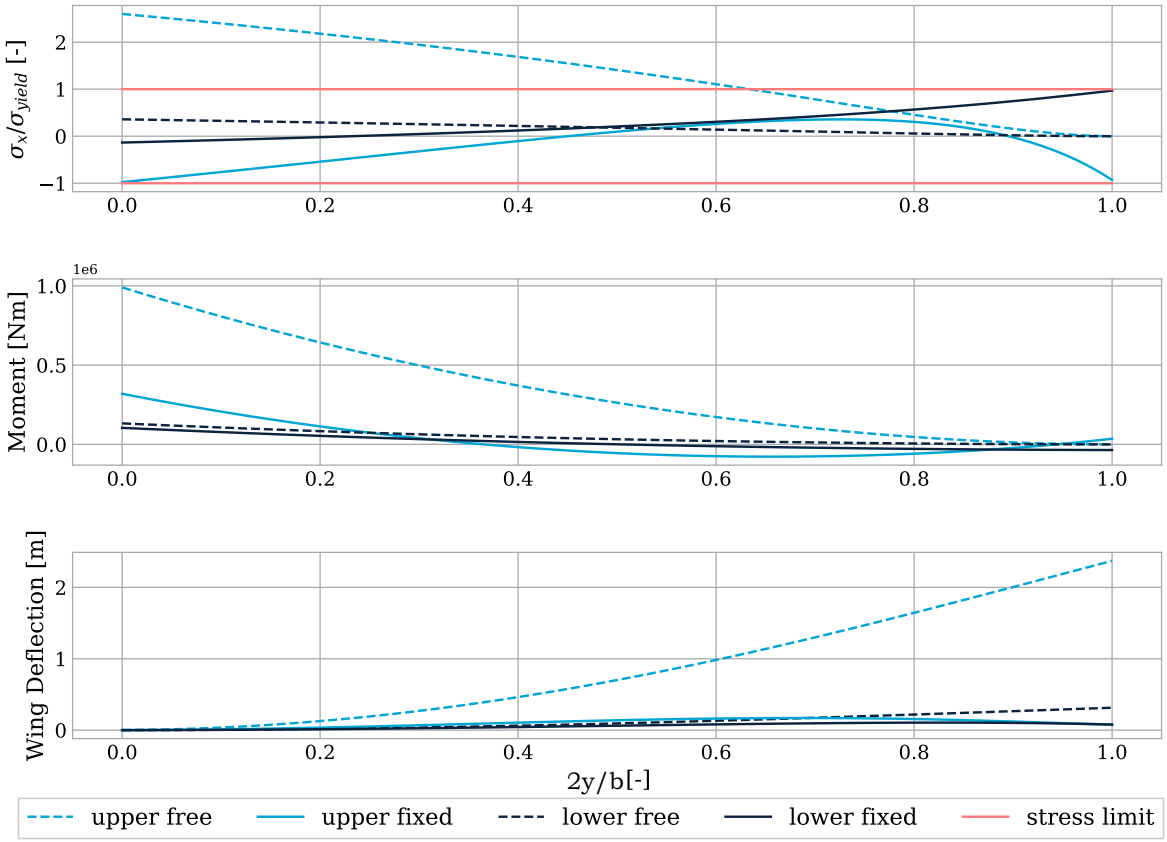

Figure 9.11: *Internal normal stress, moment and deflection of the upper and lower part of the box wing.*

In Figure 9.11, the internal moment, stresses divided by the yield stress and deflections can be seen. The thickness, defined as seen in Figure 9.9 t_1 has been set at a minimum of 1 mm, and t_2 is minimised, equalling the maximum stress to the yield stress, which can be seen as the stress ratio reaches a maximum of +-1. It is interesting to note how much more structurally efficient the wing is when the tips are rigidly connected compared to when they are not, signified by a continuous and dashed line respectively. For the same thicknesses and thus weight, the stress exceeds the yield stress by as much as a factor of 2.6. The deflection at the tip is more than 24 times as big.

A box wing without connected tips, however, has no structural benefits while experiencing less aerodynamic

efficiency. A more fair evaluation would be to compare it to a conventional straight wing. The lift and angle of attack were kept the same to make the fairest comparison. The wing was lengthened, keeping the same chord distribution, until the same Lift was reached. The same analysis was applied, with the only difference being that obviously, only one wing exists, and thus no internal forces at the tip. Altering the thicknesses again until the maximum stress is equal to the yield stress as seen in Figure 9.12.

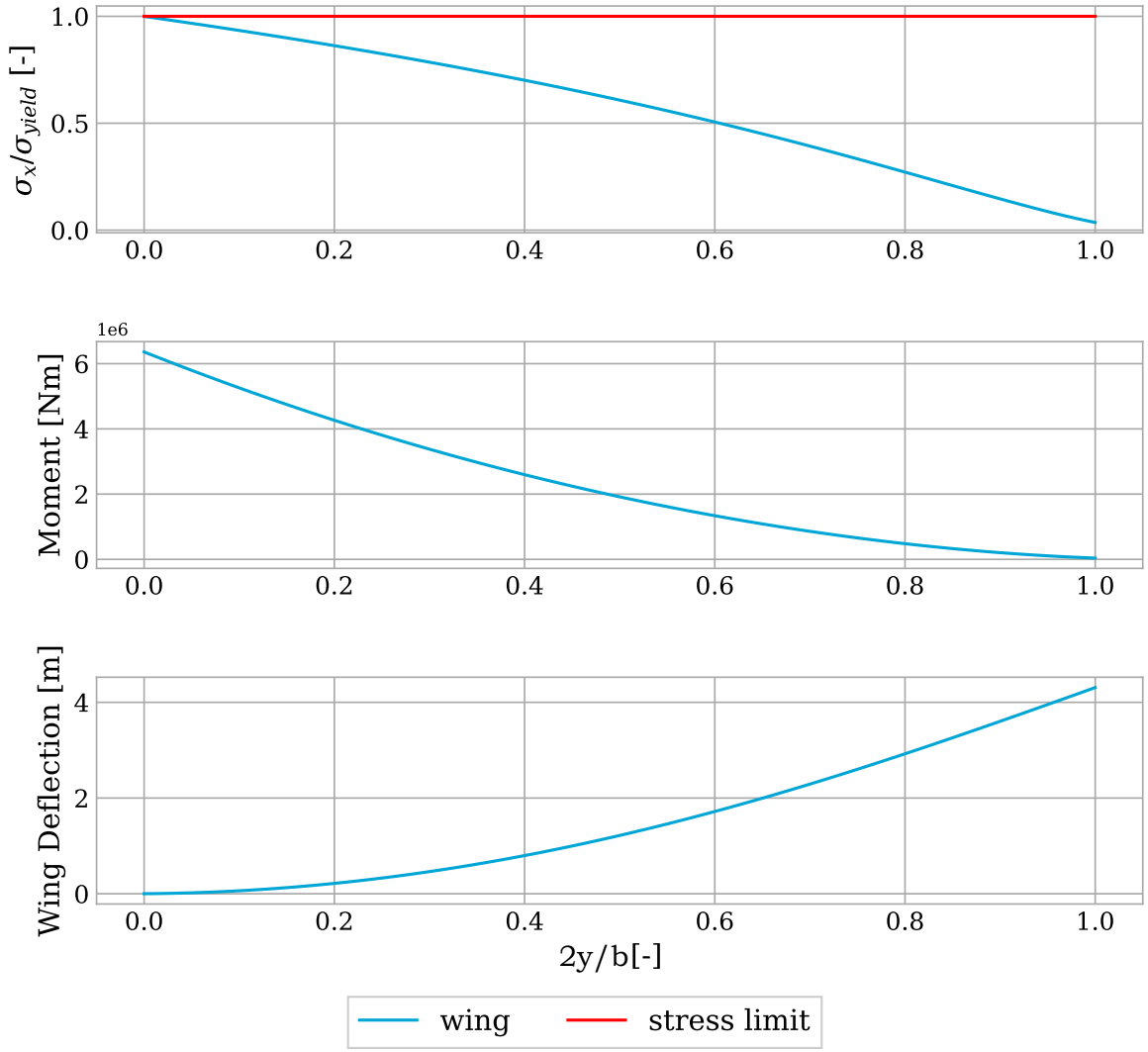

Figure 9.12: *Internal normal stress, moment and deflection of the straight wing.*

The tip deflection is well over 4 meters now, a disadvantage over the mere centimetres the box wing deflects. More important however is the weight of the wing boxes, compared to the aerodynamic efficiency, L/D. Note how these weights are not the total weights of the wings.

Table 9.3: *Structural and aerodynamic efficiency of both wings.*

	Box wing	**Straight wing**
L/D	21.9	41.8
Weight per side [kg]	235	3919

The total added structural weight of the straight wing, equal to twice that of one side, is equal to 7838 kg. Assuming the L/D will remain the same and the wing takes all the load, thus the weight is equal to the lift,

the drag can be computed. Note that the load taken by the wing is 0.92 of the normal maximum weight, 35 500 [kg] as discussed in Section 6.1.

$$D_{\text{boxwing}} = \frac{0.92 \cdot 35500 \cdot 9.81}{21.9} = 14630kN$$

$$D_{\text{straightwing}} = \frac{(0.92 \cdot 35500 + 7838) \cdot 9.81}{41.8} = 9504kN$$

The drag of the box wing is not coherent with other values in Chapter 7, as just the wing is considered, taking all the load. The straight wing is more efficient, even when its higher weight is taken into account. This, however, does not necessarily mean a straight wing should be selected. The higher efficiency comes at a cost, as the deflection is much bigger and the wing is much longer. As there shall be a shaft going through the wing, transmitting torque through the wing to the propellers on the wing, this shall bend too. Designing such a slender shaft with enough stiffness against torque, while being able to bend can be challenging. To make matters worse, the shaft is rotating, meaning that the bending stress on the shaft is cyclical. This invites fatigue-related issues, agitated when a bigger bending increases the amplitude of the cyclical stress. A longer wing has its disadvantages too. First of all, the overall dimensions of the aircraft increase. This could limit the amount of space where the aircraft could be stored, or even worse, draw water from. Secondly, the mass moment of inertia would be increased, reducing the manoeuvrability. All in all, for CHEETAH, the box wing shall be utilised as the aircraft is already rather heavy and a big deflection of the wing is undesired.

9.2. Material Characteristics

Contributors: Ivo, Merel
Authors: Ivo, Merel

When it comes to designing an aircraft, choosing materials that suit its mission profile is essential. The materials used to build an aircraft influence its weight, performance, durability, safety, sustainability and many other properties. An initial material characteristics analysis was performed in the midterm report [2]. However, these results need to be iterated since this selection was not specific to CHEETAH and many design characteristics have changed since then. For this iteration, the requirements influencing the process are first collected and their impact on each component is determined. Using this information, the material selection process for the individual components of CHEETAH can be performed. In this section, all the material data collected was retrieved from Granta[1].

The aircraft requirements serve as a good guideline for the material selection process. Nevertheless, not all of the requirements influence the material choice. Thus, the following selection of the requirements directly influencing the material selection is made:

- **FTF-SYS-OWN-02.1:** The aircraft shall have a unit cost of less than 63 million euros
- **FTF-SYS-FDS-05.15:** The aircraft shall sustain no structural damage when flying between -1 and +3.25 g at MTOW
- **FTF-SYS-FDS-07.2:** The aircraft shall be resistant to corrosion caused by salty water
- **FTF-SYS-FDS-07.3:** The aircraft shall be able to resist heat generated in the air above the fire

In this design phase, the material selection for the skin, structures, landing gear, rotor blades and rotor mast are performed. A final selection of all the materials used for these systems can be found in Table 9.4. Here, the CO_2 footprint refers to the typical grade and the primary production of the material.

Table 9.4: *Material characteristics of materials selected for CHEETAH.*

Component	Rotor skin	Landing gear	Rotor filling	Skin and structures	Rotor mast	Water tank
Material	**Epoxy and HS carbon fibre biaxial lamina**	**Low alloy steel, 300M**	**Aramid paper/phenolic honeycomb**	**Aluminium alloy 2024**	**Ti-6AI-4V**	**Aluminium alloy 6061**
Melting point [°C]	-	1430-1510	-	502-638	1610-1660	582-652
Maximum Service Temperature [°C]	140-220	220-246	-	170-200	350-420	130-150
Costs [€/kg]	49.3-54.7	1.46-1.93	27.7-39.1	3.01-4.03	20.2-25.1	2.74-3.77
Density [kg/m^3]	1540-1610	7790-7870	172-180	2750-2780	4430	2690-2730
Recyclability	No	Yes	No	Yes	Yes	Yes
Young's modulus [GPa]	62.7-68.7	200-210	4.66e3-7.86e-3	72-75.7	113-115	66.6-70
Yield strength [MPa]	627-910	1520-1680	0.216-0.315	345-381	786-898	110-128
Corrosive resistance to salt water	Excellent	Limited use	Excellent	Acceptable	Excellent	Acceptable
Fatigue strength at 10^7 cycles [MPa]	345-592	880-883	-	125-147	634-688	86.4-101
CO2 footprint [kg/kg]	45.5-50.1	1.05-1.3	15.7-17.4	7.3-8.41	17.8-21.4	7.47-8.6

9.2.1. Skin

The skin of an aircraft can be made from various materials. Typically, a type of aluminium alloy is chosen, however, composites have also been used in aircraft such as the A350 XWB [2]. The material selected for the skin of CHEETAH is Al2024 (Aluminium alloy 2024) due to its excellent heat properties, adequate strength and corrosion resistance, low cost, easy maintenance, and sustainable characteristics.

The skin must withstand significantly high temperatures since CHEETAH will be exposed to the heat generated by wildfires. In fact, the temperature at only 40 m above the wildfire can reach up to 180 °C [58]. Although CHEETAH will not be continuously exposed to such a high temperature, the skin should endure high temperatures up to 500 °C for short periods of time. Furthermore, the compound helicopter's skin should also have a high service temperature to ensure it does not melt or weaken while performing missions. Al2024 is well-suited for this purpose, as the Al2xxx series is known for its ability to perform in missions involving high temperatures, which also explains why it is commonly used in aerospace applications. Because the skin is a very thin element, heat-resistant coatings are applied to the outside of the aircraft. These coatings will protect the crew and passengers from the heat generated by the wildfires. Additionally, Al2024 is able to handle all the anticipated loads exerted on the skin. Since the fuselage of the aircraft will not be pressurised and the wing-loading will only be carried by structural elements, the skin primarily needs to withstand forces produced by wind and rain.

While the corrosion resistance of Al2024 to salty water is not outstanding compared to composites, because it is commonly used in the aerospace industry, coatings have been developed to protect the skin. On CHEETAH

[1] Granta, https://www.ansys.com/products/materials
[2] Airbus, https://safetyfirst.airbus.com/safe-operations-with-composite-aircraft

a coating similar to those used on aircraft flying in oceanic regions will be applied. Additionally, aluminium alloys also offer ease of maintenance, as cracks, dents, and other flaws can be quickly identified, often with the naked eye. Finally, repair methods are common, allowing for parts to be repaired rather than replaced for minor issues as is typically the case for composites.

At the end-of-life of CHEETAH, aluminium's recyclability allows the entire aircraft skin to be repurposed. This way sustainability is kept in mind throughout the design process.

9.2.2. Structures

The structural elements of CHEETAH will be constructed of Al2024, the same material chosen for the skin. These elements include stringers, wing boxes, spars, ribs, skin frames, longerons, and supporting beams. Al2024 is a good choice for these structural elements, not only offering all properties explained in Subsection 9.2.1, but also exhibiting proper strength and fatigue resistance. Its versatility makes it an ideal choice for all structural elements in the aircraft, including the wing boxes, which will also be used to store fuel. However, to protect the aluminium from corrosion due to the fuel, these tanks will need a coating. Further details regarding the loads on the structural elements can be found in Section 9.1.

9.2.3. Water Tank

The material selected for the water tank is Al6061, an aluminium alloy known for its excellent resistance to water corrosion. With an additional coating, it will also effectively resist corrosion caused by the retardant foam. Additionally, it is a lightweight material, allowing the tank to be easily lifted in and out of the aircraft fuselage. Furthermore, the excellent weldability of this material enables quick and cost-effective repairs if damage occurs. Finally, its heat resistance, with a minimum melting point of 582 °C, is useful as the tank will be exposed to the heat coming from the wildfires just before dropping when the fuselage doors open up.

9.2.4. Rotor Blades

The rotor blades used for CHEETAH must be stiff and durable to withstand all loads that will be applied to them, while also possessing excellent fatigue resistance. However, this can be challenging, as blades need to be lightweight. Therefore, epoxy and High Strength (HS) carbon fibre biaxial lamina were selected as material for the rotor skin. Typically, for helicopter rotor blades of this size, a honeycomb core is used to avoid the deformation of the blades while not adding any significant weight. For CHEETAH an aramid paper/phenolic honeycomb was chosen. The combination of composite skin and honeycomb for helicopter rotor blades has often been used in helicopter design. Because it is a proven design, maintenance and repair strategies are widely available.

9.2.5. Rotor Mast

The rotor mast is a hollow tube that transfers the engine power to the rotor. Titanium alloy Ti-6Al-4V was chosen for this mast due to the mast's need to handle significant amounts of torque and tensile forces. Therefore, it needs to be made from a very high-strength material with excellent fatigue resistance. Additionally, its excellent corrosion resistance to salt water is crucial, as mast failure could be catastrophic, with the rotor potentially detaching from the aircraft. Hence, the material properties have been prioritised over cost, despite it being one of the more expensive materials. Nevertheless, it is a small price to pay for the safety of the crew and passengers.

9.2.6. Landing Gear

The landing gear will be used during take-off and landing, where it must support heavy loads and endure high-impact forces. For this reason, 300M low alloy steel has been selected. This alloy has excellent strength, having a minimum fatigue strength of 880 MPa at 10e7 cycles. In addition, it is widely utilised in the aerospace industry for landing gears, ensuring manufacturers have extensive experience with its properties. While its corrosion resistance is relatively low, this can be mitigated by available coatings. Finally, the option to close off the landing gears with doors during flight should be considered, as it would provide further protection against (salty) water exposure and lead to better aerodynamic performance.

10 | System Characteristics

Apart from the characteristics specific for the propulsion, aerodynamics, stability and control and structures and material, there are some other systems that need to be designed that do not belong to one of these categories specifically. For example the design of the modular water tank and snorkel mechanism, or the fuel tank and hydraulics systems. Furthermore, a final weight estimation for CHEETAH is done and the final budgets are established.

10.1. Water Tank System

Contributors: Emma, Merel
Authors: Emma

The primary objective of CHEETAH is to fight wildfires. The water tank is a key element in the performance of extinguishing the fire and should therefore be considered carefully. The final configuration of the water tank is shown in Figure 10.1 and Figure 10.2. The system consists of a large tank for the water, with separate retardant tanks, together with a retardant-supplying system. Baffles are placed to reduce sloshing of the water. Furthermore, a snorkel and pump are installed to facilitate in-flight water refilling. A dropping mechanism is installed in such a way that the amount of water can be controlled by the crew. The tank is equipped with pressure release valves, as well as a connection to enable water loading on the ground. The design of all these sub parts is described in this section.

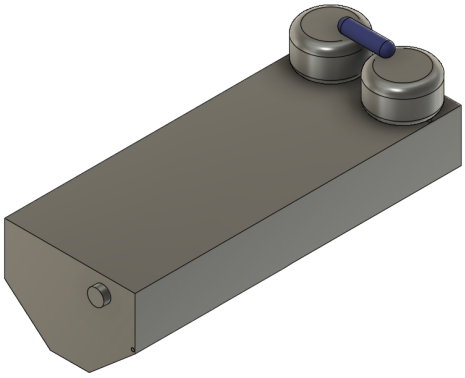

Figure 10.1: *Layout of the water tank.*

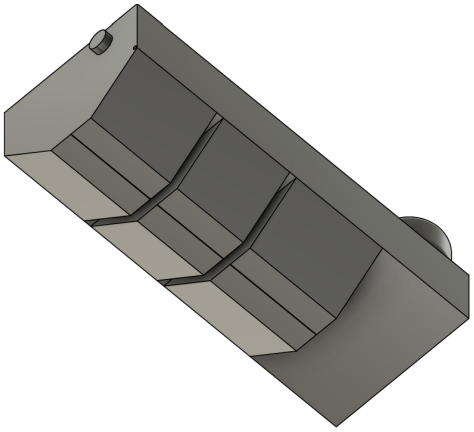

Figure 10.2: *The bottom of the water tank.*

10.1.1. Tank Design

The first step in designing the water tank system is to determine the dimensions of the water tank itself. The requirement stating a capacity of 10 000 L is needed is leading when sizing the water tank. However, the dimensions of the fuselage and the fuselage back door are already determined, which constrains the size of the water tank.

In order to be able to drop the water effectively, the water tank is placed on the bottom of the fuselage, under the cabin floor. Therefore, the floor is designed to be modular, so it can be removed when a fire fighting mission is executed, but placed when another mission is performed. A front view of where the water tank is located with respect to the cabin floor can be seen in Figure 10.3, where the floor is displayed as the dotted line. Figure 10.4 shows the dimensions of the cross-sectional area of the water tank. The width and height of the tank are made as large as possible, while still fitting through the fuselage back door. For the width, a margin of 10 cm is taken on both sides and for the height a total margin of 20 cm is taken. This results in a tank width of 2 m and tank height of 1.4 m.

To be able to fit the tank within the shape of the bottom part of the fuselage and to ensure that all the water

flows out of the tank, the part of the water tank that lies under the cabin floor has a converging shape. The 2 m width linearly decreases to 0.6 m. This is the bottom of the tank and therefore the location of the dropping doors, which will be described in Subsection 10.1.5. In Figure 10.4 the retardant tanks are shown as well. These will be elaborated on in Subsection 10.1.2.

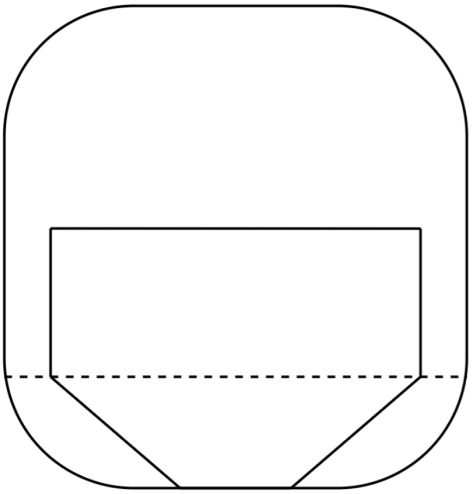

Figure 10.3: *Front view of the water tank location, with the dotted line being the cabin floor.*

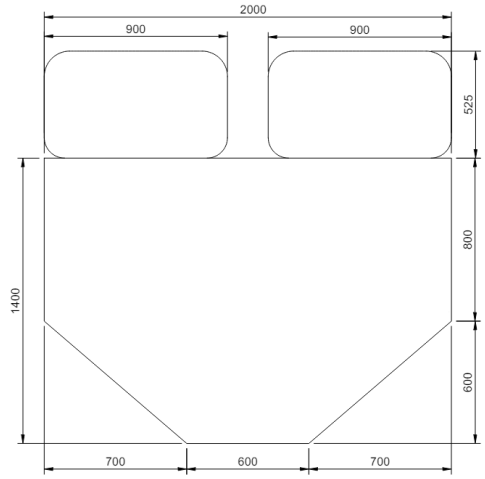

Figure 10.4: *Dimensions in millimetres of the front view of the water tank and retardant tanks.*

Due to the size of the fuselage rear door, the width and height of the tank are limited. Therefore, the length of the water tank should be sufficient to carry 10 000 L of water. However, there are more subsystems that have to fit within this space under the cabin floor. Because of the relatively small dimensions of the fuselage, the water tank has to work its way around some of these subsystems. Firstly, due to structural reasons, the vertical spars of the lower-wing wingbox go through the under-floor space. Furthermore, there needs to be a bay in the back for the retracted main landing gear and the hydraulics of the back door. These obstacles lead to some interruptions of the lower part of the water tank. To still ensure the desired water capacity, the length of the water tank needs to be equal to 5 m.

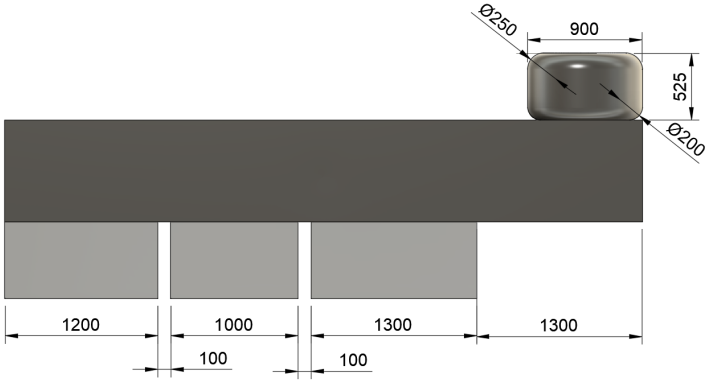

Figure 10.5: *Dimensions in millimetres of the side view of the water tank and retardant tanks.*

The cutouts for the wing spars and landing gear bay result in three separate dropping door mechanisms. The dimensions of the cutouts and remaining dropping areas are given in Figure 10.5. This layout results in a volume of 10 700 L when taking the outer dimensions. To make this quantity more accurate, a wall thickness of 10 mm is assumed. This value is likely thicker than the actual tank wall, but it is used to account for the volume occupied by structural elements such as stringers. The inner volume of the tank is then equal to 10 400 L.

In order to meet the requirement for the aircraft to be multi-role, the water tank is designed to be modular. Due to its complex shape, the loading and unloading of the tank should be considered carefully. This should be a simple process that can be performed in a short period as the tank might need to be added or removed

quickly during emergencies. The tank can be moved in or out of CHEETAH using only a cargo loader and the mechanism located in the aircraft. This mechanism consists of a railing system attached to the ceiling of the fuselage. The water tank can be attached to this system by cables running from the attachment points, located on the corners of the tank, to the railing system. These are then attached to the winch such that a force can be exerted. This force from the winch can lift the tank out of the flooring and move it to the back of the fuselage. This allows the tank to be positioned such that the cargo loader can remove it from the aircraft completely. Adding the tank to the empty fuselage can be done in the same fashion, by repeating the aforementioned process in reverse.

10.1.2. Retardant Tank System Design

The next subpart of the water tank design is the integration of the retardant. The tank is designed in a way it can be reloaded with water during flight. However, retardants are more effective in firefighting than water. Therefore, a system that adds a retardant mixture to the water is necessary. There are multiple retardant types. For aerial firefighting, class A foams are often used. They are environmentally friendly, have a very low mixture ratio, and will therefore be used for CHEETAH [59]. The mixture ratio for class A foams is 0.3-0.5% for rotary-wing aircraft and 0.6-0.8% for fixed-wing aircraft. Since CHEETAH is a both rotary and fixed-wing, a mixture ratio of 0.6% is used. To provide the entire tank with enough retardant, 60 L of the mixture is required. To be able to do multiple refills per flight, the retardant tanks are designed to carry 600 L of the retardant mixture. This means that the tank can be fully provided with retardant 10 times. Class A foams have a very high expansion factor of at least 20 times the water volume. [1] Therefore, a fully filled water tank produces at least 100 000 L of foam.

The retardant mixture is divided over two modular, cylindrical tanks. For good accessibility, the tanks are placed on top of the water tank, close to the rear door. The dimensions and placement of the tanks can be seen in Figure 10.4 and Figure 10.5. A pressurisation system comes with the retardant tanks. Pipes run through the water tank. With the pressure from the tanks, the pipes bring the retardant to the doors on the bottom. That way the retardant is only added just before the water is released. This is necessary due to the high expansion factor of the foam. The amount of retardant mixture that is supplied can be controlled by the pilot from the cockpit using valves connected to a touchscreen control system, similar to the Coulson Aviation RADS-L system. [2] How the pipes run through the tank is shown in Figure 10.6.

10.1.3. Anti-Sloshing Devices

In order to reduce sloshing induced by movement and vibrations of the aircraft, anti-sloshing devices need to be added inside the water tank. This is done by placing baffles. The cutouts for the wing spars act as a baffle for the lower part of the tank. To make them functional for the entire height of the tank, metal sheets of 10 mm thickness are placed directly on top. The sheets have holes to ensure the water can flow to all compartments when filling the tank. The size and placement of the holes is inspired by the baffle design of the Fireflighter design [60]. The lengths of the three doors lead to a distance between the baffles ranging from 1 m to 1.3 m. This is sufficient for the size of the water tank, so therefore no extra baffles are placed. The baffles are designed to still enable full use of the water tank capacity, while significantly reducing sloshing effects. The layout and location of the baffles can be seen in Figure 10.6.

[1] Application of Firefighting Foam Concentrate in Low, Medium and High Expansion, https://www.bio-ex.com/en/our-expertises/low-medium-high-expansion/ [retrieved, 2nd June 2024]

[2] State of the Art Tanking System in our CH 47 Aircraft, https://www.youtube.com/watch?v=knGhUybqTZ0 [retrieved 5th June 2024].

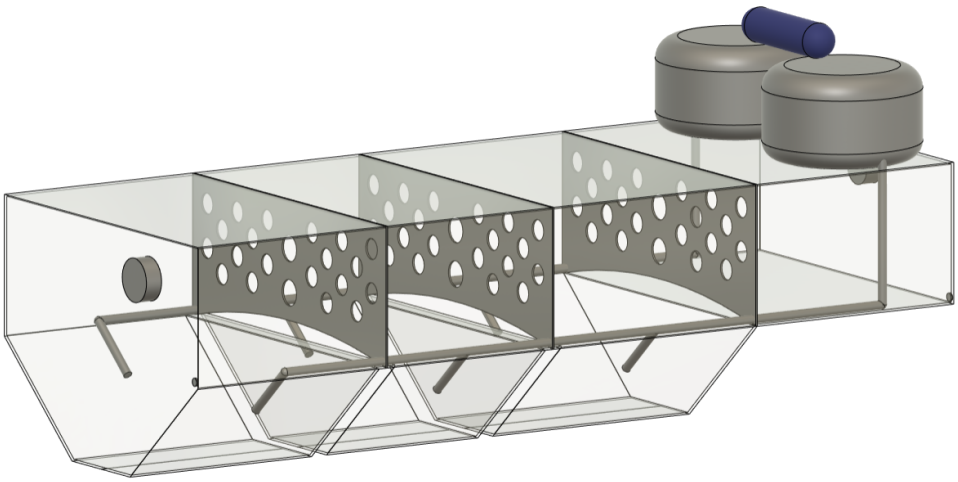

Figure 10.6: *Interior of the water tank, with retardant pipes and anti-sloshing baffles.*

Another thing to consider might be the vertical sloshing of the water. However, as for current existing fire-fighting aircraft this is not addressed as an issue, for now, it is assumed that vertical sloshing will not be problematic. In further development, it can be considered to add vertical styrofoam plates or styrofoam balls, that move along with the level of the water, as this is used in other liquid tank applications [61].

10.1.4. Snorkel and Pump Design

To facilitate in-flight water refilling, the aircraft is equipped with a snorkel and pump. In the midterm report, the Helitank HP10000 fire-fighting hover pump was selected for CHEETAH [2]. This selection was based on the availability of current industry options, the pump refill rate, the weight and power required by the pump and the ability to refill the tank in hover mode as stated in **FTF-SYS-FDS-05.2**. The specifications of this pump can be seen in Table 10.1. This pump has a refill rate of 10 000 L/min, which means that the water tank can be filled in one minute. Some extra time is counted for rolling the snorkel in and out. Assuming that this takes about a minute as well, the entire tank can be refilled in two minutes. The snorkel mechanism is controlled by the touch screen in the cockpit.

Table 10.1: *Specifications of the Helitak HP10000 pump.*

Manufacturer	Helitank
Model	HP10000 hover pump
Pump refill rate	10 000 L/min
Pump weight	35 kg
Required power	26.8 hp
Hose length	4.5 m
Type	Electric

The hose of the snorkel is integrated high into the water tank to ensure easy refilling. It is then connected to a reel to ensure that the hose can be retracted into the fuselage. This is necessary when flying at the maximum speed of 400 km/h. Since the height of the integration point is 1.15 m and some length of the hose is lost due to the attachment to the reel, the length of the hose that is suspended under the fuselage is 3 m. Therefore, the hover height when refilling the tank is maximum 3 m.

In Figure 10.6, the location of where the snorkel is connected to the tank can be seen. Due to the storage of the reel, this is not exactly in the middle of the tank. To ensure that refilling with the snorkel does not affect lateral stability, a short tube is placed inside the tank in such a way that the water flow is centred. In terms of longitudinal stability, the refilling might cause a dynamic control problem. Therefore, a control system has to be added to prevent the helicopter from becoming unstable when refilling the water tank.

Furthermore, the tank can be refilled on the ground as well by connecting a water hose with a fixed water

source at the airbase to the same inlet as where the snorkel will be connected. When ground refilling is done, the ground hose needs to be replaced with the snorkel hose to facilitate in-flight refilling

10.1.5. Dropping Mechanism

To release the water from the tank to extinguish the fire, a mechanism is needed to facilitate this. There are doors on the bottom side of the tank. These doors are controlled with the same touchscreen system in the cockpit as the snorkel and retardant adding. Each compartment has its doors, which can be operated independently. This way, each door can be opened individually, but they can also open simultaneously, depending on the amount of retardant desired. Additionally, the degree to which the doors open can be managed to control the water flow even more. The doors are electrically controlled and hydraulically operated. The layout of the doors is similar to the Firefighter. Figure 10.7 shows how the door mechanism will be placed in the tank.

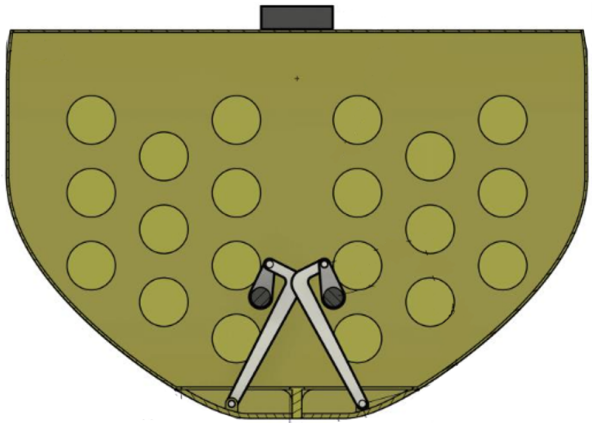

Figure 10.7: *Door mechanism of the Firefighter [60].*

With the dimension as given in Figure 10.4 and Figure 10.5, the total area that can drop water is equal to 2.1 m^2. This area can be adjusted by only opening one or two of the three doors, which is effective for spot dropping, or by only partially opening the doors, which would be more useful when line dropping. With this door mechanism, the flow rate of the water can be adjusted in the way the pilot likes.

In case of an emergency where weight needs to be released quickly, all water can be dropped at one, which would take only 2 seconds, assuming the drop is only due to the gravity and pressure of the water. Another emergency situation could be the failure of the valves of the retardant supply system, where the volume of the water will increase quickly. To prevent the tank from exploding inside the helicopter, all the water needs to be dropped as quickly as possible as well.

10.2. Fuel Tank System Design

Contributors: Emma, Merel
Authors: Merel

The fuel system of an aircraft is important as it enables the loading, storage and transport of fuel to the engines. These engines, in turn, power the rotor and electric systems, enabling the aircraft to fulfil its mission.

10.2.1. The Fuel Tanks

CHEETAH will be equipped with four main fuel storage tanks. The largest tank is located in the upper wings, spanning from one wing to the other, penetrating through the fuselage. The second and third tanks are in both lower wings, separated by the fuselage. The fourth tank is located under the flooring of the aircraft, right in front of the water tank. The combined fuel capacity of these four tanks is 9970 L. The volumes of the separate tanks can be inspected in Table 10.2.

Table 10.2: *Fuel volume per tank.*

Tank label	location	Volume [L]
FT-UW	Upper wings	5095
FT-LR	Lower right-wing	1950
FT-LL	Lower left wing	1950
FT-WT	In front of the water tank	975

These volumes are determined by considering the possible fuel volumes. In the wings, this equals the volume of the wingbox as a wet-wing configuration will be used. However, due to the possibility of lightning strikes, the last 15% of the aircraft wing remains free of fuel [62]. Additionally, 5% of each fuel tank's volume is reserved for the space occupied by the wing ribs. The ribs are not only vital to the structure of the wing box but also reduce fuel sloshing, acting as baffles.

Where necessary, the fuel tanks will be divided into smaller, separate fuel compartments. Each compartment will have a pump located at its lowest point, ensuring that the fuel flows towards the pump as it is being used by the engines. The fuel compartments furthest from the fuselage of CHEETAH will be emptied first to reduce the rolling moment of inertia. Additionally, the wing tanks will be emptied symmetrically, to keep the aircraft stable in roll-direction.

To ensure the safety of the crew and passengers, all fuel compartments will be equipped with pressure-release valves. Additionally, stainless steel plates will separate the engines from the fuel tanks in the wings and the crew and passengers from the fuel tank located in the fuselage [62]. Each tank will also be equipped with multiple fuel quantity sensors to provide accurate fuel level readings to the crew, even during extreme manoeuvres.

A more detailed platform of each fuel tank can be found in the following descriptions

FT-UW

- The fuel tank in the upper wings will be divided into several separate fuel compartments. This is to prevent the fuel from flowing to the tips due to gravity, as the upper wing is anhedral. The walls separating these compartments will be placed at 0 mm, 2422.5 mm, 4845 mm and 7268 mm from the root of the wing. These compartments will be refuelled and defuelled by means of a pumping system.

FT-LR & FT-LL

- The fuel tank in the lower right and left wing of CHEETAH will be symmetrical. However, since they are not connected, they are treated as two separate entities. These tanks have separate fuel compartments similar to the FT-UW. However, as these wings are dihedral, the tanks do not experience the same gravitational disadvantage. Therefore, each lower wing is divided into two separate compartments, with walls located at 3634 mm from the roots of the wings. The choice to minimise the number of compartments where possible was made from a weight and cost viewpoint as recommended by Roskam [62].

FT-WT

- This fuel tank is the smallest. It is located underneath the flooring, in front of the water tank. Due to its small size and convenient location, this tank will not need any separate compartments. Baffles will be placed if necessary, further research will have to be performed to determine this.

10.2.2. Fuel Flow

Properly fuelling an aircraft is of great importance as the addition of up to 9970 L of fuel shifts the balance of the aircraft and if done improperly, permanent structural damage can occur. Therefore, CHEETAH will have an advanced network of pumps, valves and pipes that distribute the fuel from the single fueling point to all four main tanks and their compartments. This process can be described, as illustrated in Figure 10.8, in seven steps;

Fuel Flow

- 1. Pump the fuel into the fuel port located on the wing of CHEETAH
- 2. Pump the fuel into **FT-WT** in the front of the fuselage
- 3. Pump the fuel up through the tube on the outside of the fuselage
- 4. Pump the fuel through the compartment up on the roof of CHEETAH
- 5. Pump the fuel through the second tube on the outside of the fuselage
- 6. Pump the fuel simultaneously into **FT-LR** & **FT-LL**, and ensure that the pumping system allows for the same mass flow into both wings to prevent tipping over
- 7. Pump the fuel into **FT-UW**, and ensure that the pumping system allows for the same mass flow into both the left and right wings to prevent tipping over

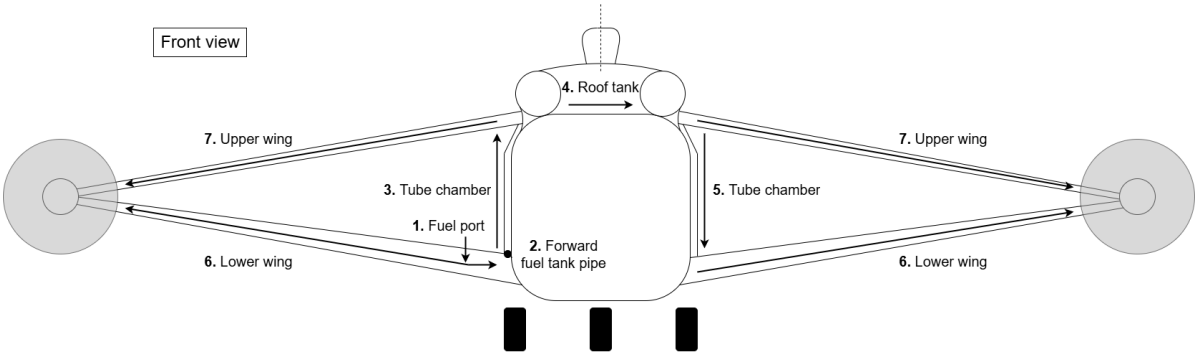

Figure 10.8: *Scheme of the fuel flow when refuelling CHEETAH.*

To be able to supply the necessary fuel to the engines, the fuel pipes and fuel pumps must be dimensioned so they can supply 1.5 times the maximum required fuel flow by the engines [62]. For the design of CHEETAH, this means that the pipes and pumps must be able to transport a fuel flow of 1.17 kg/s.

In addition to this integrated fuel system. An extra, modular fuel tank can be placed in the fuselage and connected to an additional fuel port, specific for this use. This allows CHEETAH to travel longer distances. Any fuel tank that fits the fuselage dimensions of CHEETAH and can connect to this fuel port can be used.

10.3. Hydraulics

Contributors: Merel, Ruben
Authors: Merel, Ruben

Aircraft hydraulic systems are essential for providing force to operate various mechanisms and controls. Examples of these mechanisms include the ailerons, elevators, rudder and landing gear and the doors for the dropping system. There are three main types of aircraft hydraulic systems: no hydraulics, the boosted hydraulics system, and the full hydraulic system, each type has distinct mechanisms and applications.

The hydraulic systems utilise fluid pressure to generate, control and transmit forces for operating landing gear, brakes, flight control surfaces, flaps, and other critical systems. This section will describe the various hydraulic systems, explain their operations and outline the main components present in CHEETAH.

10.3.1. Hydraulic System Configuration

Aircraft hydraulic systems can be divided into three main types: manual control, meaning no hydraulics, boosted hydraulics or full hydraulics. The choice of hydraulic system configuration depends on factors such as aircraft design, performance requirements, safety considerations and cost. Generally, helicopters with a total weight over 3000 kg cannot be operated using any hydraulics or the boosted hydraulic system [63]. This means that a full hydraulic system must be implemented for CHEETAH.

The fully hydraulic system offers higher performance, faster response times, and greater reliability compared to manual or assisted systems. This configuration is recommended for aircraft weighing more than 3000 kg

and equipped with high-response rotor systems. However, in the case of hydraulic system failure, rendering the aircraft inoperable, backup systems become imperative for ensuring safety and reliability. An example of an aircraft operating with fully hydraulic systems is the Apache. In short, the choice of hydraulic system configuration depends on factors such as aircraft design, performance requirements, safety considerations, and cost. While fully hydraulic systems offer superior performance, they also come with increased complexity and safety concerns.

In order to mitigate safety concerns, most helicopters operate dual hydraulic systems. There are two available options when deciding to use two hydraulic systems. The first option is to design each system to handle the full range of control loads, using one system as the primary and the other as a standby. In case of failure of the main system, the standby system gets activated automatically. The second option is to design each hydraulic system to handle the control loads for basic flying, with both systems together covering the entire flight spectrum. In this case, the failure of one system would still ensure minimum basic flying capability. Given that CHEETAH operates under demanding conditions, including turbulence, dense smoke, and hazardous manoeuvres, ensuring pilot safety during these situations is of great importance. Even during hydraulic system failure the pilot should still be able to navigate these conditions, this would require the first hydraulic backup system to be implemented.

According to the emerging new civil airworthiness requirements, in addition to dual hydraulic systems, an electrical backup system must also be provided for the flight control system of helicopters. This third system can also be used for preflight checks of the flight control system.

10.3.2. Hydraulic System Components

Although the hydraulic systems described in Subsection 10.3.1 vary in type, they generally comprise similar components. Hydraulic systems consist of reservoirs, pumps, filters, valves, actuators, and accumulators. It is crucial to gain an understanding of these components. Therefore, a description of these components will be provided, accompanied by Figure 10.9 to illustrate a basic hydraulic system and its components.

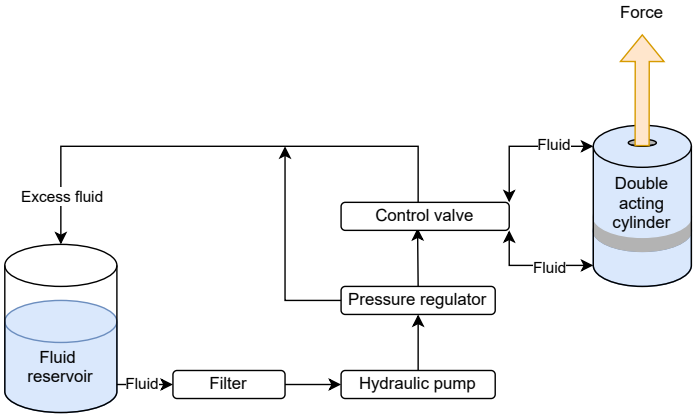

Figure 10.9: *Scheme of the hydraulic system components.*

- **Hydraulic Reservoir**
  First of all, the hydraulic system contains a hydraulic reservoir. The reservoir provides a ready source of hydraulic fluid for the hydraulic pump(s) and contains a varying volume of fluid. The reservoir supplies the hydraulic system with hydraulic fluid via a supply line and receives returns via a return line. Bleed air from the engines is often utilised to pressurise the reservoir in many scenarios; however, this task can also be performed by the engine or the Auxiliary Power Unit (APU).
- **Hydraulic Pumps**
  To pressurise the hydraulic fluid into the hydraulic system, hydraulic pumps are used. The pumps must maintain a consistent pressure while delivering the hydraulic fluid. These pumps can be powered by the engine or electrically driven by the backup system.
- **Hydraulic Filters**

To remove any impurities from the hydraulic fluid, hydraulic systems contain filters. These filters prevent damage to the hydraulic system. Often these hydraulic filters are installed before supply lines, return lines and critical components.

- **Hydraulic Valves**
  Next to the pumps, the flow of the hydraulic fluid can be controlled and regulated by hydraulic valves. To allow the fluid to flow in only one direction, a check valve can be used. The hydraulic system also contains shut-off valves that can cut off the hydraulic fluid flow during emergencies such as a leak, fire or pump fault. Moreover, to reduce the hydraulic fluid pressure in a particular line, a pressure-reducing valve can be placed in the system. Finally, selector valves can be used to change the direction of the pressurised fluid.
- **Hydraulic Actuators**
  The main component of the hydraulic system is the hydraulic actuator. The actuator converts hydraulic pressure into mechanical action. This mechanical process is used to control the flight control system and extend or retract features like flaps, slats, or the landing gear.
- **Hydraulic Accumulators**
  Finally, for a consistent supply of hydraulic fluid under varying demand and pressure conditions, hydraulic accumulators serve as a vital component. These devices store pressurised hydraulic fluid and function as a reliable backup in emergencies, such as pump failure or sudden pressure drops.

10.4. Weight Estimation

Contributors: Marinka
Authors: Marinka

The final weight estimation of the subsystems was mostly done using equations from Prouty [25]. These equations are based on helicopter statistics and are mostly related to MTOW. Some of the subsystem weights in the book were combined in our analysis for ease of overview. The cockpit controls, instruments, high avionics category and low furnishings and equipment were combined to find the weight of the cockpit subsystem. The furnishings were included in here since there will be chairs for the pilots in the cockpit and there is no furnishing elsewhere in the aircraft. To reflect the very low amount of furnishing the weight was also divided by two. Lastly, the wing weight was estimated using a formula with a coefficient to correct for box wings [64]. This formula also needed some wing parameters such as area as input. Since the estimations were dependent on MTOW they were all iterated in the calculation of the CG as well. The conceptual weight estimations were used as initial inputs for this iterative process.

10.5. Budget Breakdown

Contributors: Marinka
Authors: Marinka

In the baseline report, several budgets were set up to ensure the design would stay within a certain range. At this point, more is known about the design which enables an iteration of the budgets.

Mass

The mass budget of the operational empty weight, fuel weight, payload weight and maximum take-off weight has been updated with a more detailed calculation of the midterm report [2].

Table 10.3: *Mass budget breakdown.*

Phase	Parameter	OEW	Fuel	Payload	MTOW
First estimate	Value [kg]	18643.85	2498.15	11000	32142
	Confidence [%]	60	20	80	60
Conceptual	Value [kg]	20500	4800	11000	35500
	Confidence [%]	70	40	90	70
Preliminary	Value [kg]	16300	6700	12500	35500
	Confidence [%]	90	70	90	80

The confidence has increased greatly since the methods are more reliable compared to the initial weight estimation methods. Additionally, the operational empty weight could now be divided over the subsystems which is shown in Table 10.4.

Table 10.4: *OEW budget breakdown.*

	Conceptual		Preliminary	
Phase	**Value [kg]**	**Confidence [%]**	**Value [kg]**	**Confidence [%]**
Main rotor blades	2000	60	1200	80
Main rotor hub	1600	60	1500	80
Wing	3400	50	3700	70
Engines	1500	70	2000	90
Starboard propellers	100	60	200	90
Port side propellers	100	60	200	90
Nose landing gear	300	40	210	70
Main landing gear	600	40	410	70
Horizontal tail	300	30	80	80
Vertical tail	200	30	60	90
Fuselage	4900	40	4100	70
Cockpit	1000	30	1900	70
Pilots	200	90	200	90
Fuel tank	700	60	800	70
Water and tank	11500	90	11500	90
Retardant	1000	70	1000	90
Fuel	4000	20	6700	70

To find a first estimate of subsystem weights, weight fractions of maximum take-off weight for conventional helicopters between 14000-45000 kg were used [65]. These values are not entirely representative of a compound helicopter as there is no wing system and the propulsion system in our case is expanded with two propellers for forward thrust. For this reason, the mass allocation for the propulsion system has doubled and the wing was allocated a percentage based on aircraft statistics [66].

The second iteration was done as described in Section 10.4. Something notable is the low weight of the empennage after the second iteration. This weight has decreased drastically because, in the case of a normal helicopter, the empennage has to hold a tail rotor which means that it needs more structural strength. The weight of the horizontal tail might need to increase a bit more as CHEETAH has an H-tail so the horizontal tail will need to hold up the vertical tail. Another thing that drastically changed was the increase in weight of the propellers and engines because one extra engine and two more propellers were needed to meet the speed requirement. Lastly, the fuel has also increased by more than 50% because, in the analysis of the range, it turned out that more fuel was needed to meet the range requirements.

Power

The power budget provides an overview of the maximum power consumption for various systems and ensures efficient distribution of power resources. This includes the propulsion system, the snorkel, the avionics and control systems, as well as other smaller subsystems. Additionally, the inclusion of an APU in the power management strategy will also be evaluated. From the engine selection in Section 6.3, it was determined that the engines would deliver a total of 21252.4 kW.

- **Propulsion power**
  From Section 6.3, it was found that the full propulsion system will consume a maximum power of 20589.8 kW achieved during hover climb at 1.5g.
- **Snorkel pump power**
  A snorkel and accompanying systems will be equipped on the VTOL aircraft. It was concluded that the Helitak HP10000 Hover Pump is the best option for the mission [2]. To operate this pump, 26.8 hp (19.7 kW) is needed.
- **Avionics and control systems power**
  One of the other main power consumers are the avionics and flight control systems. Determining the exact amount of power it consumes is very hard, but an estimation can be made by looking at other aircraft. For instance, for the DC-10, the avionics need 7.25 kW and the flight controls need 14.75 kW [67]. To ensure that the power allocated is sufficient to meet the needs of the avionics and control systems, a safety margin is included in the calculations. This leads to the avionics needing 10 kW and the flight controls needing 20 kW.
- **Remaining systems power**
  The aircraft is composed of many more systems which need power. One very important system is the hydraulic system, which is responsible for operating essential components such as the landing gear, flight control systems, and brakes, among others. Additionally, power is allocated to the emergency systems, the de-icing mechanism, and smaller electric systems. However, these power demands are considered sufficiently small to be covered by the remaining 612.9 kW.
- **APU**
  An Auxiliary Power Unit is a device located on an aircraft that provides energy for various functions other than propulsion [3]. It typically powers the aircraft's electrical systems on the ground, starts the main engines, and provides cabin heating or air conditioning when the main engines are not running. Given the compound helicopter will be provided with sufficient support on the ground and that the engines provide enough power for all onboard systems, it was decided not to include an APU onboard the aircraft.

Table 10.5 gives an overview of the final power budget. For propulsion, the indicated power for the propellers is not their maximum usage, but rather the power consumption at the peak usage of the entire propulsion system.

Table 10.5: *Power budget breakdown.*

System	Power consumption [kW]
Main rotor	16410
Propellers	4179.8
Snorkel	19.7
Avionics	10
Flight controls	20
Total Power	**20639.5**

Range

Contributors: Floris, Marinka
Authors: Marinka

[3] https://www.globeair.com/g/auxiliary-power-unit-apu

This range budget will provide estimates of the aircraft's range both when fully loaded and when unloaded.

The range can be calculated with a modified Breguet-equation, Equation 10.1, which was derived in the midterm report [2].

$$\left(\frac{1}{W}\right)dW = -g\left(\left(\frac{c_{p_H}}{\eta_H}\right)\left(\frac{D}{L}\right)+\left(\frac{c_{p_V}}{V_H}\right)\left(\frac{P_V}{W}\right)\right)dx \tag{10.1}$$

with R the range in meters, V the cruise velocity in m/s (this velocity is determined by the requirements and is set to 400 km/h, or 111.11 m/s), P the power in Watts, and c_{p_H} and c_{p_V} the specific fuel consumption in $\frac{kg}{W \cdot s}$, for the propellers and the rotor respectively. Using the payload-range diagram which was set up in Section 11.1 the values in Table 10.6 were found.

Table 10.6: *Range budget breakdown.*

Phase	Parameter	MTOW+max PL	MTOW+max fuel	Ferry	Ferry+auxiliary tank
First estimate	Value [km]	1800	-	-	-
	Confidence [%]	60	-	-	-
Preliminary	Value [km]	1390	1680	1840	3975
	Confidence [%]	80	80	80	75

For the Ferry + auxiliary tank, the payload-range diagram, all payload was removed (same as Ferry), but an additional 10 000 kg of fuel was added.

As MTOW + max PL, MTOW + max fuel and Ferry all come from the same source, the confidence of all these is the same. The confidence for the auxiliary tank is less, as it is assumed that the total weight of water is replaced by the weight of fuel, instead of the volume. This would then in turn require a different tank, but as this can be a bladder, an additional 100 kg is added to the Operating Empty Weight (OEW). But because of this assumption, the confidence is a bit lower.

From Table 10.6, it can be seen that, with maximal payload and at Maximum Take-off Weight, the range is 1390 km, and as Figure 11.1 is made for a speed of 400 km/h (111.11 m/s), an endurance of 3.475 h is straightforwardly calculated.

11 | Performance

Evaluating the performance of the CHEETAH VTOL aircraft is crucial to ensure it meets operational requirements and performs effectively in diverse firefighting scenarios. This chapter investigates key performance metrics such as payload-range capabilities, transition performance, V-n diagrams, emissions, and noise levels. Understanding these parameters is essential for validating the aircraft's efficiency, reliability, and compliance with environmental and regulatory standards. A thorough analysis of these performance aspects confirms that CHEETAH is a powerful firefighting tool and a sustainable, dependable solution. This chapter outlines the methodologies and results of these evaluations, providing a comprehensive overview of the aircraft's performance characteristics.

11.1. Payload-Range Diagram

Contributors: Floris, Marinka
Authors: Floris, Marinka

A payload-range diagram can be constructed to better understand the capabilities of CHEETAH. To construct this diagram, the range of CHEETAH is determined for several combinations of payload and fuel mass.

These payload-fuel combinations start with zero fuel and a full payload. Then, fuel mass is slowly added, until MTOW is reached. From there, all extra fuel mass, until maximum fuel mass, results in the loss of an equivalent payload mass. After maximum fuel mass is reached, the payload can be removed to make CHEETAH lighter, and therefore more efficient, until the payload mass is 0 kg.

The range is calculated using a modified version of the Breguet equation, Equation 10.1, but every term is multiplied by the weight or lift, as it is assumed that the lift equals the weight. For this equation, the lift provided by the rotor is assumed to be constant, and 8 % of the MTOW of 35 500 kg, as can be seen in Equation 11.1. The equation is also rewritten to be integrated over time, instead of distance, and as the speed is constant, the distance can be calculated straightforwardly from the calculated time. The power required for the rotor is therefore also constant and equal to 2357 kW. As the same engines are used for both the rotor and the propellers, the specific fuel consumption for horizontal and vertical is equal. When these changes are incorporated, Equation 10.1 is modified to Equation 11.2.

$$L_w = W - L_r \tag{11.1}$$

$$dW = -g c_p \left(\frac{DV_H}{\eta_H} + P_V \right) dt \tag{11.2}$$

As the aircraft loses weight as it burns fuel, the weight will vary during the flight. To account for that, it is assumed that CHEETAH will fly under different angles of attack to get different lift coefficients, as can be seen in Equation 11.3, which directly influences the lift and drag generated by the wings. The angle of attack is chosen so the aircraft is in equilibrium, and the corresponding drag coefficient is then calculated. From there, the total drag is calculated using Equation 11.4, which can then be filled in Equation 11.2.

$$C_L = \frac{2L_w}{\rho V^2 S} \tag{11.3}$$

$$D = \frac{}{2} \rho V^2 S C_D \tag{11.4}$$

This process is repeated until the fuel mass reaches 0 kg, and the range for that payload-fuel combination can then be calculated. The range for all payload-fuel combinations is then calculated, the plotted version can be seen in Figure 11.1.

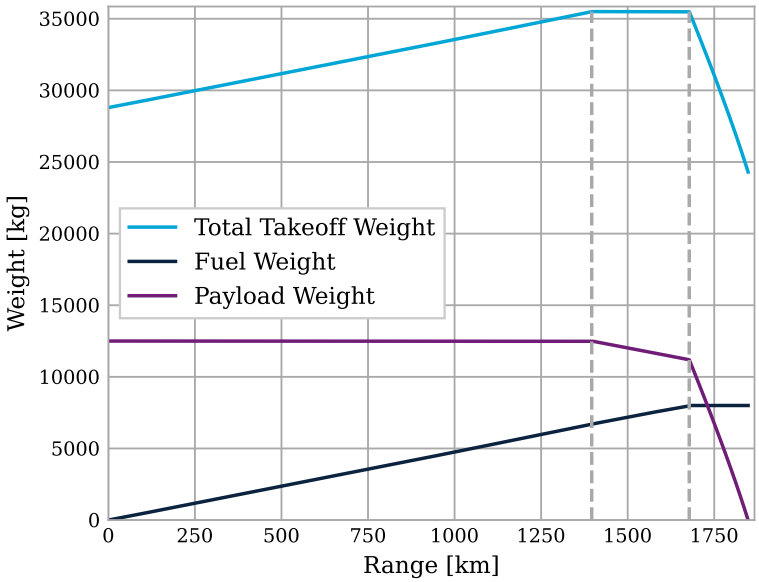

Figure 11.1: *CHEETAH's Payload-Range diagram at an altitude of* 3500 m *with a cruise speed of* 111.11 m/s

The first grey line in Figure 11.1 is the point where the MTOW is first reached, which is the combination of maximum payload and then as much fuel as possible, while the second grey line represents the combination with maximum fuel mass, and then as much payload as possible. The first grey line represents the payload-fuel combination for fire attack missions, while the second grey line marks the point from where payload mass is removed, only to reduce the aircraft weight.

Range sensitivity

A big factor influencing the range is the propeller and rotor efficiency. A quick estimate for these efficiencies was 60%. The range at MTOW and maximum payload is calculated for efficiencies between 50% and 90% and shown in Figure 11.2.

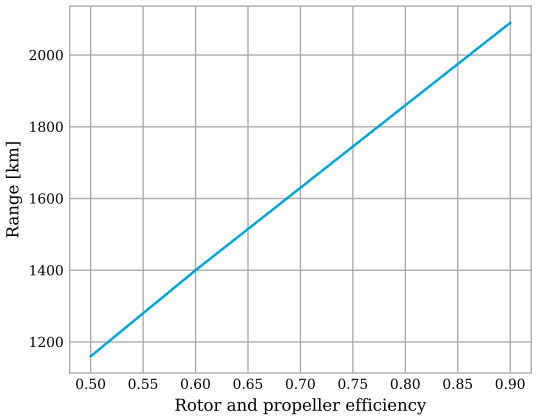

Figure 11.2: *Full payload MTOW range at different efficiencies*

For a realistic range of efficiencies, the range falls within the requirements for range and endurance. This means the design is feasible even with a different efficiency.

11.2. Transition Performance

Contributors: Sjoerd
Authors: Sjoerd

The performance of CHEETAH during the transition from hover to cruise is still vague as, for the preliminary phase, the design was only optimised for both flight profile extremes. This decision was made because it resulted in significant simplifications. It is, however, paramount for validating the design that this mission phase is analysed making sure that the design would function.

For the scope of this report, only a simplified model of the transition phase was simulated. This simulation includes the climb rate and horizontal acceleration of CHEETAH and how these are affected by the available power of solely the pusher propeller engines. The climb rate was assumed to be steady and calculated by Equation 11.5, while the horizontal acceleration was calculated by Equation 11.6.

$$RC_s = \frac{P_a - P_r}{W} \tag{11.5}$$

$$a = \frac{T - D}{m} = \frac{\left(\frac{P_a}{V}\right) - C_D q_\infty S}{m} \tag{11.6}$$

For the simulation, a ratio was determined for the power available that would be directed towards the steady rate of climb versus the horizontal acceleration. In Figure 11.3a and Figure 11.3b of Figure 11.3, the results of this simulation are shown, which represent a power available ratio for rate of climb versus horizontal acceleration of 1.5 and 9 respectively.

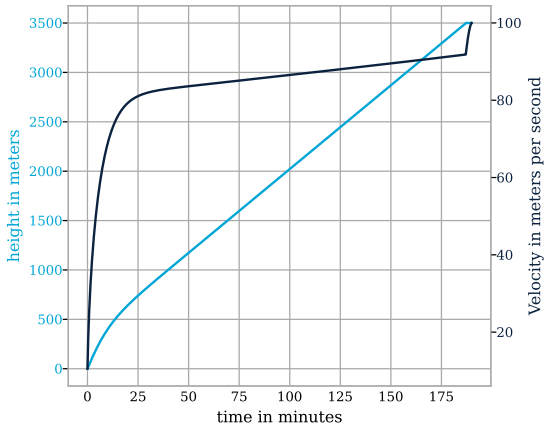

(a) *Flight profile to cruise for a power available ratio of 1.5 for rate of climb (RC) over horizontal acceleration.*

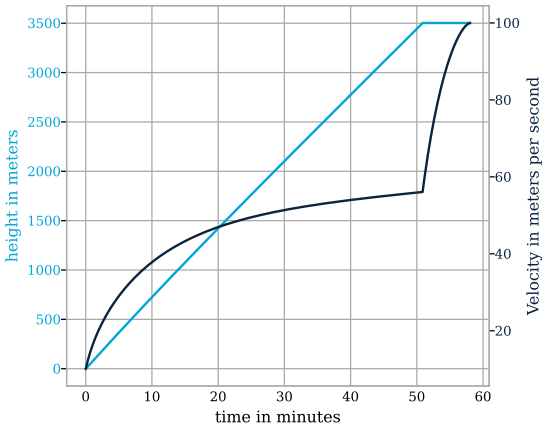

(b) *Flight profile to cruise for a power available ratio of 9 for rate of climb (RC) over horizontal acceleration.*

Figure 11.3: *Flight profile of CHEETAH for the transition from hover to cruise.*

From these graphs, it could be concluded that, for a quick transition phase, most available power should be directed towards the aircraft's climb performance. The issue, however, is that this model is still very preliminary and there are a lot of aspects and phenomena that should be incorporated before the model's confidence level will be acceptable. Furthermore, two contradicting results have arisen. According to the engine and propeller sizing in Chapter 6, CHEETAH should be able to reach the required cruise velocity of 400 km/h or 111.11 m/s. However, the transition phase model does not seem to reach this velocity and the code will need a revision.

Moreover, the most limiting factor of the transition phase is expected to stem from the rotor-wing interference as discussed in Section 7.4 of Chapter 7 and it is therefore paramount that also this phenomena will be incorporated in the model.

Overall, the transition simulation seems like a promising strategy to analyse the performance of CHEETAH in its transition from hover at sea level towards cruise conditions and should be further analysed for design validation. It should be noted, however, that the current simulation is still very limited in its accuracy and that there are several tasks required before an acceptable confidence level will be reached. These include:

- Verifying that the simulation until now is accurate and does not contain any errors.
- Expanding the steady rate of climb as the rate of climb will most likely not be steady.
- Including the induced velocity angle by the rotor on the wing as this is expected to significantly impact the wing performance.
- Account for the weight of the aircraft as the simulation assumes a constant mass while this will not be the case in practice.
- A higher rate of climb will be possible using the main rotor, this might be considered for a higher transition performance.

If these aspects have been implemented and verified, a proper estimation can be made of the time that CHEETAH will take to reach cruise conditions. Looking at the results so far as depicted in Figure 11.3a and Figure 11.3b, this might even require a revision of the cruise altitude, as it seems to take CHEETAH a very long time to reach these conditions.

11.3. Manoeuvre Loading Diagram

Contributors: Xander & Ivo
Authors: Ivo

The loading diagram of an aircraft is used to illustrate the limits in performance the aircraft has by showcasing the load factors it is able to sustain at different speeds [1]. As can be seen in Figure 11.4, for the compound helicopter, two diagrams were created. The first is similar to that of an airplane as it displays the load factor achieved solely through the wing load. The second shows a loading diagram that combines the wing load with the overall helicopter capabilities. In hover, the aircraft is designed to sustain 1.5g. Furthermore, the upper operational limit of 3.25g and lower operational limit of -1g are defined in accordance with requirement FTF-SYS-FDS-05.15 from Table 2.3, as specified by the CS-25 regulations [68]. After reaching the cruise velocity, the minimum load factor the compound helicopter is able to sustain increases linearly until reaching 0g at the diving velocity. Through this loading diagram, a better understanding of the structural and performance limits of the aircraft is achieved ensuring safe operation across all flight conditions.

[1] Flight Envelope https://www.uavnavigation.com/support/kb/general/general-system-info/flight-envelope [retrieved 18th June 2024]

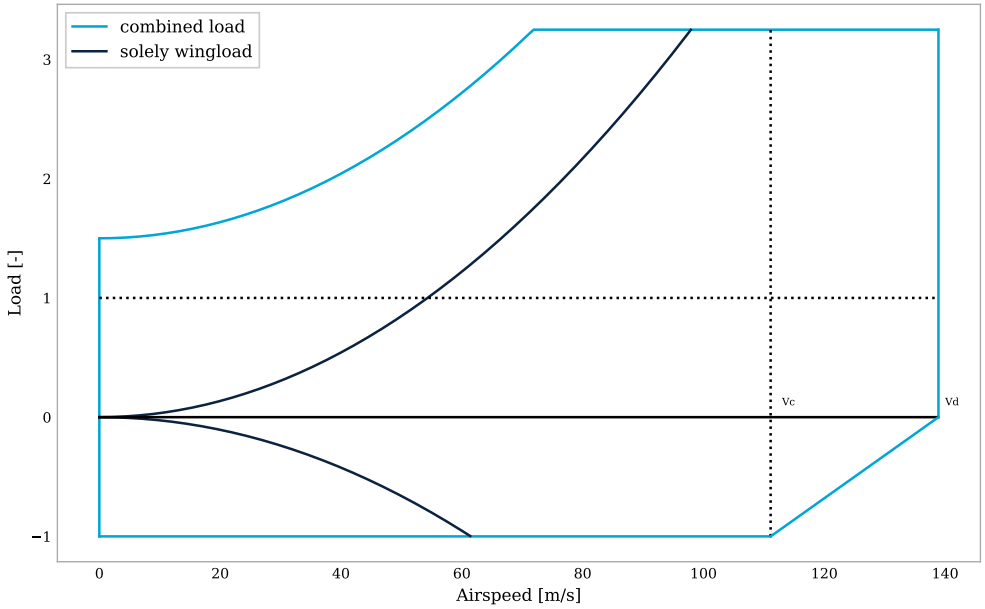

Figure 11.4: *Loading diagram compound helicopter.*

11.4. Emissions

Contributors: Ivo
Authors: Ivo

Over their lifespan, aircraft produce a significant amount of emissions, primarily stemming from the emissions produced by the combustion engine burning fuel and the production process. Although aircraft emissions represent a relatively small fraction of global emissions compared to other sectors [69], their impact is amplified due to their release at high altitudes, where they can have a stronger warming effect[2]. However, as discussed before in the midterm report [2], these emissions are negligible compared to the emissions of a wildfire. This is why, for this aircraft, the performance of the aircraft systems will always take priority over the emissions it emits. Moreover, emissions must be taken into account during the design phase of an aircraft. When the emissions of an aircraft design are known, some adjustments can be made to reduce them. As the design is still in the early design stages, some assumptions or simplifications need to be made to come up with estimations of the emissions produced.

Fuel Consumption

The emissions for the engines used will be estimated with the carbon dioxide Emission Factor (EF) of the fuel used and the BSFC of the engine. A final decision on what fuel will be used has not been made yet, but this will most likely be jet kerosene (Jet A1 or Jet A) which has an EF of 3.16 $\frac{\text{kg}_{CO_2}}{\text{kg}}$ [3]. As explained in the engine selection, four General Electric T408 engines will be used to power the rotor and the propellers. For one engine, the BSFC is 0.4 $\frac{\text{lb}}{\text{h}\cdot\text{hp}}$ and the power produced is 7500 hp. Using Equation 11.7, this results in 9480 $\frac{\text{lb}_{CO_2}}{\text{h}}$, or 4300 $\frac{\text{kg}_{CO_2}}{\text{h}}$ per engine. Assuming all the engines will operate at full power, the maximum total amount of emissions the aircraft will emit per hour is 17200 $\frac{\text{kg}_{CO_2}}{\text{h}}$.

$$\text{emissions} = \left(\text{power}\right)(BSFC)(EF) \tag{11.7}$$

[2] What is aviation's contribution to climate change? https://www.transportenvironment.org/topics/planes/airplane-pollution [retrieved 11th June 2024]
[3] CO2 Emissions https://www.offsetguide.org/understanding-carbon-offsets/air-travel-climate/climate-impacts-from-aviation/co2-emissions [retrieved 11th June 2024]

To put this into perspective, the emissions produced by the compound helicopter can be compared to those produced by wildfires. As explained in the baseline report [1], the emissions produced during a wildfire are dependent on many factors including the type of vegetation and humidity. In 2023, wildfires burned nearly 400 million hectares of land worldwide [70], resulting in approximately 2170 megatonnes of carbon emissions [71]. This translates to approximately 5425 kg of CO_2 released per hectare burned. Given that wildfires typically cover areas over 1000 hectares, the emissions produced by the firefighting fleet are minimal compared to those produced by the wildfire.

Production

The production phase of the aircraft can be divided into different steps. Each step produces its own amount of emissions, which can be added up at the end of production to get the total amount of emissions. Since the final designs of both aircraft are not known yet, most emissions will be given in terms of the mass of the material. The first step of the production phase is material production. In Section 9.2, several materials were considered for different parts of the aircraft. Since no final decision has yet been made on the quantities in which they will be used, Table 11.1 gives an overview of the carbon footprint of all those materials per kg.

Table 11.1: *Material characteristics of materials considered for the aircraft (see Section 9.2).*

Material	**CO2 footprint** [kg_{CO_2}/kg]
Epoxy and HS carbon fibre biaxial lamina	45.5-50.1
Low alloy steel, 300M	1.05-1.3
Aramid paper/phenolic honeycomb	15.7-17.4
Aluminium alloy 2024	7.3-8.41

The next step in production would be the transportation of the materials. The final design of the compound helicopter will be composed of many different materials. The most used material will be aluminium, which is mostly produced in China, India and Russia [4]. Assuming the aircraft is assembled in Rotterdam, The Netherlands, the main aluminium producer that is furthest away would be China. Since 90% of goods are shipped by ocean freight [5], which is also one of the most eco-friendly ways of transporting cargo[6], it will be assumed that this is also the case for the materials used for the compound aircraft. In addition to this, it is also assumed the aluminium used will be shipped from Beijing, China. This would mean the ship would have to cover a distance of 11347 nautical miles, or 21014 km [7]. Knowing that 1000 km of shipping freight for 2 kg of cargo is equivalent to 0.03 kg of CO_2 [7], shipping aluminium from Beijing to Rotterdam will emit 0.630 kg of CO_2 for every 2 kg of material. On the other hand, although China is one of the leading countries in carbon fibre production, it makes more sense to use the carbon fibre produced in Germany, which is also one of the leading carbon fibre producers in the world [72]. Additionally, it will be assumed the carbon fibre will be produced in Willich, an SGL Carbon production site close to the border with the Netherlands. This time, the carbon fibre will be transported by truck, which will have to cover a distance of 210 km to get to Rotterdam [8]. The average CO_2-emission factor recommended by McKinnon for road transport operations is 0.062 kg_{CO_2}/tonne-km [73]. Therefore, the transport of carbon fibre will emit 0.013 kg_{CO_2}/kg_{carbon}. Finally, the steel used for the aircraft will also come from Germany. The biggest steel production site in Europe is located in Duisburg, 207 km from Rotterdam [9]. With this distance being very close to the distance between Willich and Rotterdam, the transport of steel will have a similar carbon footprint to that of the transport of carbon fibre. The emissions produced during manufacturing depend on various parameters, including the type of manufacturing process, the type of material, and the mass of the material. Once these parameters are known, the total amount of energy used can be converted into the carbon footprint of the manufacturing process. As of 2023, 1 kWh

[4] Which are the main aluminium producing countries in the world?, https://www.laminazionesottile.com/en/blog/the-main-aluminum-producing-countries. [retrieved 11th June 2024]

[5] Shipping from Beijing, Beijing to Rotterdam: Air, Sea & Container Freight, https://freightos.com/routes/route/cn-beijing-beijing/nl-rotterdam

[6] Carbon Footprint: Freight | Shipping, https://www.co2everything.com/co2e-of/freight-shipping [retrieved 11th June 2024

[7] Rotterdam to Beijing By Air freight, Cargo ship or Road, https://www.fluentcargo.com/routes/rotterdam-nl/beijing-cn [retrieved 11th June 2024

[8] Our sites – SGL Carbon around the world https://www.sglcarbon.com/en/company/about-us/sites/ [retrieved 11th June 2024

[9] Industrial Heritage, https://www.duisburg.de/microsites/visit_duisburg/discover_the_city/industrial_heritage/index.php [retrieved 11th June 2024]

of energy produces approximately 421 grams of CO_2 in the Netherlands.[10] Using this conversion factor, the total emissions can be calculated.

The final part of the production phase is the assembly of different systems. Unfortunately, at this stage of the design phase, too little is known to estimate the emissions produced during this part of the process.

11.5. Noise

Contributors: Marco
Authors: Marco

As discussed in the midterm report [2], helicopters made purely for firefighting are exempt from the noise regulations of International Civil Aviation Organization (ICAO) Annex 16 Volume I [74]. However, as also stated in the midterm report, CHEETAH will still comply with these regulations since it is supposed to be used in other missions as well. In this section, the existing regulations are listed, and rudimentary calculations for noise levels are performed, after which the validity of the results will be discussed.

There are no existing noise regulations for compound helicopters; the regulations for normal helicopters are reported in Table 11.2 below. Maximum noise levels are displayed as Effective Perceived Noise in Decibel (EPNdB) values. The EPNdB values for 80 000 kg are the ones specified explicitly, and the ones at CHEETAH's 35 500 kg are the adjusted values with the correction factor mentioned in the regulations. The distance at which this noise is measured is reported at the bottom of the table.

Table 11.2: *Maximum EPNdB for helicopters of different masses in different flight phases, as regulated by ICAO Annex 16 Volume I [74].*

MTOW [kg]	Take-off	Overflight	Landing
80 000	106	104	109
35 500	102	100	105
Measuring distance [m]	500	150	120

No in-depth aeroacoustic analysis has been performed for CHEETAH's design, as this is outside of the scope of this project, so more rudimentary methods have to be used. Here, the procedure from Appendices B & C of [75] was followed: for the propellers and rotor, semi-empirical calculations were performed, and their results were summed. The results are tabulated below in Table 11.3:

Table 11.3: *Estimated noise levels from [75] for CHEETAH in cruise, measured at a distance of 150 m below the aircraft.*

Noise Source	Noise Level [dB]	Remarks
Rotor – Rotational Noise	119	Excludes blade slap; result may be too high
Rotor – Vortex Noise	95	Result may be too high
Propellers	100	Sum of all propellers
Total	**119**	Result seems too high, due to extrapolation of components

These results, obtained for overflight at cruise velocity, measured at 150 m below the aircraft, seem to be quite high, due to the rotor's rotational noise being high. The probable cause for this is that the model from [75] was not made for helicopters of this size, but another possibility is that the model used presents outdated results (the source was published in 1970) and that the state of the art is much more advanced. It should be noted that the values obtained here are in unweighted decibels, and not in EPNdB as regulations prescribe. The conversion from dB to EPNdB is time- and frequency-dependent, and was deemed both too uncertain to estimate and, even if possible, outside the scope of this project. Another note is that this analysis only includes the propellers and rotor and that there are more sources of noise present in CHEETAH. These sources include the following [76]:

- **Rotor:** Apart from the rotational and vortex noise estimated, another very important component of rotor noise is blade-vortex interaction (BVI), otherwise known as blade slapping. This source of noise

[10] Current emissions in the Netherlands, https://www.nowtricity.com/country/netherlands/ [retrieved 16th June 2024].

arises when a rotor blade encounters the vortex coming off a preceding blade. This usually occurs when the aircraft is descending;[11]

- **Propellers:** a non-negligible extra source of noise relating to the propellers is the interference of fast-moving air from the propellers with the wings mounted behind them;
- **Engines:** helicopters' turboshaft engines can become the main source of noise at takeoff. Engine noise mostly comes from combustion and air radiated at the outlet of the engines [77];
- **Airframe:** this covers all the noise that does not come from the propulsion system, essentially, the noise that would be generated if the aircraft was a glider;
- **Other instances of interference:** this is the hardest part to predict, and it is impossible to do so with just rudimentary calculations. Since for CHEETAH, the rotor, propellers, wings and body are placed tightly together, the interference that these components experience from each other is assumed to be significant.

In short, the noise values estimated in Table 11.3 paint far from the whole picture, and the actual noise value will likely increase. The hard truth is that the aircraft may not fly in any other role than active firefighting if it does not comply with the regulations from Table 11.2, and these regulations will likely get more stringent in the future. Even if the EPNdB value will turn out (far) lower than the total from Table 11.3, care must be taken during further development to limit how loud CHEETAH will become. It is therefore recommended that resources be allocated to the development of more silent propellers, rotors, engines, etc. and that a better understanding of the magnitude of interference effects be sought.

[11] Tiltrotor Aeroacoustic Model Summary, https://rotorcraft.arc.nasa.gov/Research/Programs/tramprogram.html [retrieved 17th June 2024].

12 | Return on Investment

In order to determine whether an aircraft is feasible, it should be investigated how expensive it is to develop the aircraft and how much it would cost to actually produce each individual aircraft. It should also be investigated how much demand there is for such an aircraft, and for that, it is also good to know the operating costs of the aircraft. From the costs, and the desired profit, or profit margin, a selling price can be determined. Then, all costs and revenues can be computed, and from there, a Return on Investment (ROI) can be calculated.

12.1. Costs

Contributors: Floris
Authors: Floris

In the baseline report [1], some first estimations of acquisition, operating and crew costs were made. The estimation has been broken down into several subsystems, such as rotor, wings, powerplant and more. Not all of the articles and reports used in this section, give the prices in FY24 $, so to account for inflation, the costs were multiplied by the total inflation[1] between the year the article or report was published, and 2024.

Production

For the breakdown of the production costs, a combination off methods was used. For the production cost, a PhD thesis [78] was found to estimate some key systems of helicopters, next to that, the costs of the engines [2] and the propellers [3] were found online. Lastly, an article that breaks the costs of subsystems for aircraft down in percentages [79], was found to calculate the costs of the rest of the subsystems.

Table 12.1: *Overview of production cost broken down per subsystem, based on 50 produced aircraft [79] [78].*

Subsystem	**Costs** [million$]
Avionics	5.81
Airframe	7.14
Electrical	2.09
Empennage	0.78
Gear	0.78
Nacelles	1.18
Flight Control	1.49
Total General	19.27
Rotor	1.64
Drivetrain	1.32
Propulsion	12.32
Total Helicopter	15.28
Wing	2.74
Forward Drivetrain	0.26
Propeller	0.34
Total Aircraft	3.35
Assembly	7.58
Total Cost	45.47

[1] https://www.in2013dollars.com/us/inflation/1956?amount=1 [retrieved 3rd June 2024]
[2] http://tealgroup.com/images/TGCTOC/sample-wpsba2.pdf [retrieved 3rd June 2024]
[3] https://hartzellprop.com/wp-content/uploads/2021-Price-List.pdf [retrieved 6th June 2024]

For the forward drivetrain, it is important to note that it was assumed that this drivetrain would cost 20 % of the main rotor drivetrain, as a big part of this would be shared. For the equations found by Gilliland [78], a number of to-be-produced aircraft was required, this number is assumed to be 50, but this will be changed later on, in Section 12.3, when the number of expected CHEETAHs that will be sold is computed.

Development

The development costs are estimated using a method by Roskam, presented in his eight book of the "Airplane Design" series [80]. This method estimates the costs for Research, Development, Testing and Evaluation (RDTE). For this estimation, it was assumed that six aircraft should be produced to be tested, it was also assumed that the difficulty factor should be 1.5, as the design is not straightforward, but is using existing technology. An overview of these, and all other values, can be seen in Table 12.2. The Computer Assisted Drawing (CAD) capability factor was estimated to be 1.1. The costs of avionics can be found in Table 12.1, and the engines at the website mentioned in Section 12.1. It was furthermore assumed that two aircraft are used for static testing. CHEETAH is designed to be primarily constructed out of aluminium alloys, so the material factor was estimated to be 2.0.

Table 12.2: *Assumed values for the RDTE cost estimation.*

Parameter	Symbol	Value
Produced aircraft for RDTE	N_{RDTE}	6
Difficulty factor	F_{diff}	1.5
CAD factor	F_{CAD}	1.1
Aircraft used for static testing	N_{st}	2
Material factor	F_{mat}	2.0

For all other values, the example value provided by Roskam was used. These values resulted in costs for every RDTE phase and can be found in Table 12.3. Please note that it was determined that no profit was made during the RDTE-phase, but that the program also did not need to be financed.

Table 12.3: *RDTE budget breakdown.*

Phase	Costs [million$]
Airframe Engineering and Design	159
Development Support and Testing	35
Flight Test Airplanes	778
Flight Test Operations	19
Test and Simulation Facilities	99
Total RDTE costs	**1090**

Operational

For the operating costs, the direct operating costs, excluding crew costs were estimated using Roskam [80], where the current fuel price was gathered from the internet [4], the crew costs themselves are copied from the baseline report. The indirect operating costs, only the maintenance costs, are found in the literature.

The maintenance costs were estimated using two reports from the American military, the first one was used to estimate the maintenance costs of different subsystems, based on weights [81] and the second breaks maintenance costs down to the subsystems [82] and was thus used to fill in the gaps.

As can be seen in Table 12.4, the wing subsystem does not have a source, this is because in aircraft, this is integrated into the airframe subsystem, and for helicopters, it does not exist. As the production costs of the wing subsystem are half that of the airframe, and as the wing is mostly a structural component, the assumption was made that the maintenance costs are half that of the airframe.

[4] https://jet-a1-fuel.com/ [retrieved 5th June 2024]

Table 12.4: *Overview of maintenance costs per flight hour, broken down per subsystem [81] [82].*

Subsystem	**Costs per flight hour** [$/h]
Rotor maintenance	1670
Drivetrain maintenance	980
Propulsion maintenance	445
Airframe maintenance	225
Wing maintenance	110
Flight Control maintenance	110
Hydraulic maintenance	75
Inspection maintenance	330
Other maintenance	290
Total Maintenance costs	4235

As the maintenance costs per flight hour are now known, it is possible to make an overview of the operating costs per mission. This overview is presented in Table 12.5. The considered missions are: active firefighting, dropping retardant, (Combat) Search and Rescue ((C)SAR), and transport, at both grey lines, as described in Section 11.1.

Table 12.5: *Overview of operating costs for different missions.*

Parameter	**Active Firefighting**	**(C)SAR**	**Transport (maximum payload)**	**Transport (maximum fuel)**
Mission length [h]	3	4.5	3	4
Crew [-]	2	3	2	2
Fuel costs [$] [80]	4360	5580	4360	5580
Oil and Lubricants cost [$] [83]	131	167	131	167
Salary [$/h] [1]	400	600	400	400
Retardant Costs [$] [84]	2378	N/A		
Direct Operating Costs [$]	8069	8448	5691	7348
Direct Operating Costs per hour [$/h]	2690	1877	1897	1837
Maintenance costs per hour [$/h]	4235			
Total Operating Cost per hour [$/h]	**6925**	**6112**	**6132**	**6072**

It should be noted that ground handling costs, as well as insurance and financing costs, are not considered, as it is not sure whether they apply (a government does not insure their vehicles), and ground handling costs vary widely.

An overview of these costs, as seen from an operator of the aircraft, can be seen in Figure 12.1.

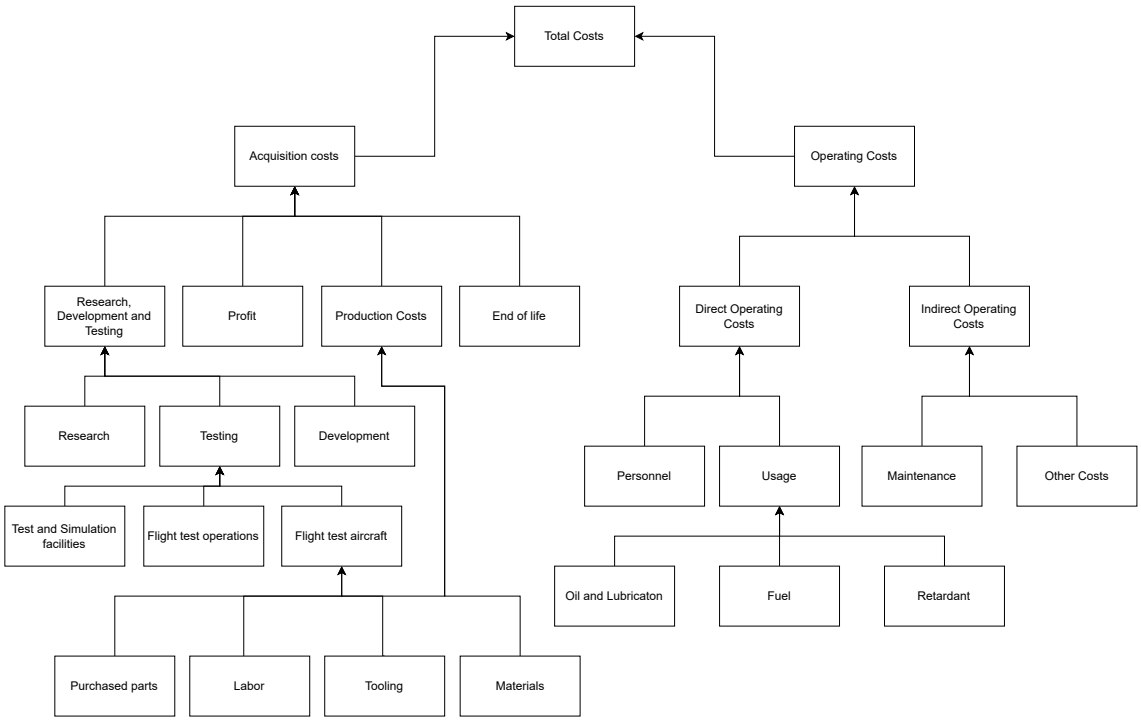

Figure 12.1: *Cost breakdown structure as seen from a user*

12.2. Revenue

Contributors: Floris
Authors: Floris

Potential Customers

CHEETAH is a compound helicopter specifically designed to be able to participate in aerial firefighting. However, the design is modular, and CHEETAH's missions are not limited to only aerial firefighting. As discussed in Subsection 3.2.3, CHEETAH can also be used for search and rescue missions, during medical emergencies and for more general transportation to and from difficult-to-reach places or as a replacement for heavy helicopters. However, there are more efficient aircraft for search and rescue, as well as aircraft used for medical emergencies. This does not exclude CHEETAH from doing these missions, but it is assumed that CHEETAH will not be sold solely for this purpose.

There is however one exception to this assumption, if a (military) aircraft has crashed in or near an active combat zone, a combat search and rescue operation will need to be carried out. These are normally carried out by aircraft that are VTOL capable and have longer ranges than standard helicopters.

Another mission CHEETAH can perform for the military is carrier onboard delivery (COD, resupplying aircraft carriers). VTOL-capable aircraft are preferred on carriers, as other transport aircraft would need an upgrade to be able to sustain the loads exerted from the arresting cables.

Almost all heavy-lift helicopters are originally designed for the army, navy or airforce, thus the assumption was made that the military market would be the best indicator.

Offshore operations usually require a small landing footprint, thus for this analysis, it is assumed that CHEETAH will not be ordered specifically for this purpose.

Achievable Market share

To analyse how big the aerial firefighting market is, an overview of different aircraft used for aerial firefighting, with a similar capacity to CHEETAH, is composed. After that, it is determined how many of these specific aircraft are used specifically for aerial firefighting and then, the market price for these aircraft is found. This

overview of this can be seen in Table 12.6.

Table 12.6: *Overview of comparable aerial firefighting aircraft.*

Aircraft	Number in service	Price [million $]	Market Money [million $]
Cl-415	96	35	3360
DHC-8	19	46.765	888.535
BAe 146	22	36.5	803
S-2T	35	4.23	148.05
C-130	7	21.43	150
Type 1 Helicopters	177	20	3540

The same is done for the heavy lift helicopters from Western militaries, as it is expected that countries outside the sphere of influence of North Atlantic Treaty Organization (NATO) will not be able to buy CHEETAH for the military, this overview can be seen in Table 12.7.

Table 12.7: *Overview of comparable heavy-lift helicopters.*

Aircraft	Number in service	Price [million $]	Market Money [million $]
CH-47	950	40	38000
CH-53K	220	79.14	17411

For combat search and rescue, as well as carrier onboard delivery, V-22 Ospreys are used, in Table 12.8, it can be seen how many are used in the earlier mentioned categories. After comparing the capabilities of CHEETAH with the capabilities of the Osprey, it was concluded that CHEETAH has a higher payload, lower speed, and at the same payload, a higher range. It is therefore estimated that CHEETAH can perform at least half the tasks the Osprey can, and thus, it is estimated that 50 % of the Ospreys can be replaced with CHEETAH, as long as the costs of CHEETAH do not exceed those of the Osprey.

Table 12.8: *Overview of V-22 usage.*

Aircraft	Number in service
CSAR	48
COD	38
Other usage	314

It is estimated that CHEETAH can obtain a market share of 30 % of the identified aerial firefighting market, which is 75 % of the market share that the CL-415 currently has. This would then result in an achievable market share of 2.7 $ billion. As CHEETAH will not be cheaper than the CH-47, or have a higher payload than the CH-53K, it is assumed that the market share CHEETAH can achieve is 10 %, which will result in a market share of 5.5 $ billion. And 50 % of the 400 Ospreys currently in service would result in 200 additional orders.

12.3. Pricing

Contributors: Floris
Authors: Floris

From Airbus, the ratio of the profit before taxis and interest and the costs was taken, this was a margin of 8.3 % [85]. This ratio was chosen to price CHEETAH, it should be noted that for this ratio, for Airbus, the research costs are already subtracted from the profit, while this ratio will cover those costs for CHEETAH. However, as it is not the goal to make the largest possible profit for CHEETAH, this is considered to be desired. After some iteration, a price of 42.5 $ million was established. With this price, 62 CHEETAHs are sold to the firefighting market, while 330 are sold to the military. From these 330, 130 are sold for heavy lifting, and 200 are sold to replace the V-22s, as 42.5 $ million is less than the 72 $ million that the V-22 costs. In Table 12.9, the final production costs per subsystem can be seen. This is based on 398 produced aircraft, as the testing airframes

used in Table 12.1 also have to be considered as the marginal production costs for each aircraft decrease [78] [80].

Table 12.9: *Overview of production cost broken down per subsystem, based on 398 produced aircraft.*

Subsystem	**Costs** [million$]
Avionics	5.01
Airframe	4.69
Electrical	1.80
Empennage	0.68
Gear	0.68
Nacelles	1.01
Flight Control	1.29
Total General	15.16
Rotor	1.27
Drivetrain	1.03
Propulsion	12.32
Total Helicopter	14.62
Wing	2.36
Forward Drivetrain	0.21
Propeller	0.34
Total Aircraft	3.91
Assembly	6.54
Total Cost	39.23

With these prices, a total revenue of 16.660 $ billion is achieved, while the total costs are 16.469 $ billion. Thus, a profit of 191 $ million is made. This leads to a ROI of 0.0116 (1.16 %), according to Equation 12.1.

$$ROI = \frac{\text{Total Revenue} - \text{Total Costs}}{\text{Total Costs}} \tag{12.1}$$

This means that CHEETAH is financially feasible as well.

13 | Technical Risks and RAMS

In the demanding field of aerial firefighting, the reliability and safety of an aircraft is crucial to the success of the mission. To ensure safety and reliability, the potential risks both in flight and on the ground are examined. Subsequently, mitigation strategies can be formulated to reduce the likelihood and impact of possible incidents. Through this approach, the compound helicopter's performance is optimised, and the downtime is minimised. This chapter provides detailed insights and recommendations that are essential for maintaining the operational effectiveness and safety of CHEETAH in firefighting missions. This will be done through the technical risk analysis, identifying all the risks that were recognised before starting this phase of the design. Additionally, the Reliability, Availability, Maintainability, and Safety (RAMS) characteristics will provide a detailed analysis of the primary risks the aircraft will face during operation.

13.1. Technical Risk Assessment

Contributors: Merel, Sjoerd
Authors: Sjoerd

No design is perfect, including that of the CHEETAH. The design process comes with assumptions and uncertainties which makes for technical risks to arise in every aspect and subsystem of the aircraft. Throughout the design process, these risks have been identified and this section serves as a summary of all these risks, including mitigation strategies to cope with possible incidents.

The midterm report already mentioned several technical risks, however, these were not yet categorised in subsystems [2]. For this iteration of the technical risk analysis, the risks in the midterm report have been revised and categorised in their subsequent technical departments. Moreover, some technical risks have been added to aim for a more complete list ultimately reducing the chance of unexpected incidents. If more elaboration is demanded on the definition, interpretation or quantification of technical risks in this report, the midterm report can be informed, as this report serves as a sequel on the latter [2].

Some risks from the midterm report are considered general risks as they do not specifically relate to one technical department. Therefore, these are not reintroduced in this report and they can be found in the midterm under the identifiers: **TR19**, **TR20**, **TR21**, **TR22**, **TR24**, **TR25** and **TR29**. These will now continue under the ID's **TR-GEN-01**, **TR-GEN-02**, **TR-GEN-03**, **TR-GEN-04**, **TR-GEN-05**, **TR-GEN-06** and **TR-GEN-07** respectively.

As a further side note for all the coming tables, abbreviations have been introduced for the magnitudes of likelihood and impact. These are as follows:

Likelihood Levels:
- **VL**, Very Low
- **L**, Low
- **M**, Moderate
- **H**, High
- **VH**, Very High

Consequence Levels:
- **N**, Negligible
- **M**, Marginal
- **CR**, Critical
- **CS**, Catastrophic

All the risks and mitigation strategies are listed in the tables Table 13.1 until Table 13.12. These tables are structured in the following way with subsequent risks and mitigation per department:

1. Risk Table ASM department
2. Mitigation Strategy ASM department
3. Risk Table FPP department
4. Mitigation Strategy FPP department

Where the same structure will continue for the additional technical departments: aerodynamics, stability & control, operations, communication & electrical systems.

Table 13.1: *List of technical risks related to ASM.*

Risk Code	Requirement	Risk	Likelihood	Impact	Consequence
TR-ASM-01	FTF-SYS-FDS-07.3	The heat resistance of the aircraft structure is lower than accounted for	H	CS	The structural integrity of the aircraft is compromised
TR-ASM-02	FTF-STK-FDS-01	The tank erodes because of the composition of retardant	L	M	Unexpected maintenance on the tank, resulting in extra expenses
TR-ASM-03	FTF-SYS-FDS-07.2	The aircraft will experience corrosion after being exposed to an environment with salty water for a longer period of time	H	CR	Unscheduled maintenance has to be performed on the aircraft, and some parts might need replacing sooner than anticipated, costs will be higher than expected
TR-ASM-04	FTF-SYS-FDS-05.3	Too much rotor-blade tip deflection after retardant drop	M	CR	Rotor-blade will collide with tail resulting in damage of both components
TR-ASM-05	FTF-SYS-FDS-05.3	Rotor-blade will break due to high stresses after retardant drop	L	CR	Instability of main rotor system and therefore the whole aircraft
TR-ASM-06	FTF-SYS-REG-02.8	Rotor-blade will fail due to fatigue	L	CR	Instability of main rotor system and therefore the whole aircraft
TR-ASM-07	FTF-SYS-FDS-05.15	Failure of wing structure	L	CS	Aircraft will lose stability and capability to produce sufficient lift

Table 13.2: *Mitigation plan for technical risks related to ASM.*

Risk Code	Category	Mitigation Strategy	Verification	Likelihood	Impact
TR-ASM-01	Reduction	Implement sufficient safety factors and choose materials typical for the firefighting industry	Heat laboratory testing	L	CS
TR-ASM-02	Reduction	Creating a manual that highlights which retardants are allowed to be used and a warning system in case a wrong retardant is placed in the tank	Extensive material analysis using several different types of retardants	VL	N
TR-ASM-03	Reduction	Choose coatings or materials that can resist this for the parts of the aircraft that can come into contact with salty water	Testing in a laboratory by exposing materials to salty water solutions and seeing how they react	VL	M
TR-ASM-04	Avoidance	Ensure for sufficient stiffness	Model simulation of deflection due to payload drop	VL	CR
TR-ASM-05	Avoidance	Ensure for sufficient strength	Calculate maximum stress in rotor-blade during operation. Lab tests	VL	CR

Continued on next page

Table 13.2 – continued from previous page

Risk Code	Category	Mitigation Strategy	Verification	Likelihood	Impact
TR-ASM-06	Avoidance	Design for sufficient life-cycles	Perform a fatigue analysis and research	VL	CR
TR-ASM-07	Avoidance	Design wing structure such that it will not break due to expected loads	Stress analysis and make sure yield stress is above expected stresses in the wing	VL	CS

Table 13.3: *List of technical risks related to FPP.*

Risk Code	Requirement	Risk	Likelihood	Impact	Consequence
TR-FPP-01	FTF-SYS-FDS-05.1	The engines do not supply enough power for the aircraft to perform VTOL at MTOW	L	CR	Loss of VTOL capabilities during take-off/tanking/landing as planned
TR-FPP-02	FTF-SYS-REG-01.3	Lower engine power than expected due to different atmospheric conditions during operations	VH	CS	Aircraft will not be compliant with engine power ratings as stated in CS-E 40
TR-FPP-03	FTF-SYS-PIL-04.3	Inability to maintain rotor RPM after abrupt engine loss	M	CR	Unpredictable loss of altitude
TR-FPP-04	FTF-SYS-PIL-04.3	Failure of shared drive shaft causing asymmetric thrust	L	CS	Insufficient controllability
TR-FPP-05	FTF-SYS-PIL-04.3	Autorotation capability not sufficient	H	CS	Powerless glide impossible
TR-FPP-06	FTF-SYS-PIL-04.3	Hard clutch engagement occurs	L	CS	Key components are damaged and the aircraft starts moving erratically
TR-FPP-07	FTF-STK-FDS-04	Pusher propeller failure	L	CR	The aircraft will still be able to take off and land, however, it cannot achieve the speed necessary for a successful mission anymore, also stability might be impaired
TR-FPP-08	FTF-SYS-FDS-05.1	Main rotor failure	L	CS	Sudden loss of lift, impaired VTOL capabilities

Table 13.4: *Mitigation plan for technical risks related to FPP.*

Risk Code	Category	Mitigation Strategy	Verification	Likelihood	Impact
TR-FPP-01	Reduction	Thorough testing of the engines, monitoring different circumstances such as wind to ensure VTOL capability	Tests are supervised by certified independent experts	VL	CR

Continued on next page

Table 13.4 – continued from previous page

Risk Code	Category	Mitigation Strategy	Verification	Likelihood	Impact
TR-FPP-02	Reduction	Test engine power with atmospheric conditions encountered during operations	Tests are supervised by certified independent staff	M	CR
TR-FPP-03	Reduction	Introduce requirements for a stable autorotation	Test the autorotation capabilities in the desired condition	L	CR
TR-FPP-04	Reduction	Introduce requirements for maintaining controllability after engine loss, such as sufficient margin and control surfaces	Conduct a simulation of aircraft parameters after engine loss	VL	CR
TR-FPP-05	Reduction	Introduce requirements for minimum rotor size to allow autorotation	Test the autorotation capability of the aircraft under operational conditions in case of sudden power loss of all engines	L	CS
TR-FPP-06	Reduction	Design the drive shaft to be able to handle the shock load of a sudden engine loss	Test the drive shaft in case of a sudden engine failure under operational conditions	VL	CS
TR-FPP-07	Reduction	Elaborate rotor testing by certified professionals and design for aerial firefighting conditions. Implementing automatic system checks	Wind tunnel testing, software testing	VL	CR
TR-FPP-08	Transfer	Regular maintenance check-ups by the maintenance instance and implementing system warnings	Log every check-up and any findings, software testing	VL	CS

Table 13.5: *List of technical risks related to aerodynamics.*

Risk Code	Requirement	Risk	Likelihood	Impact	Consequence
TR-AERO-01	FTF-SYS-FDS-04.1	The aircraft has too much drag	L	CR	The aircraft is too slow and cannot reach the required cruise speed at MTOW
TR-AERO-02	FTF-SYS-FDS-04.1	The aircraft wing has too much of an induced AoA due to rotor-induced velocity	H	CR	The wing will not be able to generate positive lift
TR-AERO-03	FTF-SYS-FDS-05.16	Flow separation over the airfoil in horizontal flight	H	CR	Sudden loss in lift by the wing
TR-AERO-04	FTF-SYS-FDS-04.1	Pressure fields of both box wing levels will interact	H	CR	Wing will not be able to produce sufficient lift

Table 13.6: *Mitigation plan for technical risks related to aerodynamics.*

Risk Code	Category	Mitigation Strategy	Verification	Likelihood	Impact
TR-AERO-01	Reduction	Perform tests of the autonomous flight system in operational conditions	Tests are supervised by certified independent staff	VL	CS
TR-AERO-02	Reduction	Design the wing at a constant AoA. Design the wing to include HLD for more lift at low AoA	Simulate induced angle of attack during flight conditions	M	CR
TR-AERO-03	Transfer	Select an airfoil that is optimised for Reynolds numbers at which the aircraft will be flying	Check with XFLR5 or CFD software whether flow separation will occur	L	CR
TR-AERO-04	Reduction	Space the upper and lower wing apart as much as possible. Choose an airfoil that has a spread-out pressure field rather than a high-pressure peak.	Check with XFLR5 or CFD software how critical this interaction effect is	H	N

Table 13.7: *List of technical risks related to stability and control.*

Risk Code	Requirement	Risk	Likelihood	Impact	Consequence
TR-SC-01	FTF-STK-PIL-01	The aircraft is uncontrollable in autonomous operations	L	CS	Losing control of the aircraft and mission failure
TR-SC-02	FTF-SYS-FDS-01.3	Due to system malfunction the aircraft cannot remain stable during the water/retardant release phase	L	CR	The dispersion of the water/retardant will not be optimal, hindering the fire fighting operation
TR-SC-03	FTF-SYS-PIL-03.1	The aircraft tail stability surfaces experience wake from the main rotor	H	CR	The aircraft becomes unstable and difficult or impossible to fly
TR-SC-04	FTF-SYS-PIL-03.1	Stability control loop system malfunctioning	L	CS	Dynamic instability of the aircraft
TR-SC-05	FTF-SYS-PIL-03.1	CG located further backwards than designed for due to incorrect loading procedure	M	CS	Static longitudinal instability of the aircraft
TR-SC-06	FTF-SYS-PIL-03.1	Control system is over sensitive	M	CR	Very tiring for the pilots to fly the aircraft

Table 13.8: *Mitigation plan for technical risks related to stability and control.*

Risk Code	Category	Mitigation Strategy	Verification	Likelihood	Impact
TR-SC-01	Reduction	Detailed analysis of the control surfaces in the aircraft	Wind tunnel testing of the aircraft to see if the results agree with calculations	VL	CR

Continued on next page

Table 13.8 – continued from previous page

Risk Code	Category	Mitigation Strategy	Verification	Likelihood	Impact
TR-SC-02	Reduction	Design the aircraft to remain stable even when big load-changes occur	Testing of the system in extreme situations such as gusts of wind	VL	M
TR-SC-03	Avoidance	Design such that the tail surfaces remain out of the rotor-wake during flight	Simulate flight conditions using CFD software	VL	CR
TR-SC-04	Avoidance	Design with redundant control loop systems	Practical tests on the proper functioning of the control loops	VL	CS
TR-SC-05	Avoidance	Provide proper loading procedures and loading sheets for pre-flight checks	Confirm with operators that they properly use the procedures and loading sheets	L	CS
TR-SC-06	Avoidance	Design for a control system that is adjusted to pilot preference	Extensive practical testing with pilots	L	CR

Table 13.9: *List of technical risks related to aircraft operations.*

Risk Code	Requirement	Risk	Likelihood	Impact	Consequence
TR-OPR-01	FTF-SYS-FDS-05.2	Failure of the pumping system when refilling the water/retardant tank	L	CR	The tank cannot be refilled and there is not enough water for the extinguishing of fires
TR-OPR-02	FTF-STK-PIL-01	Malfunction of sensors while performing the autonomous operations	M	CR	The aircraft loses control and the pilot has to take over
TR-OPR-03	FTF-STK-FDS-09	Malfunction of the night vision system	L	CS	The aircraft cannot fly at night and perform nighttime operations
TR-OPR-04	FTF-SYS-FDS-01.3	Failure of the water dispersion system	L	CR	Inefficient fire prevention strategy
TR-OPR-05	FTF-SYS-REG-01.1	The ice protection system fails to activate due to a technical malfunction	L	CS	Ice build-up can't be combated in flight
TR-OPR-06	FTF-STK-PIL-04	Emergency door not opening	VL	CS	The safety of the crew is jeopardised
TR-OPR-07	FTF-SYS-FDS-02.1	The tank meter incorrectly displays the water/retardant level.	L	CR	The tank isn't filled and the aircraft cannot effectively extinguish fire
TR-OPR-08	FTF-SYS-FDS-01.1	The dropping mechanism is defective	L	CR	No effective drops can be performed during the mission
TR-OPR-09	FTF-STK-FDS-11	Malfunction of the Helicopter Flight Rescue System (HFRS)	VL	M	Evacuations and drop-offs cannot be performed in-flight anymore, the aircraft will have to land before cargo and/or passengers can enter or leave the vehicle

Continued on next page

Table 13.9 – continued from previous page

Risk Code	Requirement	Risk	Likelihood	Impact	Consequence
TR-OPR-10	FTF-SYS-FDS-05.7	Malfunction of the heat monitoring system	L	M	When the heat caused by the fire cannot be monitored anymore it is hard to determine whether the aircraft is being exposed to more heat than it is designed for, resulting in system overheating or component damage

Table 13.10: *Mitigation plan for technical risks related to aircraft operations.*

Risk Code	Category	Mitigation Strategy	Verification	Likelihood	Impact
TR-OPR-01	Reduction	Perform tests of the pumping system in operational conditions	Tests are supervised by certified independent staff	VL	CR
TR-OPR-02	Reduction	Implement a fail-safe sensor system	Test the fail-safe sensor system in operational conditions	M	N
TR-OPR-03	Reduction	Use of battery powered night vision system independent of aircraft electrical power [86]	Check the battery percentage	VL	M
TR-OPR-04	Reduction	Implement a fail-safe release mechanism	Test the fail-safe release mechanism in operational conditions	L	M
TR-OPR-05	Transfer	Establish routine check-up procedures for the ice protection systems in the maintenance manual	Log every check-up and any findings	VL	CR
TR-OPR-06	Reduction	Introduce requirements on the safety equipment with redundant systems	Test the emergency equipment in various conditions	VL	CS
TR-OPR-07	Reduction	Implement a tank volume measurement system with redundancies	Test the detection levels in the laboratory in various scenarios	VL	CR
TR-OPR-08	Reduction	Elaborate testing of the dropping system and regular inspection during maintenance operations	Testing by certified professionals	L	M
TR-OPR-09	Reduction	Using an already proven design and having a qualified maintenance crew performing regular maintenance on the aircraft	Researching available options extensively	VL	N
TR-OPR-10	Transfer	Look into special coatings that can withstand this as well as selecting and designing components that can handle this heat	Heat laboratory testing	VL	M

Table 13.11: *List of technical risks related to aircraft communication and electrical systems.*

Risk Code	Requirement	Risk	Likelihood	Impact	Consequence
TR-CES-01	FTF-STK-CRW-02	Communication system interference/malfunction	M	CR	Lack of communication with the ground crew
TR-CES-02	FTF-STK-ATC-01	Malfunction of the transponder	VL	CS	Critical data not being sent to the dispatcher, traffic collision and avoidance system (TCAS) inactive
TR-CES-03	FTF-SYS-REG-01.1	The caution/master caution information system is defective	L	CS	The flight crew is not alerted when the anti-ice or de-ice system is not functioning normally

Table 13.12: *Mitigation plan for technical risks related to communication and electrical systems.*

Risk Code	Category	Mitigation Strategy	Verification	Likelihood	Impact
TR-CES-01	Reduction	Implement anti-cyber attack measures such as in-system warnings and ensuring high safety of network [87]	Perform communication system tests	L	CR
TR-CES-02	Reduction	Implement a fail-safe transponder system	Test the fail-safe transponder system in operational conditions	VL	N
TR-CES-03	Transfer	Establish routine check-up procedures of the caution information system in the operations manual	Log every check-up and any findings	VL	CR

13.2. Risk Map

Contributors: Sjoerd
Authors: Sjoerd

The likelihood and impact of all risks mentioned in Section 13.1, including the general risks which are elaborated upon in the midterm report, have been included in Figure 13.1a. From the map, the technical departments FPP, aerodynamics and ASM seem to be the most critical when it comes to a combination of likelihood and impact.

Moreover, Figure 13.1b shows the likelihood and impact of all the risks after the mitigation strategy has been applied. The map clearly shows how the risks are expected to either become less likely to occur or to be reduced in expected impact.

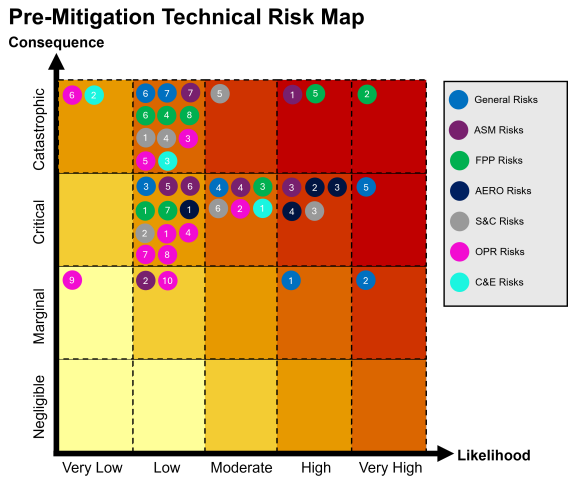

(a) *Technical risk map pre-mitigation.*

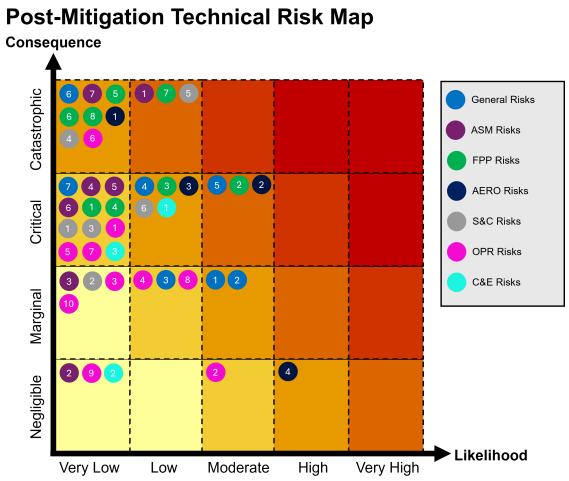

(b) *Technical risk map post-mitigation.*

13.3. Reliability, Availability, Maintainability, and Safety

Contributors: Ivo
Authors: Ivo

The RAMS disciplines are a set of tools that make it possible to ensure that a product, process, or system fulfils the mission for which it was designed, all under the conditions of reliability, maintainability, availability, and well-defined safety [1]. Each discipline can be defined as follows [88]:

- **Reliability:** The ability of a system to accomplish a required function, in given conditions, during a given time interval.
- **Availability:** The ability of a system to be able to accomplish a required function, in given conditions, at a given moment, supposing that the external means are present.
- **Maintainability:** The ability of a system to be restored in an operating state, during a time interval, when the maintenance operations are accomplished with given means, as a determined program.
- **Safety:** The ability of a system to generate to itself and its environment, in given conditions, catastrophic or hazardous events with an acceptable level of risk.

Reliability, Availability and Safety

At this stage of the design of the CHEETAH, the reliability is hard to quantify due to the lack of data for similar aircraft. Therefore, to get a preliminary understanding of the reliability, availability, and also the safety of the aircraft, a Functional Hazard Assessment (FHA) was conducted. This FHA, shown in Table 13.13, is closely linked to the Technical Risk Assessment, covering the most relevant failures that may occur during the operational mission, and serving as a guide to construct other useful reliability and safety tools such as the Failure Mode Effect Analysis (FMEA) and the fault tree analysis in regards to safety further in the design.

For each failure mode, a classification of the severity of the risk was given. The classifications of the risk used in Table 13.13 are mentioned below [89]:

- Category 1 (C1): Catastrophic (death or system loss).
- Category 2 (C2): Critical (severe injury, major property damage, major system damage, mission loss).
- Category 3 (C3): Marginal (minor injury, minor property damage, minor system damage, delay or loss of availability or system degradation).
- Category 4 (C4): Minor (no injury, property damage, or system damage but unscheduled maintenance or repair may be necessary).

[1] RAMS Engineering https://www.byhon.it/rams-engineering/ [retrieved 16th May 2024]

Table 13.13: *Functional Hazard Assessment.*

Function	Failure	Classification and Effect	Mitigation
Propulsion	One engine failure	C4: Loss in power meaning the aircraft has to fly at reduced speeds.	Proper maintenance and regular inspections. Follow the proper start-up and shut-down procedures. Avoid big sudden changes in power.
	Two engine failures	C2: This is a significant loss in power. First, the full water payload must be dropped. Next, the pilot should look for the closest runway as the aircraft can only make a conventional landing with this amount of power.	Proper maintenance and regular inspections. Follow the proper start-up and shut-down procedures. Avoid big sudden changes in power.
	Three engine failures	C2: Nearly complete loss of power. The aircraft must drop the full water capacity and make an emergency landing. The pilot shall attempt autorotation, using the upward airflow to make sure the rotor keeps spinning, allowing for a controlled descent.	Proper maintenance, regular inspections and pilot emergency training. Follow the proper start-up and shut-down procedures. Avoid big sudden changes in power.
	Four engine failures	C2: Full loss of power. The aircraft must drop the full water capacity and make an emergency landing. The pilot shall attempt autorotation, using the upward airflow to make sure the rotor keeps spinning, allowing for a controlled descent.	Proper maintenance, regular inspections and pilot emergency training. Follow the proper start-up and shut-down procedures. Avoid big sudden changes in power.
	Engine(s) overheating	C4: The pilots must decrease power to allow the engines to cool down.	Provide sufficient cooling to the engines.
	Main rotor failure	C1: In case the main rotor fails, the aircraft loses a large amount of lift, stability, and controllability, making a crash very likely.	Proper maintenance and regular inspections, including Non Destructive Testing (NDT). Additionally, sensors can be used to possibly detect the failure at an early stage.
	One Propeller failure	C4: On the opposite side power shall be reduced to maintain controllability.	Proper maintenance and regular inspections, including NDT.
	Two propeller failures (same side)	C3: On the opposite side, power shall be reduced and reverse thrust may be used if necessary.	Proper maintenance and regular inspections., including NDT.
	Two propeller failures (opposite side)	C4: Loss in forward propulsion meaning the aircraft can only fly at reduced speeds.	Proper maintenance and regular inspections, including NDT.

Continued on next page

Table 13.13 – continued from previous page

Function	Failure	Classification and Effect	Mitigation
	Three propeller failures	C3: Significant loss in forward propulsion. The aircraft shall increase rotor power, reduce propeller power and use reverse thrust if necessary.	Proper maintenance and regular inspections, including NDT.
	Four propeller failures	C2: The aircraft loses all forward propulsion. The pilots must use the main rotor to make an emergency landing	Proper maintenance, regular pilot emergency training and inspections, including NDT.
Water tank	Leakage	C4: No aerial firefighting possible, the aircraft shall return to base.	Proper maintenance and regular inspections. Additionally, sensors could be used to supervise the condition of the tank.
Snorkel	Does not deploy	C4: No aerial firefighting possible, the aircraft shall return to base.	Proper maintenance and regular inspections.
	Does not retract	C4: No aerial firefighting possible, the aircraft shall return to base at a lower speed to avoid damaging the snorkel.	Proper maintenance and regular inspections.
Fuel system	Leakage	C2: The aircraft shall drop the full water capacity and make an emergency landing as soon as possible.	Proper maintenance and regular inspections. Additionally, sensors could be used to supervise the condition of the tank
	Fuel contamination	C2: This will seriously influence engine performance potentially causing a failure. The helicopter shall therefore make an emergency landing as soon as possible.	Regular inspection of the fuel system used to refill the aircraft. Properly seal this tank and place it in a dedicated refuelling area. Have regular quality checks and clean refuelling equipment after use.
Avionics	Electrical system failure	C3: Loss of multiple systems (such as the navigation system, communication system...).	Proper maintenance and regular inspections. Additionally, a backup electrical system can be installed for the more important systems
	Instruments malfunction	C3: The pilot shall fly using visuals and return to base as quickly as possible.	Regular inspections and pilot training. Have backup instruments for the most crucial instruments.
	Autopilot failure	C4: The pilots shall continue the mission in manual flight. In case of long missions, the pilot may return to base earlier.	Regular inspections and pilot training

Continued on next page

Table 13.13 – continued from previous page

Function	Failure	Classification and Effect	Mitigation
Hydraulics	Leakage	C3: Loss in hydraulic pressure, causing a loss in control. The aircraft shall return to base as quickly as possible. In case the hydraulic leakage is too hard to manage for the pilots, the aircraft shall make an emergency landing.	Proper maintenance, regular inspections and pilot emergency training.
	Pump failure	C3: Loss in hydraulic pressure, causing a loss in control. The aircraft shall return to base as quickly as possible. In case the hydraulic leakage is too hard to manage for the pilots, the aircraft shall make an emergency landing.	Proper maintenance, regular inspections and pilot emergency training.
Landing gear	Does not deploy	C3: The pilots shall land the compound helicopter vertically, damaging the aircraft in the process.	Proper maintenance and regular inspections.
	Does not retract	C4: The aircraft will fly at reduced speeds.	Proper maintenance and regular inspections.

The safety of the aircraft follows closely from the reliability of the different subsystems. The failure modes, effects and mitigation strategies of each type of potential failure should be considered. The fault tree analysis diagrams in Appendix E give a more detailed view of each failure mode, by specifying how they can potentially be caused.

Maintainability

In a firefighting context, maintainability is very important as the aircraft is constantly exposed to harsh conditions. It involves systematically inspecting, repairing, and overhauling components to prevent failures. During the wildfire season, the aircraft should spend as little time as possible on maintenance as this time loss could be critical in fighting a fire. Maintenance can be categorised into two different types, corrective and preventive [2]. While corrective maintenance is performed after the component fails, preventive maintenance is scheduled beforehand. It is typically used for more critical components whose failure can have significant consequences, such as safety risks, production halts, or high repair costs. Other than the pre-flight, post-flight, and other scheduled inspections, helicopters typically go through base maintenance every 12 months or after up to 300–400 flight hours [90]. Each component has a designated overhaul interval during which it is completely disassembled for thorough maintenance.

Factors such as the helicopter's model, usage frequency, and operational environment all influence maintenance schedules [91]. At this stage of the design phase, it is hard to get a more detailed prediction of the overhaul intervals of different components of the compound helicopter. Nevertheless, it can be assumed that the overhaul intervals will be similar to those of the Bell 412 helicopter, which can also be used for firefighting. Table 13.14 gives an overview of the overhaul intervals of different components of the Bell 412 helicopter [92].

[2] Corrective Maintenance vs. Preventive Maintenance: A Comprehensive Guide, https://www.fracttal.com/en/blog/corrective-maintenance-vs-preventive-maintenance [retrieved 13th June 2024]

Table 13.14: *Overhaul time of different components of the Bell 412 helicopter.*

Component	Overhaul interval [h]
Rotors	
Rotor Blades	2500
Power Train	
Rotor Brake Quill	3000
Driveshaft Assembly	3000
Transmission	6000
Flight Control Hydraulics	2500
Powerplant	
Gearbox	4000
Starter Generator	1000

Furthermore, the overhaul intervals of other subsystems can also be estimated. For instance, the water tank used by firefighting trucks typically undergoes an annual check which includes component checks, tank cleaning, and the necessary repairs.[3] It can be assumed that the compound helicopter's water tank will have similar maintenance requirements and a similar overhaul interval. Since the fuel tank shares similar properties with the water tank, the same overhaul interval can be applied to the fuel tank. When it comes to the landing gear, it tends to be overhauled every 10 years [93]. However, this is only the case for aircraft. Given that the compound helicopters will make many vertical landings and take-offs, the landing gear will be subjected to high-impact loads less often. This reduced stress on the landing gear components can lead to an increased lifespan. For the avionics and the snorkel, other than the pre-flight and post-flight inspections, they will they will undergo monthly maintenance checks. Additionally, they will be taken apart either after a failure or on a five-year basis.

For the avionics and the snorkel, maintenance will include regular pre-flight and post-flight inspections. Additionally, they will undergo monthly maintenance checks. Finally, they will be disassembled for comprehensive maintenance either after a failure occurs or on a five-year interval basis.

[3]Fire Suppression Tank Maintenance https://oneclarion.com/fire_suppression_tanks_maintenance [retrieved 13th June 2024]

14 | Verification and Validation

Verification and Validation (V&V) is an important procedure to make sure no errors have been made in the design. The requirements should be met and errors in the models can result in unexpected surprises.

14.1. Requirement V&V

Contributors: Marinka
Authors: Marinka

In the midterm report, a list was given of all the requirements which would be verified during DSE [2]. The verification entails confirming that the design theoretically adheres to the requirements that were set. An overview of all the requirements that have been verified can be found in Table 15.1. In this table it is also stated in which section the calculation or analysis needed to confirm that the requirement has been met can be found.

14.2. Model V&V

Contributors: Marinka
Authors: Marinka

Models have been used to find many of the values during the design process. The accuracy of the design depends on the correctness of the models. For each model, several checks have been used to see if the output is as expected and if it makes sense compared to reality.

14.2.1. Rotor model

The rotor model was verified by doing a sanity check on the order of magnitude of the outputs. All of the outputs were in a logical range. The results were also similar to the values that were obtained with an earlier somewhat less accurate analysis.

The verification for hover is still somewhat doable but for forward flight, it is harder to find results to compare with. Flapping has a significant influence on the performance of a rotor but it is too complicated to implement ourselves. The inaccurate implementation of flapping leads to a large discrepancy between values from the literature and the model results. Despite this, the optimal load factor of the rotor in forward flight was found to be 0.11 which is low but not zero which is similar to values found in the literature for compound helicopters [34][35][36].

14.2.2. Aerodynamic model

At first, CFD was set up to find out more about the aerodynamics of the aircraft. However, after careful consideration, it was concluded that the results would not be accurate enough because of errors in setting up the model. After this, a model of the wing was made in XFLR to find some data on the performance of the airfoil in our conditions and the aerodynamics of a simplified box wing.

In general, XFLR5 is considered a widely validated program but some sanity checks were still performed. The upper and lower wings were analysed separately to see if they gave reasonable results. The combination of the two was done using the biplane option. However, the wingtips do not touch in this simulation which means the reduction of vortices due to the closed wing ends is not taken into account properly. The lift and moment resulting from the simulation should be fairly accurate but the simulated drag is probably higher than in reality.

14.2.3. Static stability model

The static stability model consists of the calculation of the centre of gravity using moment balance, sizing the horizontal tail using a scissor plot and sizing the vertical tail for counter-torque.

The centre of gravity was verified by inputting known values for the locations and weight of subsystems of an example helicopter from [25] and checking if this resulted in the same location. With the wing taken out

of the equation, it gave the same results. The wing had to be taken out since the example moment balance was for a conventional helicopter. Furthermore, the CG is located around 40% of the fuselage length which is similar to the most forward CG of existing helicopters[1] [2] [3] [4]. The weight of the horizontal and vertical tail dependent on its size was done using multiple different methods which all gave weights within a range of 10 kg.

The stability equation was checked by calculating by hand if the moment balance is zero for the chosen horizontal tail area which is the case. As validation, the size of the horizontal tail was compared to that of the Sikorsky UH-60A which has a span of 4.4 m and a tail arm of 9 m [25]. Our aircraft has a span of 6.7 m and a tail arm of 16.3 m which seems reasonable as the Black Hawk is significantly smaller in general.

The calculation of the side force of the vertical tail was checked once by hand before the code was run to find it for the whole range of speeds. This value could not be compared to any existing aircraft as airplanes do not have the main rotor torque problem and helicopters usually have a tail rotor to counteract the torque. For aircraft like the RACER and X3 the information is not publicly available yet and they are smaller and lighter which means they will have a relatively smaller rotor torque and thus need a smaller vertical tail.

14.2.4. Dynamic stability model

In the dynamic stability model, the values are all converted from metric to imperial units first. Next, the eigenvalues are calculated in hover using only the main rotor in hover stability derivatives. Lastly, all the derivatives for the horizontal tail, vertical tail and fuselage have been implemented in Python and the eigenvalues are found from the roots of the characteristic equation.

Firstly, all the conversions have been checked by hand to see if they were performed properly. Next, a sanity check was done for several of the variables compared to existing helicopters. The Lock number of 13.4 is on the high side but still in a feasible range of 3-14[94]. The torque coefficient solidity ratio that was calculated is close to the expected value from [25]. The thrust coefficient and the thrust coefficient over solidity ratio are also approximately in the right range for a twist of 5° in hover conditions with a value of 0.004 [95].

A unit test was performed on all derivatives separately with known input values from [25] to see if that gave the expected output. The outputs were exactly the same which indicates that the equations were implemented correctly in Python. It was also checked if the np.roots function in Python from NumPy gave the correct results with known inputs and outputs of a general polynomial.

14.2.5. Structural model

The structural model calculates the moments and deflections in the box wing and rotor blades. This is done using boom area for the area moment of inertia.

It was checked if the model produced accurate outputs by using a simple point load and moment. In addition to that, it was validated that the distributed lift and weight add up to the right total by integrating them. Finally, a sanity check was done on the results to check if they were in the right order of magnitude compared to helicopters of similar size.

14.2.6. Range model

A model was written to make the payload-range diagram. First, all the variables are defined and the weights for different amounts of fuel are calculated. The program then loops over the lift needed for the current weight and the corresponding drag for the power that needs to be provided by the propellers. With this, the fuel burned in a certain time step is calculated and this loop is repeated until all fuel is gone. The total time is then multiplied by the speed to find the range.

To validate the program some unit tests were performed. A check was done by hand if the right drag coefficient was imported for a certain lift coefficient. The range was also calculated and checked for one set fuel weight before the program looped through all the different initial fuel weights.

[1] https://www.boeing.com/defense/ch-47-chinook#overview [Retrieved 1 May 2024]
[2] https://shergoodaviation.com/wiki/index.php?title=Chinook_CH-47/Weight_and_Balance [Retrieved 1 May 2024]
[3] https://shergoodaviation.com/wiki/index.php?title=S-64/Weight_and_Balance [Retrieved 1 May 2024]
[4] https://sikorskyarchives.com/home/sikorsky-product-history/ [Retrieved 1 May 2024]

15 | Further Development

The design of CHEETAH was performed to a certain level. To improve the level of details, the feasibility and the reliability of the design, further development has to be performed in future design phases. This chapter describes the requirements that still need to be meet, the manufacturing, assembly and integration of the vehicle and other post-DSE activites that will have to be executed in the future.

15.1. Requirement Compliance

Contributors: Emma
Authors: Emma

To see if the requirements of the design are being met, a requirement compliance matrix is constructed. In this matrix, all the requirements are displayed, followed by a colour and the section in which the requirement is achieved. Green (✓) means the requirement is met, orange (✓/×) means that the requirement is partially met and red (×) means that the requirement is not met or that it was not considered or Not Addressed (NA) yet in this stage of the design. First a compliance matrix was established for the user requirements in Table 15.1. These user requirements are decoupled into system requirements, for which the compliance matrix is given in Table 15.2.

Table 15.1: *User requirements compliance matrix.*

Identifier	Requirement	Met?	Section
FTF-UR-01	The aircraft shall suppress wildfires effectively using water and/or retardant.	✓	10.1
FTF-UR-02	The aircraft shall have Vertical Take-off and Landing (VTOL) capability.	✓	6.1
FTF-UR-03	The aircraft shall have the ability to refill water tanks in a hover.	✓	10.1
FTF-UR-04	The aircraft shall have a water/retardant tank capacity of at least 10 000 L.	✓	10.1
FTF-UR-05	The aircraft shall have a maximum cruise speed of at least 400 km/h.	✓	6.2
FTF-UR-06	The aircraft shall have a reliability and operational availability equal to or better than that of comparable aircraft.	×	NA
FTF-UR-07	The aircraft shall provide a systems and avionics architecture that will enable autonomous operations in cruise.	✓	5.3
FTF-UR-08	The aircraft shall be capable of Visual Flight Rules (VFR) flight with an autopilot.	✓	5.3
FTF-UR-09	The aircraft shall be capable of Instrument Flight Rules (IFR) flight with an autopilot.	✓	5.3
FTF-UR-10	The aircraft shall be capable of flight in known icing conditions.	✓	5.3
FTF-UR-11	The aircraft shall meet applicable certification rules in CS Part 25/29 depending on applicability.	×	

Table 15.2: *System requirements compliance matrix.*

Identifier	**Requirement**	**Met?**	**Section**
FTF-SYS-FDS-01.1	The aircraft shall be able to drop retardant at least twice per refill.	✓	10.1
FTF-SYS-FDS-01.2	The aircraft shall withstand the effects of sloshing liquids in the tank.	✓	10.1

Continued on next page

Table 15.2 – continued from previous page

Identifier	Requirement	Met?	Section
FTF-SYS-FDS-01.3	The aircraft shall remain longitudinally statically stable during the release phase of the water and retardant.	✓	8.2
FTF-SYS-FDS-02.1	The aircraft shall have a water/retardant tank capacity of at least 10 000 L.	✓	10.1
FTF-SYS-FDS-03.1	The aircraft shall have a ferry range of at least 3000 km.	✓	10.5
FTF-SYS-FDS-03.2	The aircraft shall have a minimum endurance of 3 hours.	✓	10.5
FTF-SYS-FDS-03.3	The aircraft shall have a full retardant tank range of at least 500 km in cruise.	✓	10.5
FTF-SYS-FDS-04.1	The aircraft shall have a cruise speed of at least 400 km/h.	✓	6.2
FTF-SYS-FDS-05.1	The aircraft shall have VTOL capability.	✓	6.1
FTF-SYS-FDS-05.2	The aircraft shall be able to refill the water tanks while hovering.	✓	10.1
FTF-SYS-FDS-05.3	The aircraft shall be able to drop all its water/retardant load at once (spot-dropping).	✓	10.1
FTF-SYS-FDS-05.4	The aircraft shall be able to drop its water/retardant load over a longer distance (line-dropping).	✓	10.1
FTF-SYS-FDS-05.5	The aircraft shall be able to be (re)filled with water and retardant by ground tanking equipment.	✓	10.1
FTF-SYS-FDS-05.6	The aircraft shall be equipped with a system to monitor the fire visually.	✓	5.3
FTF-SYS-FDS-05.7	he aircraft shall be equipped with a system to monitor the the infrared radiation emitted by the fire.	✓	5.3
FTF-SYS-FDS-05.8	The aircraft shall be able to evacuate people.	✓	5.4
FTF-SYS-FDS-05.9	The aircraft shall be able to drop objects in forward flight.	✓	5.4
FTF-SYS-FDS-05.10	The aircraft shall be able to drop objects in hover.	✓	5.4
FTF-SYS-FDS-05.11	The aircraft shall be able to drop personnel in forward flight.	✓/×	5.4
FTF-SYS-FDS-05.12	The aircraft shall be able to drop personnel in hover.	✓	5.4
FTF-SYS-FDS-05.13	The aircraft shall be able to adjust the water/retardant dispersion settings.	✓	10.1
FTF-SYS-FDS-05.14	The aircraft shall be capable of stable hovering at different altitudes.	✓/×	8.3
FTF-SYS-FDS-05.15	The aircraft shall sustain no structural damage when accelerating between -1 and +3.25 g at MTOW.	✓	9.1
FTF-SYS-FDS-05.16	The aircraft shall have a service ceiling of 5000 m above sea level.	✓	7.1
FTF-SYS-FDS-05.17	The aircraft shall be capable of a minimum rate of climb (ROC) of 5.5 m/s at MTOW in hover mode at sea level.	✓At SL	6.1
FTF-SYS-FDS-06.1	The aircraft shall have a maintenance downtime of less than 10 hours per operational hour.	×	NA
FTF-SYS-FDS-06.2	The aircraft shall be able to take off within 30 minutes from an emergency call.	×	NA
FTF-SYS-FDS-06.3	The aircraft shall make use of proven technology.	✓/×	
FTF-SYS-FDS-06.4	The aircraft shall be able to be serviced by an Approved Maintenance Organisation (AMO).	×	NA
FTF-SYS-FDS-06.5	The aircraft shall be compatible with a widely used refuelling system.	×	NA
FTF-SYS-FDS-06.6	The aircraft shall have a turnaround time of 20 minutes.	×	NA
FTF-SYS-FDS-07.1	The aircraft shall be able to operate in known icing conditions.	✓	5.3

Continued on next page

Table 15.2 – continued from previous page

Identifier	Requirement	Met?	Section
FTF-SYS-FDS-07.2	The aircraft shall be resistant to corrosion caused by (salty) water.	✓	9.2
FTF-SYS-FDS-07.3	The aircraft shall be able to operate as required, despite of heat generated by the fire whilst flying in the air above the fire.	✓	9.2
FTF-SYS-FDS-08.1	The aircraft shall contain a night vision system for the pilots.	✓	5.3
FTF-SYS-FDS-09.1	The aircraft shall contain a system that enhances the pilot's perception in smoke.	✓	5.3
FTF-SYS-PIL-01.1	The aircraft shall be capable of autopiloted flight in compliance with VFR.	✓	5.3
FTF-SYS-PIL-01.2	The aircraft shall be capable of autopiloted flight in compliance with IFR.	✓	5.3
FTF-SYS-PIL-01.3	The aircraft shall be equipped with an auto-land feature.	✓	5.3
FTF-SYS-PIL-02.1	The aircraft shall not require higher physical control effort from the pilot compared to the Sikorsky S-70 Firehawk.	×	NA
FTF-SYS-PIL-03.1	The aircraft shall be statically longitudinally stable.	✓	8.2
FTF-SYS-PIL-03.2	The avionics software used shall be user-friendly and similar to use as existing aircraft.	✓	5.3
FTF-SYS-PIL-04.1	The aircraft shall be equipped with safety features to ensure the safety of the crew when flying over a fire.	×	NA
FTF-SYS-PIL-04.2	The aircraft shall be equipped with safety features to ensure the safety of the crew in case of an aircraft malfunction (e.g. crash or emergency landing).	×	NA
FTF-SYS-PIL-04.3	The aircraft shall be able to sustain one-engine-inoperative flight.	✓	6.3
FTF-SYS-PIL-04.4	The aircraft shall have crash-resistant fuel systems.	✓	10.2
FTF-SYS-PIL-05.1	The aircraft shall be ergonomic such that a 95th% percentile male can fly missions of endurance specified in FTF-SYS-FDS-03.2 without inducing physical discomfort.	✓	5.3
FTF-SYS-INV-01.1	The preliminary design of the aircraft shall be performed by a team of 10 students working full-time.	✓	
FTF-SYS-INV-02.1	The aircraft design shall be modular.	✓	5.4
FTF-SYS-INV-02.2	The aircraft shall be capable of search and rescue missions.	✓	5.4
FTF-SYS-INV-02.3	The aircraft shall be capable of cargo missions.	✓	5.4
FTF-SYS-INV-02.4	The aircraft shall be capable of landing on a surface as soft and as wet and boggy grass.	✓	8.4
FTF-SYS-OWN-01.1	The aircraft shall comply with environmental regulations for the coming 20 years, from 2024 onwards.	×	NA
FTF-SYS-OWN-02.1	The aircraft shall have a unit cost of less than 63 million euros.	✓	12.2
FTF-SYS-GFC-01.1	The aircraft shall be equipped with radio communication equipment capable of reaching ground crews.	✓	5.3
FTF-SYS-ATC-01.1	The aircraft shall be equipped with radio communication equipment capable of reaching air traffic control.	✓	5.3
FTF-SYS-ATC-01.2	The aircraft shall be equipped with satelite communication equipment.	✓	5.3
FTF-SYS-ATC-02.1	The aircraft shall not make use of low observable (LO) Technology materials.	✓	9.2
FTF-SYS-ATC-02.2	The aircraft shall be equipped with a transponder.	✓	5.3
FTF-SYS-LOC-01.1	The aircraft shall be able to create fire lines.	✓	10.1

Continued on next page

Table 15.2 – continued from previous page

Identifier	Requirement	Met?	Section
FTF-SYS-REG-01.1	The aircraft shall be compliant with icing conditions requirements as stated in CS25.1419.	×	NA
FTF-SYS-REG-01.2	The aircraft shall be compliant with one engine inoperative climb rate requirements as stated in CS29.67.	×	
FTF-SYS-REG-01.3	The aircraft shall be compliant with engine power ratings as stated in CS-E 40.	✓	6.3
FTF-SYS-REG-01.4	The aircraft shall be compliant with engine fire requirements as stated in CS-E 130.	✓	6.3
FTF-SYS-REG-01.5	The aircraft shall be compliant with critical engine part integrity requirements as stated in CS-E 515.	×	NA
FTF-SYS-REG-01.6	The aircraft shall be compliant with ingestion of foreign matter requirements as stated in CS-E 540.	×	NA
FTF-SYS-REG-01.7	The aircraft shall be compliant with cockpit visibility requirements as stated in CS29.773.	✓	5.3
FTF-SYS-REG-01.8	The aircraft shall be compliant with fire protection requirements of critical parts as stated in CS29.855.	✓ / ×	10.2
FTF-SYS-REG-01.9	The aircraft shall be compliant with emergency evacuation requirements as stated in CS25.803.	✓	5.3
FTF-SYS-REG-01.10	The aircraft shall be compliant with the installation of systems requirements as stated in CS25.901.	×	NA
FTF-SYS-REG-01.11	The aircraft shall be compliant with engine placement requirements as stated in CS29.903.	×	NA
FTF-SYS-REG-01.12	The aircraft shall be compliant with gust and turbulence requirements as stated in CS25.341.	×	NA
FTF-SYS-REG-01.13	The aircraft shall be compliant with deformation characteristics as stated in CS25.305.	✓	9.1
FTF-SYS-REG-01.14	The aircraft shall be compliant with landing gear requirements as stated in CS29.731.	✓	8.4
FTF-SYS-REG-02.2	The aircraft shall have SC certification for fireproof systems.	×	NA
FTF-SYS-REG-02.4	The aircraft shall have SC certification to utilise a refilling device while hovering.	×	NA
FTF-SYS-REG-02.5	The aircraft shall have SC certification to carry a drop tank.	×	NA
FTF-SYS-REG-02.6	The aircraft shall have SC certification to withstand waterload conditions.	×	NA
FTF-SYS-REG-02.8	The aircraft shall have SC certification according to VTOL.2235 regarding the proof of structure.	×	NA
FTF-SYS-REG-02.9	The aircraft shall have SC certification in accordance with VTOL.2230, VTOL.2235 and VTOL.2240 for each critical loading condition.	×	NA
FTF-SYS-REG-02.10	The aircraft shall have SC certification in accordance with VTOL.2500 b) and VTOL.2510 for the development of the Flight Guidance Systems (FGS).	×	NA
FTF-SYS-AIR-02.1	The aircraft shall be compliant with engine power ratings as stated in CS-E 40.	✓	6.3
FTF-SYS-SUP-01.1	The aircraft shall operate within a temperature range specified by the construction materials supplier.	×	
FTF-SYS-SUP-01.2	The aircraft shall be able to operate with a widely available type of fuel for the chosen engine configuration.	✓	6.3

Continued on next page

Table 15.2 – continued from previous page

Identifier	Requirement	Met?	Section
FTF-SYS-SUP-01.3	The aircraft shall be able to host off-the-shelf avionic systems.	✓	5.3

15.2. Feasibility Analysis

Contributors: Emma
Authors: Emma

In the feasibility analysis, the requirements that are not met are discussed. Starting off with the system requirements, since they together form the user requirements.

- **FTF-SYS-FDS-05.11**: The aircraft will be able to drop personnel in forward flight, as the aircraft can fly horizontally. However, dropping personnel in hover will be the preferred option. Therefore, no detailed look is taken at dropping personnel in forward flight.
- **FTF-SYS-FDS-05.14**: The aircraft is not capable of stable hovering without a control system. With a control system to correct for the instability, the aircraft will be able to hover stably.
- **FTF-SYS-FDS-06.3**: The largest part of the aircraft does make use of proven technology, but some of the technologies are not proven yet. Therefore it can not be said that the aircraft only uses proven technology.
- **FTF-SYS-REG-01.2**: The aircraft can not climb with one engine inoperative. This could be solved by adding an extra engine. However, since the aircraft can still glide and land safely with one engine inoperative, it is decided that the extra weight and complexity of an extra engine is not worth it.
- **FTF-SYS-SUP-01.1**: The aircraft operates within the temperature range. However, this was achieved the other way around. The materials were chosen, such that it can operate within the temperatures.

There are also quite some requirements that were not met due to that they are not addressed at all. This does not necessarily mean that the requirement will not be met, but it does mean that those requirements have to be considered in the further development of the aircraft. Some examples are given below. Since there are relatively many unaddressed requirements, not all of them are discussed. The reasons for these requirements is similar to the examples given below.

- **FTF-SYS-FDS-06.2**: During the design phase, it was kept in mind that the initial response time should be as low as possible. However, no analysis is yet performed that determines the exact initial response time.
- **FTF-SYS-PIL-02.1**: When determining the control characteristics, they were not compared to other aircraft.
- **FTF-SYS-ATC-02.2**: Simply not considered yet. Shall be considered in later stages.
- **FTF-SYS-REG-02.**: All Special Conditions (SC) certifications are not met. This does not necessarily mean that the design contradicts the certifications, but it means that it is not checked yet if it complies with the certification standards. If it does not comply, iterations are necessary to make them comply. Most of these requirements are too specific for this design stage.

Next, the feasibility of the user requirements is discussed. A summation of the reasons for system requirements not being met is the reason for the user requirements that are not met.

- **FTF-UR-05**: Most of the operational reliability and availability is not analysed yet. It was kept in mind throughout the design phase, but no detailed calculations were yet made. This will be one of the first steps in the next phase of the design.
- **FTF-UR-11**: As described before, for certifications the requirement is not met due to the missing of the actual checking and connecting the design to the certification rules. This will have to be done in the following stages of the design. This will probably lead to new iterations of the design parameters.

15.3. Viability of CHEETAH

Contributors: Jorrit
Authors: Jorrit

Though CHEETAH meets most of its user requirements, the real feasibility of the aircraft will be largely dependent on the market. This can be further analysed using a simulation like the one created by Wissam Chalabi in 2023 [96]. From there the effectiveness can be determined and the true value of CHEETAH in a firefighting fleet can be found.

As can be seen from Chapter 12, a large part of the produced aircraft will be sold to the military. This makes the continuation of the project not only a financial matter but also an ethical dilemma. The target of the project was to develop a multi-role VTOL aerial firefighter that can bridge the capability cap of traditional firefighting helicopters and fixed-wing aircraft. The "multirole" aspect could imply further use in other sectors like the military, however, from the nature of this project, the intent of the statement was likely to develop a multirole aircraft with the purpose of saving lives, property and the environment.

The main issue with selling to military organisations is the indirect contribution CHEETAH would have to the loss of life. Though the aircraft would largely be used for search and rescue missions, dropping of personnel and dropping of supplies, history has shown that military organisations add large guns or other weapon systems to these types of aircraft. This conflicts with the personal values of the team or the corporate values focused on humanitarian efforts. Selling to military organisations would also be a risk to the reputation of the company. However, since most aircraft manufacturers are also involved in the military circuit, this is likely not a large risk.

Since a non-profitable aircraft will not continue into the next phase, a mitigation strategy will have to be created and executed. As shown in Chapter 12, the profits will largely come from the military side, which cannot be changed. Keeping the personal values of the project members in mind, the decision was made to continue the project even though sales would be made to the military. The key to this decision was the way CHEETAH is likely going to be used in the military. Even though militaries will likely mount weaponry on the aircraft, the main purpose of its missions will not be direct combat. It will more commonly be used in search and rescue, cargo missions and crew transport, which do not directly influence the loss of lives. The argument can even be made that a more efficient aircraft will lead to a more efficient and effective organisation, which in turn leads to fewer innocent lives lost. The reputation risk can be tackled with a marketing strategy. The aim will be to only market CHEETAH to the public as a firefighting and humanitarian aid aircraft while leveraging the profits from the military sales to subsidise the firefighting organisations.

15.4. Manufacturing, Assembly and Integration

Contributors: Ivo
Authors: Ivo

When producing an aircraft or a series of aircraft, the Manufacturing, Assembly, and Integration (MAI) Plan outlines the strategy and steps taken for successful production. The MAI plan, indicated in Appendix D, highlights the key elements of the production process such as part manufacturing, (structural) sub-assembly, installation of the sub-assemblies and finally, the finished product.

The various components that need to be produced or integrated are arranged in a chronological sequence. Although the exact time required for manufacturing and assembling these components is not yet known at this stage of the design, the goal is to complete the entire production of an aircraft within six months. The process is divided into several stages:

- **Component production:** Smaller parts needed for the fuselage, tail and wings are produced.
- **Subsystem structure assembly:** The first structures of certain subsystems are assembled together. Additionally, new components are manufactured or purchased from external suppliers.
- **Subsystem assembly:** The smaller components are assembled into larger systems such as the fuselage, tail and wing. Each system undergoes quality checks and testing to ensure all parts meet the requirements.
- **Final integration:** All the systems are integrated together into one final product. Additionally, some

tests are performed to make sure the assembled aircraft meets the desired quality. Moreover, smaller components such as the avionics, communication system, and navigation system are installed. The final integration is completed with the installation of the main rotor, thereby marking the end of the production phase of the compound helicopter.

15.5. Post-DSE Activities

Contributors: Jorrit
Authors: Jorrit

A plan was set up to continue work on the project after the end date of the DSE. As the project is finishing its feasibility analysis phase the specific steps to take in the future are difficult to determine. Therefore the plan was kept top-level for now. A flow diagram and GANTT chart can be found in Appendix C.

The plan was divided into 6 phases (identifier P-XX), which contain activities(identifier A-XX), milestones (no identifier) and stage gates (identifier SG-XX). The stage gates are points where the viability of the project is identified and the project can be shut down if needed. The first of which is the feasibility analysis that was done in Section 15.2.

The following phase will be the detailed design of the aircraft. Here all parts of the aircraft will be designed and integrated. This is a feedback loop to ensure the integration of all parts of the aircraft. Testing will also be performed in this phase such that all individual aspects of the design can be verified and validated already. An example would be testing the effects of the spinning main rotor on the box wing in a wind tunnel. In cockpit tests the cockpit mock-up could be built in a flight simulator like SIMONA at TU Delft and tested by pilots to get feedback on the cockpit layout. The detailed design phase is planned to last about 2.5 more years to ensure an optimised design. Naturally, changes to the design can still be made during the prototype and certification phase. A second feasibility analysis will be performed after the detailed design process to decide if the aircraft is still worth building.

If the design is deemed feasible, a prototype will be developed. Simultaneously, a detailed certification plan will be set up that builds on the V&V plans discussed earlier in Chapter 14. A design presentation will also be held to start off the marketing campaign for the aircraft, which will continue well into the production and delivery phases. The first milestone will be hit after this when the first orders of CHEETAH roll in. The production of the prototype will be performed the same as the rest of the production as outlined in Section 15.4. A year is taken for the prototype phase.

When the prototype is finished the v&v and certification testing phase will start. This will be done with several tests that can be categorised underground, flight, safety and structural tests. The flight tests will also include tests of the dropping system. From there the last full project stage gate will be passed as all certifications will be obtained. If certifications cannot be obtained with the current design, the project can go back to the detailed design phase or be cancelled immediately. Due to the nature of the design, the testing phase is planned to take 3 years.

From here production will be started up. This means setting up and managing the supply chain as well as setting up the production and assembly lines. The production process is again outlined in Section 15.4. Each aircraft will go through a rigorous quality control process, where it will be approved for delivery once it passes. Pilot training and maintenance programmes will also be started up once the first deliveries have been completed. Spare parts will have to be created for the aircraft to ensure smooth maintenance processes. A launch event will be held where the first produced aircraft will be rolled out. The aircraft will be in production for 10 years, wherein the production of 400 aircraft is targeted.

16 | Conclusion and Recommendations

Author: Sjoerd

The design and development of CHEETAH represent a significant advancement in the capabilities of aerial firefighting. There is an urgent need for new firefighting aircraft to effectively combat the increasing intensity and spread of wildfires, which threaten both nature and society. To help manage wildfires, an aircraft was created to make the largest possible impact on any firefighting fleet. The objective was to design a multirole VTOL aerial firefighter that outperforms helicopters in capacity, range, and speed while offering more versatility than fixed-wing aircraft. By integrating the versatility of VTOL technology with the capacity and speed of fixed-wing aircraft, CHEETAH fills a critical gap in the current market. This innovative aircraft is designed to enhance firefighting efficiency, particularly in remote and difficult-to-reach areas, while also emphasising sustainability and environmental impact.

16.1. Key Findings and Limitations

CHEETAH successfully combines VTOL capabilities with the high capacity and speed of traditional fixed-wing firefighting aircraft. This design ensures that CHEETAH can operate efficiently in varied and challenging environments. Key innovations include hover capabilities, which allow for precise water or fire retardant drops, high-speed performance that enables rapid response to fire outbreaks, and substantial payload capacity to carry significant amounts of firefighting materials. Additionally, the modular design allows for CHEETAH to be adapted for other critical roles such as search and rescue operations, medical evacuations, and logistical support. The aircraft's flexibility in different operational contexts makes it a valuable asset for emergency response teams, potentially saving more lives and property during wildfire incidents.

In terms of technical progress, the propulsion system development is well underway, with the multi-engine setup proving to be reliable in initial tests, providing sufficient lift and thrust across various flight conditions. Aerodynamic design efforts have focused on minimising drag and maximising efficiency, which have shown promising results in achieving higher speeds and improved fuel efficiency. The structural integrity of the aircraft has been enhanced through the use of advanced composite materials, which not only increase durability but also reduce weight, thereby enhancing overall performance and safety. For stability and control, the horizontal and vertical tail designs are being refined to ensure static and dynamic stability in both hover and forward flight modes. Dynamic stability analysis has indicated that while all eigenmotions are stable in forward flight, further design adjustments are required to address instability in hover mode.

Despite these promising findings, several limitations were identified that need to be addressed in future work. One significant limitation is the technical challenge of noise reduction, which is crucial for operations in populated areas and for minimising disturbance to wildlife. Rotor-wing interference, which affects the aerodynamic efficiency and stability of the aircraft, requires further optimisation to ensure safe and reliable performance. Moreover, there are substantial uncertainties, assumptions, and risks associated with key technical areas including propulsion systems, aerodynamics, and structural integrity. These uncertainties need careful management and mitigation in subsequent development phases. Furthermore, the sustainability analysis, although thorough, indicated the need for continuous improvement in reducing the environmental impact of CHEETAH's operations and manufacturing processes. Another limitation is the reliance on projections and assumptions in market analysis, which may not fully account for future market dynamics and technological advancements. These limitations underscore the importance of ongoing research, development, and testing to fully realise the potential of the CHEETAH aircraft.

16.2. Viability of CHEETAH

Though CHEETAH meets most of its user requirements, its real feasibility will largely depend on market acceptance and addressing ethical considerations related to potential military applications. The project's financial sustainability hinges on military sales, posing an ethical dilemma. However, the primary humanitarian use and potential non-combat military applications, such as search and rescue, support the continuation of the project. A targeted marketing strategy can help mitigate reputational risks by emphasising CHEETAH's

primary role as a firefighting and humanitarian aid aircraft.

16.3. Recommendations

Given the findings and limitations discussed, several key recommendations have been formulated to ensure the successful development and implementation of the CHEETAH VTOL firefighting aircraft. These recommendations aim to address the technical and ethical challenges identified in the report, establishing CHEETAH as a crucial asset in aerial firefighting and beyond.

1. **Technical Enhancements and Validation:** Further invest in technical validation and optimisation, particularly in noise reduction, rotor-wing interference, and aerodynamic performance, to ensure regulatory compliance and operational efficiency. Improving these aspects will enhance the overall performance and acceptance of the aircraft in various markets.
2. **Sustainability Initiatives:** Continue integrating sustainability into the design and operation of CHEETAH. Explore the use of sustainable fuels, optimise fuel efficiency, and ensure that manufacturing processes are environmentally friendly to minimise the aircraft's carbon footprint and enhance its long-term viability.
3. **Risk Management and Mitigation:** Develop comprehensive risk management strategies to address the uncertainties, assumptions, and risks identified in the technical departments. This includes ongoing research and development efforts, stakeholder engagement, and continuous evaluation to mitigate potential challenges and ensure the successful introduction of CHEETAH.
4. **Market Simulation and Analysis:** Conduct further market analysis using advanced simulations to evaluate the effectiveness of CHEETAH in firefighting fleets. This will help determine its true value and operational benefits in real-world scenarios.
5. **Ethical Considerations and Marketing Strategy:** Develop a comprehensive marketing strategy that emphasises CHEETAH's role as a firefighting and aid aircraft. Address ethical concerns by highlighting the aircraft's non-combat applications and leveraging profits from military sales to support firefighting organisations.
6. **Model Expansion, Verification, and Validation:** To, expand, verify, and validate the existing models created during the project. This step is essential to ensure the models' accuracy and reliability in predicting the aircraft's performance and effectiveness in various scenarios.

By following these recommendations, the CHEETAH project can move forward confidently, addressing both the technical and ethical challenges while maximising its impact as a pioneering aerial firefighting solution.

Bibliography

[1] DSE Groups 13 and 14, "Baseline Report for the Design of a VTOL Firefighter Aircraft," , 2024.

[2] DSE Groups 13 and 14, "Midterm Report for the Design of a VTOL Firefighter Aircraft," , 2024.

[3] MacCarthy, J., Richter, J., Tyukavina, S., Weisse, M., and Harris, N., "The Latest Data Confirms: Forest Fires Are Getting Worse," World Resources Institute, August 2023. URL https://www.wri.org/insights/global-trends-forest-fires, accessed 01/05/2024.

[4] ESA, "Counting wildfires across the globe," *ESA Website*, 2023. URL https://www.esa.int/Applications/Observing_the_Earth/Copernicus/Sentinel-3/Counting_wildfires_across_the_globe.

[5] Department, L. A. C. F., "Analysis of Current Wildland Firefighting Aircraft Program & Other Aircraft Types," 2016.

[6] James, O., "Frégate-F100, le pari fou d'un Canadair Made in France," *L'Usine Nouvelle*, 2023.

[7] Insights, B. R., "Aerial Firefighting Market Size, Share, Growth, And Industry Analysis by Type (Multi-Rotor, Fixed Wing, Helicopter) by Application (Firefighting Organizations, Military & Others) and Regional Insights and Forecast to 2032," Tech. rep., Buisness Research Insights, 2024.

[8] Research, A. M., "Firefighting Aircraft Market Size, Share, Competitive Landscape and Trend Analysis Report by Aircraft Type, by Tank Capacity, by Maximum Takeoff Weight, by Range : Global Opportunity Analysis and Industry Forecast, 2023-2032," Tech. rep., Allied Market Research, 2024.

[9] Keeley, J. E., "Fire management impacts on invasive plants in the western United States," *Conservation Biology*, Vol. 20, No. 2, 2006, pp. 375–384.

[10] Keeley, J. E., and Zedler, P. H., "Large, high-intensity fire events in southern California shrublands: debunking the fine-grain age patch model," *Ecological Applications*, Vol. 19, No. 1, 2009, pp. 69–94.

[11] Stephens, S. L., and Ruth, L. W., "Federal forest-fire policy in the United States," *Ecological Applications*, Vol. 15, No. 2, 2005, pp. 532–542.

[12] Swanson, M. E., Franklin, J. F., Beschta, R. L., Crisafulli, C. M., DellaSala, D. A., Hutto, R. L., Lindenmayer, D. B., and Swanson, F. J., "The forgotten stage of forest succession: early-successional ecosystems on forest sites," *Frontiers in Ecology and the Environment*, Vol. 9, No. 2, 2011, pp. 117–125.

[13] Shakesby, R., and Doerr, S., "Wildfire as a hydrological and geomorphological agent," *Earth-Science Reviews*, Vol. 74, No. 3-4, 2006, pp. 269–307.

[14] Smith, J. K., "Wildlife responses to fire," *USDA Forest Service, General Technical Report RMRS-GTR-42-volume 1*, 2000.

[15] Wettstein, Z. S., Hoshiko, S., Fahimi, J., Harrison, R. J., Cascio, W. E., and Rappold, A. G., "Cardiovascular and cerebrovascular emergency department visits associated with wildfire smoke exposure in California in 2015," *Journal of the American Heart Association*, Vol. 7, No. 8, 2018.

[16] Liu, J. C., Pereira, G., Uhl, S. A., Bravo, M. A., and Bell, M. L., "A systematic review of the physical health impacts from non-occupational exposure to wildfire smoke," *Environmental Research*, Vol. 136, 2015, pp. 120–132.

[17] Bladon, K. D., Emelko, M. B., Silins, U., and Stone, M., "Wildfire and the future of water supply," *Environmental Science & Technology*, Vol. 48, No. 16, 2014, pp. 8936–8943.

[18] Donovan, G. H., and Rideout, D. B., "An integer programming model to optimize resource allocation for wildfire containment," *Forest Science*, Vol. 49, No. 2, 2003, pp. 331–335.

[19] Penman, T. D., Bradstock, R. A., Price, O. F., and Penman, S. H., "Reducing wildfire risk to urban developments: Simulation of cost-effective fuel treatment solutions in south eastern Australia," *Environmental Modelling & Software*, Vol. 52, 2014, pp. 166–175.

[20] Oum, T. H., Yu, C., and Wang, J., *Aviation and the Environment*, Springer, Berlin, Germany, 2021.

[21] Westerling, A. L., Hidalgo, H. G., Cayan, D. R., and Swetnam, T. W., "Warming and earlier spring increase western US forest wildfire activity," *Science*, Vol. 313, No. 5789, 2006, pp. 940–943. doi:10.1126/science.1128834.

[22] Human Factors Standardization SubTAG, "Human Engineering Design Data Digest," Tech. rep., Department of Defense Human Factors Engineering Technical Advisory Group, 2000.

[23] U.S. Department of Defense, "Chapter 608 – System 463L Pallets and Nets," *Defense Transportation Regulation*, 2023.

[24] Boeing, *Pallets and containers*, 2012.

[25] Prouty, R., *Helicopter Performance, Stability, and Control*, PWS Publishers, 1986.

[26] Gudmundsson, S., "Propeller Efficiency," *General Aviation Aircraft Design*, 2014.

[27] "Janes," Online, April 2021. Jane's All the World's Aircraft database. Engine: Rolls Royce AE 1107C.

[28] "Janes," Online, April 2021. Jane's All the World's Aircraft database. Engine: Rolls Royce AE 1107F.

[29] "Janes," Online, April 2021. Jane's All the World's Aircraft database. Aircraft: Sikorsky CH-53K.

[30] "Janes," Online, April 2021. Jane's All the World's Aircraft database. Engine: Rolls Royce Turbomeca RTM 322.

[31] "Janes," Online, April 2021. Jane's All the World's Aircraft database. Engine: General Electric T700.

[32] Prandtl, L., "Induced Drag of Multiplanes," NASA Technical Report 672, National Advisory Committee for Aeronautics, August 1965. Reproduced for NASA by the Scientific and Technical Information Facility.

[33] Gagnon, H., and Zingg, D. W., "Aerodynamic Optimization Trade Study of a Box-Wing Aircraft Configuration," *Journal of Aircraft*, Vol. 53, No. 4, 2016, pp. 971–981. doi:10.2514/1.C033592.

[34] Sugawara, H., Tanabe, Y., and Kameda, M., "Effect of Lift-Share Ratio on Aerodynamic Performance of Winged Compound Helicopter," *Journal of Aircraft*, Vol. 58, No. 5, 2021, pp. 997–1008. doi:10.2514/1.C036163.

[35] Yeo, H., and Johnson, W., "Optimum Design of a Compound Helicopter," *Journal of Aircraft*, Vol. 46, No. 4, 2012, pp. 1210–1220. doi:10.2514/1.40101.

[36] NASA and the US Army Aviation Development Directorate, "Design and Aeromechanics Investigation of Compound Helicopters," *Aerospace Science and Technology*, Vol. 88, 2019, pp. 158–173. doi:10.1016/j.ast.2019.03.010.

[37] Vos, D. R., "Aerospace Design & Systems Engineering Elements I," TU Delft, BSc Aerospace Engineering, 2023/2024. Accessed on 01/06/2024.

[38] Anderson, J., *Introduction to Flight*, McGraw-Hill Education, 2016.

[39] Unknown, "XFLR5," , 2023. URL http://www.xflr5.tech/xflr5.htm, accessed: 2024-06-01.

[40] Russo, A., and Others, "Box-Wing and Induced Drag: Compressibility Effects in Subsonic and Transonic Regimes," *Aerospace Science and Technology*, Vol. 97, 2020, p. 105684.

[41] Ning, S. A., and Kroo, I., "Multidisciplinary Considerations in the Design of Wings and Wing Tip Devices," *Journal of Aircraft*, Vol. 47, No. 2, 2010, pp. 534–543. doi:10.2514/1.41833.

[42] Kunze, P., and Wentrup, M., "Aerodynamic Analysis and Optimization of Wings and Tail Surfaces of a Compound Helicopter with Box Wing," *New Results in Numerical and Experimental Fluid Mechanics XII*, edited by A. Dillmann, G. Heller, E. Krämer, C. Wagner, C. Tropea, and S. Jakirlić, Springer International Publishing, Cham, 2020, pp. 372–381. doi:10.1007/978-3-030-25253-3_36.

[43] Leishman, J. G., *Principles of Helicopter Aerodynamics*, 2nd ed., Cambridge University Press, Cambridge, UK, 2006.

[44] N. Miller, A. P., J.C. Tang, "Theoretical and Experimental Investigation of the Instantaneous Induced Velocity Field in the Wake of a Lifting Rotor," Technical Note -, Dynasciences Corperation, Blue Bell, Pennsylvania, 1968.

[45] Walter Castles, J., and Gray, R. B., "Empirical Relation Between Induced Velocity, Thrust, and Rate of Descent of a Helicopter Rotor as Determined by Wind Tunnel Tests on Four Model Rotors," Technical Note 2474, National Advisory Committee for Aeronautics, Washington, October 1951.

[46] White, F. M., *Fluid Mechanics 6th edition*, McGraw-Hill Publishing Company, 2016.

[47] Roskam, J., *Airplane Design Part VI: Preliminary Calculation of Aerodynamic Thrust and Power Characteristics*, DARcorporation, 1989.

[48] Vos, D. R., "Systems Engineering & Aerospace Design," TU Delft, BSc Aerospace Engineering, 2023/2024. Accessed on 14/06/2024.

[49] Sturgeon, W., and Phillips, J., "A Mathematical Model of the CH-53 Helicopter," Technical Memorandum NASA-TA-812 38, National Aeronautics and Space Association, Ames Research Center, California, 1981. Accessed: 2024-06-12.

[50] EASA, "Certification Specifications for European Technical Standard Orders (CS-ETSO)," , October 2003.

[51] Torenbeek, E., *Synthesis of Subsonic Airplane Design*, Kluwer Academic Publishers, 1982.

[52] Tyre, M. A., "Aircraft tire Engineering Data," , unknown.

[53] Oliviero, D., "Aerospace Design & Systems Engineering Elements II," TU Delft, BSc Aerospace Engineering, 2022/2023. Accessed on 07/06/2024.

[54] Sridharan, A., Chopra, I., and Govindarajan, B., "A Scalability Study of the Multirotor Biplane Tailsitter Using Conceptual Sizing," *American Helicopter Society*, 2019, pp. 012009–5. URL https://www.researchgate.net/publication/336773459_A_Scalability_Study_of_the_Multirotor_Biplane_Tailsitter_Using_Conceptual_Sizing.

[55] Wahl, L., Maas, S., and Waldmann, D., "Shear Stresses in Honeycomb Sandwich Plates: Analytical Solution, FEM and Experimental Verification," Master's thesis, University of Luxembourg, 2011.

[56] Alambra, K., and Swanson, N., "Beam Deflection Calculator," *Omni Calculator*, 2024.

[57] Prouty, R., "Helicopter performance, stability, and control," *Krieger Pub*, 1986, pp. 683–702.

[58] Soprunenko, E., Valeriy, P., Vladimir, R., and Egor, L., "Simulation of impact assesment of crown forest fires on boudary layer of atmosphere using software PHOENICS," Tech. rep., XXI International Symposium Atmospheric and Ocean Optics. Atmospheric Physics, 2015. doi:10.1117/12.2205474.

[59] Ansul, "SILV-EX Plus "Class A" Fire Control Concentate," , unknown.

[60] Ler, H., Tock, P., Tamas, W., Neoh, S., Lee, K. E., Tang, C., and W.Y., "AIAA 2021-2022 Design Competition," Tech. rep., Nanyang Technological University, Singapore, 639798, May 2014.

[61] Ning, D., Su, P., and Zhang, C., "Experimental Study on A Sloshing Mitigation Concept Using Floating Layers of Solid Foam Elements," *Chinese Ocean Engineering Society*, 2018.

[62] Roskam, J., *Airplane Design Part IV: Layout Design of Landing Gear and Systems*, DARcorporation, 1989.

[63] Viswanath, S., and Nagarajan, R., "HELICOPTER HYDRAULIC SYSTEM," , 2002.

[64] Jemitola, P. O., Monterzino, G., and Fielding, J., "Wing mass estimation algorithm for medium range box wing aircraft," *The Aeronautical Journal*, Vol. 117, No. 1189, 2013, p. 329–340. doi:10.1017/S0001924000008022.

[65] Stepniewski, W. Z., and Shinn, R. A., *A Comparative Study of Soviet vs. Western Helicopters Part 2 - Evaluation of Weight, Maintainability, and Design Aspects of Major Components*, 1983.

[66] Roskam, J., *Airplane Design Part V: Component Weight Estimation*, 5th ed., Design, Analysis and Research Corporation, 2018.

[67] Ravinka Seresinhe, C. L., "Electrical load-sizing methodology to aid conceptual and preliminary design of large commercial aircraft," *SageJournals*, Vol. 229, No. 3, 2014.

[68] *Certification Specifications for Large Aeroplanes CS-25*, European Aviation Safety Agency, sep 2007.

[69] Lee, D., Fahey, D., Skowron, A., Allen, M., Burkhardt, U., Chen, Q., Doherty, S., Freeman, S., Forster, P., Fuglestvedt, J., Gettelman, A., De León, R., Lim, L., Lund, M., Millar, R., Owen, B., Penner, J., Pitari, G., Prather, M., Sausen, R., and Wilcox, L., "The contribution of global aviation to anthropogenic climate forcing for 2000 to 2018," *Atmospheric Environment*, Vol. 244, No. 117834, 2021.

[70] COUSTAL, L., "Forest fires: a record year," *PHYS ORG*, 2023.

[71] Service, A. M., "2023: A year of intense global wildfire activity," *Opernicus*, 2023.

[72] *Globe Newswire*, 2023, pp. 2015–2035.

[73] *Guidelines for Measuring and Managing CO2 Emission from Freight Transport Operations*, issue 1 ed., mar 2011.

[74] ICAO, *Annex 16, to the Convention on International Civil Aviation – Volume I - Aircraft Noise*, ICAO, 2017.

[75] Marte, J. E., and Kurtz, D. W., "A Review of Aerodynamic Noise From Propellers, Rotors, and Lift Fans," Tech. rep., Jet Propulsion Laboratory, 1970.

[76] Hubbard, H. H., "Aeroacoustics of Flight Vehicles: Theory and Practice – Volume 1: Noise Sources," Tech. rep., NASA, 1991.

[77] Blacodon, D., and Lewy, S., "Source localization of turboshaft engine broadband noise using a three-sensor coherence method," *Journal of Sound and Vibration*, Vol. 338, 2015, pp. 250–262.

[78] Gilliland, J. J., "The Establishment of Helicopter Subsystem Design-to-Cost Estimates by use of Parametric Cost Estimating Models," Ph.D. thesis, North Texas State University, August 1979.

[79] Lammering, T., Franz, K., Risse, K., Hoernschemeyer, R., and Stumpf, E., "Aircraft Cost Model for Preliminary Design Synthesis," *American Institute of Aeronautics and Astronautics*, 2012.

[80] Roskam, J., *Airplane Design Part VIII: Airplane Cost Estimation: Design, Development, Manufacturing and Operating*, Design, Analysis and Research Corporation, 1990.

[81] SCHNEBLY, F. D., "TRANSPORT HELICOPTER OPERATING COST ANALYSIS METHODS," Tech. rep., HILLER HELICOPTERS, 1955.

[82] Reddick, H. K., "ARMY HELICOPTER COST DRIVERS," Tech. rep., U. S. ARMY AIR MOBILITY RESEARCH AND DEVELOPMENT LABORATORY, 1975.

[83] Satpathy, N., and Murari, K., "Life Cycle Cost of a Six Ton Helicopter," *Journal of Aerospace Science and Technology*, Vol. 57, No. 2, 2005. doi:10.61653/joast.v57i2.2005.766.

[84] Solutions, P., "WD881, class A foam concentrate," https://www.perimeter-solutions.com/wp-content/uploads/2022/08/PC-WD881-Class-A-Brochure_PCC-2019046-3_EN.pdf, 2020. [Accessed 05-06-2024].

[85] "Airbus Financial Statements 2023," , 2023.

[86] "Night Vision Imaging System (NVIS) | SKYbrary Aviation Safety — skybrary.aero," , 2023. [Accessed 02-05-2024].

[87] Concepts, F. C. S. O., and Team, R., "A COMMUNICATIONS OPERATING CONCEPT AND REQUIREMENTS FOR THE FUTURE RADIO SYSTEM VERSION 2.0," , 2005. About risks for communication systems.

[88] ENAC, "RAMS Analysis for Aeronautics," , nov 2023. Lecture slides SDF.

[89] Hamann, R., and van Tooren, M., *Systems Engineering & Technical Management Techniques - Part 2*, 1st ed., January 2006. Lecture Notes.

[90] Corley, T., *How Often Does a Helicopter Need Maintenance?*, JSSI, 2022.

[91] Storm, E., *How Often Do Helicopters Need Maintenance?*, Start Pac, 2024.

[92] BELL, *Bell 412/412EP maintenace manual*, Vol. 1, BELL TEXTTRON INC., 2022.

[93] sasadmin, "EASA Landing Gear Maintenance Considerations," *Sofema*, 2018.

[94] Stamps, F. B., "ROTOR ASSEMBLY WITH HIGH LOCK-NUMBER BLADES," , June 2019. EP 3 345 829 B1.

[95] Sieradzki, A., "Aeroelastic Analysis of Helicopter Rotor using Virtual Blade Model and Equivalent Beam Model of a Blade," *Journal of KONES. Powertrain and Transport*, Vol. 23, 2016, pp. 297–304. doi:10.5604/12314005.1213508.

[96] Chalabi, W., "The Vehicle Routing Problem for Aerial Firefighting," Master's thesis, TU Delft, 2023.

A | Functional Flow Diagram & Functional Breakdown Structure

Contributors: Ruben, Xander
Authors: Ruben, Xander

Functional Flow Diagram (FFD)

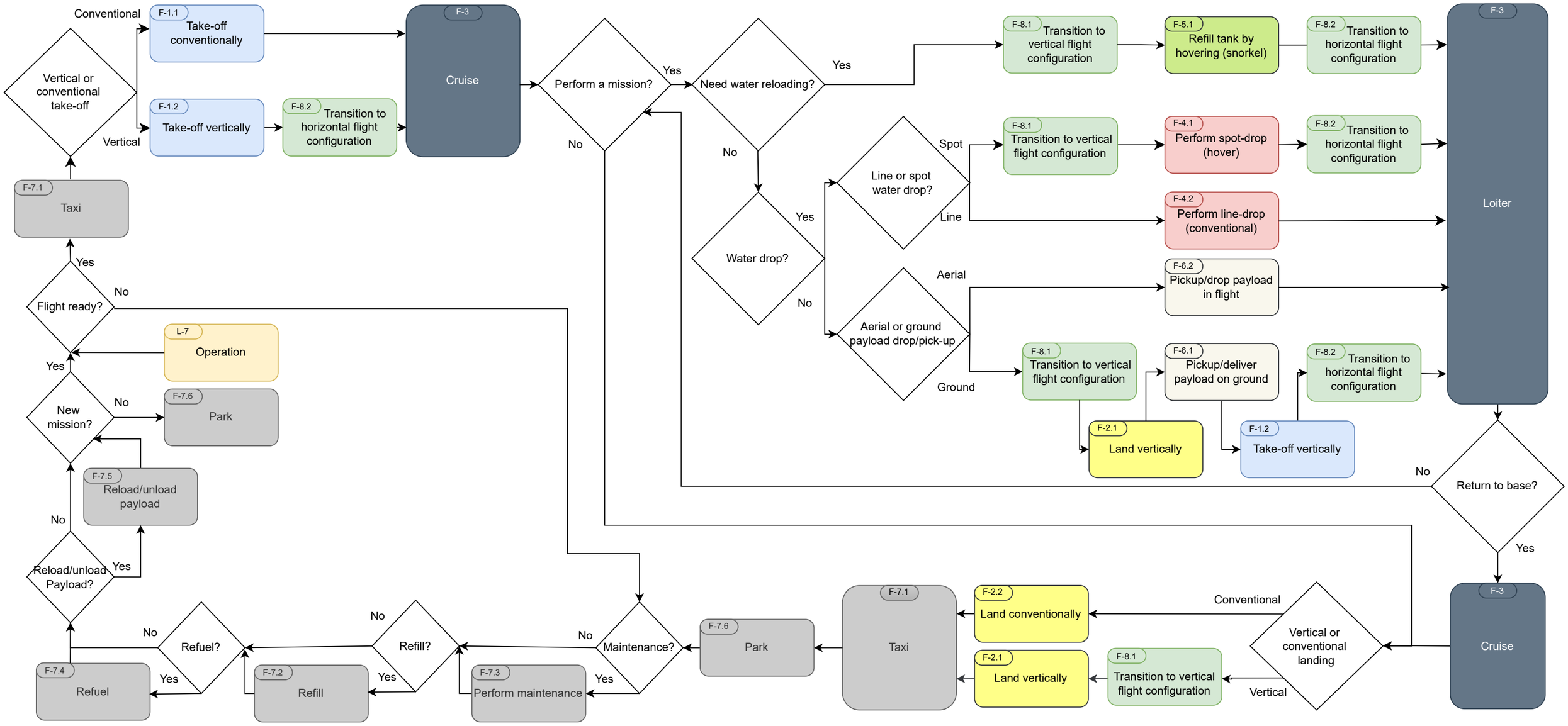

Functional Breakdown Structure (FBS)

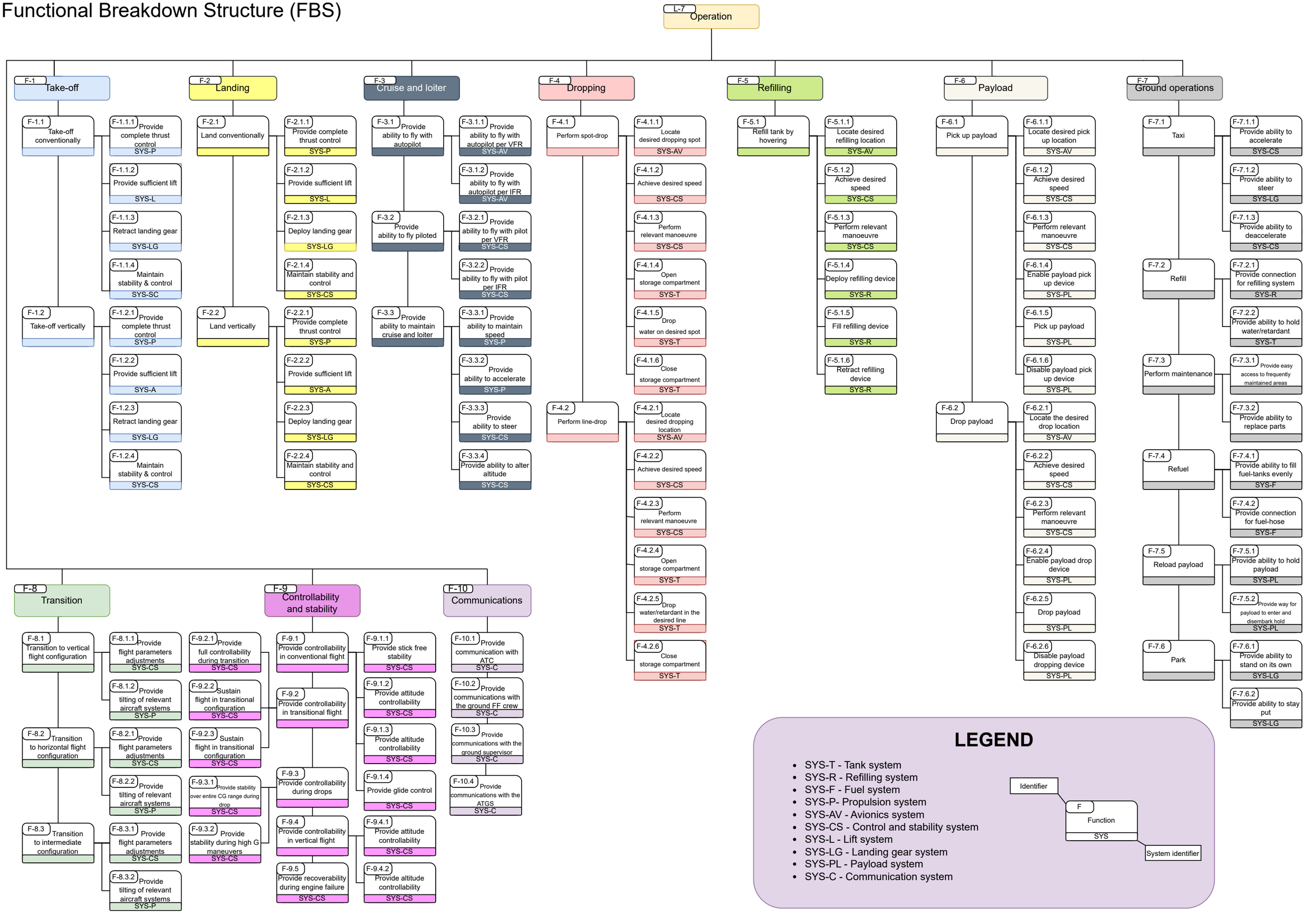

LEGEND

- SYS-T - Tank system
- SYS-R - Refilling system
- SYS-F - Fuel system
- SYS-P- Propulsion system
- SYS-AV - Avionics system
- SYS-CS - Control and stability system
- SYS-L - Lift system
- SYS-LG - Landing gear system
- SYS-PL - Payload system
- SYS-C - Communication system

B | System Drawings & Block Diagrams

Contributors: Marco
Authors: Marco

In this appendix, the Three-View Drawing, and the Hardware, Software & Data Handling, and Electronics Block Diagrams for CHEETAH are reported. Explanations for the elements appearing can be found in Section 5.2 and 5.3.

CHEETAH Three-View Drawing

Dimensions in metres

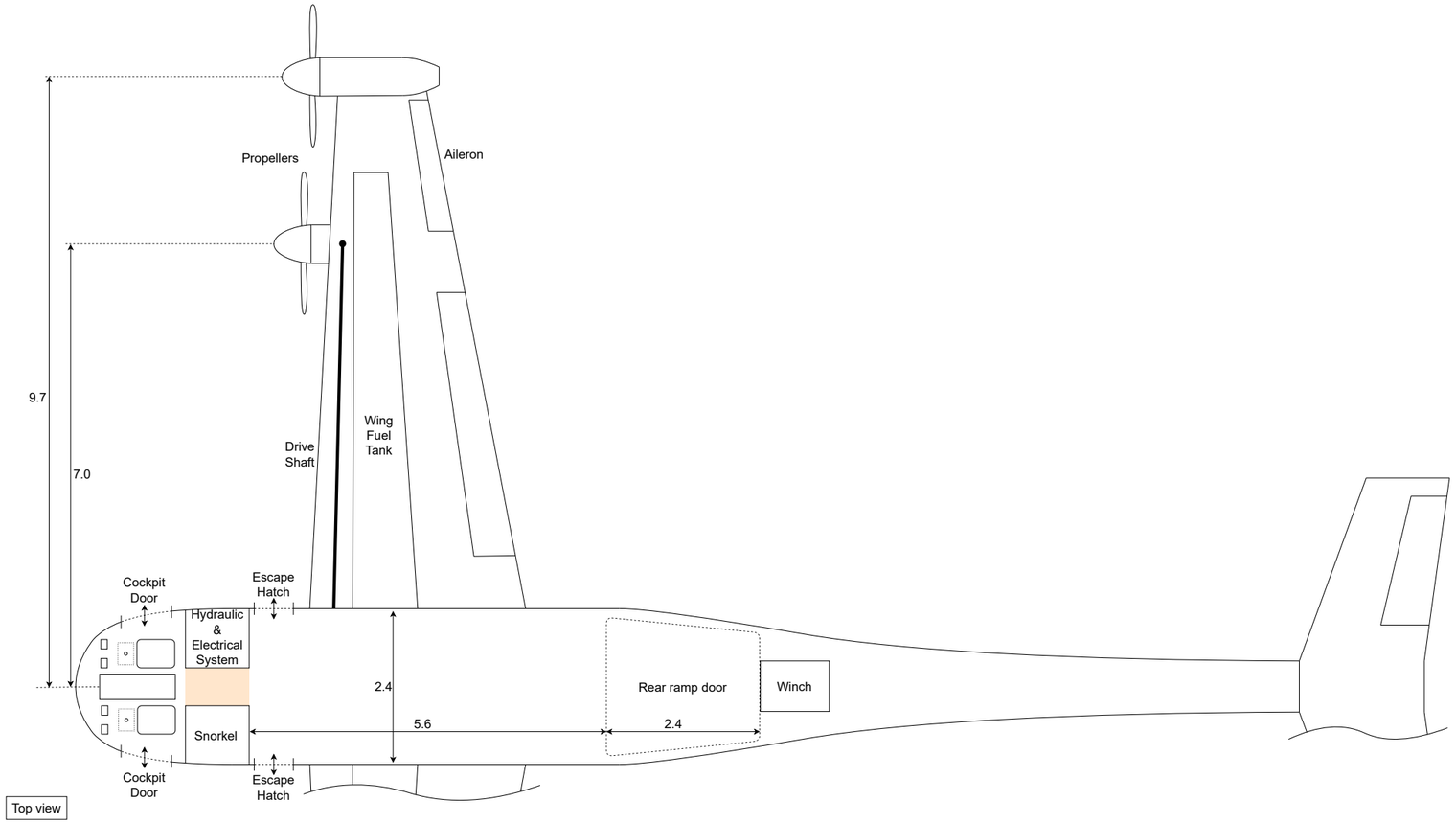

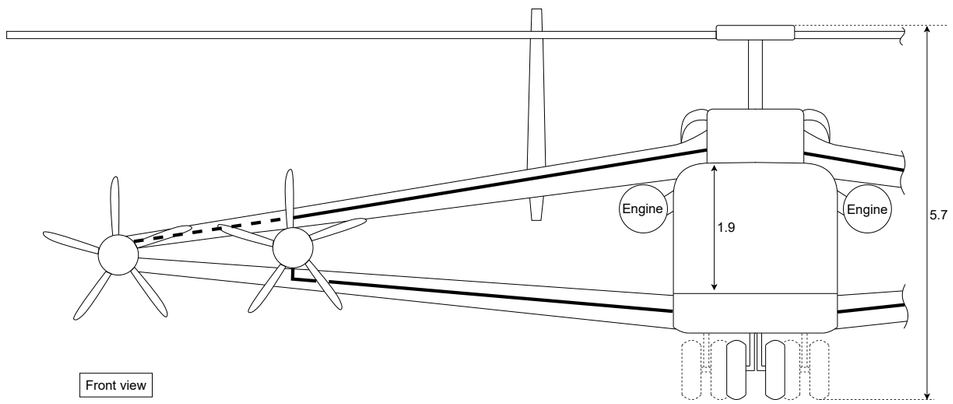

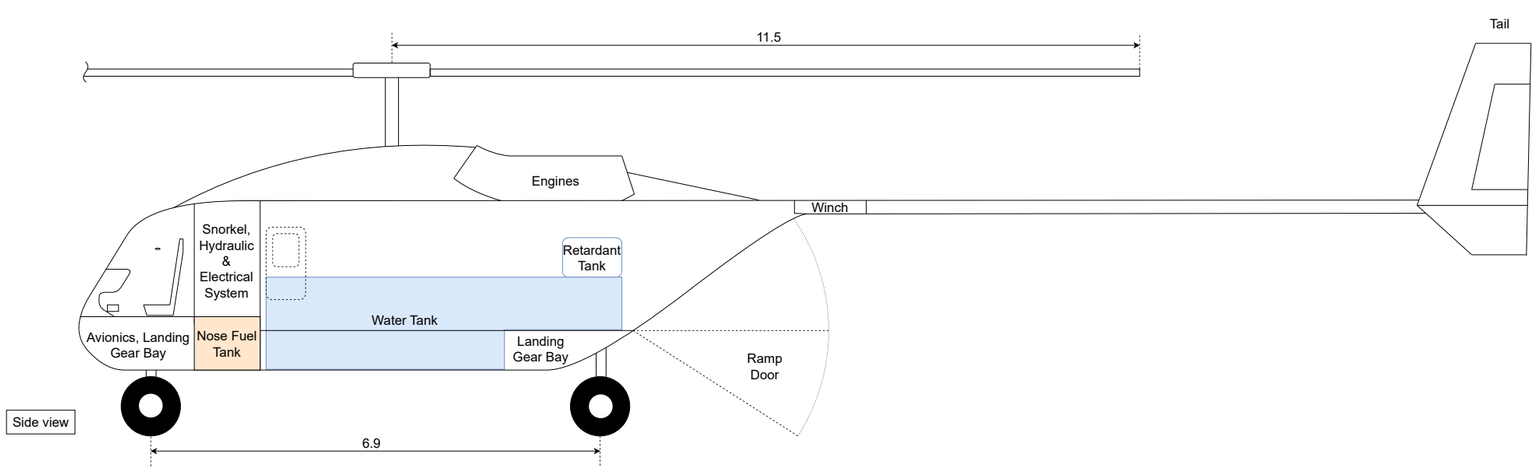

CHEETAH Hardware Block Diagram

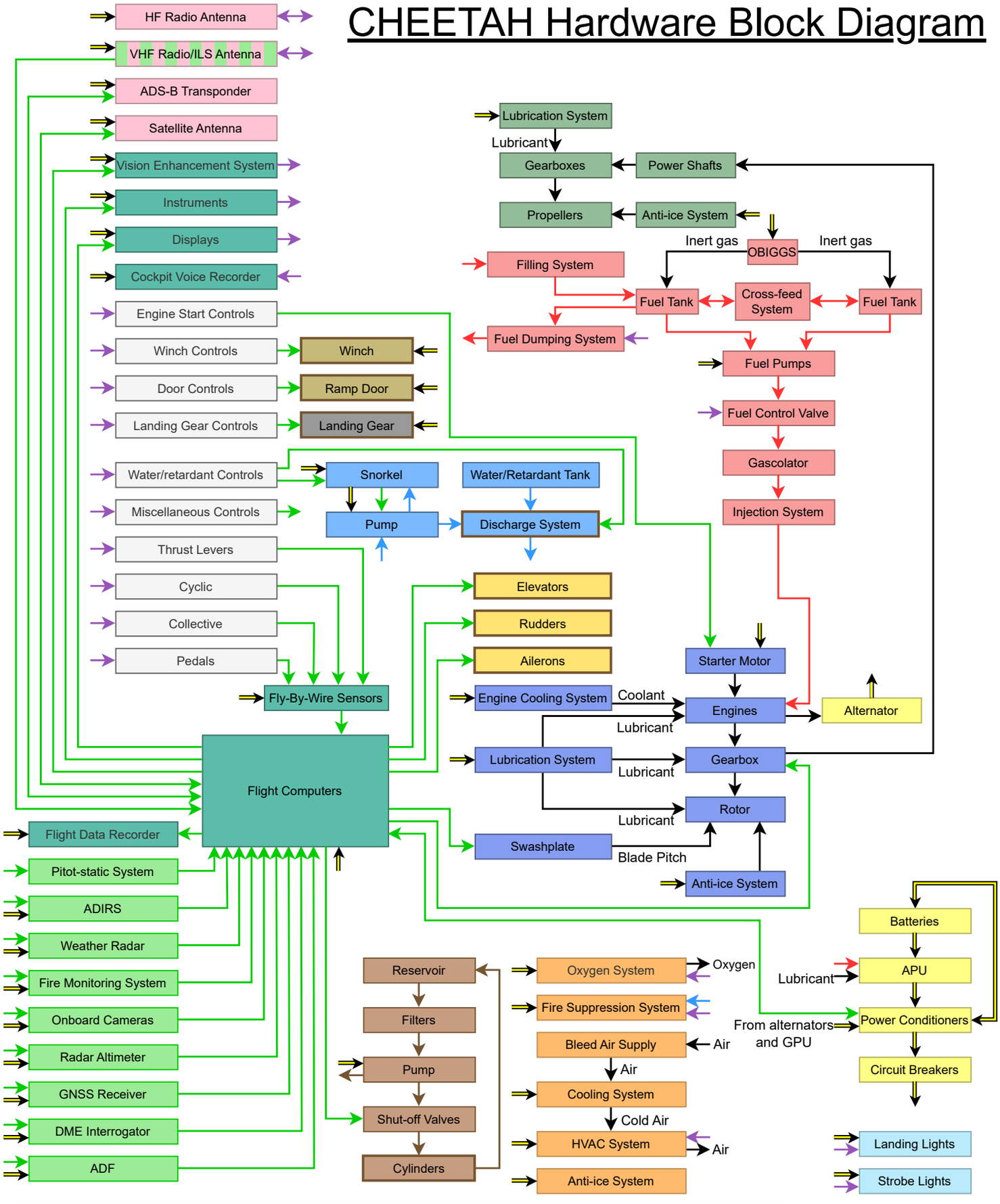

CHEETAH Software & Data Handling Block Diagram

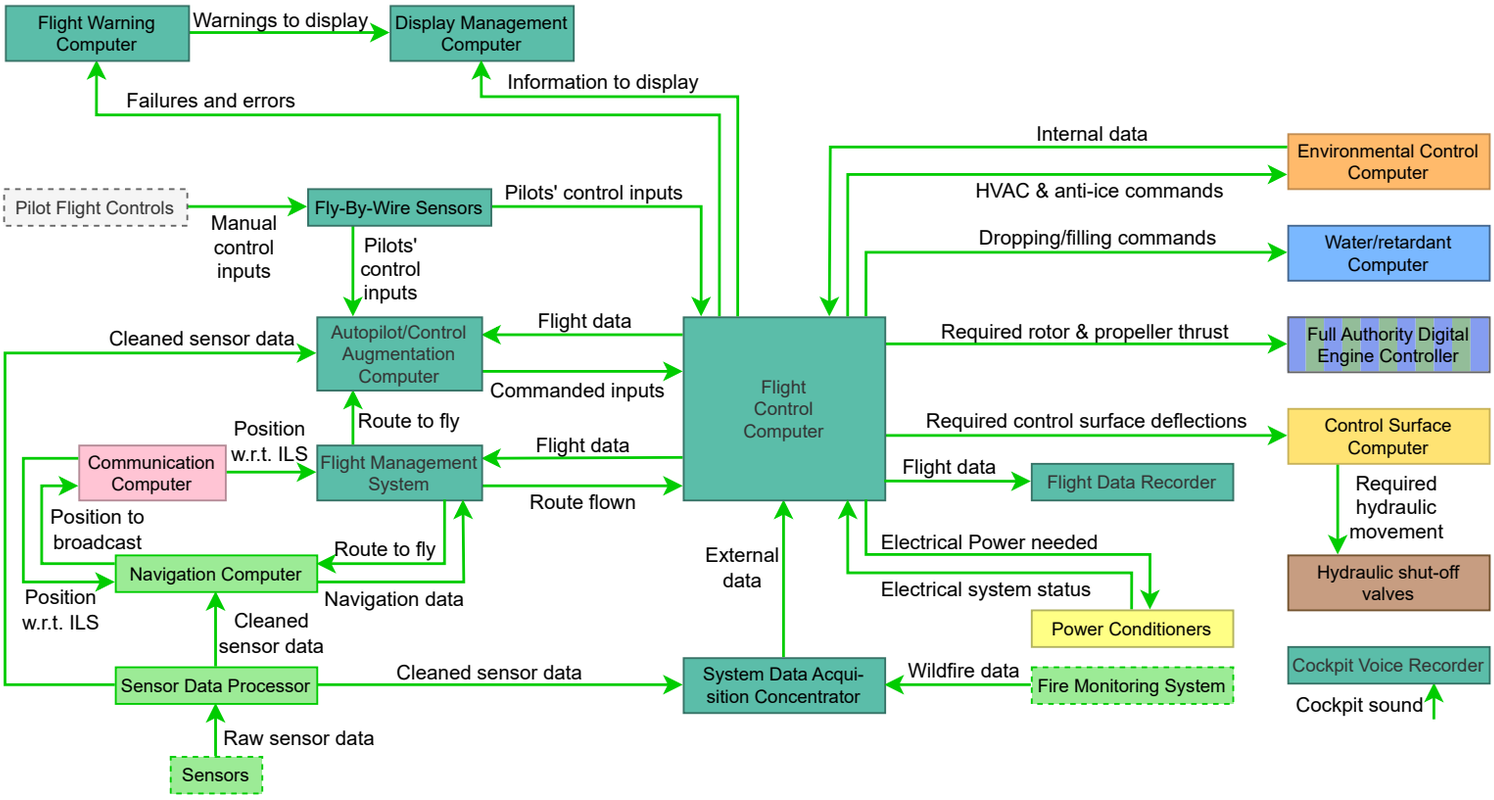

CHEETAH Electronics Block Diagram

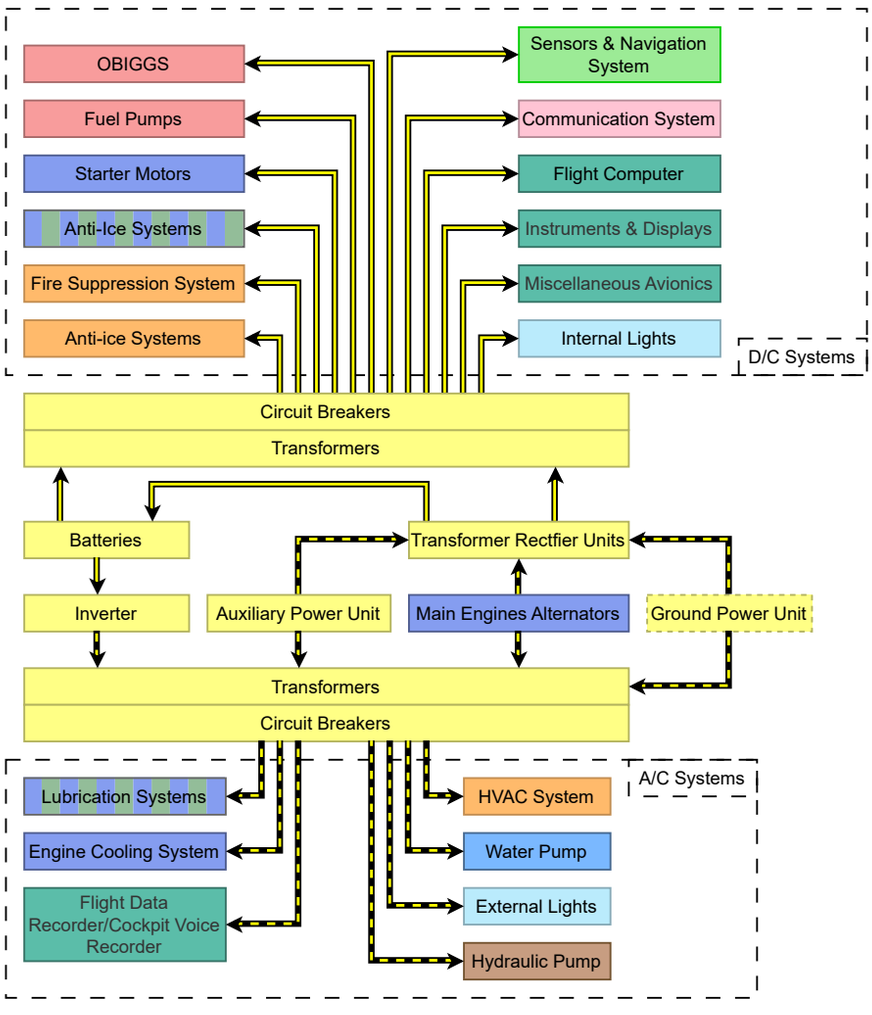

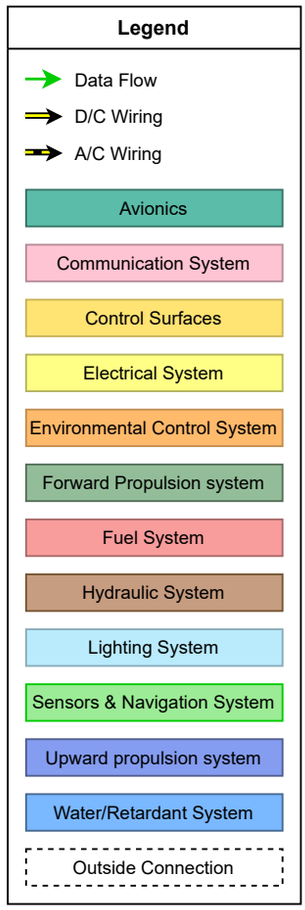

C | Post-DSE Flow Diagram

Contributors: Jorrit
Authors: Jorrit

In this appendix, the post-DSE flow diagram for CHEETAH are reported. Explanations for the diagrams can be found in Section 15.5.

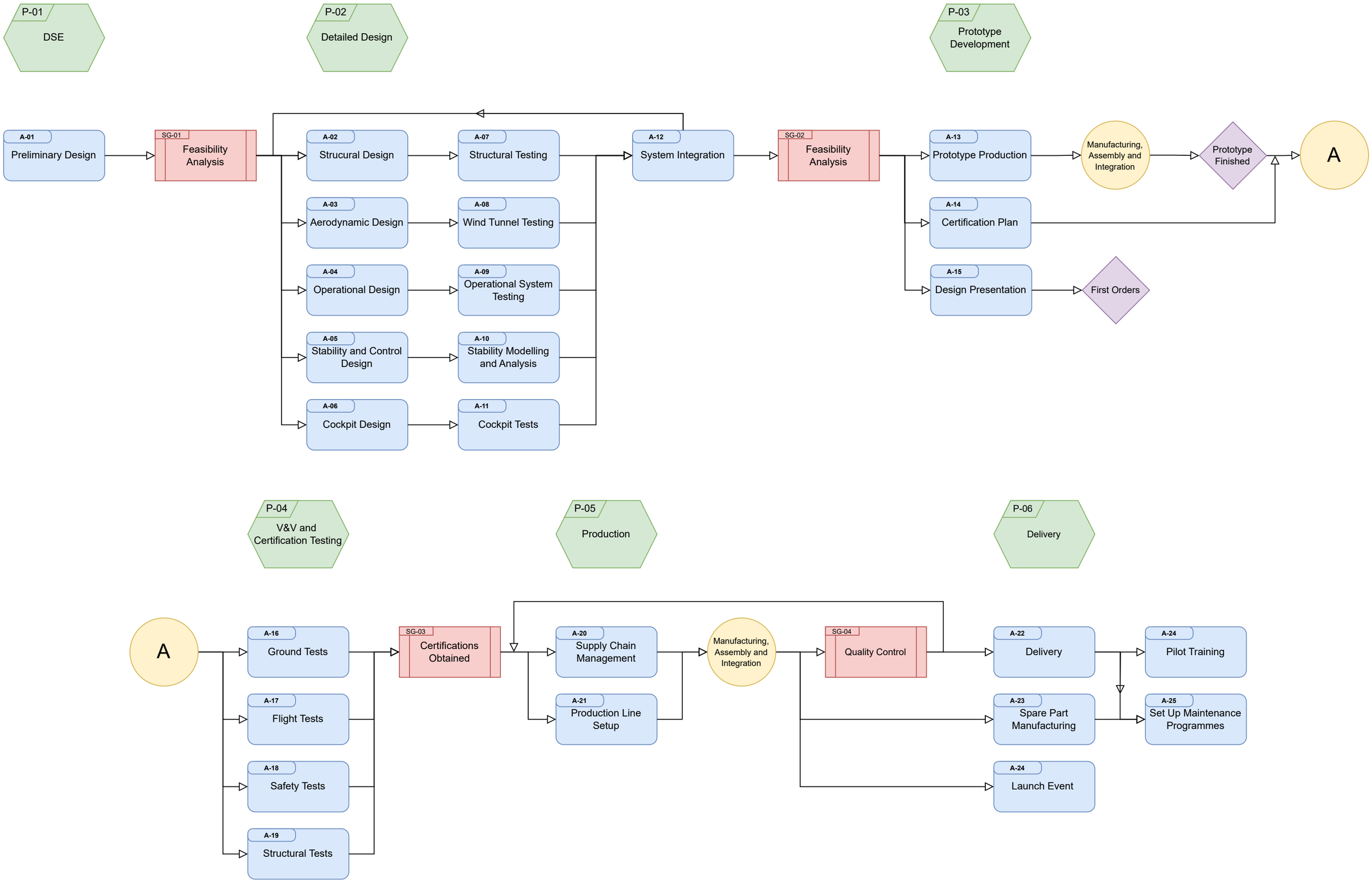
P-01
DSE
P-02
Detailed Design
P-03
Prototype Development
A-01
Preliminary Design
SG-01
Feasibility Analysis
A-02
Strucural Design
A-07
Structural Testing
A-12
System Integration
SG-02
Feasibility Analysis
A-13
Prototype Production
Manufacturing, Assembly and Integration
Prototype Finished
A
A-03
Aerodynamic Design
A-08
Wind Tunnel Testing
A-14
Certification Plan
A-04
Operational Design
A-09
Operational System Testing
A-15
Design Presentation
First Orders
A-05
Stability and Control Design
A-10
Stability Modelling and Analysis
A-06
Cockpit Design
A-11
Cockpit Tests
P-04
V&V and Certification Testing
P-05
Production
P-06
Delivery
A
A-16
Ground Tests
SG-03
Certifications Obtained
A-20
Supply Chain Management
Manufacturing, Assembly and Integration
SG-04
Quality Control
A-22
Delivery
A-24
Pilot Training
A-17
Flight Tests
A-21
Production Line Setup
A-23
Spare Part Manufacturing
A-25
Set Up Maintenance Programmes
A-18
Safety Tests
A-24
Launch Event
A-19
Structural Tests

ID	Name
1	DSE
3	Preliminary design
2	Feasibility analysis
6	Detailed Design
4	Aerodynamic Design
9	Wind Tunnel Testing
5	Structural Design
10	Structural Testing
7	Operational Design
11	Operational System Testing
8	Stability and Control Design
12	Stability Modelling and Analysis
13	Cockpit Design
14	Cockpit Testing
15	System Integration
16	Feasibility Analysis
17	Prototype Development
18	Prototype Production
19	Certification Plan
20	Design Presentation
37	Prototype Finished
21	V&V and Certification Testing
22	Ground Tests
23	Flight Tests
24	Safety Tests
25	Structural Tests
26	Certifications Obtained
27	Production
28	Supply Chain Management
29	Production Line Setup
30	Production
31	Quality Control
33	Delivery
32	Delivery
34	Spare Part Manufacturing
35	Pilot Training
36	Set up maintenance programmes

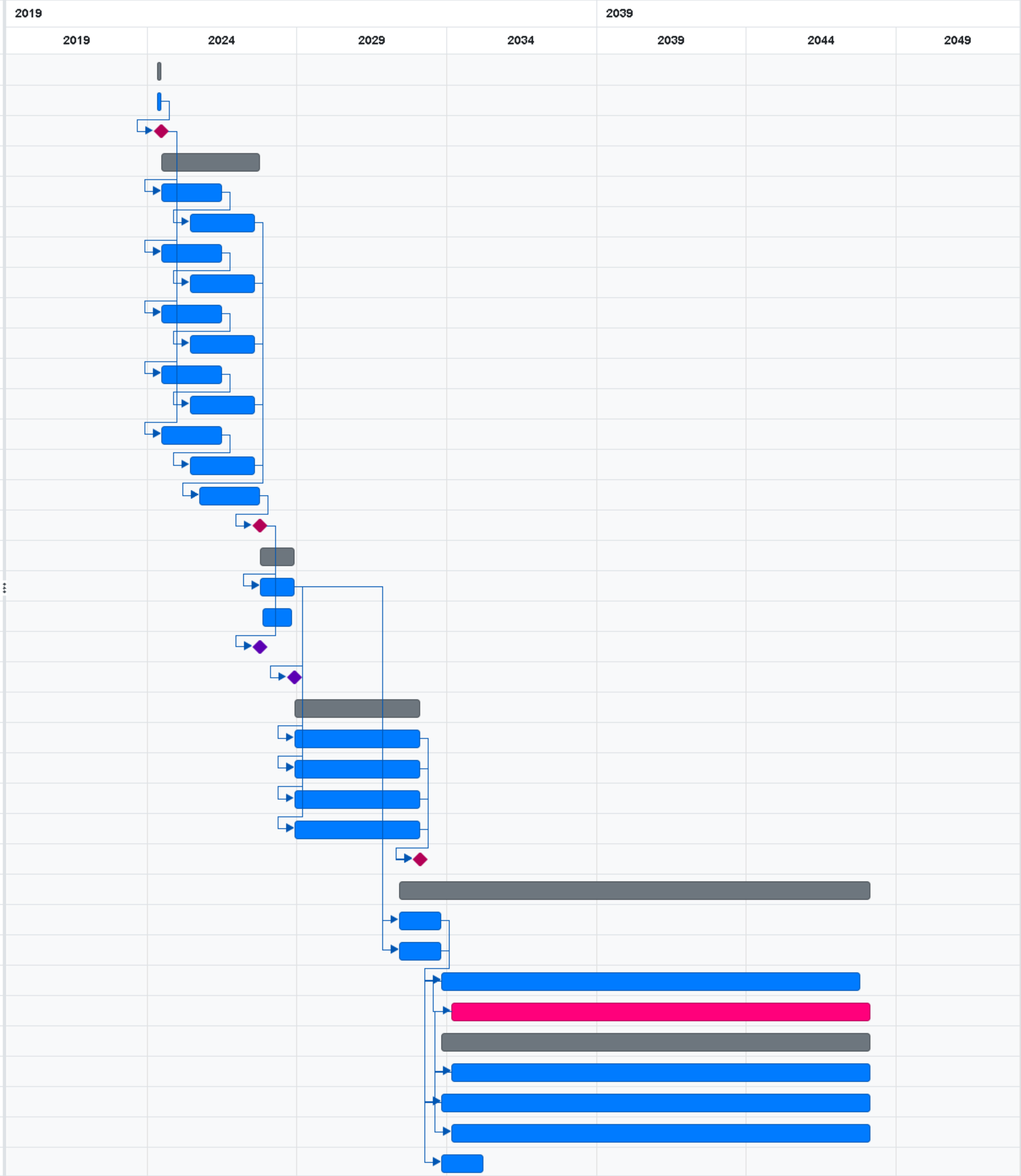

D | Manufacturing, Assembly, Integration Plan

Contributors: Ivo
Authors: Ivo

In this appendix, the MAI plan for CHEETAH can be found. Explanations for the plan can be found in Section 15.4.

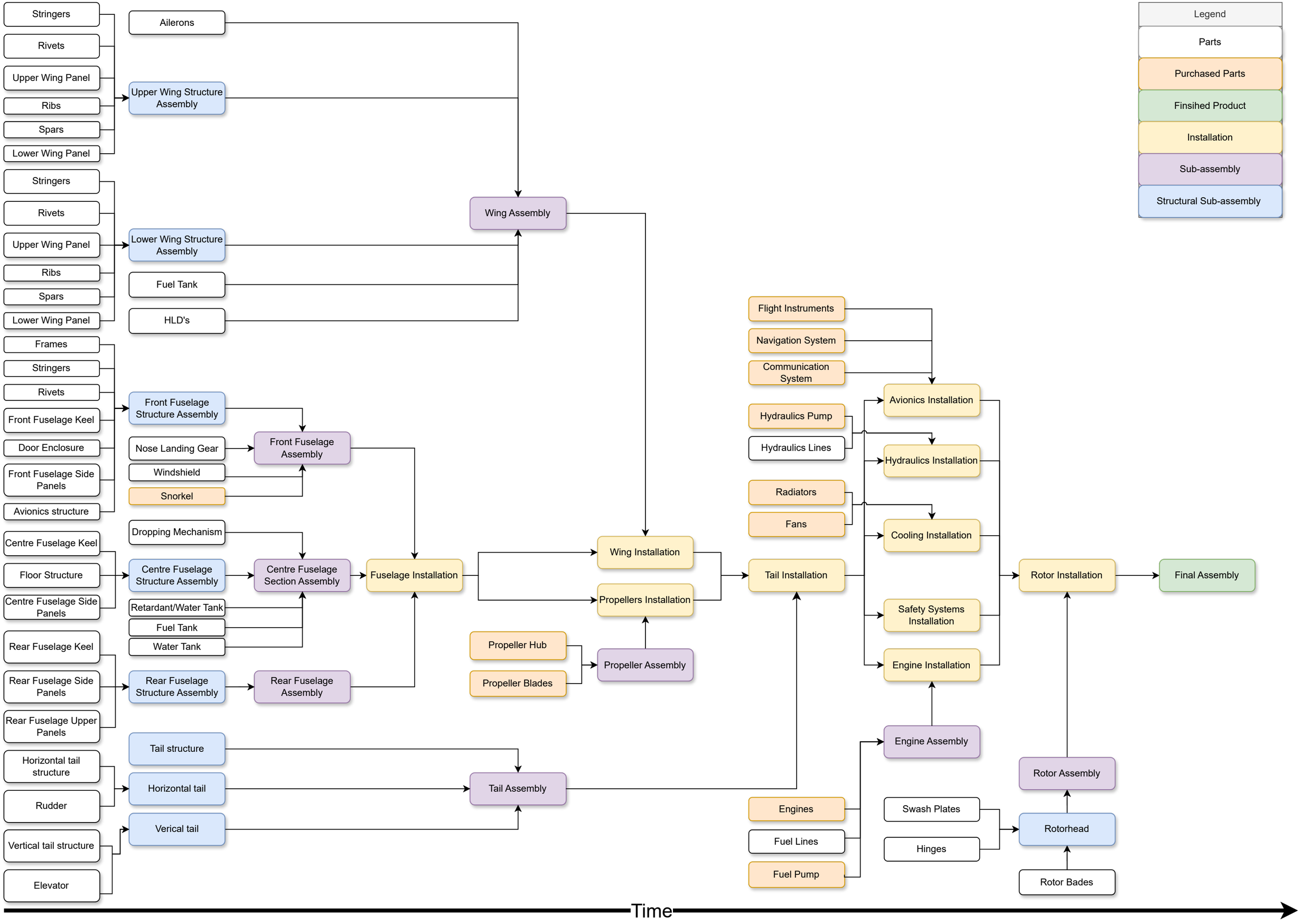
Legend
Parts
Purchased Parts
Finsihed Product
Installation
Sub-assembly
Structural Sub-assembly
Stringers
Rivets
Upper Wing Panel
Ribs
Spars
Lower Wing Panel
Ailerons
Upper Wing Structure Assembly
Stringers
Rivets
Upper Wing Panel
Ribs
Spars
Lower Wing Panel
Lower Wing Structure Assembly
Fuel Tank
HLD's
Wing Assembly
Frames
Stringers
Rivets
Front Fuselage Keel
Door Enclosure
Front Fuselage Side Panels
Avionics structure
Front Fuselage Structure Assembly
Nose Landing Gear
Windshield
Snorkel
Front Fuselage Assembly
Dropping Mechanism
Centre Fuselage Keel
Floor Structure
Centre Fuselage Side Panels
Centre Fuselage Structure Assembly
Centre Fuselage Section Assembly
Retardant/Water Tank
Fuel Tank
Water Tank
Rear Fuselage Keel
Rear Fuselage Side Panels
Rear Fuselage Upper Panels
Rear Fuselage Structure Assembly
Rear Fuselage Assembly
Fuselage Installation
Wing Installation
Propellers Installation
Propeller Hub
Propeller Blades
Propeller Assembly
Tail structure
Horizontal tail structure
Rudder
Horizontal tail
Vertical tail structure
Elevator
Verical tail
Tail Assembly
Tail Installation
Flight Instruments
Navigation System
Communication System
Avionics Installation
Hydraulics Pump
Hydraulics Lines
Hydraulics Installation
Radiators
Fans
Cooling Installation
Safety Systems Installation
Engine Installation
Engine Assembly
Engines
Fuel Lines
Fuel Pump
Swash Plates
Hinges
Rotorhead
Rotor Assembly
Rotor Bades
Rotor Installation
Final Assembly
Time

E | Fault Tree Analysis Diagrams

Contributors: Ivo
Authors: Ivo

In this appendix, the fault tree analysis diagrams for the RAMS characteristics can be found. Further details about these failure modes can be found in Section 13.3.

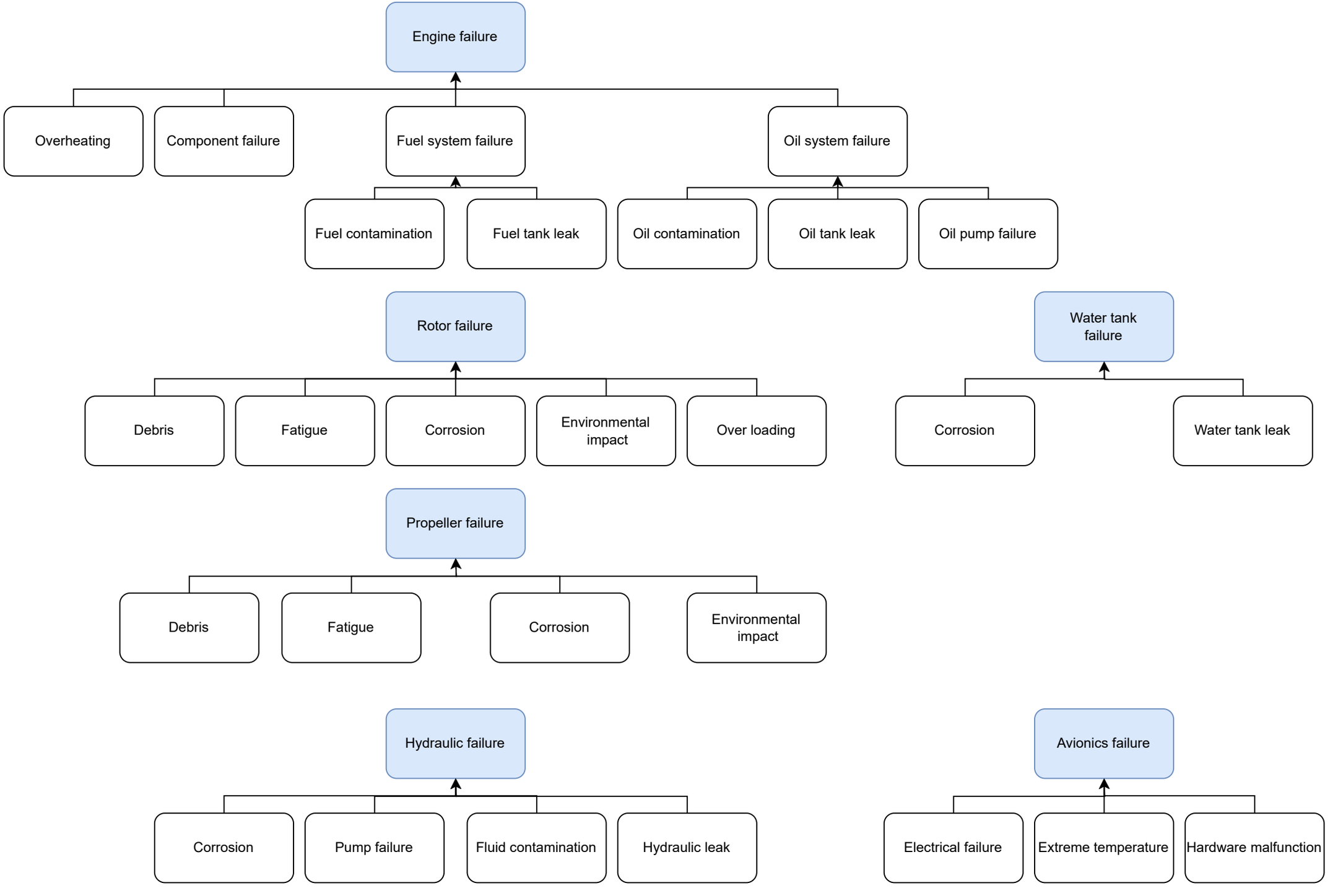
Engine failure
Overheating
Component failure
Fuel system failure
Oil system failure
Fuel contamination
Fuel tank leak
Oil contamination
Oil tank leak
Oil pump failure
Rotor failure
Debris
Fatigue
Corrosion
Environmental impact
Over loading
Water tank failure
Corrosion
Water tank leak
Propeller failure
Debris
Fatigue
Corrosion
Environmental impact
Hydraulic failure
Corrosion
Pump failure
Fluid contamination
Hydraulic leak
Avionics failure
Electrical failure
Extreme temperature
Hardware malfunction